A thesis entitled

An Accustic Investigation of the Viscoelastic Properties of High Polymers

submitted for the degree of

Doctor of Philosophy

in the

University of London

and for the

Diploma of Imperial College

by

Leslie Massey, M.Sc. (Yale), B.Sc., A.R.C.S.

1967

ABSTRACT

Velocity dispersion in short cylinders is shown to be similar to that in an infinitely long one for a wide range of values of the ratio of the diameter of the cylinder to the wavelength, subject to the condition that Young's modulus (and possibly Poisson's ratio) of the materials of the cylinders investigated are dependent on frequency. This similarity holds for both high- and low-loss materials. The magnitude of the end-effects in short cylinders is critically dependent on the knowledge of the variation of Young's modulus and Poisson's ratio with frequency. Anisotropy is the most likely cause of deviations of the behaviour of cylinders from the exact theory of wave propagation.

The Q values of resonances of cylinders of different dimensions but the same frequency are shown to be independent of the dimensions of the cylinders, for a range of values of the ratio of the radius to the length of the cylinder up to 0.1. Variations in the Q values of cylinders of nominally the same polymer and at the same frequency are most likely due to the different thermal histories of the specimens. The purity of commercially-produced blocks of polystyrene is shown to be open to doubt, the density of such specimens being likely to be 4 - 5% lower than that of the pellets from which they were made. Pressure experiments on polystyrene in the rubber-like state followed by cooling to the glass-like state indicate the existence of molecular motion below T_g of an extent not previously demonstrated.

ACKNOWLEDGEMENTS

The author wishes to thank Dr. R.W.B. Stephens of the Acoustics Group, Imperial College, for his constant guidance and encouragement throughout the project, and to Professor P.M.S. Blackett and Professor C.C. Butler for the laboratory facilities provided. He wishes to thank the technical staff of the Physics Department, in particular Mr. A. Sutherland, Mr. O. Millbank, Mr. F. Martin and the workshop staff under Mr. W. Shand for much assistance. He is grateful to the Cotton, Silk and Man-made Fibre Research Association, Manchester, for the provision of a research bursary, and thanks are due to I.C.I. Limited, Shell Chemical Co. Limited., Monsanto Chemicals Limited and Mill Plastics Limited for specimens. Finally, he wishes to thank his parents for the educational opportunities they offered and his wife for her encouragement, particularly during the final stages of the production of this thesis.

CONTENTS

CHAPTER 4 VELOCITY DISPERSION MEASUREMENTS

CHAPTER 5 DISCUSSION OF THE Δf CORRECTION TERM

LIST OF PRINCIPAL SYMBOLS

A	reflection coefficient
a	radius of cross-section of cylinder
c_n	correction for dispersion at n^{th} resonance of a finite cylinder
d	diameter of cross-section of cylinder
E, E^*, E', E''	Young's modulus, complex Young's modulus, real and imaginary parts of complex Young's modulus
$F(n,m)$	assymetric modes of propagation of elastic waves
f_n	frequency of n^{th} resonance
f_E	frequency associated with Young's modulus mode of propagation
f_s	fundamental shear mode resonant frequency
G	Gibbs' function
$G(t)$	distribution of relaxation times
g	deviation of n from an integer
J_n	Bessel function of order n
J^*	complex compliance
j	$(-1)^{\frac{1}{2}}$
$L(n,m)$	symmetric modes of propagation of elastic waves
L, L_n	wavelength, wavelength at n^{th} resonance
l	geometric length of cylinder
m,n	integers
P	pressure

Q	3 db quality factor of a resonance curve
R	rate of temperature change
r	coordinate
S	tensile strain
T_{xy}, etc.	stress components
T, T_g, T_d	temperature, glass transition temperature, dynamic glass transition temperature
t	time
$\bar{u}$	displacement vector of components u_r, u_θ, u_z
v_E	phase velocity of elastic waves governed by Young's modulus
v_l	phase velocity of longitudinal mode elastic waves
v_n	phase velocity associated with n^{th} resonance of a finite cylinder
v_s	phase velocity of shear mode elastic waves
Z	coordinate
α	real part of complex propagation constant
β	imaginary part of complex propagation constant
γ, γ^*	propagation constant, complex propagation constant
Δf	correction to resonant frequencies
δ, δ_E	damping factor, damping factor in Young's modulus mode
θ	coordinate, phase angle of reflection coefficient

λ , λ^*	Lamé elastic constant, complex Lamé elastic constant
μ , μ^*	Lamé elastic constant which is the shear modulus, complex Lamé elastic constant (complex shear modulus)
ρ	density of a medium
σ , σ^*	Poisson's ratio, complex Poisson's ratio
τ	relaxation or retardation time
ω , ω_o	angular frequency, ideal angular frequency

CHAPTER 1

VELOCITY DISPERSION IN CYLINDERS

(a) Introduction

Various authors (Abramson (1958); Miklowitz (1960)), and particularly Zemaneck (1962) have written substantial reviews of the development of the theory of wave propagation in elastic cylinders. Following Zemaneck, the word "mode" is reserved exclusively for reference to the type of wave motion in the propagation of the elastic wave, e.g. the torsional mode. When resonances of a rod of finite dimensions are referred to, they will be referred to as resonances of a particular mode of propagation.

Pochhammer (1876) first attempted to solve the problem of longitudinal wave propagation in an infinite cylinder, and Chree (1899) obtained the same equation independently. This equation which relates the frequency of the resonances, or the phase velocity, to the appropriate elastic modulus governing the propagation consists of two terms, one of which having been previously obtained by Rayleigh (1877) by considering the lateral inertia of the cylinder, the other resulting from regarding the cylinder as a rigid body.

The corrective term for the flexural mode was obtained by Pochhammer (1876) in accounting for the rotary inertia of the cylinder and Timoshenko (1921) obtained a second corrective term for the flexural mode by taking into consideration the transverse shear stress.

Bancroft (1941) was the first to calculate phase velocity dispersion values as a function of Poisson's ratio and the ratio of the diameter of the cylinder to the wavelength of the propagation. He was also the first to note that the solution of the frequency equation resulted in a number of dispersion curves, which are termed "branches".

Hudson (1943) calculated the phase velocity curve for the lowest flexural mode from the Pochhammer equation, though he overlooked the existence of higher branches of this flexural mode, and Holden (1951) first established their existence. Hudson did, however, note the existence of higher flexural modes.

Bancroft (1941) showed that for wavelengths small compared with the diameter of the rod, the phase velocity approaches the Rayleigh wave velocity for the first branch of the first symmetric mode, and that for higher order branches of this mode, the phase velocity approaches the velocity of propagation of shear waves.

Others (Hughes (1949); Holden (1951); Abramson (1957); Kynch (1957)) established the existence of further antisymmetric modes, each with a number of branches. Sittig (1957) showed that an infinite number of symmetric and antisymmetric modes exist. Adem (1954) first established that the frequency equation has complex roots which will be shown later to be necessary in the solution of the wave equation when applied to a cylinder of finite length.

More lately, interest has centred on the development of the theory for short cylinders, and those made of materials which could not be considered as loss-less.

(b) Velocity dispersion in cylinders

The equation of motion for an isotropic elastic cylinder is:-

$$(\lambda + 2\mu)\,\nabla(\nabla.\bar{u}) - \mu\,\nabla \times \nabla \times \bar{u} = \rho.\frac{\partial^2 u}{\partial t^2} \qquad (1.1)$$

where λ and μ are the Lamé constants of the elastic material, see App.1, (μ is the shear modulus), $\bar{u}$ is the displacement vector, t is the time, and ρ the density of the medium. The full analysis of this equation is given in Appendix 2.

Employing cylindrical co-ordinates r, θ , z, the components of $\bar{u}$ are given as:-

$$u_r = U(r).\cos(n\theta).\exp\{ j(\gamma z - \omega t)\}$$

$$u_\theta = V(r).\sin(n\theta).\exp\{ j(\gamma z - \omega t)\} \qquad (1.2)$$

$$u_z = W(r)\cos(n\theta).\exp\{ j(\gamma z - \omega t)\}$$

where U(r), V(r), W(r) are functions of Bessel functions of r of order n and of three independent constants A, B, C, and z is direction of propagation. These constants are evaluated by applying the boundary conditions that the cylindrical surface of the body is free. The resulting equation is a 3 x 3 determinant which is generally known as the frequency equation as it relates phase velocity to wavelength; this equation is given in full as equation (A2.17) in Appendix 2.

This equation has two sets of solutions represented by L(n,m) and F(n,m), n and m being integers. L(n,m) represent the symmetric modes of propagation which include the commonly called longitudinal mode. F(n,m) are the antisymmetric ones or flexural modes. Thus there exists an infinite series of both symmetric and antisymmetric modes

specified by n = 0,1,2,3,4 .... to infinity for the former, and n = 1,2,3,4 .... to infinity for the latter.

For each mode given by n, there exists an infinite series of dispersion curves of phase velocity specified in both L(n,m) and F(n,m) by m = 1,2,3,4 .... to infinity, and these are called "branches". The first branch of the first symmetric mode is thus given by L(0,1) and the first branch of the first antisymmetric mode by F(1,1).

Setting n = 0 in equation (A2.17) yields

$$kaJ_0(ka) - 2J_1(ka) = 0 \qquad (1.3)$$

Writing $\Omega = (\omega a/v_s)$

$$\left\{\Omega^2 - 2(\gamma a)^2\right\}^2 . J_0(ha).J_1(ka) + 4(\gamma a)^2 . hakaJ_0(ka).J_1(ha)$$

$$- 2.\Omega^2 . haJ_1(ha).J_1(ka) = 0 \qquad (1.4)$$

Equation (1.3) is the frequency equation for torsional waves and determines an infinite set of roots given by $ka = Y_q$, q being an integer which specifies the mode, see Mason (1964, p.134). The simplest solution is given by ka = 0 and represents the lowest order torsional mode in which the phase velocity is v_s. This phase velocity is

independent of frequency and is therefore non-dispersive; it is given by:-

$$v_s = \left\{\frac{\mu}{\rho}\right\}^{\frac{1}{2}} \qquad (1.5)$$

Equation (1.4) is the frequency equation for the first longitudinal mode which is the mode of particular interest here. To solve it requires the application of the boundary conditions that the shear and normal stresses T_{rz} and T_{zz} vanish on the end faces of the rod, i.e. at $z = 0$ and l, where l is the geometric length of the rod. These boundary conditions apply <u>exactly</u> only when l approaches infinity.

(c) <u>Velocity dispersion at low frequencies</u>

For frequencies less than those given by $\frac{\omega a}{v_s} = 2.6036$ Zemaneck (1962)* has shown that T_{rz} is zero at the centre and at the edges of the end-face of the cylinder and is generally two orders of magnitude less than T_{zz}. T_{zz} is an odd function of Y and can therefore be made to vanish at the end-face if the incident wave is reflected internally with no pressure phase shift.

The resultant normal stress due to the incident and reflected wave assumes the form:-

---

* Mason (1964) carries a review of Zemaneck's main findings.

$$T_{zz} = A.\sin(\gamma z) \tag{1.6}$$

which is the low frequency assumption and results in the familiar resonance condition:-

$$L = 2l/n \tag{1.7}$$

where L is the wavelength and n is an integer (see Appendix 2).

Assuming that T_{zz} and T_{rz} are zero at the end-faces of the rod, equation (1.4) yields the dispersion curve of phase velocity as a function of frequency for the first symmetric mode, L(0,1). Expanding J_0 and J_1, the Bessel functions, in the power series of ha and ka, and neglecting terms in a^2 and higher, Love (1944, p.287) has shown that the velocity of propagation v_1 is given by:-

$$v_1 = \left\{\frac{E}{\rho}\right\}^{\frac{1}{2}} \tag{1.8}$$

E being Young's modulus of the material. We shall in future refer to the velocity given in equation (1.8) as v_E to differentiate between the two velocities v_E and v_1 the latter symbol being used as the solution of equation (1.4). Equation (1.8) is the solution which results from

the simple equation of the elastic cylinder under longitudinal excitation:-

$$S = E \frac{\partial u}{\partial z} \qquad (1.8a)$$

where S is the tensile ~~strain~~ stress, u the displacement in the z-direction (along the axis) and E is Young's modulus - see Kolsky (1953, Chapter 3).

Retaining terms in a^2 in equation (1.4) produces a second approximation:-

$$v_1 = \left\{\frac{E}{\rho}\right\}^{\frac{1}{2}} \left(1 - \frac{\sigma^2 \, a^2 \, \pi^2}{L^2}\right) \qquad (1.9)$$

σ is Poisson's ratio, given by $\frac{\lambda}{2(\lambda + \mu)}$. All the other symbols have been defined before. This second approximation was derived by Rayleigh (1877, p.252) from considerations of the lateral inertia of the rod.

Bancroft was the first to calculate the roots of equation (1.4). He showed that the variables in this equation could be reduced to the three given below:-

$$x = (1 + \sigma) \left\{\frac{v_1}{v_E}\right\}^2$$

$$\Phi(y) = y \frac{J_0(y)}{J_1(y)}$$

$$\beta_0 = \frac{1 - 2\sigma}{1 - \sigma} \qquad (1.10)$$

By defining two more parameters:-

$$P = \frac{2\pi}{L} (\beta_0 x - 1)^{\frac{1}{2}}$$

$$Q = \frac{2\pi}{L} (2x - 1)^{\frac{1}{2}} \qquad (1.11)$$

equation (1.4) can be written as:-

$$(x - 1)^2 . \Phi(Pa) - (x\beta_0 - 1). \{ x - \Phi(Qa)\} = 0 \qquad (1.12)$$

From this point, v_1 will be written as v_n, the subscript n being the integer of equation (1.7) and specifying the harmonic resonances of the first symmetric mode, n = 1 being the fundamental. It is not the "n" of the symbol L(n,m), the "n" here having been set to zero to obtain equation (1.4).

The theoretical values of the dispersion of the phase velocity v_n (given by $f_n . L_n$ where f_n is the frequency of

the harmonics of the cylinder and L_n is the wavelength of the propagation at the appropriate resonance) from the "Young's modulus velocity" v_E (i.e. the phase velocity of an infinitely long and thin cylinder) are given in the Bancroft paper (1941) as a function of d/L_n (d is the diameter of the cylinder) and Poisson's ratio, σ.
For practical purposes, the intervals between the values of d/L_n and σ for which v_n/v_E have been calculated by Bancroft are too great and Bradfield (1964) has produced tables (interpolated from Bancroft's original table) with smaller intervals of σ and d/L_n, though the latter's maximum value is 0.45.

The author has used an Elliot 803 computer to extend the range of d/L_n values to 1.00 by stages of 0.05 for the same range of σ as Bradfield's and has tabulated them in Appendix 3.

(d) <u>The "universal point"</u>

The assumption that T_{rz} is identically zero everywhere is in fact true for only one frequency which is given by:-

$$\frac{\omega a}{v_s} = 2.6036 \ldots.$$

$$\text{or} \quad \gamma a = 1.841 \ldots. \qquad (1.13)$$

This frequency, called the "universal point" by Hudson who first noted it (1943) is universal in the sense that at this value of $\omega a/v_s$ equation (1.12) is independent of Poisson's ratio. The criterion is

$$\frac{\omega a}{v_s} = 2^{\frac{1}{2}} . (\gamma a) \qquad (1.14)$$

where γa is the first non-zero root of $J_1'(\gamma a) = 0$, for the L(0,1) mode. (See Morse and Feshbach (1953, p.1565)). In fact for each branch of the first symmetric mode, given by L(0,n), there is a universal point, see Mason (1964, p.146

Equation (1.14) gives as a condition for the universal point that $v_n/v_s = (2)^{\frac{1}{2}}$ when $d/L = 0.5860_6$ (from equation (1.13)), and hence v_s can be deduced from v_n and d/L_n values.

(e) Dispersion theory at high frequencies

In order to arrive at the solution of the frequency equation in section (b), it was assumed that the shear stress on the end faces of the rod were negligibly small (at frequencies less than those given by $\frac{\omega a}{v_s} = 2.6036$), and that the normal stress was made to vanish by assuming that the incident wave was reflected with no pressure phase change.

At higher frequencies than $\frac{\omega a}{v_s} = 2.6036$, T_{rz} becomes increasingly greater than zero, however, and both components of stress can be made to vanish only if it is assumed that higher branches of the propagating mode are so generated at an end face as to cancel out the excess strain. This excess is the strain which remains after that due to the directly reflected wave only is considered.

For the L(0,1) mode, Zemaneck (1962) has shown that these higher branches are the infinite number whose propagation constants are complex when the frequency is lower than that given by $\frac{\omega a}{v_s} = 3.68$. For higher frequencies than this, these branches include a finite number having real and having imaginary propagation constants and an infinite number having complex propagation constants.

Therefore below this frequency, the L(0,1) mode is the only propagating symmetric mode. At this frequency, the first two "complex" modes become propagating, i.e. the L(0,2) and L(0,3) modes - see Appendix 2. As the value of $\frac{\omega a}{v_s}$ increases, more and more pairs of branches become propagating and thus for frequencies greater than $\omega a/v_s = 3.68$, one can no longer refer to a particular resonance of a cylinder as belonging to the L(0,m) mode,

for more than one propagating branch of the mode is making a contribution to the frequency of the resonance. Appendix 2 states that above $\frac{\omega a}{v_s} = 3.68$, an infinite number of pairs of branches have to be considered when calculating the frequency of a specific resonance of the cylinder.

(f) "End effect" and reflection coefficient

In arriving at an exact solution for the non-infinite rod, it was stated in section (d) that one has to consider the reflection of the wave at the end face of the rod. The derivation in Appendix 2 defines the reflection coefficient as having amplitude A and phase θ such that

$$A = (A) \cdot \exp (j\theta) \qquad (1.15)$$

In employing the relation $L_n = 21/n$ to give L_n, the wavelength, one is ignoring a possible end effect in equation (1.15). Zemaneck allows for this possibility by writing equation (1.7) as

$$L_n = 21/(n - g) \qquad (1.16)$$

where g is the deviation of n from an integer. In calculating v_n, the form $v_n = f_n \cdot L_n$ is employed, and in

applying equation (1.16) to this equation for v_n, the following equation is obtained:-

$$v_n = (f_n + \Delta f) . \frac{21}{n} \qquad (1.17)$$

where Δf is the amount by which the ideal resonant frequency is reduced on assuming that the actual wavelength is given by $L_n = 21/n$.

(g) Effect of internal friction on the frequency equation

In all that has preceded this section, it has been assumed that the material of the cylinder is loss-less. In recent years, interest has been shown by many workers in the effect of internal friction in the material on the theory of dispersion in cylinders.

Snowdon (1964) has amended equation (1.9) to account for finite but small losses in rods having a diameter to length ratio of 1:5. The principal finding of this work is that the strain amplitudes of the resonances are less than would be predicted for cylinders of the same dimensions but entirely loss-less. There is no effect on the values of the frequencies of the resonances.

Edmonds (1961) has amended the frequency equation (1.12) by assuming that λ, μ (the Lamé constants), v_1 and ω are each complex to account for energy loss, e.g. $\lambda^{*} = \lambda' + j\,\lambda''$ where λ'' is the imaginary component. In Appendix 2, a more complete development is given, but in retaining only the first order imaginary terms and on separating the equation into its real and imaginary parts, the former gives the dispersion equation as before, whereas the latter relates the Q factor of the resonances (see Appendix 1) to λ''/μ'' and $\omega\, a/v_R$. This loss effect will be referred to in Chapter 5.

To date, no attempt has been made to calculate the second order effect of internal friction on the frequencies of the resonances as given by equation (1.12). Parfitt (1954) introduces a frequency dependent loss factor δ into the simple equation for the solution of the elastic cylinder under longitudinal excitation (see equation (1.8a)). The effect at resonance is to produce an amplitude of vibration at the end of the rod remote from the driving force of

$$u = \frac{U_o \cdot \omega_o}{\pi \cdot \omega} \left\{ \frac{2}{(1 + \delta_E^{\,2})^{\frac{1}{2}} (\cosh 2\alpha 1 - \cos 2\beta 1)} \right\}^{\frac{1}{2}} \qquad (1.18)$$

where U_o is a constant, $\omega_o = \frac{\pi}{l}\left\{\frac{E}{\rho}\right\}^{\frac{1}{2}}$, the ideal angular frequency, ω is the angular frequency as measured, α and β are given by

$$\alpha^2 = \frac{\omega^2\rho}{2E'} \cdot \frac{(1 + \delta_E^2)^{\frac{1}{2}} - 1}{(1 + \delta_E^2)} \qquad (1.19)$$

$$\beta^2 = \frac{\omega^2\rho}{2E'} \quad \frac{(1 + \delta_E^2)^{\frac{1}{2}} + 1}{(1 + \delta_E^2)} \qquad (1.20)$$

and δ_E by $E^* = E'(1 + j\delta_E)$.

In retaining terms in δ_E^2 where they make a contribution approaching 1% or more, Parfitt has shown that

$$\omega = n\,\omega_o \left\{ 1 + \frac{\delta_E^2}{8}(1 + 2p + 1/8\ (3 + 2p)\ b\ \delta_E^2) \right\}^{-1} \qquad (1.21)$$

where $b = \pi^2 n^2/6$ and p is a parameter describing the manner in which δ_E is a function of ω, i.e. δ_E is proportional to $(\omega)^{-p}$. As can be seen, no term in δ_E exists, which supports Edmond's conclusion.

(h) Review of previous experimental work

There are three problems that could be examined by the experimentalist.

1. To find if the measured phase velocity dispersion follows the dependence on d/L and σ as given by the theory.
2. To find if there are any measurable end-effects in short cylinders.
3. To examine if internal losses of the material of the cylinder produce any deviations from the theory.

Bancroft (1941) has published data to show that if end effects exist at all in short lengths (5 - 15 cm.) of 3/8" diameter steel rod, then they are less than 2 parts in 5000. The experiment he performed consisted of cutting two cylinders, one 15 cm. long and the other 5 cm. long, from the same length of drill rod. The fundamental resonant frequency of the 5 cm. rod is equivalent in d/L value to the third harmonic of the 15 cm. rod, if the end effects are ignored. Hence, assuming that Poisson's ratio remains constant for the two cylinders, the only effect that could produce a change in the calculated phase velocity would be the existence of an end effect. To within the accuracy quoted above, none was detected. Bancroft did not attempt to measure the Poisson's ratio of the material of the rod, nor did he refer to the possibility of anisotropy in a rod.

Hudson (1943) applied Shear's(1940)data to test the validity of the dispersion curves as a function of d/L and Poisson's ratio. He found that the data for longitudinal wave propagation fitted the dispersion curve for $\sigma = 0.38$, whereas that for the flexural wave fitted the curve for $\sigma = 0.49$. He ascribed this variation in Poisson's ratio to anisotropy introduced in the rod when subjected to a hard-drawing process. Shear's data was taken from silver rods of dimensions 25 cm. in length and 0.5 cm. in diameter, so that d/21 is of the order of 0.01.

Spinner et al. (1960, 1962) experimented with a steel rod of length 15 cm. and diameter 1.2 cm.; thus d/21 = 0.04. They measured the resonant frequencies of the rod in the longitudinal mode, shortened the rod and found the frequencies once again. Repeating the procedure once more resulted in a rod of dimensions given by d/21 = 0.10. They used n.d/21 to give d/L values, derived v_E from the fundamental resonant frequency of the longest rod (dispersion is small for these values of d/L and is only very slightly dependent on the value of σ) and found that $\sigma = 0.292$ gave the best fit to the theoretical curves for values of d/L up to 0.3. Recognising that an independent check on the value of Poisson's ratio was desirable, they measured the first torsional mode

resonant frequency and employed the equation:-

$$\sigma = \tfrac{1}{2}\left\{\frac{f_E}{f_s}\right\}^2 - 1 \qquad (1.22)$$

where f_E is the fundamental frequency of Young's modulus mode (suitably corrected for dispersion) and f_s is the fundamental frequency of the shear mode (which is dispersionless). This method produced a value of 0.262 for Poisson's ratio and the authors ascribed this difference to anisotropy in the rod.

By far the most complete work on velocity dispersion in cylinders has been carried out by Zemaneck (1962) and a joint paper with Rudnick (1961) reported findings for an aluminium alloy cylinder, well-annealed, 3" in diameter and 120" in length, giving a value of d/21 = 0.0125. The first few resonances in the longitudinal mode are practically dispersionless and hence an accurate value of v_E can be determined. The wavelength was measured by means of a strain detector which traversed the surface of the cylinder in an axial direction, and therefore d/L could be determined without use of the formula n.d/21, thus avoiding end-effect corrections. Equation (1.22) was used to calculate Poisson's ratio, and it was found that Rayleigh's approximate

solution (equation (1.9)) fitted the experimental data better than the exact solution for d/L values up to 0.16. The deviation from the exact theory is only 0.2% at the worst, however.

Zemaneck and Rudnick also show that the dispersion in the first flexural mode is according to Timoshenko's correction as opposed to the exact theory, though again the deviations are small. Dispersion in the shear mode was found to be less than 0.01% over the range covered.

Edmonds and Sittig (1957) have reported work carried out on an aluminium cylinder 24 cm. long by 4.9 cm. in diameter, i.e. d/21 = 0.102. They expressed their results in a manner which is more sensitive to deviations from the theory, particularly in the region of the universal point, than is obtained from plotting v_E/v_n as a function of d/L and σ , see Figure (1.1). As can be seen, the experimental plot Y should lie between plots (a) and (b), if the material of the cylinder has a value of Poisson's ratio lying between 0.3 and 0.4. This experimental plot should pass through the universal point ($\frac{d}{L} = 0.5860_6$, Y = 0) as should all theoretical and experimental curves. Figure (1.1) shows that neither of these conditions is held for the experimental values obtained by Edmonds and Sittig.

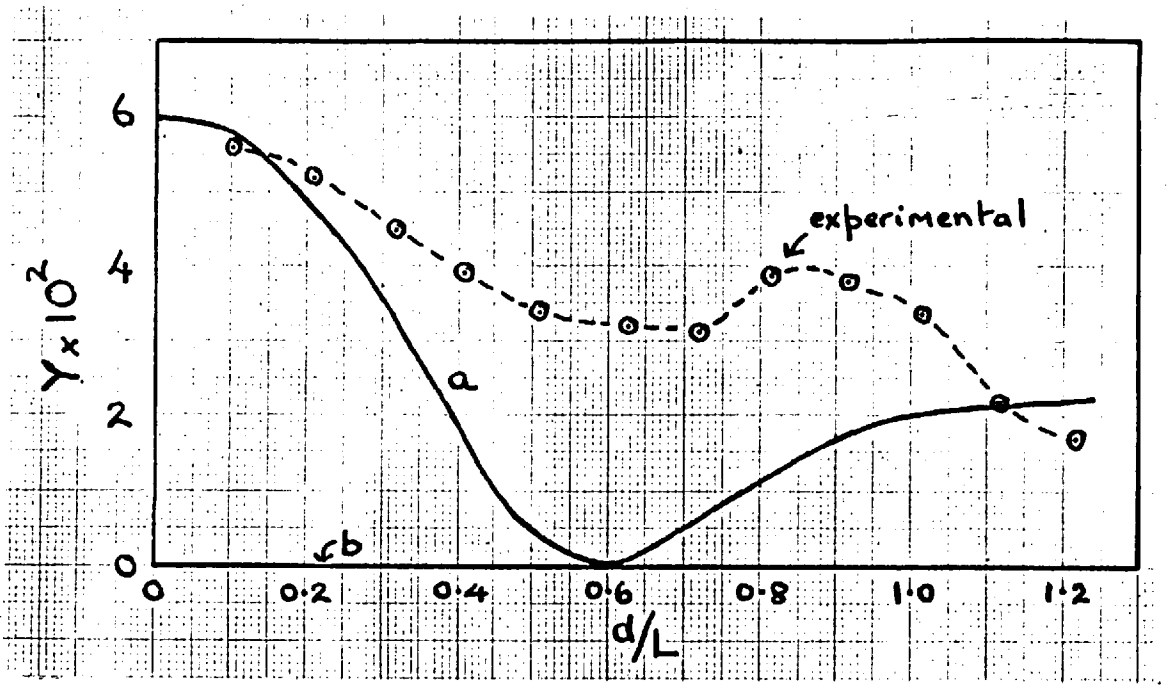

FIGURE (1.1). Edmonds' and Sittig's method of display of velocity dispersion data.

$$Y = \left(\frac{v_n}{v_s}\right)_{\sigma} - \left(\frac{v_n}{v_s}\right)_{0.30}$$

(a) $\sigma = 0.40$, theoretical values.

(b) $\sigma = 0.30$, theoretical values.

For the experimental points, (v_n/v_s) is calculated from the experimental values of v_n and v_s.

Using an experimental technique as described above, they detected the positions of the nodes along the surface of the cylinder and showed that, from about the sixth resonance, the positions of nodes began to move in from both ends of the rod towards the centre. This effect is at a maximum at about the ninth resonance and has disappeared again at the eleventh. As the deviation from the theory occurs before the sixth resonance, this shifting of the nodal distribution cannot be the only explanation of the deviation from theory, and possibly anisotropy in the rod may be a contributing cauce.

(i) Present investigation of velocity dispersion

From the previous section, it seems that it is always possible to find a value of Poisson's ratio which will adequately fit the experimental data of v_E/v_n as a function of d/L. The doubt still remains whether this value of Poisson's ratio can be obtained by other experimental methods, even for cylinders which are loss-less and perfectly isotropic. Zemaneck has shown that consistent values of Poisson's ratio can be obtained for relatively long cylinders using the dispersion values and the first longitudinal and first shear mode resonances.

It was felt, therefore, that insufficient data was available for short isotropic cylinders and it was decided to investigate these. Other techniques of measuring Poisson's ratio independently of the velocity dispersion measurements were thought to be necessary.

The velocity dispersion behaviour of cylinders made from materials with high internal losses has been theoretically investigated, though no experimental data on these materials seems to be available, and an investigation of the behaviour of cylinders made from such materials was thought to be advantageous.

Three methods of deducing Poisson's ratio are available, using

1. The dispersion data.
2. The interpolated value of f_s and the measured value of f_s, along with f_E obtained from f_1 for the longitudinal mode in equation (1.22).
3. The shear velocity v_s and the "true" longitudinal velocity v_1 (i.e. that governed by $\lambda + 2\mu$ and not E as modulus) obtained from the propagation of the appropriate 5 mc/s pulses through samples of the material. This apparatus will not be described, a full report having been given by Smith (1965).

CHAPTER 2

Free Volume Effects in Glass-like Polymers

(a) Nature of the glass transition

The parameters which determine whether an amorphous polymer behaves as a glass are temperature (or frequency) and pressure. Above a temperature T_g, called the glass transition temperature, the behaviour of the polymer is rubber-like in that the value of its Young's modulus is $\sim 10^7$ dynes/cm^2 whereas below this temperature, the polymer is hard and brittle and has a Young's modulus of the order of 10^{10} dynes/cm^2. Kovacs (1964) has defined glasses as an "important class of materials whose mechanical properties are comparable to those of crystalline solids whilst having a molecular arrangement similar to those of liquids". On increasing temperature, the properties of a glass change more or less abruptly to those more like a rubber and this process is called the glass transition. Kauzmann (1948), Davies and Jones (1953), Condon (1954) and Saito (1963) have written articles on the nature of the glass transition.

The glass transition is not a phase transition in the thermodynamic sense (Flory, 1955). In classical

thermodynamics (see Zemansky, 1957, Chapter 2, for example), there are two kinds of transition, a first order transition and a second order transition. The former is characterised by a discontinuity in both the entropy and volume of the sample which are given by $\left(\frac{\partial G}{\partial T}\right)_P$ and $\left(\frac{\partial G}{\partial P}\right)_T$ respectively, where G, T, P are the Gibbs function, temperature and pressure respectively; crystallisation and vapourisation are particular examples. A second order transition is characterised by a continuous change in the entropy and volume of the sample and a discontinuous change in the heat capacity, thermal expansion coefficient and compressibility of the sample, which depend upon the second derivatives of the Gibbs function with respect to T, to P and T together, and to P respectively; a specific example is the order-disorder transition that occurs in some alloys. Figure (2.1) due to Zemansky shows how entropy and volume change for first and second order transitions.

Although the glass transition exhibits these second order transition features, Flory (ibid.) has shown that glasses are not even in a state of <u>metastable</u> equilibrium, but tend to approach such a state at an infinitely slow rate when the temperature of the sample is lower than T_g. Richards (1936) was one of the first to recognise that

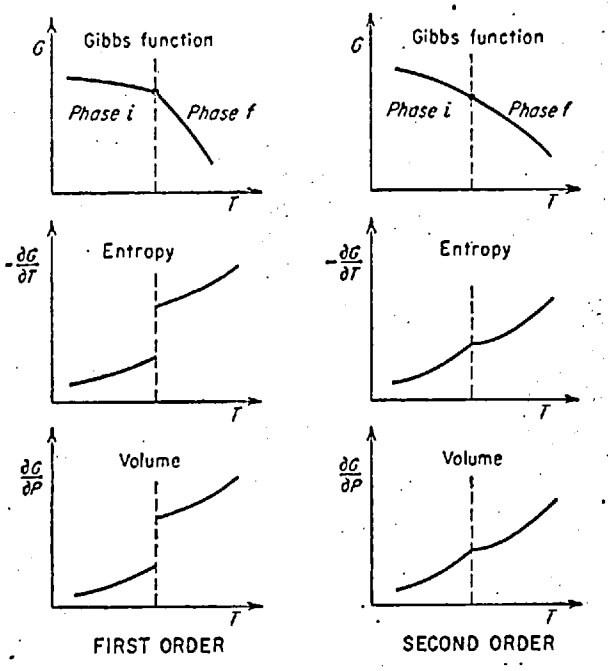

FIGURE (2.1) First and second order phase transitions, after Zemansky (1957).

Gibbs function can be written as $dG = V.dP - S.dT$ for an infinitesimal reversible process, where V, P, S and T are the volume, pressure, entropy and temperature respectively. From this definition, it follows that

$$V = \left\{\frac{\partial G}{\partial P}\right\}_T \qquad S = \left\{\frac{\partial G}{\partial T}\right\}_P$$

Heat capacity, $C_P = T.\left\{\frac{\partial S}{\partial T}\right\}_P = -T.\left\{\frac{\partial^2 G}{\partial T^2}\right\}_P$

Compressibility, $K = -\frac{1}{V}.\left\{\frac{\partial V}{\partial P}\right\}_T = -\frac{1}{V}.\left\{\frac{\partial^2 G}{\partial P^2}\right\}_T$

Volume expansion coefficient, $\alpha_o = \frac{1}{V}.\left\{\frac{\partial V}{\partial T}\right\}_P = \frac{1}{V}.\left\{\frac{\partial^2 G}{\partial T \partial P}\right\}$

the transition from the rubbery to the glass-like state is one of a "freezing in" of disorder of the molecules, this state representing a particular form of a supercooled liquid, but one in which the entropy remains greater than that of the theoretical crystalline form right down to the absolute zero of temperature (Simon, 1930, 1931).

The glass transition appears, therefore, to be concerned with the freedom of movement of the polymer molecules within the bulk of the sample. At temperatures below T_g, the molecular segments are localised in potential energy wells, whereas above T_g the motion of the molecules tends to approach free rotation about single bonds in the polymer chain (Ellerstein, 1964). On increasing the temperature through the glass transition molecules relax, a process which would lead to viscous flow in a liquid, but which in a polymer results in the highly elastic deformation characteristic of rubber-like elasticity.

No review of the glass transition would be complete without some reference to the effect of molecular weight on T_g. Below values of the number average (n) molecular weight, $\bar{M}_n$, of about 20,000, the value of T_g for a homologous series is found to increase asymptotically with $\bar{M}_n$ according to the equation $T_g = T_{g,\infty} - k_p/\bar{M}_n$,

where k_p is a constant, and $T_{\bar{g},\infty}$ is the value of T_g as $n \longrightarrow \infty$. Above this value of $\bar{M}_n$, the effect of neighbours on molecular motion can no longer be described solely in terms of local frictional forces, and the visoelastic properties reveal an additional coupling to neighbours which appears to be localised at a few widely separated points along the molecular chain. This effect is known as entanglement coupling (Ferry, 1961, page 23). Ellerstein (1964) has reported on this subject and refers to the various theories governing the dependence of T_g on molecular weight. ~~It is found that the centigrade temperature of viscous flow in the polymer is of the order of twice that of the glass transition.~~

In describing the glass transition, attention will be directed to the mobility of the molecule comprising the polymer and in turn to the shape, size and flexibility of the main backbone chain and its pendant side groups.

(b) Molecular mobility and its effect on T_g

The principal description of the glass transition temperature is that point at which the convolutions of the backbone of the polymer molecule are largely immobilised. Thus the viscoelastic properties of the glassy state must

result from limited local molecular motion, which is usually ascribed to the rearrangements of the side groups along the polymer chain (Ferry, 1961, page 306). However, steric hindrance and bulkiness of the side groups are often difficult to separate from lack of backbone flexibility. As Nielsen (1962, Chapter 2) points out, steric hindrance can increase the value of T_g, as is illustrated by the difference in T_g between that of poly (p-methyl styrene) and of poly (o-methyl styrene), 101°C and 125°C, respectively. It is thought that the methyl group in the ortho-position of the benzene ring restricts the motion of the backbone.

Increasing bulkiness of the side group also elevates the temperature of the glass transition. This is illustrated by comparing the values of T_g for polyethylene, polypropylene, polystyrene and poly-vinyl carbazole in which the side groups are, from left to right:

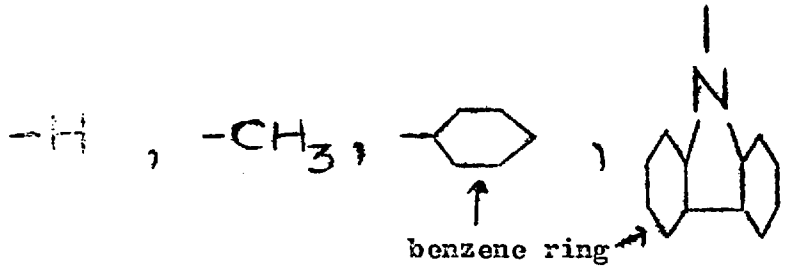

The values of T_g for these polymers is, in the same sequence, 153°K, 264°K, 373°K, 481°K.

However, the glass transition temperature depends on the flexibility of the side group, for in the series polymethyl acrylate, polyethyl acrylate, polybutyl acrylate, T_g decreases as the side group gets larger.

Mixtures of polymer with its monomer and other plasticisers (Dudek, 1965) and with other polymers (Krause, 1965a) results in a lowering of the glass transition temperature T_g, although in some two component mixtures of polymers three transitions have been reported, one for each component and one for the mixture (Krause, 1965a).

The tacticity of the polymer molecule also affects the glass transition temperature. The value of T_g for isotactic PMMA ($-COOCH_3$ groups all "on one side") is 159°C, whereas that for the syndiotactic form (the group alternating "from side to side") is 30°C. An equal mixture of the two forms has a T_g of 94°C (Krause, 1965b). Figure (2.2) shows diagrammatically the difference between isotactic, syndiotactic and atactic polymers.

Multiple glass transitions in cellulose 2-5 acetate have been reported by Daane (1964), each one being ascribed to a specific rotation of portions of these complex molecules. The glass transition can therefore be linked quite specifically with molecular motion, the motion of the

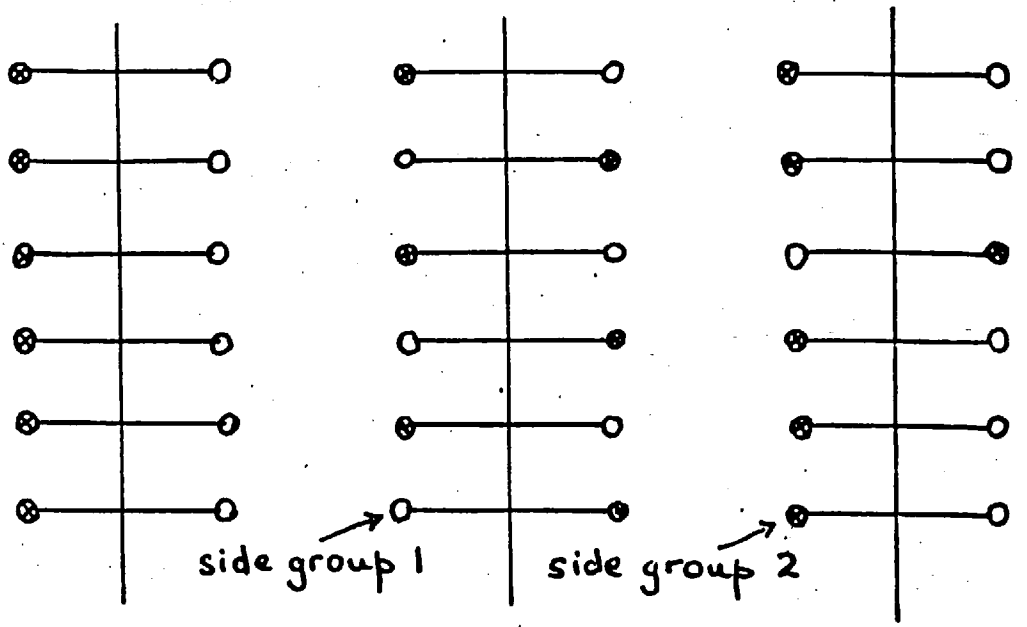

ISOTACTIC SYNDIOTACTIC ATACTIC
(random)

FIGURE (2.2) Diagrammatic representation of stereoregularity in polymers.

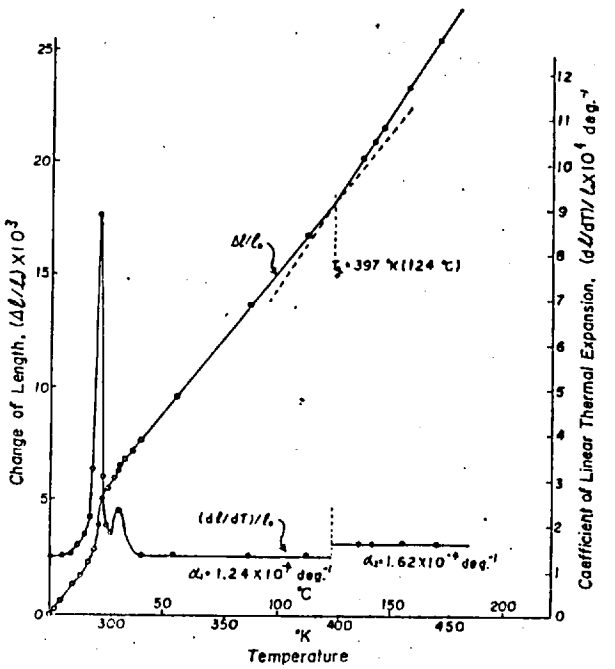

FIGURE (2.3) Linear thermal expansion coefficient of poly(tetrafluoroethylene) as a function of temperature, after Araki, (1965).

main backbone chain of the polymer being that which is "frozen out" as the temperature is reduced to T_g. Other transitions have been reported on a transition in polystyrene which is observed at 50°C. This is the β-transition, so called because it is the next lowest in temperature below that of the α-transition (glass). Still lower temperature transitions are signified by the appropriate Greek letter taken in sequence. The β-transition in polystyrene is ascribed to a "freezing out" of the motion of the phenyl group. PMMA shows a β-transition (Heijboer's article in Prins, 1965) at 25°C, due to the stopping of the motion of $-COOCH_3$ groups around the C-C link, though in most of these secondary transitions, there is some evidence for interference by the backbone chain.

Monaglio (1963) and Wunderlich (1964) have both reported

(c) Observation of the glass transition

The investigation of any property of the glass which influences or is influenced by molecular mobility will demonstrate the glass transition. Boyer and Spencer (1946) have reviewed the experimental field, though since this time much more data has accrued, particularly in the field of nuclear magnetic resonance. The easiest method of observation of the glass transition is by noting how the volume of the sample changes with temperature within the appropriate range. Other

methods include observation of the elastic moduli, internal friction and viscosity, such thermodynamic functions as thermal conductivity and specific heat, nuclear magnetic resonance measurements such as second moment and spin-lattice relaxation time of the proton, dielectric constant, refractive index measurements and X-ray pattern measurements, all as a function of temperature or pressure.

(i) Thermodynamic functions

Pasquino (1964) has shown that a change in slope of the thermal conductivity of polystyrene exists at a temperature which was found by dilatometer studies to be the glass transition temperature. Wunderlich (1964) has used a differential thermal analysis technique* to show both the α- and the β-transitions in this polymer.

---

* In conventional differential thermal analysis, the temperatu of the outer surfaces of blocks of identical shapes, one of the substance under investigation and the other of a material of known thermal properties (the reference block) is raised at a constant rate and the temperature difference between the centres of the two blocks observed. At steady state, the difference will be constant, but whenever the temperature passes through some point of thermal transition, the extra amount of heat absorbed tends to retard the rate of temperatur rise of the specimen under test. Thus a transition point presents a pattern of irregularity in the temperature difference. In Wunderlich's experiments, the specific heat of the polymer is approximately equal to the temperature difference between the sample and the reference block. Smothers (1958) reviews in detail the manifold uses of D.T.A. techniques.

Allen (1961) has measured P_i, the internal pressure, of samples of polyvinyl acetate and PMMA around T_g. P_i was calculated from $P_i = \frac{\partial U}{\partial V} \sim \frac{T\alpha_o}{K}$ where α_o and K are the coefficients of thermal expansion and isothermal compressibility respectively, and U is the internal energy. These authors observe a decrease in P_i at T_g and explain the effect in terms of a relative lack of molecular mobility in the glassy state. Araki (1965) has shown that a discontinuity on the linear thermal expansion coefficient versus temperature plot for poly (tetra-fluoroethylene) at about $400^{\circ}K$ is a glass transition in the amorphous regions of this otherwise crystalline polymer, see Figure (2.3).

(ii) Dielectric constant measurements

The behaviour of the dielectric constant of poly (oxy-methylene) has been investigated by Read (1961) who shows that a broad relaxation peak exists at - $85^{\circ}C$, a temperature at which the behaviour of dynamic mechanical properties also implies a relaxation process. O'Reilly (1962) has investigated the effect of pressure on the dielectric relaxation in polyvinyl acetate, showing that it occurs at higher temperatures when the sample is subjected to pressure.

(iii) Dynamic mechanical properties

Possibly the most complete experimental work done in this

field is that of Wada, Hirose and Asano (1959). They showed that the real part of the shear modulus, the bulk modulus, and the Young's modulus for polystyrene, PMMA and polyvinyl acetate show changes in the dependency on temperature at values of T_g, these being detected by dilatometer measurements. The loss tangents in both the shear mode and the Young's modulus mode have maxima (the α-transition), at some temperature T_d which is sometimes called the dynamic glass transition temperature. The value of T_g is slightly lower than that of T_d, and is explained by the authors as due to the difference between the onset of mobility and its maximum value. Lewis (1963) made an empirical analysis of the variation of T_d as a function of frequency of measurement and Heijboer (Prins, 1964) followed up by estimating that there is a $3^{\circ}C$ increase in T_d for each decade rise in frequency.

The application of pressure on samples at temperatures above T_g can bring about the glass transition (Paterson, 1964; Matsuoka, 1958). Working on polyisobutylene, Singh and Nolle (1959) have shown that the glass transition temperature as observed in the behaviour of Young's modulus is increased by $0.025^{\circ}C$ per atmosphere rise in pressure, which value is supported by the work of McKinney (1960).

(iv) Nuclear magnetic resonance methods

Both the spin-lattice relaxation time T_1 and the second moment of the broad line resonance ΔH_2^2, are dependent upon the mobility of the protons in the polymer molecule; see Appendix 4 for definitions of these parameters. Powles (1956) has shown steps in the graph of second moment vs. temperature for PMMA at 150°K and 400°K, but not at the 25°C transition as reported by other workers. The constant value of the second moment between these two temperatures has been calculated as arising from the motion of one half of the $-CH_3$ groups, either those in the $-COOCH_3$ or those existing independently as side groups, but Powles has not been able to differeniate between them. The transition at 150°K occurs when one half of the $-CH_3$ ceases rotating, which is consistent with the idea that the 25°C transition is the $-COOCH_3$ group transition. The decrease in second moment and T_1 both occur at the temperature T_d observed in shear for both polystyrene and PMMA (Powles, 1962, 1964) and he has observed the different values of T_g for isotactic and syndiotactic PMMA (1963).

For reasons that are not yet apparent, however, transitions observed by one method are not always observed by another, oneexample of this being given above. Crissman

(1965) has detected in polystyrene a transition at 38°K (5.6c/s) or 48°K (6kc/s), thus supporting Heijboer's value of shift in T_d with frequency. He has attributed the effect as due to the "wagging" (small amplitude oscillation) of the phenyl group. He was unable to observe this transition in broad line n.m.r. experiments, however.

(v) Dilatometer measurements

The observation of the volume of a sample as a function of temperature change over the appropriate range is the easiest method of observing the glass transition, and the temperature at which the slope of the curve changes is that temperature which is usually referred to as the glass transition temperature (Kovacs, 1964). Most authors reporting on these experiments quote Bekkedahl (1949) for the basis of the technique. Kovacs (1964) is the most prolific reporter of dilatometer studies.

(vi) Optical properties

Boyer and Spencer (1946) quote the findings of McPherson and Cummings (1935) which show that a rubber containing 19 per cent sulphur shows a change in refractive index at a given temperature, but point out that this temperature is a lower one than that observed for a similar type of relaxation in the thermal expansion coefficient noted by others in the same

material. It is suggested that the refractive index change anticipates that of the thermal expansion transition because of the slight change in the polarisability of the electrons brought about by decreasing force fields associated with neighbouring molecules. As described earlier in this section, the onset of the transition as observed will depend upon the effect of temperature on the particular aspect of the motion of the molecules which is being observed.

(vii) X-ray diffraction patterns

Krim and Tobolsky (1951) have obtained X-ray diffraction patterns for both polystyrene and PMMA. Being amorphous, these materials present very simple patterns consisting of two rings which have uniform intensity. The inner ring is associated with intermolecular interference in the form of interaction between carbon atoms of adjacent rings. The outer ring (less intense than the inner one) is thought to be associated with phenyl-phenyl group interactions of a single polymer chain - an intramolecular effect. Krim and Tobolsky have noted that the ratio of the intensities of the second (outer) to the first ring is constant below 80°C and above 170°C, but that between these two temperatures, this ratio diminishes at a constant rate from the low temperature constant value to the high temperature constant value. This effect is most

marked for polystyrene, and less marked for PMMA. The authors offer the explanation that this is due to increasing numbers of intermolecular interactions, as the decrease in the ratio described above results from an increase in the intensity of the inner ring rather than a decrease in intensity of the outer one. Thus the implication is that phenyl group interactions are little affected by temperature, whilst those of the main chain are governed by the temperature.

(d) Rate dependence of T_g

One of the first facts which becomes obvious to the experimenter observing the glass transition is that the glass transition temperature is dependent upon the rate of temperature change. Krause (1965a) has obtained values of T_g for polystyrene as different as 97°C and 89°C for rates of temperature change of 1°C per minute and of some hours (total time one week) respectively, and in pressure experiments, Paterson (1964) has shown that the hysteresis observed in the change of Young's modulus at the glass transition is dependent upon the rate of pressure application and release.

Kovacs (1964, page 409) describes this time dependency very well. He considers a sample above its glass transition reacting to a change in temperature from T_o to T_f, $T_o > T_g > T_f$. Above T_g, the rate of cooling of the sample

is slower than the rate at which the molecular segments can adjust thermodynamically to the new (lower) temperature as time increases. At any temperature between T_o and another temperature T_θ, $T_o > T_\theta > T_g$, the state of the molecular configuration is defined by the temperature and pressure of the environment of the sample. At a time t_e when the temperature T_e is arrived at, the rate of cooling of the sample and the rate at which the configuration is adjusted to temperature change can be considered to be the same. After this point, (T_e, t_e), the molecular configuration is no longer in phase with the temperature of the sample. At the end of the cooling process when temperature T_f is reached, the molecular configuration is not defined by T_f but by some "fictive" temperature, T^*_e (first used by Tool, 1931) which lies between T_e and T_f. T^*_e is not a measurable quantity but serves only the purpose of theoretical analysis.

As can be seen, the fictive temperature will depend on the rate of cooling of the sample, and as some relationship must exist between T^*_e and the onset of the glass transition, T_g must also be rate dependent. Indeed, so dependent is the value of T_g on the rate and direction of the temperature change that some authors (e.g. Wunderlich, (1964)) prefer to refer to a glass transition <u>range</u> or <u>interval</u>.

(e) Free volume

From the description of the rate dependence of the molecular configuration, it follows that below the glass transition temperature an amorphous polymer will have a density which will in part be rate dependent, since the molecular configuration arising from a slow cooling through T_g will occupy a smaller volume than that resulting from a more rapid one. Free volume has been defined in different ways as reviewed by Kovacs (1964, page 484) and Haward (1966) but the latter has shown that in many cases these are equivalent. These definitions consist of two groups, the first being for theoretical purposes and invoking such concepts as volume of the molecule at $0^{o}K$, i.e. the "actual" space taken up by the molecule, and the volume resulting from inter-molecular action due to van der Waals' forces. For experimental purposes, Kovacs defines free volume as $v - v_{\infty}$, where v is the instantaneous total volume and v_{∞} is the total volume after an infinite time. A fractional free volume is defined as $(v - v_{\infty})/v_{\infty}$.

Saito (1963) has calculated the effect on free volume of the rate of cooling through T_g. For a change in cooling rate from $10^{-3}{}^{o}C$/sec. ($0.36^{o}C$/hour) to $10^{-5}{}^{o}C$/sec., the change in fractional free volume at temperatures well below T_g would be from 0.022 to 0.020.

Saito calculated these values from a phenomenological theory whose starting point is the equation

$$\delta T = (1/a_F).\ \delta f + (\tau/a_F).\ \frac{d.(\delta F)}{dt} \qquad (2.1)$$

where $\delta T = T - T_o$ and $\delta F = F - \bar{F}_o$, T_o and $\bar{F}_o$ defining the equilibrium state of the glass. It is to be noted that this equation can be compared with that governing the behaviour of a Voigt solid (spring of elastic constant $1/a_F$ and dashpot of viscosity (τ/a_F) connected in parallel) subjected to the stress $(T - T_o)$. The retardation time τ is defined as

$$\tau = \tau_o . \exp(1/F) \qquad (2.2)$$

following Doolittle's (1951) theory of liquid viscosity.

The temperature dependence of the equilibrium value of free volume defines a_F according to

$$\bar{F} = \bar{F}_o + a_F(T - T_o) \qquad (2.3)$$

whereupon the equation used by Saito to calculate the values above is derived as

$$\frac{dF}{d\bar{F}} = - \frac{F - \bar{F}}{a_F.R.\ \tau_o .\exp(1/F)} \qquad (2.4)$$

where R is the rate of cooling, and the values of τ_o and a_F are set at 10^{-13} sec. and $(4.8) \times 10^{-4}$/deg.C respectively.

Saito's theory is only one such theory that attempts to produce the observed free volume dependence on temperature,

most of which are based on some two state concept of the transition. Kovacs (1964) has produced much experimental data in this field and has reviewed the applicability of the theories to this data.

Kovacs' mode of attack, both experimentally and theoretically, is to note and consider the reaction of samples to a sudden change in temperature; the samples are small so that temperature equilibrium is reached very shortly after the temperature change, though the volume continues to relax for some time after depending upon the temperature jump, the thermal history of the sample and the closeness of the equilibrium temperature to T_g.

One of the experimental facts which any theory must account for is the non-linear and asymmetric behaviour of the approach to equilibrium of the volume of the sample when approaching it by dilatation (a positive temperature jump), as opposed to its behaviour on contraction (a negative temperature jump). The non-linearity is observed in that a change in volume by contraction requires a smaller temperature jump than does the same change by dilatation. A more difficult effect to express theoretically is the "autocatalytic" behaviour in dilatation. Unless

the amplitude of the temperature jump is great enough, the relaxation of volume will not be of the same form as in contraction. The volume dilatation takes place as if a certain amplitude of temperature change is required to break up the molecular configuration, after which the process of rearrangement can take place. Kovacs (1961b) has shown that a simple relaxing solid model (see Appendix 1) exhibits this autocatalytic behaviour.

Kovacs concludes that all the theories are incorrect in that they assume that a single relaxation time dependent upon temperature controls the approach to equilibrium of the volume. Although some success has been achieved by the theories, Kovacs concludes that τ should be replaced by a distribution of such relaxation times, each component of which being dependent not only on temperature but also on free volume. For polyvinyl acetate, he claims that the deviations from theory are best explained by the different dependence of each component on some distribution with temperature, whereas for glucose, he has had considerable success in fitting a narrow rectangular distribution of relaxation times (all similarly dependent upon free volume and temperature) to the experimental data.

(f) Behaviour of a polymer below its glass transition temperature

It is not the purpose of the present work to investigate the behaviour of amorphous materials above their glass transition. Many authors (e.g. Alfrey, 1948; Treloar, 1958; Ferry, 1961) have covered this field, and the theoretical work is both detailed and broad and is supported by much experimental evidence.

Below the glass transition, comparatively little theoretical work has been done except on the singularities in behaviour which are due to relaxation processes, more or less well-understood as the onset of motion of specific groups of molecules - the α-, β- , γ- etc. transitions (Ferry, 1961, Chapter 14). For polystyrene, the α- , β- and γ- transitions occur at 100°C, 50°C and (about) 40°K and are accounted for by main chain mobility (the glass transition), by rotation of the phenyl groups, and by "wagging" of the phenyl groups, respectively. For PMMA, they occur at 120°C, 25°C and 150°K and seem to be due to main chain mobility (the glass transition), to motion of the $-COOCH_3$ group and to motion of the $-CH_3$ group, respectively.

The theories of molecular mobility away from these

transition regions (Parfitt, 1956; Turnbull, 1961; Ellerstein, 1963) are based on the "hindered rotation" concept, and have been used to analyse the phenomenon of an internal friction more or less independent of frequency at frequencies away from the transitions. This frequency independent background level of damping has been noted by many authors, a review of whose work appears in Parfitt's thesis (1954). More recently Benbow and Wood (1958), and Ferry (1961, Chapter 14), have restated the fact, the former noting that the level of damping can be correlated with the estimated degree of flexibility of the molecules involved.

Parfitt (1954, 1956) has shown that the internal friction of samples of polystyrene below T_g is dependent in part upon the amount of free volume trapped in the sample by different annealing techniques. Melchore and Mark (1953) have shown that the heat distortion temperature of polymers can be increased by a slower cooling of the samples through T_g. McLoughlin and Tobolsky (1951) working with polyvinyl acetate, have shown that a more rapid relaxation of stress takes place in those samples which had been more rapidly cooled through T_g. Kovacs, Stratton and Ferry (1963) working above T_g, have shown that types of relaxation associated with volume, internal friction and shear

modulus changes were equivalent for a sample of polyvinyl acetate as it responded to an abrupt temperature change.

(g) Hindered rotation theories of molecular mobility

Rubber-like elasticity is generally typical of a relaxation or retardation process, characterised by a relaxation time, τ , as described in Appendix 1. Although there may be relaxation processes which can be expressed in terms of one relaxation time, even the secondary transitions which occur in polymers (and which are generally explained in terms of very specific rotations of particular side groups) are found to be governed by a distribution of relaxation times (Ferry, 1961, Chapter 14) and the background level of damping upon which these transitions can be considered to be superimposed can only be explained mathematically in terms of relaxation times given by the function G(t) where t is time and which generally is finite for all values of t.

The ratio of the complex strain amplitude to the complex stress amplitude, called the complex compliance and denoted by J^*, has been shown by Alfrey (1948) to be such that the loss term, J", is given by

$$J''(\omega) = \int_0^\infty \frac{G(t).dt}{1 + \omega^2 t^2} \qquad (2.5) .$$

and the main theoretical problem is then to derive the distribution G(t) from the structure of the polymer.

Very little of this kind of analysis has been undertaken. Parfitt (1956) has considered a very specific rotation of sections of the backbone chain of the polymer. The rotation of these segments can be idealised as subject to two constraints in the form of potential energy wells, the first defines the free rotation of the segment and the second describes the hindrance to this free rotation arising from the presence of the other molecules. Parfitt arbitrarily defined the former well as being sinusoidal and the "hole" potential well as being rectangular. Turnbull and Cohen (1961) considered the possibility of the first well as being Lennard-Jones in shape and Ellerstein (1963) defined both as sinusoidal.

Only Parfitt has tested the validity of his assmptions by applying experimental data to his findings. By a suitable choice of theoretical constants, Parfitt is able to reproduce from his theory the frequency dependence of the damping coefficient that was observed experimentally. The increase in damping that this theory gives suggests that the fractional free volume in the material at T_g is of the order of 0.4 per cent whereas Kovacs quotes a

value, obtained experimentally, of about 2.5 per cent. However, the amount by which Parfitt could change the free volume in the glassy state using different annealing processes was only 0.15%, an amount much less than that deduced from Saito's theory, see section (2.e).

(h) Factors affecting damping in glass-like polymers

The previous section showed that the rate of cooling of the polymer through its glass transition affects the free volume and hence the damping occurring in the material. What might be called "artificial" methods of altering the level of damping also exist, for example, by cross-linking (produced either chemically or by irradiation), or by the addition of plasticisers and, possibly, of fillers. The effect of these changes of molecular environment of the specimen are considerable at temperatures above T_g, although below this temperature the effect is slight, showing principally in the changes in the moduli of the material and hardly at all in the damping, except in the position and width of the secondary transitions. Ferry (1961) reports the effects of these changes, particularly above T_g. Little experimental work has been done below T_g.

Charlesby and Hancock (1953) have shown that Young's modulus increases with increasing cross-linking at temperatures below the glass transition temperature. Rady (1957) has shown that the β-transition peak in the damping of polyethylene which has been cross-linked in varying degrees by irradiation shifts to higher and higher frequencies as the irradiation dose (and hence cross-linking) increases, and the peak disappears altogether for very high doses. It is considered that the β-transition in this polymer is due to the amorphous side chains which can exhibit motion below T_g except when the backbone chains are highly cross-linked. Rady has some data on the effect of cross-linking on the damping coefficient. Up to doses of about 8 units*, there seems to be no effect on the damping. Above this dosage, however, the damping suddenly increases and then diminishes at which stage the material becomes very brittle; this occurs when the cross-linking is very

---

* Rady defines one unit as being equivalent to 10^{17} slow neutrons/cm^2 plus the associated fast neutrons and gamma irradiation for the polyethylene samples. These last two components are considered to be proportional to the slow neutron flux density. Thus, Rady defines

1 unit = (40 - 50) x 10^6 rontgen = (2.2 - 2.7)x 10^{21} ev/gm

high. It should be pointed out that polyethylene is not normally considered to be a glass at these frequencies and temperatures and it is only the effect of cross-linking that produces these glass-like properties for the material. The heavily cross-linked, brittle material, produced by irradiating with a dosage of 149 units does not exhibit the glass transition as normally given by more lightly cross-linked polyethylene. For this material the characteristic change in the specific volume versus temperature plot was observed by Rady although no existence of a glass transition was observed for the brittle material.

The addition of plasticisers reduces the "brittleness" of the material, and lowers the glass transition temperature. Plasticisers can be looked upon as lubricating the motion of the molecules and are generally of a much lower molecular weight than the polymer to which they are added. The effect of such diluents is to depress sharply the value of T_g, linearly at first according to $T_g = T_g^o - k_2 w$, where w is the weight fraction of the diluent, T_g^o is the glass transition temperature of the pure polymer, and k_2 is a constant ranging between 200°C and 500°C for polystyrene, see Ferry (1961) and Jenckel (1953). This decrease in T_g is

ascribed to the creation by the diluent of more free volume in the material, though Yamamoto and Wada (1957) have shown that addition of about $\frac{1}{4}$ per cent of water to a methacrylate polymer resulted in a shift in the β-transition to higher temperatures, implying a "filling up" of the free volume by the water. Illers and Jenckel (1958) have investigated lightly cross-linked polystyrene swollen with diethyl phthalate for which the β-transition shifts to lower temperature, whereas the γ-transition shifts to a higher one, as the proportion of the diluent increases. Heijboer (1956) has shown that PMMA plasticised with dibutyl phthalate has a β-transition which has shifted to a temperature lower than that of the pure material and that the amplitude of the peak has increased by about 50-100 per cent as the plasticiser content increases, which implies an increase in the number of groups participating in the transition signified by this peak.

Table (2.1) shows the effect of these diluents on the positions of the secondary transitions. It is obvious that the behaviour of plasticisers is not a simple one.

TABLE (2.1)

The effect of diluents on the positions of secondary transitions in polystyrene (PS) and polymethyl methacrylate (PMMA)

DILUENT	TRANSITION		REPORTER
	β	γ	
dibutyl phthalate in PMMA	shifts to lower temperature	-	Heijboer (1956)
¼% water in PMMA	shifts to higher temperature	-	Yamamoto (1957)
diethyl phthalate in cross-linked PS	shifts to lower temperature	shifts to higher temperature	Illers (1957)

Fillers such as woodflour and the various forms of carbon have a large effect on the properties of polymers above their glass transition, an increase in such properties as abrasion resistance and in the moduli being the general result. Very little seems to be available on the effect of fillers at temperatures below T_g, however.

(i) Present investigation

It has been shown that the free volume of a glass is dependent upon the rate of cooling of the sample through its glass transition and that increased free volume implies increased internal friction.

Whilst some authors have investigated the effect of rate of cooling through T_g on the free volume and damping in the material, there seems to be little published data on the combined effect of pressure and temperature on the free volume of polymers below their glass transition.

It was decided therefore to investigate this field using polystyrene (PS) and polymethyl methacrylate (PMMA), these materials being the most commonly used polymer glasses and of a sufficiently low internal friction to make for easy investigation by the method employed.

As described in Chapter 1, some doubt exists as to the validity of the values of damping factor as previously derived from the Q values of rods in longitudinal mode resonance, and so the effect of rod dimensions on the damping factor has been investigated.

CHAPTER 3

THE EXPERIMENTAL SYSTEM

(a) The experimental method

The method employed to excite the cylinders into the longitudinal mode is the electrostatic method of Ide (1935) and of Bancroft and Jacobs (1938). Excitation is provided by the electrostatic force between one flat face of the cylinder (rendered conducting if necessary) and a parallel electrode placed a small distance away, when an alternating potential is applied between them. The same system is used for the measuring of the relative displacement of the other end face of the rod, the physical basis of the driving principle being used in reverse. The sensitivity of this system of excitation and detection has been considered by Parfitt (1954) who showed that maximum tensile strains of the order of 10^{-6} are produced in a material like polystyrene; the present system can detect displacements of the order of 10^{-8} cm which is equivalent to a smallest detectable strain of the order of 10^{-9}.

The frequency of the resonances and the 3 db points on the resonance curve are measured directly either by a Hewlett-Packard frequency counter or a Schomandl frequency

synthesiser. The former gives an accuracy of measurement of the order of 1 c/s over all ranges, the latter (being tunable to the Droitwich standard) an accuracy approaching 0.2 c/s. The damping coefficient (or damping factor) of the Young's modulus mode, given by δ_E in the equation $E^* = E'(1 + j\delta_E)$, see Appendix 1, is obtained directly from a measurement of the quality factor, Q

$$\delta_E = 1/Q \qquad (3.1)$$

Parfitt (1954) has shown that this definition of damping factor is applicable to the simple resonance theory of cylinders. A detailed discussion of measuring both E' and δ_E is given by Parfitt, and Edmonds (1961) has investigated theoretically the more exact relationship between δ_E and Q_E, see section (1.g) and Appendix 2. By measuring the Q values of the range of detectable harmonics, the frequency dependence of δ_E can be obtained. The value of Young's modulus is given by the dimensions of the cylinder under test and the resonant frequencies, from the relationship

$$f_n \cdot c_n/n = \frac{1}{2l} \cdot \left\{ \frac{E'}{\rho} \right\}^{\frac{1}{2}} \qquad (3.2)$$

where f_n is the frequency of the n^{th} resonance, l is the length of the rod, ρ is the density of the material of the rod, and c_n is the correction for velocity dispersion due to

the finite diameter of the rod.

(b) Experimental system

Figure (3.1a) shows a diagrammatic view of the experimental system which is more completely reported by Parfitt (1954). Figure (3.1b) is a photograph of the apparatus. Details of the electronic circuits are given in Appendix 5.

The oscillator whose circuit diagram is shown in Figures (A5.1a) and (A5.1b) is of a basic RC design but incorporates two fractional detuners which are constant at all frequencies. The rectified detected signal is displayed on a d.c. milliammeter from which the 3 db drop in amplitude of the signal is observed when the oscillator frequency is adjusted by one of these fractional detuners. The detection amplifier (see Appendix 5) may be tuned over the required frequency range whenever background noise becomes great. When the tuned amplifier is employed, the Q has to be modified according to the relation

$$Q_t/Q_m = 1 + (Q_m/Q_a)^2 \qquad (3.3)$$

where Q_t is the true Q factor of the rod,

Q_m is its measured Q, and

Q_a is the Q of the tuned circuit of the amplifier.

This equation only holds when $(Q_m/Q_a)^2$ is fairly small, which is the case for all materials used in this investigation.

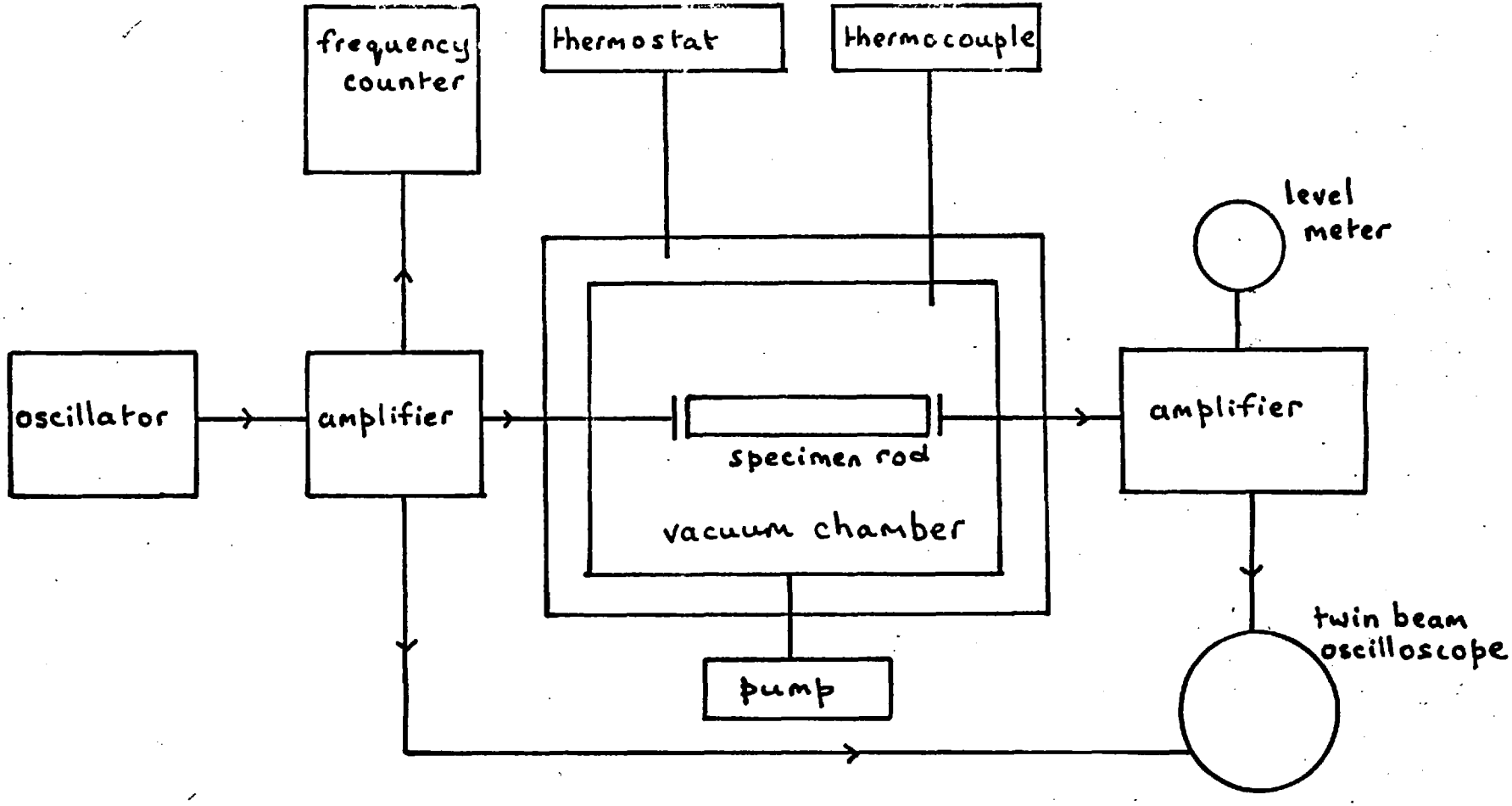

FIGURE (3.1a) DIAGRAMMATIC VIEW OF THE APPARATUS

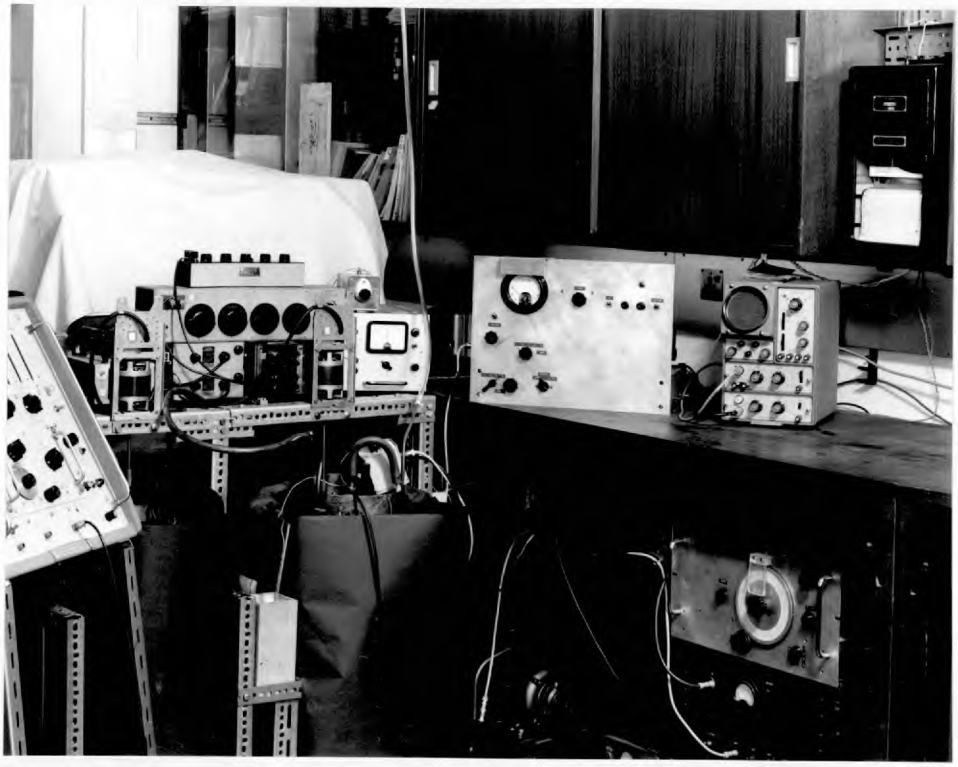

FIG.(3.1b) General view of the apparatus.

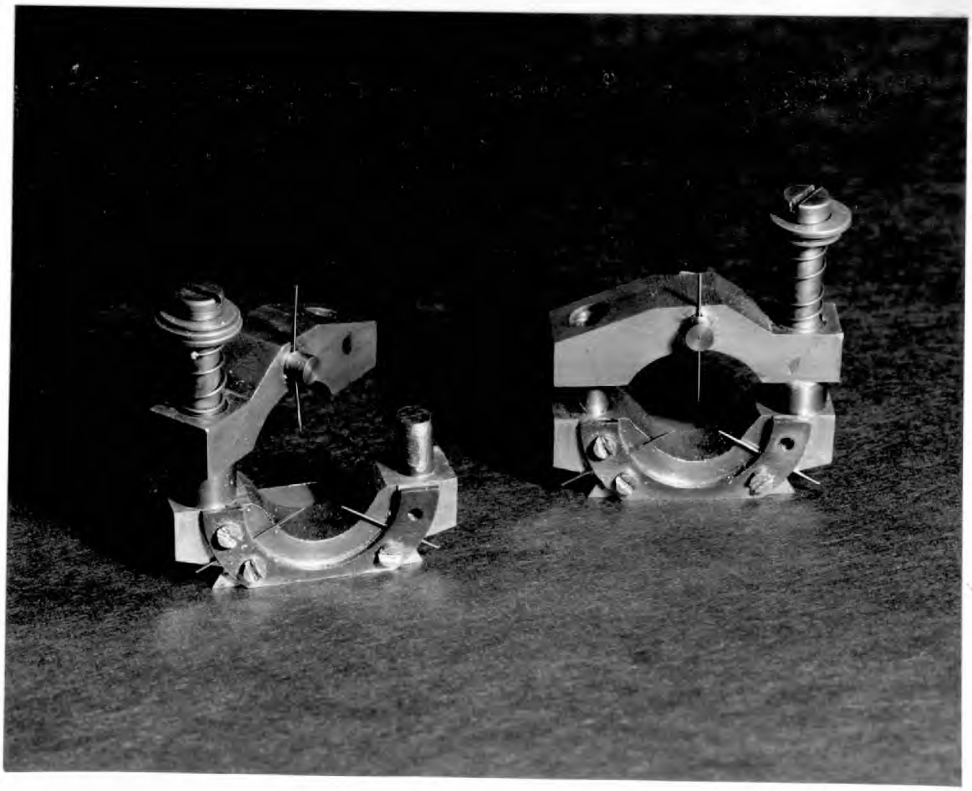

FIG.(3.2) The pin support system.

A twin beam oscilloscope monitors both the drive and the detected potentials and ensures that the peak-to-peak value of the drive voltage is constant. Observation of these potentials also tells the experimenter when the rod is driven into resonance at harmonics of the drive frequency.

(c) Method of supporting the cylinder under test

The rod is firmly but lightly clamped in position by means of one or two of the support systems shown in Figure (3.2). The principle of a variable length for the pins, one of which is spring mounted is not original, though the particular design shown in Figure (3.2) is new. Parfitt (1954) concluded that this system of support has least effect on the resonances of the rod under test. He has shown experimentally that the values of Q of the resonances decrease when the rod is tightly clamped at the positions of the anti-nodes of the standing wave pattern set up in the rod; this can be largely avoided by lightly clamping the rod. However, a decrease in Q can arise if the resonance anti-nodal positions do not coincide with the pin supports. Generally, more of these "randomly" decreased Q values occur if the rod is supported by more than one set of pins, and the existence of possible complex couplings was suggested by Parfitt. The question of the effect of the supports on the

measurements made in the present work will be discussed in Chapter 4.

(d) Method of driving the rod into resonance

(i) Normal condenser microphone technique.

For rods made of non-conducting material, the end faces of the rod are coated with a conducting material like "Aquadag" (a water based suspension of graphite) to which electrical contact is made by means of a fine wire attached with "Durofix". The separation between the rod end-face and the earthed brass plate of the condenser microphone was adjustable by use of the control rods shown in Figure (3.3); the phosphor bronze bellows act not only as vacuum seals but also as springs. The control head shown in Figure (3.3) was developed by Rady (1957) from Farfitt's original design (1954), except for the air inlet pipe whose purpose will be described later. Tufnol joints in the control and support rods of the chassis and expanded polystyrene baffles placed between the control head and the sample under test help to maintain temperature stability. Figure (3.4) shows a polystyrene specimen in position.

For materials which are conducting, the rod is earthed through the pin supports, and the brass plates

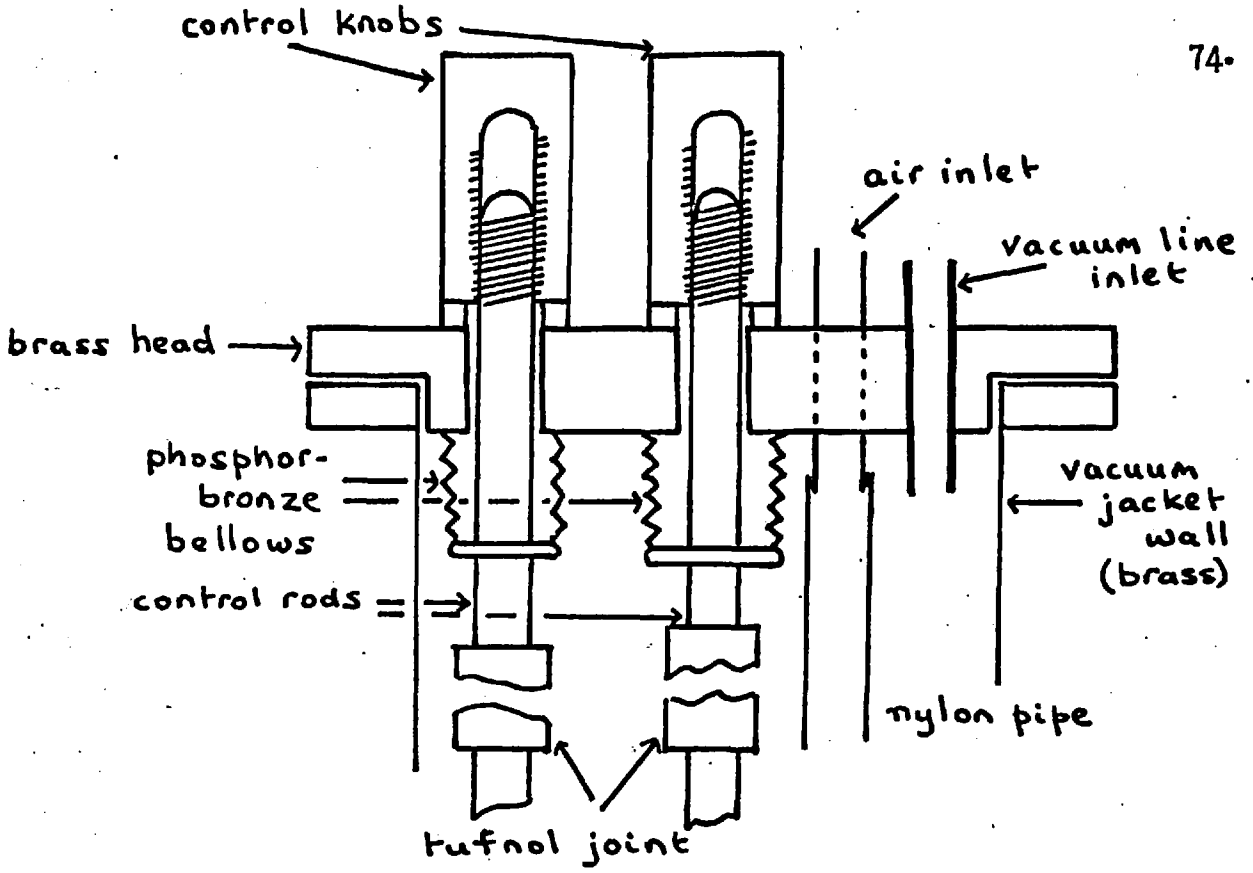

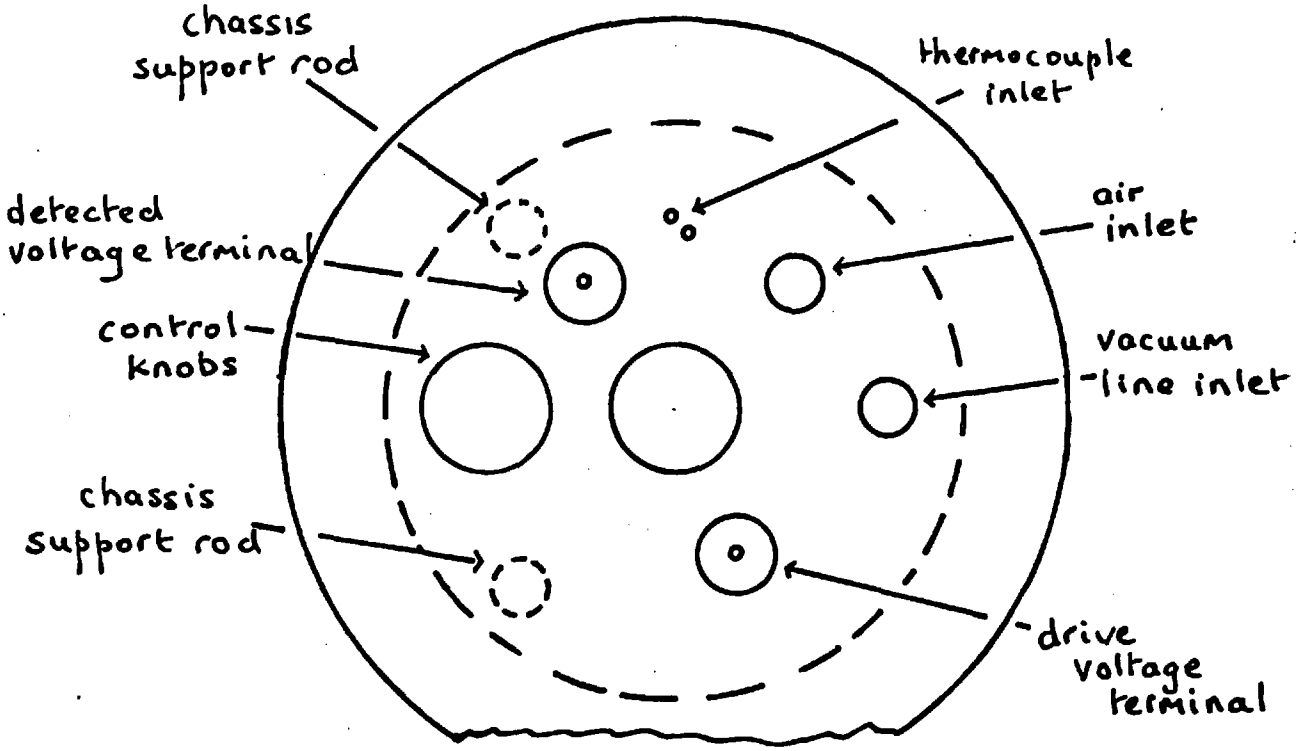

FIGURE (3.3) CONTROL HEAD OF THE VACUUM CHAMBER

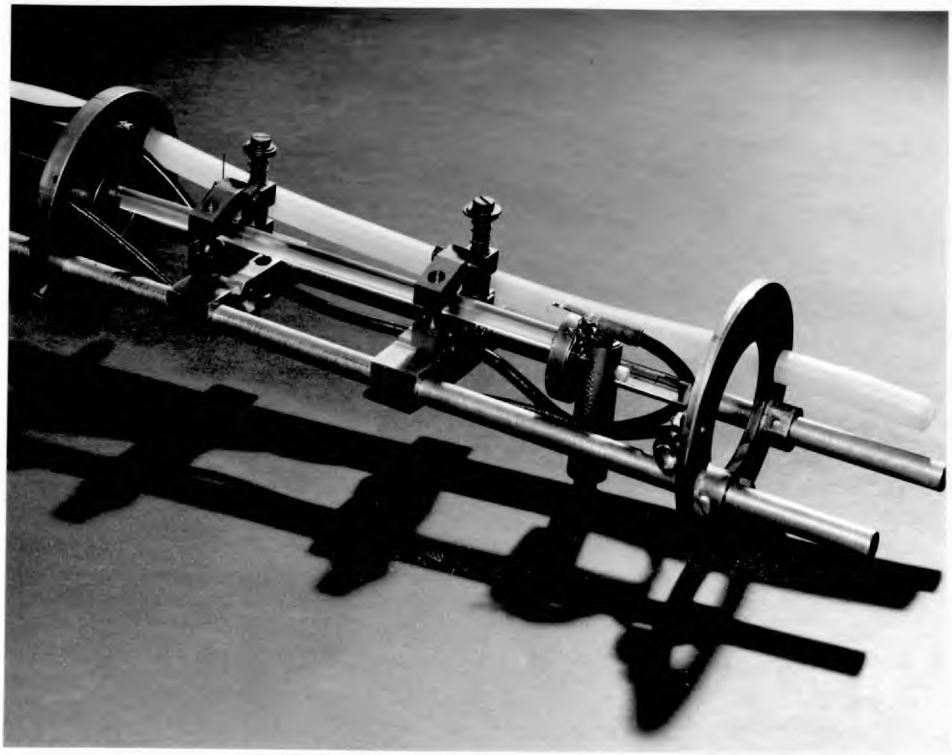

FIG.(3.4) Polystyrene rod held in position in the condenser microphone system.

are now insulated from the chassis and become the high potential electrodes of the condenser microphone system. An advantage of this method of exciting metal rods into resonance is that the only loading on the rod is that arising from the pin supports.

(ii) Excitation of shear mode resonances.

Cylinders of high Q materials can be excited into shear mode resonances by means of a coil which is wound on the end of the specimen cylinder as shown in Figure (3.5). When placed in a magnetic field as shown, application of a polarising voltage and an oscillatory potential of the appropriate frequency will exert a torque sufficient to drive the cylinder into shear mode resonance. Detection of the resonance is by means of a similar coil at the other end of the cylinder.

(iii) Electrostrictive technique.

Figure (3.6) is a photograph of an aluminium rod, r, placed in an alternative drive and detection system which has been shown by the author (by trial and error) to work only for low-loss, low density specimens. In this method the specimen is inserted between diaphragms of "Meculon" which is a polymer film of thickness 0.001" and coated on one side with an aluminium film a few angstroms thick.

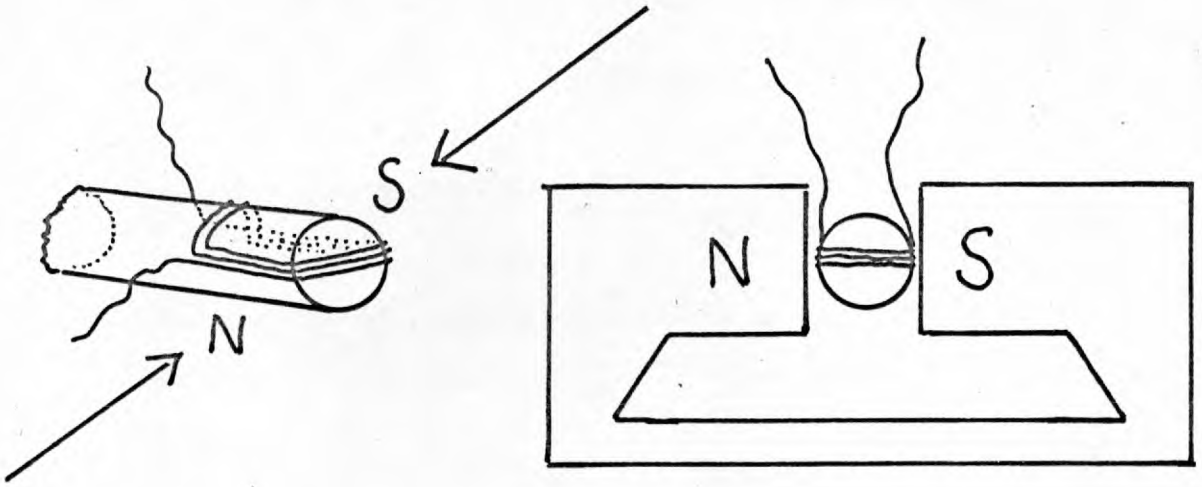

FIGURE (3.5) METHOD OF EXCITATION OF SHEAR MODE RESONANCES

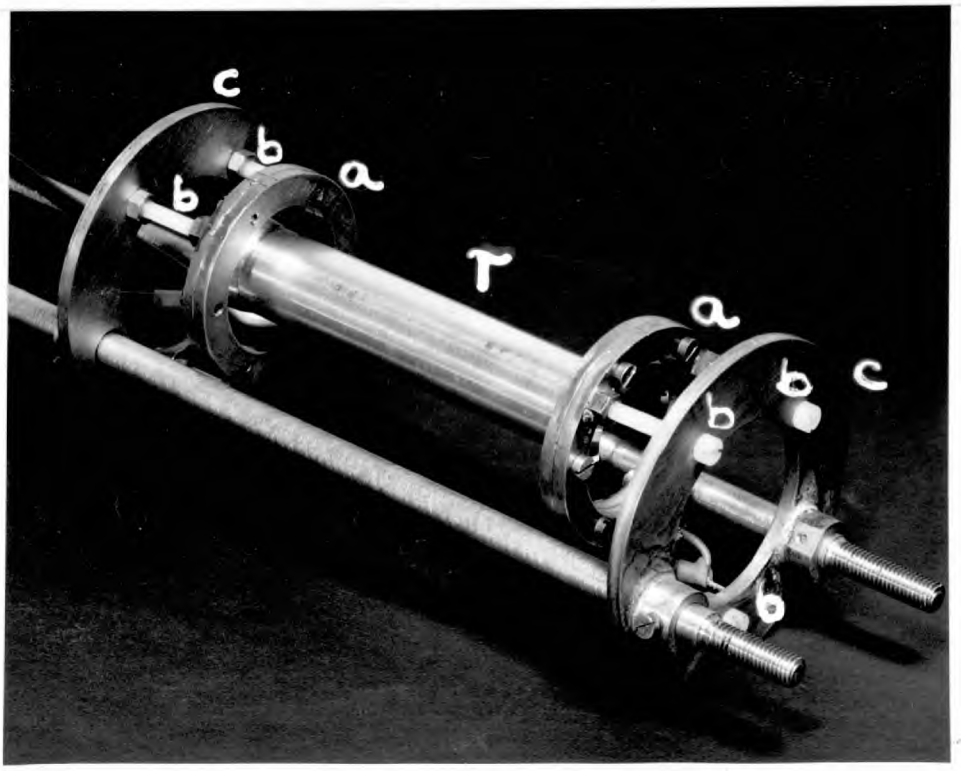

FIGURE (3.6) ALUMINIUM CYLINDER IN DIAPHRAGM SYSTEM.

In Figure (3.6) the rod is kept in the horizontal position by driving it into each diaphragm. For the vertical position of the rod, as is the case in all investigations carried out, the rod merely rests on the bottom (drive) diaphragm, and the top diaphragm is brought lightly down on to the other end. The non-metallised surface of the diaphragm is in contact with the ends of the rod. The rod is earthed by means of a fine wire and the driving and polarising e.m.f.s. are applied between the metallised surfaces and the rod. If the rod is non-conducting, its end faces are coated with "Aquadag".

The diaphragm is held by the two $1\frac{1}{4}$" diameter brass rings (a) and these are fastened to supports (c) by nylon bolts (b). The supports can slide along the chassis to take rods of various lengths. The method of making the diaphragm is as follows. Figure (3.7a) shows the rings (a) which together form the support of the diaphragm shown in Figure (3.6) separated prior to making the diaphragm from an initial diaphragm as formed between the two 4" diameter rings and which is also shown in Figure (3.7). This latter diaphragm does not have to be under a particularly great tension. Nuts (d) are used to fix the diaphragm support (a) to the supports (c) by nylon bolts (b). Figure (3.7b) shows how the final diaphragm is made from the initial one.

FIG.(3.7a)

FIG.(3.7b) Method of making diaphragms.

The first ring which forms this final diaphragm, and which cannot be seen, is placed on a platform; the diaphragm is placed on top of it and the second ring of the diaphragm is placed on top of this. By breathing on the "Meculon" the positions of the bolt holes in the ring underneath can be clearly seen. The tension in the final diaphragm is achieved by pressing down on the outer ring as shown. The supports (c) and the two sets of rings which form the two diaphragms are all made out of 1/8" brass sheet. The supports (c) are readily removable from the chassis, leaving it free to receive the components of the other excitation system.

The advantages that this drive system has over the air-gap method are

1. No pins are required to support the rod.
2. The sensitivity of the system is much greater due to the smaller and more uniform gap between the condenser plates.

The disadvantages are

1. For some reason yet unknown, neither polystyrene nor PMMA rods can be excited by this method. It is possibly due to the relatively low Qs of the resonances of these rods.
2. Considerable pressure on the diaphragm reduces the sensitivity of the system drastically and seems to act as a load on the ends of the rod, reducing the frequencies

of the resonances. This is observed when the pressure is increased by bringing the two diaphragms too close together and also when very heavy cylinders are used, e.g. brass cylinders. The principle of its operation is considered to arise from the electrostrictive nature of the polymer film.

(e) Effect on resonant frequency of loading the rod

For those rods whose ends have to be coated with "Aquadag", it is necessary to correct the resonant frequencies as measured by an amount given by equation (3.4) below:-

$$\omega = \frac{\omega_o}{1 + A} \qquad (3.4)$$

where ω_o is the resonant frequency of the unloaded rod. The factor A depends on the mode excited. If the rod is resonating in the Young's modulus mode, A = m/M, where m is the mass of the one end of load on the specimen and M is the mass of the cylinder. If the rod is excited into shear mode resonance, $A = I/I_o$, where I_o is the moment of inertia of the rod about its longitudinal axis and I is the moment of inertia of the loading masses about the same axis.

In all calculations concerning resonant frequency, it is

to be assumed that correction for any loading that might exist has been carried out according to equation (3.4).

(f) The vacuum system

The chamber containing the rod is evacuated to eliminate loading effects due to air at atmospheric pressure; a pressure of 2 - 3 mm of mercury is adequate for this task. More important, however, is the fact that a reduced pressure avoids the occurrence of a resonance of the air between the end of the rod and the brass plate. This resonance is so broad as to make damping measurements impossible for the first 3 or 4 resonances. In the case of the diaphragm drive system, the loading of the air on the diaphragm is sufficiently strong to reduce considerably the sensitivity of the system.

(g) Measurement of damping at elevated temperatures

For temperatures above room temperature, the vacuum chamber is placed in a bath of oil maintained at the required temperature. A diagram of such a bath is shown in Figure (3.8). An electric motor drives a stirrer which runs on a nylon nipple resting in a smooth brass bush at the bottom of the tank. The oil (Shell Vitrea Oil, grade 33) is heated by a 1 Kwatt electric heating element which is fed, through a rheostat, from the 250 volt A.C. mains supply.

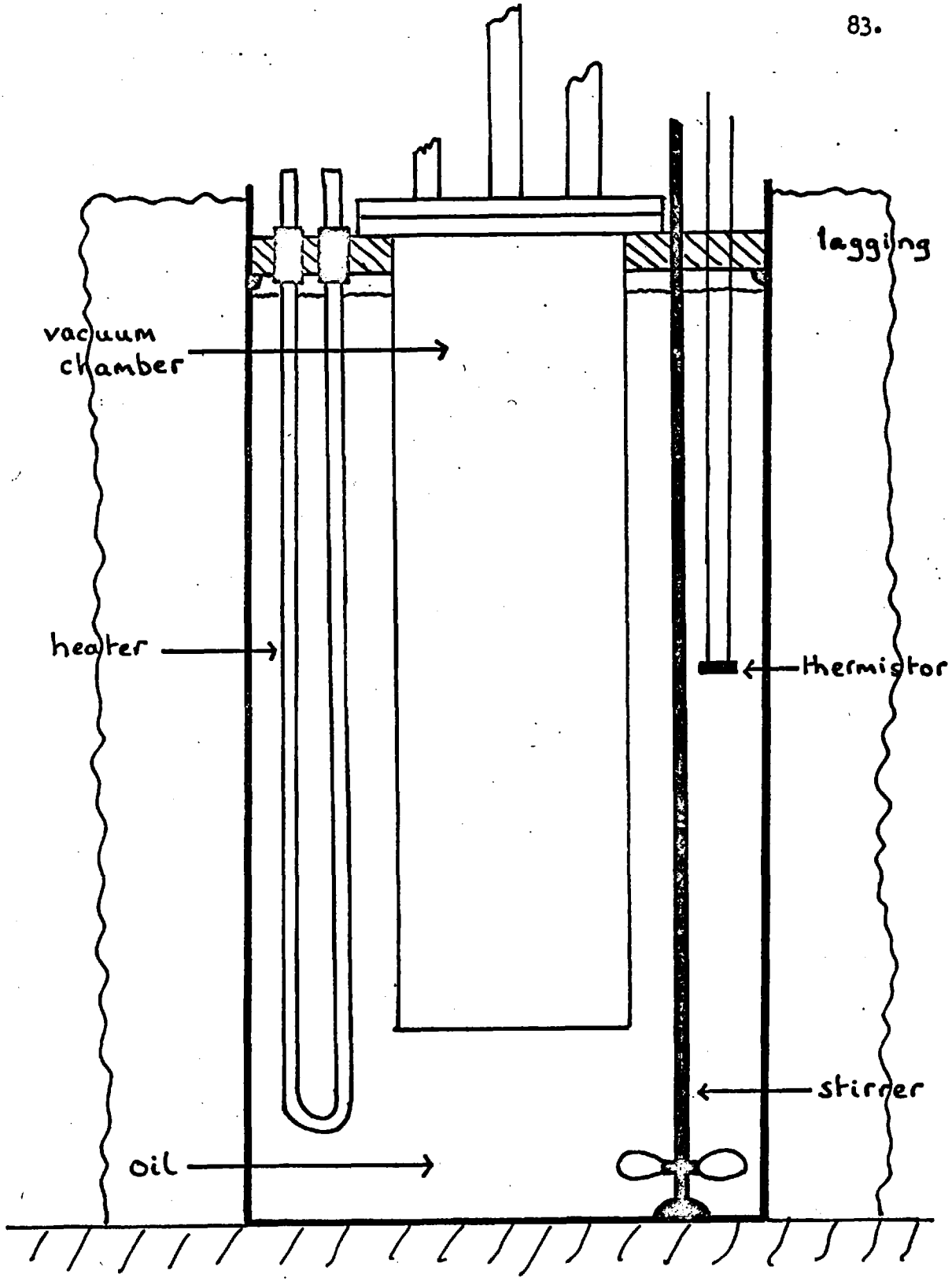

FIGURE (3.8) CONSTANT TEMPERATURE BATH

Control and measurement of the temperature bath system are described in following sections.

Two baths of the type described were made so that a sudden increase (or decrease) in the temperature of the sample could be achieved by transferring the vacuum chamber from one bath to the other. Due to the large thermal inertia of the brass vacuum chamber, it was found necessary to speed up the rate of change of temperature of the sample by blowing air at the required temperature through the chamber. To do this, air from the laboratory's compressed air-line was passed through a copper tube which was coiled four or five times around the inside of the appropriate oil-bath and then led into the top of the chamber containing the sample through a pipe on the top of the chamber, see Figure (3.3). As can be seen in Figure (3.4) the hot (or cold) air circulates round the sample from the bottom and comes out at the top through the (for this procedure) unused vacuum line.

(h) <u>The temperature control system</u>

The temperature of the oil in the bath is controlled by a thermistor (a temperature sensitive resistor), which is placed in the oil bath, in the circuit shown in Figure (3.9c). To produce the temperature required, resistance box R is set at the value of the thermistor at that temperature, the temperature/resistance characteristic of the thermistor

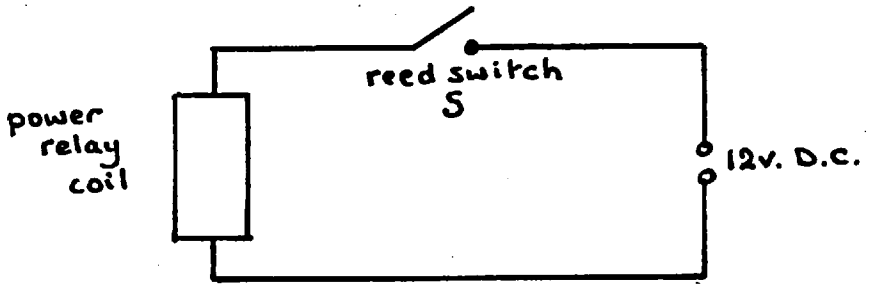

(a)

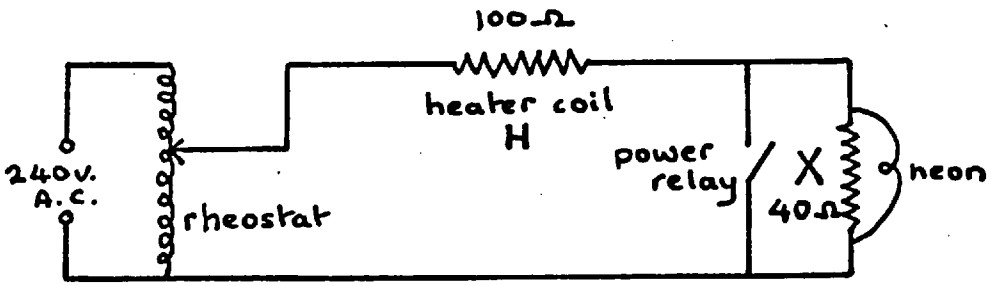

(b)

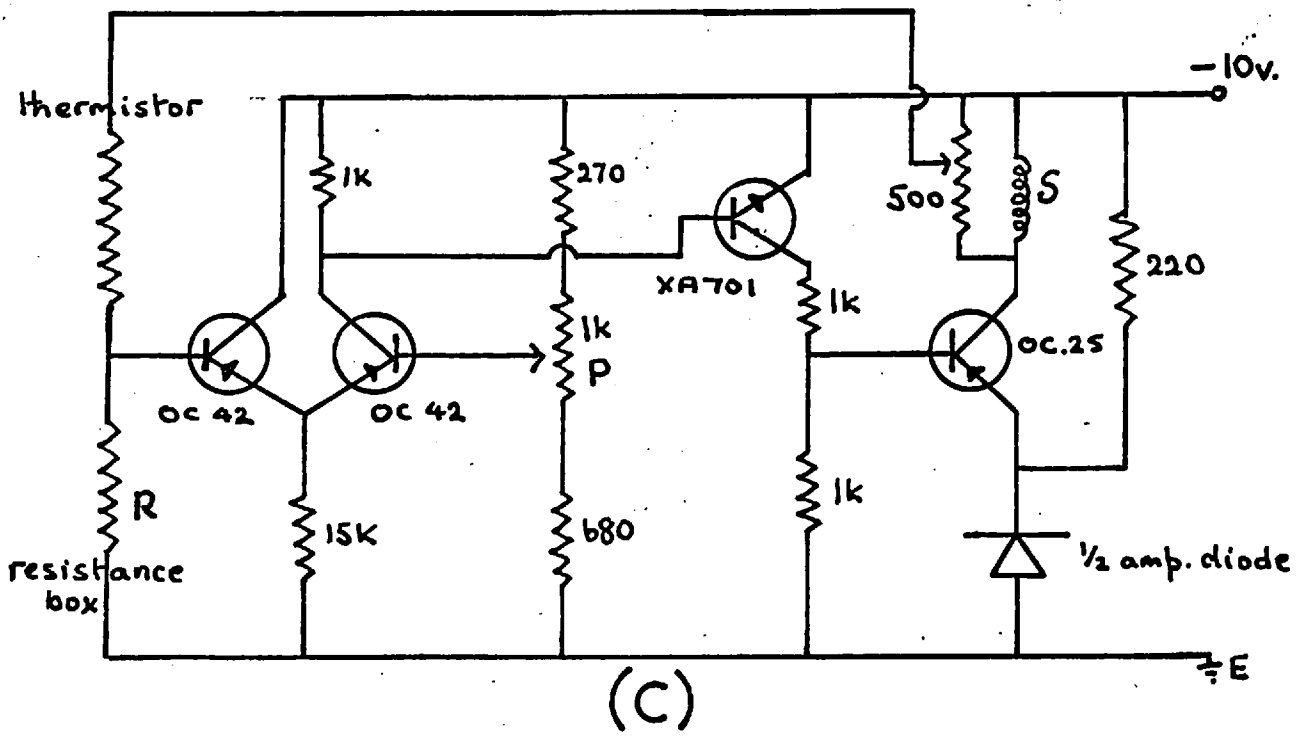

(c)

FIGURE (3.9) (a) SWITCHING CIRCUIT FOR POWER RELAY
(b) SWITCHING CIRCUIT FOR HEATER
(c) CIRCUIT OF TEMPERATURE-CONTROL BRIDGE

having been previously determined.

The reed switch (S), Figure (3.9a), is in circuit with the heating coil H and a subsidiary resistance X, as is shown in Figure (3.9b). Whilst heating up to the set temperature, the switch is open, hence the power relay is open and therefore maximum current goes through the heater coil H. As soon as the set resistance (temperature) is reached, switch S closes thereby bringing the subsidiary resistance X into the circuit. With the values of H and X shown in Figure (3.9b), the switching of S produces a reduction of about one half in the power dissipated by the heating coil. By adjusting the rheostat, the system can be made to operate with only a small power dissipation in the resistor X, the neon lamp being in circuit to show when X is in circuit and thus helps to avoid overheating X.

Figure (3.9c) is the circuit diagram of the bridge network which controls the switching of S. This circuit is not set for all values of R and has to be set each time a different temperature is required. This is done by putting another resistance box of equal value to the first in circuit in place of the thermistor and by then adjusting the 1kohm potentiometer P until the reed switch S is just about to switch on; the thermistor is then replaced and the heating up starts.

The bridge circuit which is novel (Figure (3.9c)) was designed to cause S to switch for an out of balance of $\frac{1}{4}$ deg.C which at 90°C, is equivalent to a swing of 10 ohms in 500 ohms from the I_b/V_b characteristic of the thermistor. With a - 10 volt operating voltage, a setting of 500 ohms in R will give, at balance, a current flow of 0.01 amp through the thermistor and through R. At this current, a change in the resistance of the thermistor from 500 ohms to 510 ohms will produce a change of 100 millivolts in the voltage on the base of the first transistor, the OC 42. This change in voltage produces a base current of 50 microvolts, which is sufficient to cut off the two OC 42 transistors. This action causes sufficient current to flow in the 1kohm resistor in the collector arm of the second OC 42 to switch on the next transistor (XA 701). The purpose of transistors XA 701 and OC 25 is to amplify the current sufficiently to operate the reed switch coil.

Two features are introduced for greater stability of the circuit. The $\frac{1}{2}$ amp diode on the emitter of the OC 25 transistor is in circuit to eliminate the possibility of the reed switch being operated by leakage currents through the last two transistors; leakage current is also avoided by adopting a long-tailed pair arrangement of the two OC 42 transistors. The 500 ohm variable resistance strapped

across the reed switch coil is to introduce a little feedback into the system. Without this, "kicks" in the voltages throughout the circuit produced by the switching of S can re-activate the circuit, thus producing a continuous feedback from the "on" to the "off" positions. This produces a continuous vibration of the reed switch which is obviously undesirable. It is the inclusion of the 500 ohm potentiometer which results in the need for readjusting the circuit (via potentiometer P) every time a new temperature is required.

(i) The temperature measuring system

The temperature of the sample under test is measured by means of a copper/constantan thermocouple which is embedded in a piece of perspex of the same lateral dimensions as the test rods, i.e. about $\frac{1}{4}$" in diameter. The e.m.f. from the thermocouple is amplified by a D.C. amplifier (Pye, 11370) and recorded on a 1 milliamp f.s.d. pen recorder (Evershed and Vignoles, Murray system) which is "padded" with a 10 k ohm resistor.

The temperature can be measured in two ways. The first method is to display the output of the D.C. amplifier directly on to the calibrated chart of the pen recorder. However, instantaneous measurement of temperature can be achieved by the use of the bias device whose circuit diagram is shown in

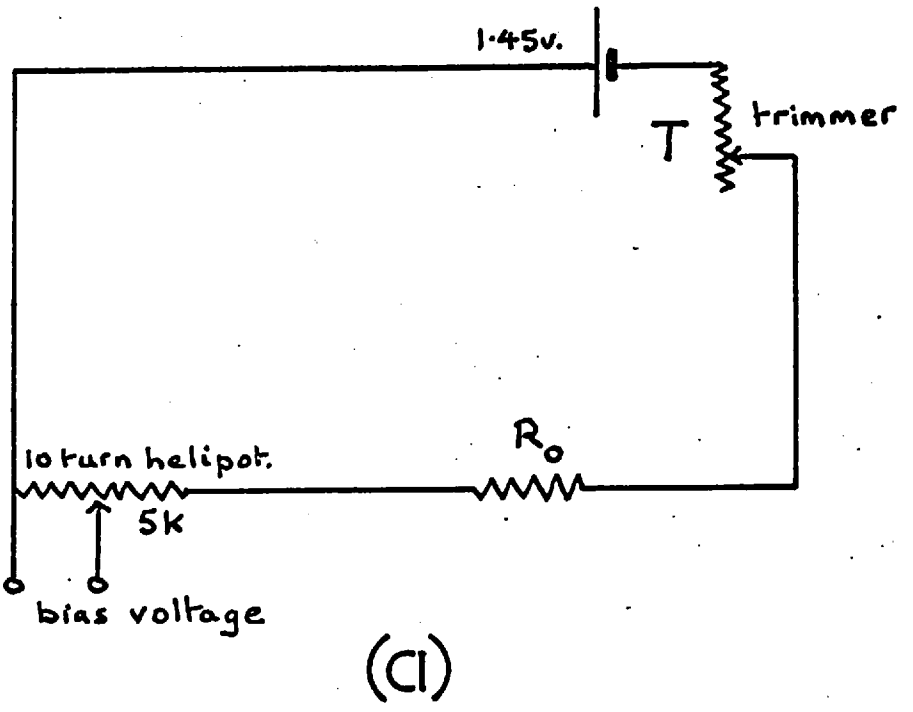

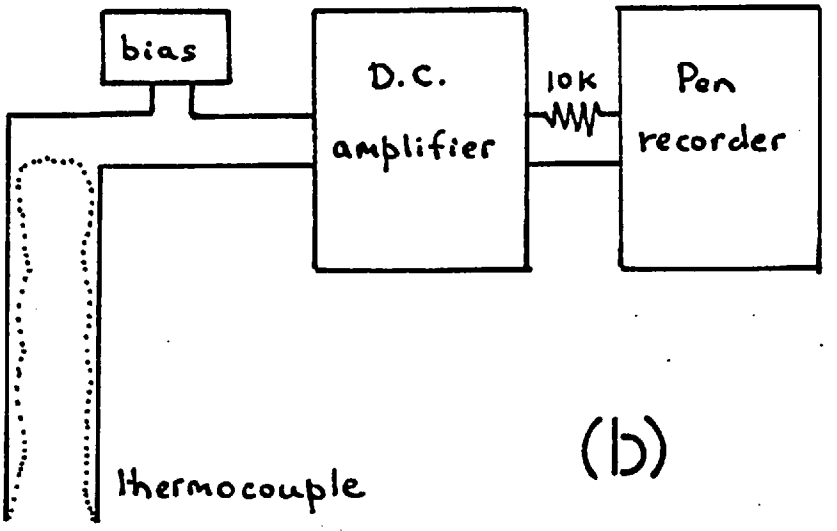

FIGURE (3.10) (a) BIAS DEVICE CIRCUIT
(b) TEMPERATURE MEASURING CIRCUIT

Figure (3.10a). By suitably choosing the value of R_o and by adjusting the potentiometer T, the voltage drop across the 5 k ohm 10 turn helical potentiometer can be set (as measured on a commercial bridge) to 5 millivolts. The temperature can be read by noting the setting of the helical potentiometer which produces a zero reading, either on the chart of the pen recorder, or (more easily) on the meter of the D.C. amplifier when the e.m.f.s' of the bias device and the thermocouple are put in opposition across the terminals of the D.C. amplifier.

A further use exists for the bias device. For high temperatures (about 100°C), the e.m.f. from the thermocouple is of the order of 4 millivolts. The scales of the D.C. amplifier are such that insufficient accuracy can be obtained in the display of this magnitude of e.m.f. on the pen recorder. However, by applying a suitable bias in opposition to the thermocouple e.m.f., the most sensitive range of the D.C. amplifier/pen recorder system can be used; this range gives a full scale deflection of 2°C. The bias device can also be used when cooling or heating the sample, for which an instantaneous temperature may be required later. By adjusting the bias at suitable times throughout the heating or cooling process, a continuous record of temperature on the more accurate ranges of the D.C. amplifier/pen recorder system

can be obtained.

Figure (3.10b) shows the circuit of the temperature measuring system. The cold junction of the thermocouple is either water at room temperature or ice, depending on the time scale of the experiment in progress.

When transferring the specimen chamber from one temperature bath to the other, the initial temperature of the sample is measured by the null method. After transference the stability of temperature inside the chamber is observed by placing the "cold" junction in the bath in which it is contained. Once stability has been observed, the temperature can once more be measured by the null method for which the "cold" junction is return ed to the ice or room temperature water bath.

The setting of the temperature bath can only be achieved to within 2 or 3°C, but once set, it stabilises to within $\pm \frac{1}{2}$°C; tests within the specimen chamber show variations of the temperature is no worse than this. However, tests along the axis of the chamber suggest that there is about a $\frac{1}{2}$°C drop in moving from the bottom to the top; this is more than the length of the sample by about a factor of two.

(j) The compression apparatus

The apparatus used to compress hydrostatically the samples is shown diagrammatically in Figure (3.11). It has a maximum pressure of 8000 p.s.i., which is achieved by compressing water by the pistons from the compression chamber into the pressure vessel, which is surrounded by a jacket through which hot water can be pumped.

Compression of the water in the pressure vessel is obtained as follows. Valve B is closed, the pressure vessel head is put in place and the pressure vessel topped up with water through a bleed valve on the head, which is then closed. Valve A is opened and the piston is screwed back, drawing water into the compression chamber. Valve A is closed and Valve B opened, after which the water in the compression chamber is driven into the pressure vessel by means of the piston. This procedure is repeated until the pressure required is obtained.

Because polymers absorb water, it is not advisable to place the samples directly in contact with the compression fluid, particularly at the high pressures obtained. For example, a sample of polystyrene under 5000 p.s.i. for 10 hours at room temperature absorbed sufficient water to increase its mass from 5.743 gm to 5.763 gm and a slight increase in the internal friction was noted.

FIGURE (3.11) COMPRESSION APPARATUS

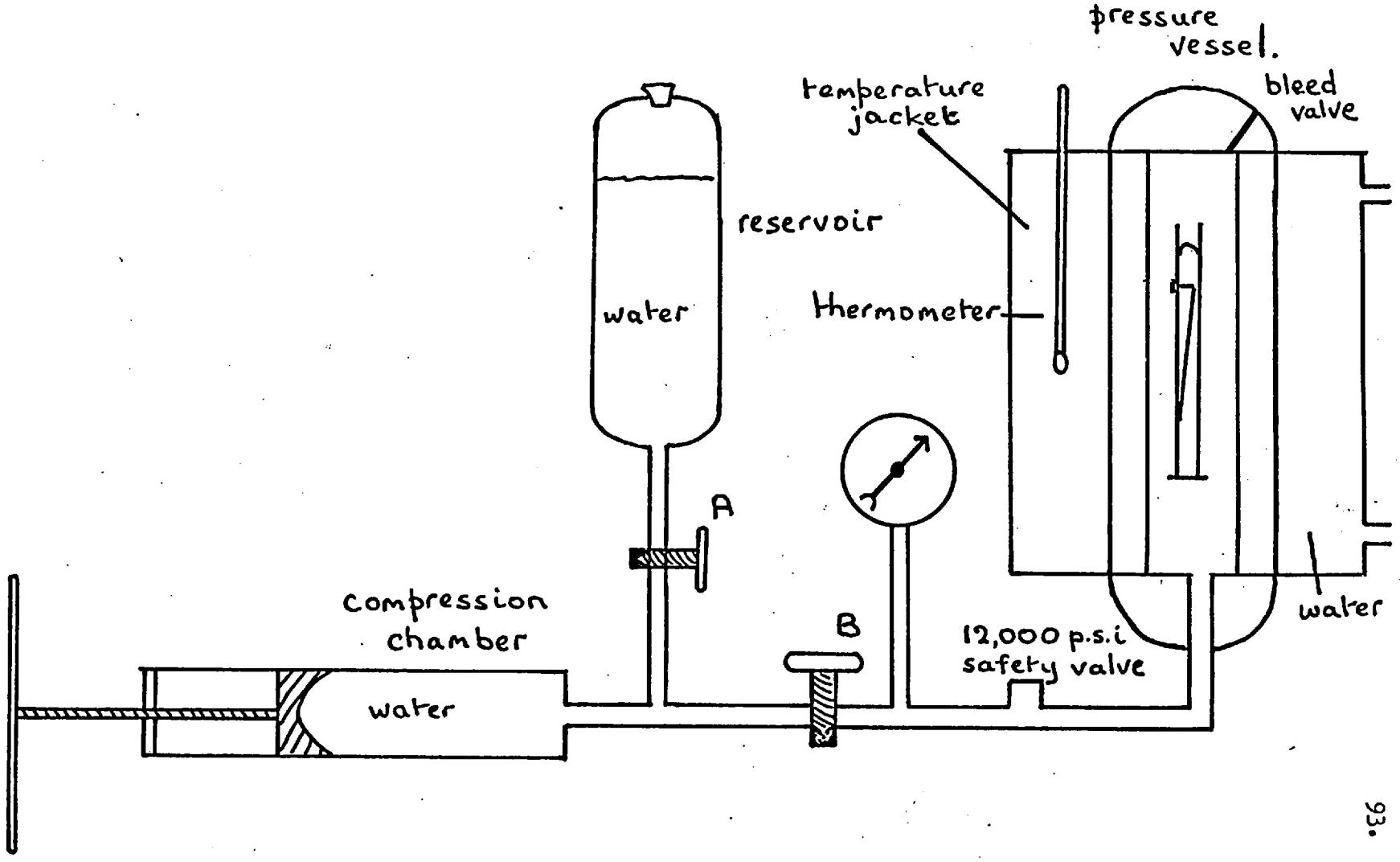

Therefore, the samples were placed in a brass cylinder sealed at one end and with a screw across the open end wide enough to stop the sample coming out. Mercury was then poured into the cylinder until the sample was covered, and this container was placed in the compression chamber. Weighing and damping measurements at room temperature showed that no water (or mercury) was being absorbed. A diagram of this containing cylinder is shown in the pressure vessel of Figure (3.11).

CHAPTER 4

VELOCITY DISPERSION MEASUREMENTS

(a) Choice of materials

In choosing a material from which to test the validity of the exact theory, the following conditions must be satisfied:

1. Its density must be very uniform.
2. It must be readily and accurately formable into the required shape.
3. If metallic, the grain size must on average be less than 0.1 mm to avoid inaccuracies brought about by the scattering of the 5 mc/s pulses.
4. It must have a low damping coefficient to produce high Q resonances in the cylinder for accuracy of measurement of the resonances, and so that the 5 mc/s pulses might traverse samples of the material.

Much time was spent in trying to obtain an aluminium alloy sample (8% zinc, 92% aluminium by weight) which satisfied these conditions. Conditions 2 and 4 are applicable, but 1 and 3 were very difficult to achieve. This alloy was chosen because its crystal structure is spatially a relatively uniform one. However, this quality

was found to be completely discounted by the existence of air holes in the sample as obtained from the manufacturers, who had been asked not to extrude the material which would have removed the air holes but at the expense of introducing strain into the sample. Such strains could have been removed by careful annealing, but this process (unless well controlled) would have led to a growth in the grain size of the metal.

With these difficulties in mind, it was decided to use an optical quality glass, although this material does not satisfy condition 2. The cross-section of the rod could be formed accurately by the technique of centre-less grinding, but slight chipping occurred on cutting and grinding the ends of the rod. The glass (Chance-Pilkington) had a quoted refractive index of 1.523 ± 0.001. To remove any strains induced in the grinding of the rod, it was maintained at $540^{\circ}C$ for three hours and was then allowed to cool to $200^{\circ}C$ over 5 hours after which it was cooled to room temperature overnight in the oven.

Throughout this chapter, reference will be made to samples which are "anisotropic" or "annealed". Little attempt has been made to investigate the particular form

of the anisotropy, whether due to strains induced by machining, due to spatial variations in density or due to grain-size variations and orientations. Annealing can obviously remove strains, but in the case of metals it can lead to growth of grain-size. In the case of glasses (optical glass, perspex and polystyrene) where there is no ordering of the molecules in crystal formations, the terms anisotropic and annealed are used in a mutually excluding sense; thus annealing removes anisotropy arising from internal strains.

(b) Calculation and display of results

If the exact theory is valid for short cylinders, a constant value of Poisson's ratio should result from the velocity dispersion as measured from each resonant frequency.

The dispersion, v_E/v_n, is given by nf_E/f_n and the value of d/L is given by n.d/21 assuming that no end-effect corrections are necessary. The value of f_E is given by the value of f_1 suitably adjusted for dispersion. The value of d/L for this resonance is known, but the value of σ to be used is not, and three methods of deriving a value of σ are available, see Table (4.1).

TABLE (4.1)

Methods of calculating Poisson's ratio from dispersion measurements

Method	(1) v_E/v_n given by:	(2) f_E derived from:	(3) σ derived from:
1.	$n.f_1/f_n$	f_1	Dispersion as given in (1) and value of d/L_n using tabulated values*; re-iteratively.
2.	$n.f_1/f_n$	f_1	f_s derived from interpolation, and f_1 used in equation (1.22) re-interatively.
1A.	$(n+1).f_n/n.f_{n+1}$	f_n/n	Dispersion as given in (1) and value of d/L_n using tabulated values*; re-iteratively.

*The theoretical values of v_E/v_n as a function of d/L and σ as given by Appendix 3 and Bradfield (1964).

The first method starts from a calculation of the dispersion at the value of d/L given by n.d/21 as $n.f_1/f_n$, from which an approximate value of σ can be derived from the theoretical predictions of velocity dispersion, which is used to give the correction to be applied to f_1 for a better approximation to f_E. Used reiteratively, method 1 produces a value of σ and of f_E for each value of n.

Alternatively, a value of the fundamental shear mode frequency, f_s, can be obtained from the value of f_n/n at the universal point (given by $d/L = 0.5860_6$) see section (1.d) for details. A value of f_s is obtained by means of a linear interpolation between the eleventh and twelfth values of f_n/n for a 5" x $\frac{1}{2}$" cylinder. Use of f_s and f_1, the latter being a first approximation to f_E, in equation (1.22) gives a value of σ which is then used to correct f_1 to give a more accurate value of f_E, and so on, until the final values of f_E and σ are obtained. This is method 2.

Use of $n.f_1/f_n$ to give the dispersion relies on the fundamental resonant frequency to give an accurate value of f_E. This can be avoided by use of $(n+1).f_n/nf_{n+1}$ to

give the dispersion, the re-iterative process described above being then employed. It will be shown that both of these methods of calculating the velocity dispersion produce the same results in terms of the average values of f_E and σ . This method is referred to as method 1A.

The dimensions of all the specimen rods used were known to 0.001". For ease of calculation, the ideal dimensions of the rods were such that the values of d/L resulting from n.d/21 were those of the tables of predicted values of dispersion, see Appendix 3 and Bradfield (1964), so that a minimum of interpolation was necessary. Thus, a rod of length 5.000" and diameter 0.500" gives values of d/L_n of n.(0.050).

The advantage of quoting values of Poisson's ratio calculated in the manner described above compared with displaying the values of velocity dispersion is demonstrated by reference to Figures (4.1) and (4.2). Figure (4.1) shows velocity dispersion calculations for a glass and a polystyrene cylinder compared with the theoretical predictions for two chosen values of Poisson's ratio. Figure (4.2) shows the values of Poisson's ratio for three sets of data as calculated from the theoretical

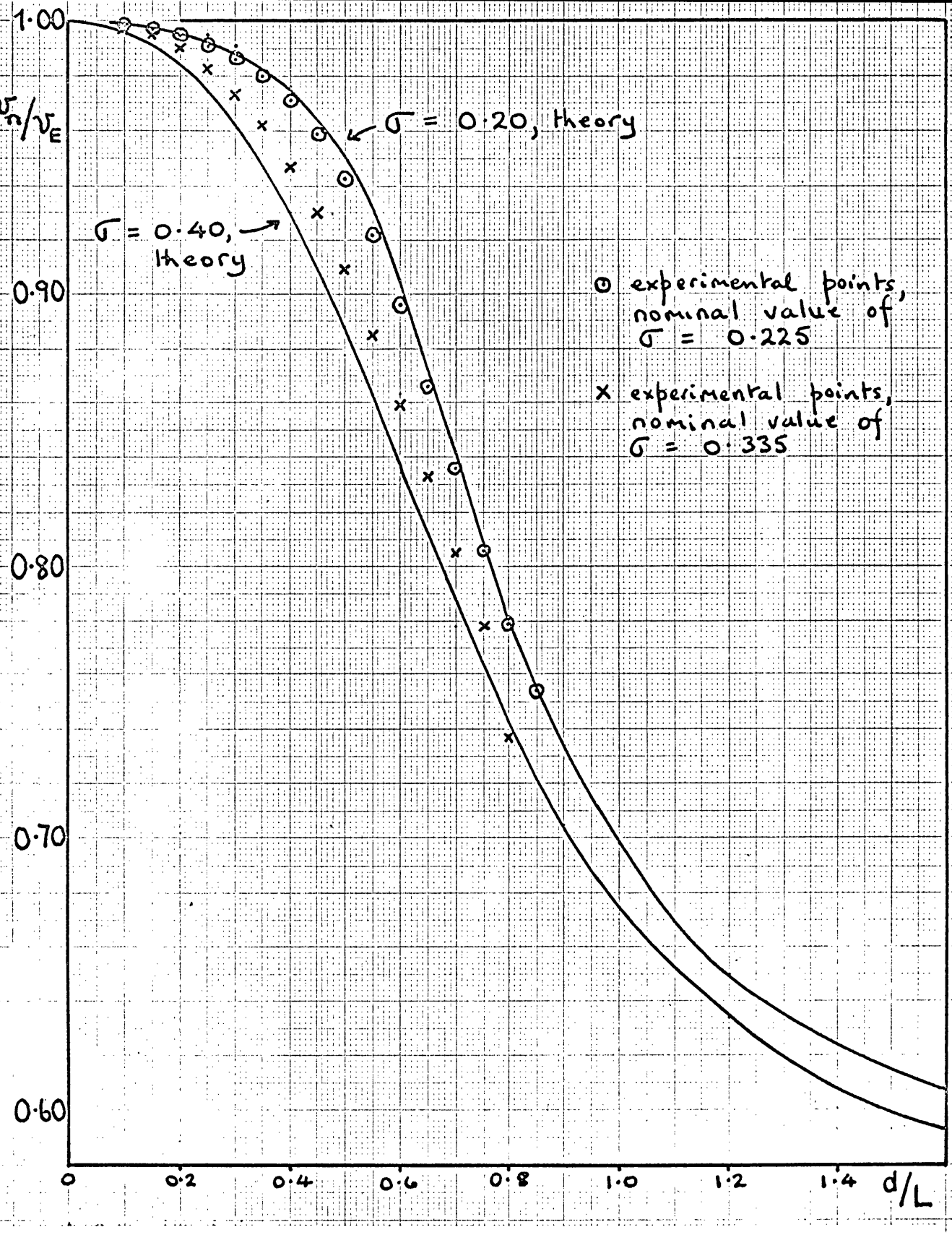

FIG.(4.1) Experimental values of velocity dispersion vs. d/L in two 5" x $\frac{1}{2}$" cylinders compared with exact theory values.

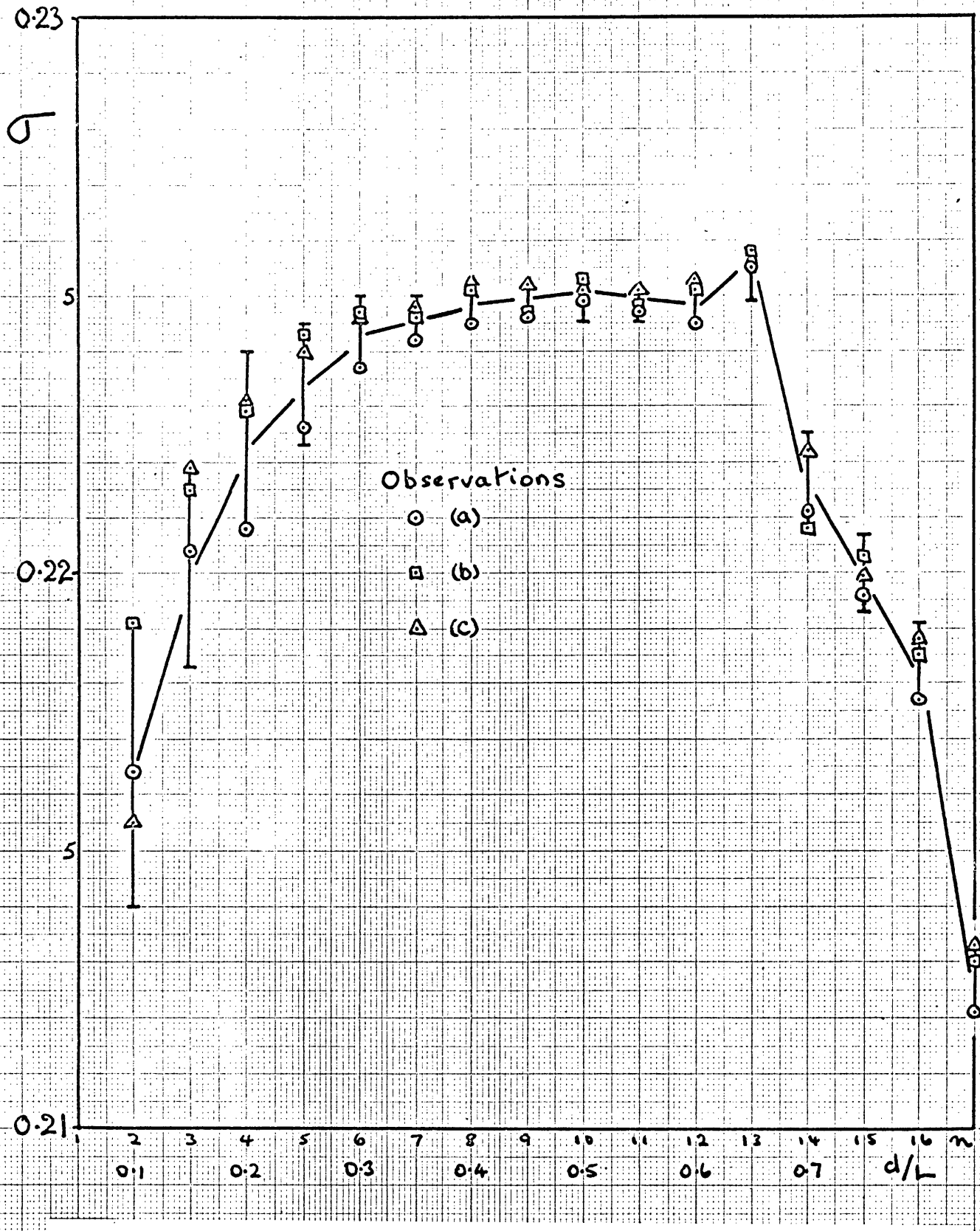

FIG.(4.2) Poisson's ratio calculated from the velocity dispersion in a 5" x $\frac{1}{2}$" glass cylinder using the exact theory, for three sets of experimental observations.

predictions, and (a) is equivalent to the data of the given glass cylinder shown in Figure (4.1).

(c) Glass cylinder measurements

(i) Results and discussion for the 5" x $\frac{1}{2}$" cylinder.

Figure (4.2) shows the values of Poisson's ratio computed by method 2 for the glass cylinder of nominal dimensions 5" x $\frac{1}{2}$". Three sets of data are given, (a) from the resonant frequencies of the rod when excited by the diaphragm technique, (b) from the rod similarly excited but with a slightly heavier loading of the top diaphragm on the rod, (c) from the rod when excited by the condenser microphone technique and held centrally by one support system. The limits of the vertical lines define the extreme values of σ obtained from the large number of observations of the resonant frequencies, using both techniques of excitation. The accuracy with which the values of f_n/n are determined is of the order of $\pm$ 1 c/s. The specimen cylinder was placed in the chamber for a period of about one hour before measurements were taken to ensure the attainment of temperature equilibrium, following which 3 or 4 measurements of the resonant

frequencies were made. Temperature stability over the measurement period was within $\pm\frac{1}{2}^{\circ}$C which, for a coefficient of linear thermal expansion of 10^{-5}/deg.C., is equivalent to a possible error in f_n/n of about 0.1 c/s for values of f_n/n of 20 kc/s, which is the case for cylinders described in this section.

An error of this magnitude in f_n/n produces an error of the order of $\pm$ 0.00007 in the dispersion. The values of the dispersion for d/L = 0.2 at σ = 0.21 and 0.22 are 1.00111 and 1.00122 respectively; hence such an error in the dispersion is equal to an error of $\pm$ 0.006 in the value of Poisson's ratio calculated at d/L = 0.2. The accuracy of the experimental points in Figure (4.2) was improved therefore by taking many different measurements of the resonant frequencies, each set of resonant frequencies being used to calculate Poisson's ratio; the spread of values so obtained is shown as the vertical lines in Figure (4.2).

The values of Poisson's ratio at low d/L values shown in Figure (4.2) suggest that some correction is necessary to the values of the resonant frequencies in order to obtain a constant value of σ ; the

deviation from a constant value of σ at high d/L values (i.e. > 0.65) will be dealt with in more detail in Chapter 5. The form of the deviation suggests that the correction is more important at low frequencies than at high. It was therefore decided to calculate a correction, to be called an "end-effect" correction, and symbolised by Δf, from the following equation:

$$n.(f_1 + \Delta f).c_1 = (f_n + \Delta f).c_n \qquad (4.1)$$

where c_n are the corrections due to dispersion for the n resonances. This equation is derived from that for phase velocity corrected for end-effect, see equation (1.17). Figure (4.3) shows the values of Δf as a function of n for the three sets of data of Figure (4.2), and the values of Poisson's ratio which result from a calculation of dispersion from the resonant frequencies to which had been added the average value of Δf for each set of data. The average values of Δf, the values of f_E and of f_s, are given in Table (4.2).

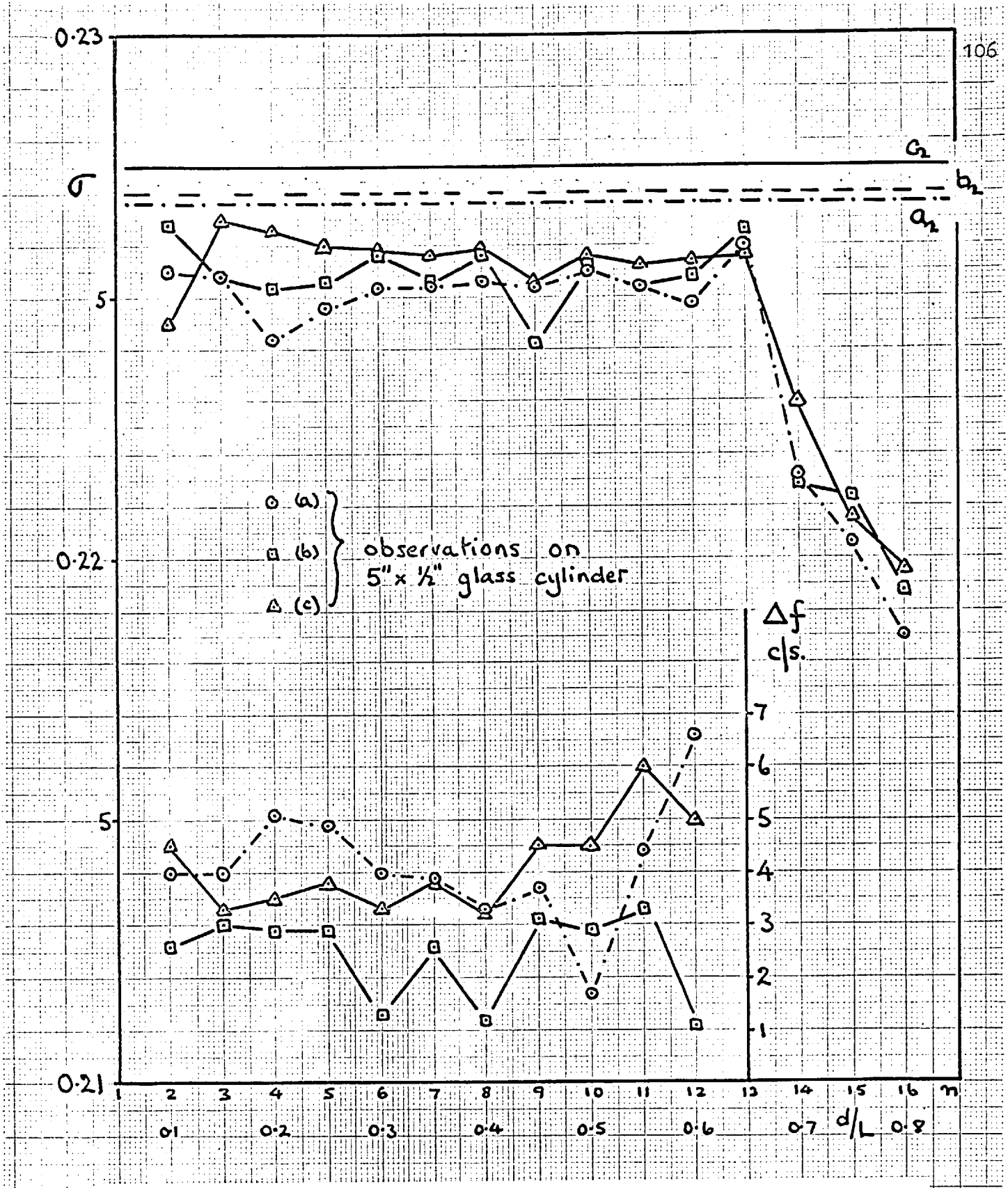

FIG.(4.3) Corrected values of Poisson's ratio and corresponding Δf values for three sets of experimental observations.

TABLE (4.2)

Calculated values of Δf, f_E and f_s for

5" x ½" glass rod

Data	(a)	(b)	(c)
(1) Δf, c/s	4.2 ± 1.3	2.4 ± 0.6	4.1 ± 0.7
(2) $f_E(1)$, kc/s	20.614	20.612_5	20.619_5
(3) $f_E(2)$, kc/s	20.615	20.615	20.619
(4) $f_s(1)$, kc/s	13.160	13.158	13.160
(5) $f_s(2)$, kc/s	13.167	13.164	13.168

Notes:

(2) calculated from f_1 and method 2, error is ± 1 c/s.

(3) average of first 9 values resulting from method 1, ± 5 c/s.

(4) result of linear interpolation between eleventh and twelfth resonances, ± 1 c/s.

(5) result of computer interpolation, using values of f_n/n up to d/L = 0.60; ± 2 c/s.

The values of σ shown in Figures (4.2) and (4.3) have been calculated from method 1. The values of f_E resulting from the use of this method are given as $f_E(2)$ in Table (4.2) and can be seen to agree very well with $f_E(1)$ which is calculated from f_1 by method 2. The average value of f_E resulting from the first 8 values given by method 1A was equal to the values of f_E shown in Table (4.2), within experimental error. Table (4.2) also gives two values of f_s; $f_s(1)$ results from a linear interpolation of f_n/n between the eleventh and twelfth resonances, and $f_s(2)$ is calculated from an interpolation of f_n/n at the universal point by means of a curve fitting of all of the resonances below d/L = 0.65, which was carried out using an Elliot 803 computer. Use of a curve-fitting program avoided the problem of deciding which value of σ to use.

Values of the Poisson's ratio calculated in various ways from the data shown in Figure (4.3) are given in Table (4.3).

TABLE (4.3)

Calculated values of Poisson's ratio for glass cylinder

Data	(a)	(b)	(c)	Standard deviation
(1)	0.2252	0.2254	0.2257	± 0.0005
(2)	0.2268	0.2270	0.2275	± 0.0005
(3)	0.2255	0.2259	0.2260	± 0.0007
(4)	0.2252	0.2252	0.2258	± 0.0010

Notes:

(1) average of first twelve values of Figure (4.3).

(2) using $f_E(1)$ and $f_s(1)$ of Table (4.2).

(3) using $f_E(1)$ and $f_s(2)$ of Table (4.2).

(4) average of first eight values using method 1A.

The horizontal lines shown in Figure (4.3) and labelled a_2, b_2 and c_2 are the values of σ shown in Table (4.3) as row (2). The error in the correction due to dispersion applied to f_1 to give f_E resulting from this value of Poisson's ratio, as compared with the value of Poisson's ratio obtained from the computer interpolation is insignificant; the corrections at d/L = 0.05 for σ = 0.2268 and 0.2255 are 1.00032 and 1.00031_7, respectively.

Use of the uncorrected values of f_n to give f_E and f_s only affects the value of the former, as the latter is in fact computed from f_n/n. The uncorrected value of f_E for data (a) of Table (4.2) is 20.610 kc/s which with f_s = 13.167 kc/s gives a value of σ from equation (1.22) of 0.2250 $\pm$ 0.0002.

Figure (4.4) is the data labelled (a) of Figures (4.2) and (4.3) shown together with the values of σ calculated using method 1A, which is shown as plot (d). The lines C_1 and C_2 are the values of σ calculated from f_E and a linearly-interpolated f_s, which were themselves calculated from the values of f_n being respectively unadjusted and adjusted, for the end-effect.

Some mention should be made of the difference in the values of f_E between those for data (a) and (b) and that

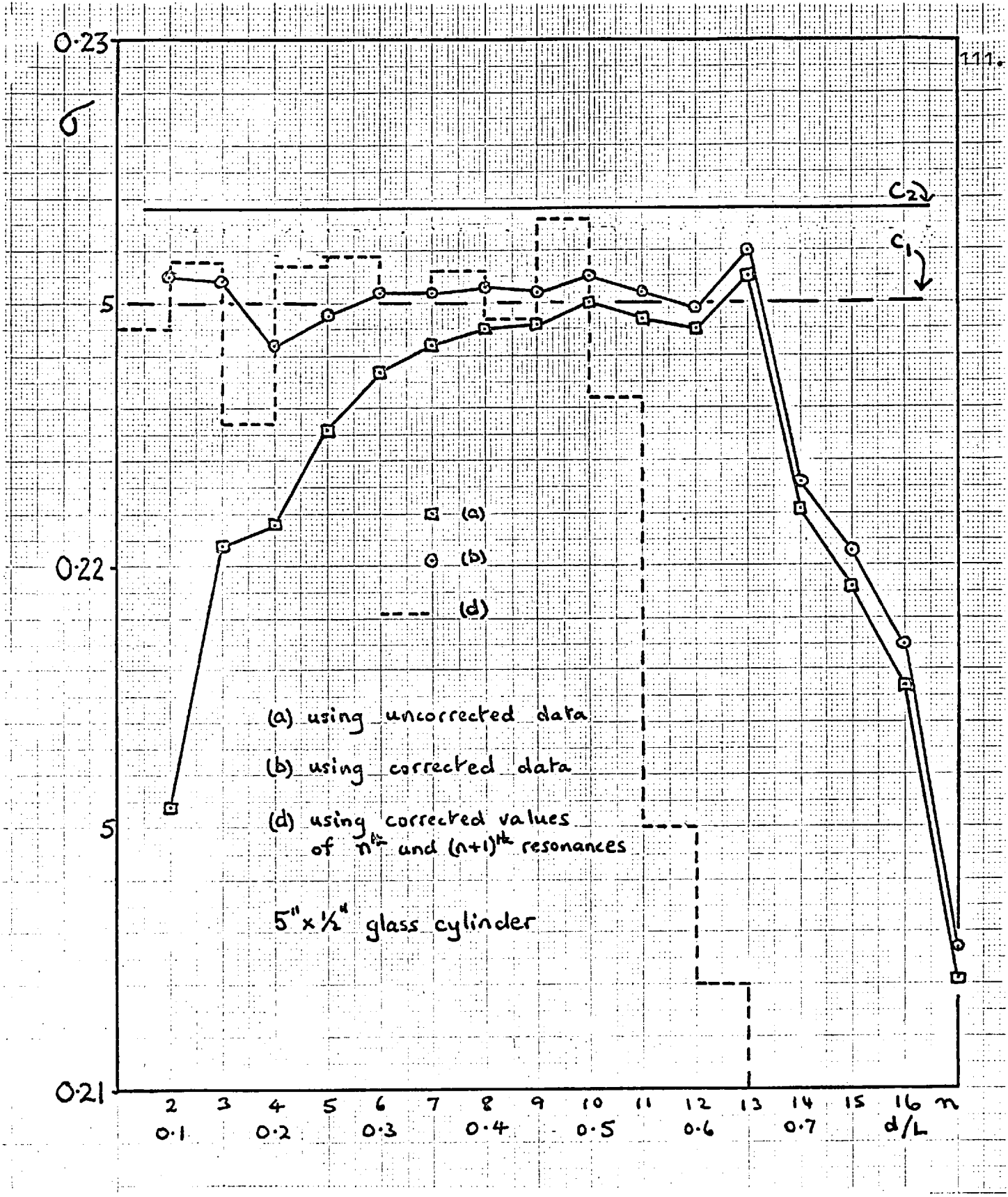

FIG.(4.4) Poisson's ratio obtained by various methods of calculation using the same experimental observations as (a) of FIG.(4.3).

for data (c), see Table (4.2). The diaphragm drive method ((a) and (b)) must produce some load on the specimen and this is considered to be the cause of the lower values of f_E resulting from this method of drive. Using the value of f_E of data (a) as the "loaded" value, and that of (c) as the "unloaded" one, equation (3.4) gives a value of 0.006 gm as the mass loading on each end which is equivalent to the loading produced by the diaphragm. This is about four times that due to the average loading of the wire and "Aquadag" on the ends of the rod. The explanation of the reduced values of f_E for data (a) and (b) (an effect noted in all observations made using this method of excitation, though not necessarily by the amount shown in Table (4.2)), is further supported by the observed decrease in the values of f_n when the diaphragms were pushed tightly into the ends of the rod. A maximum decrease in f_1 of the order of 30 c/s was noted and substantial distortion of the shape of the resonance curve occurred. No equivalent increase in the value of f_s is noted for data (c), see Table (4.2).

The values of the end-effect correction as shown in Table (4.2) agree within experimental error. The difference in values of f_E for data (a) and (b) is due

mostly to the difference in values of Δf for these two sets of data. It is shown in Chapter 3 that the effect of loading the rod produces a correction which is proportional to f_n whereas the end-effect correction seems to be constant for all f_n. Therefore the effect of the increased load due to the diaphragm of data (b) should not affect the value of Δf.

From the results shown in this section, the following conclusions can be drawn.

1. The velocity dispersion in the 5" x $\frac{1}{2}$" glass cylinder can be explained in terms of the exact theory up to values of d/L of 0.65, subject to the condition that a constant end-effect correction is made to the values of the resonant frequencies, this correction being given by equation (4.1).

2. Above d/L = 0.65, the value of the correction necessary to produce the same constant value of σ above and below d/L = 0.65 has to be increased by a factor of 10.

3. The position of the universal point at d/L = 0.5860_6 as predicted by the exact theory is supported by the measurements taken from the non-infinite glass cylinder, in the sense that the value of σ derived from the theory of the universal point is equal to that resulting from the

dispersion measurements when the end-effect is taken into consideration.

Four aspects of velocity dispersion in short cylinders still need investigating:

1. The dependence of the value of Δf on rod dimensions, see section (4.c.ii).

2. The dependence of Δf on the material of the rod, see Chapter 5.

3. The reproducibility of the value of σ by methods independent of the dispersion measurements, see section (4.c.iii).

4. The effect of anisotropy of the material of the rod on the measurement of Poisson's ratio, see section (4.g).

(ii) Variation of the dimensions of the given cylinder.

The cylinder was shortened to $2\frac{1}{2}$" in length and annealed as described in section (4.a). Values of the resonant frequencies were measured many times using the condenser microphone technique (to avoid any possible inaccuracy due to loading to the diaphragm, incurred in the diaphragm method) until typical values had been obtained.

The rod was then "ground down" to $\frac{1}{4}$" in diameter, thus producing a rod of the same relative dimensions as the original one. After annealing, the values of the resonant

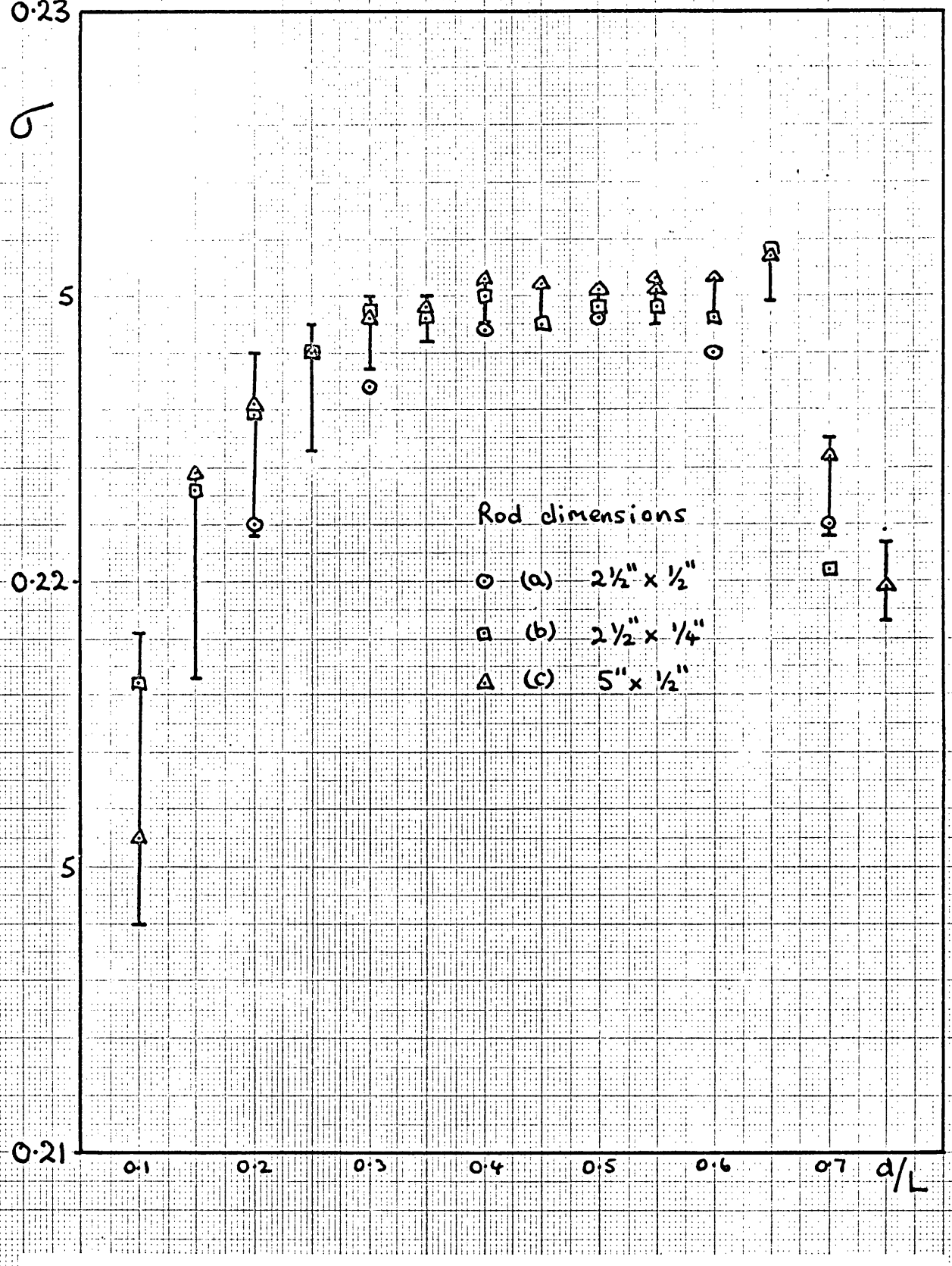

FIG.(4.5) Poisson's ratio calculated from the velocity dispersion in three glass cylinders of different dimensions using the exact theory.

frequencies were measured a number of times using the condenser microphone system.

Figure (4.5) shows the values of Poisson's ratio calculated from the uncorrected values of the resonant frequencies of the three rods by method 1. The experimental points (a), (b) and (c) are for the rods of dimensions $2\frac{1}{2}$" x $\frac{1}{2}$", $2\frac{1}{2}$" x $\frac{1}{4}$" and 5" x $\frac{1}{2}$" respectively, data (c) of this graph being the same as data (c) of Figure (4.2). The vertical lines shown in Figure (4.5) are the spread of values obtained from the calculation of σ from the many sets of resonant frequencies for rod (c). Similar ranges of values of σ exist for data (a) and (b), but have not been shown in order to avoid confusion. Bearing this in mind, it is possible to conclude that the value of σ calculated in this manner is dependent only on the value of d/L at which it was calculated.

Figure (4.6) shows the data of Figure (4.5) amended by the addition of an end-effect correction calculated from equation (4.1). The value of this correction is an average of the values shown in Figure (4.6), which is shown in Table (4.4) which also gives values of v_E and v_s and σ derived from the same data.

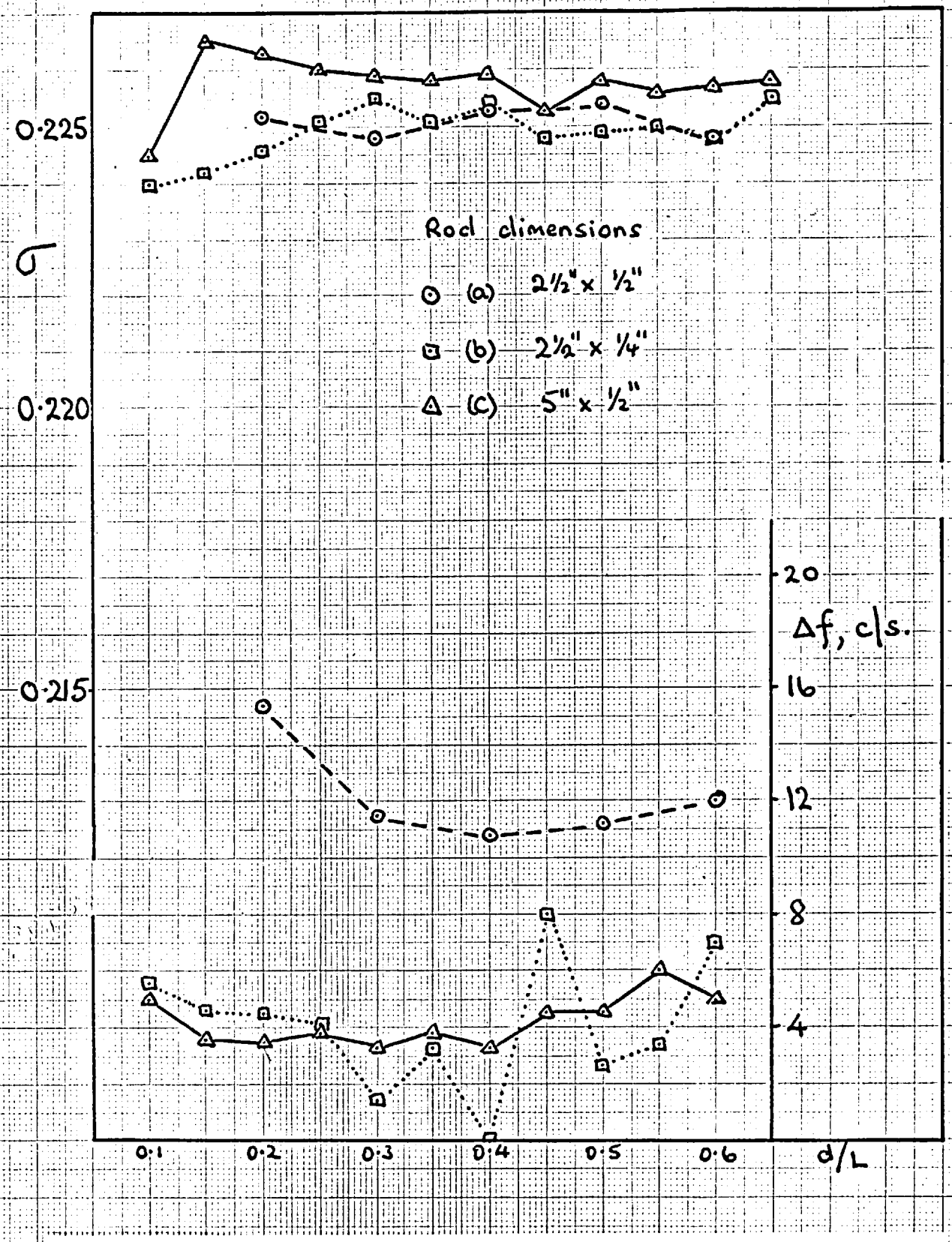

FIG.(4.6) Corrected values of Poisson's ratio and corresponding Δf values for three glass cylinders of different dimensions.

TABLE (4.4)

Calculated data for glass rods of different dimensions

Data	(a)	(b)	(c)
Dimensions	$2\frac{1}{2}$" x $\frac{1}{2}$"	$2\frac{1}{2}$" x $\frac{1}{4}$"	5" x $\frac{1}{2}$"
(1) Δf, c/s	12.2 ± 1.6	4.3 ± 2.3	4.1 ± 0.7
(2) v_E, Kc/s	5238 ± 2	5236 ± 2	5237 ± 1
(3) v_s, kc/s	$3345 \pm 1\frac{1}{2}$	$3344 \pm 1\frac{1}{2}$	$3345 \pm 1\frac{1}{2}$
(4) $\sigma(1)$	0.2251 ± 0.0005	0.2249 ± 0.0005	0.2257 ± 0.0005
(5) $\sigma(2)$	0.2258 ± 0.0006	0.2256 ± 0.0006	0.2260 ± 0.0006

Notes:

(2) and (3): principal error due to error in length measurement

(4): average of values of Figure (4.6)

(5): obtained from f_E (calculated from f_1) and f_s (computer-interpolated at universal point) in equation (1.22).

It is seen from Table (4.4) that the values of Poisson's ratio calculated from the dispersion data obtained from rods of three different dimensions are the same, within experimental error. The universal point is seen to occur at the same value of d/L as given by the exact theory in all three rods, as demonstrated by the constant values of v_s and σ predicted by this theory. The value of v_E obtained from the fundamental resonant frequency suitably adjusted for dispersion and end-effect is seen to be constant within the experimental error.

The end-effect correction appears to be dependent on the value of d/21 for the rod under test although this conclusion is only supported by observations on rods having two values of this ratio. Chapter 5 deals in detail with the end-effect correction, and further comment is made there.

(iii) Poisson's ratio measurements using various other techniques

As described in section (1.i), two methods, independent of dispersion measurements, are available for obtaining Poisson's ratio for the material of the rods.

The first technique comes from a measurement of the fundamental shear mode resonance, which was excited and

measured in the 5" x $\frac{1}{2}$" rod by a technique described in section (3.d). Four turns of onamelled copper wire (S.W.G. 36) were wound on each end of the rod, as shown in Figure (3.5), "Durofix" being used to cement the winding in place. The frequency of the resonance was measured, after which one turn was removed from each end. This procedure was repeated until only one turn remained. The mass and dimensions of each turn were determined and the appropriate form of equation (3.4) was used, giving a fundamental shear mode frequency of 13.14 $\pm$ 0.02 kc/s. The error quoted arises from the poorness of the estimation of the loading effect due to the difficulty of deciding what effective length of the leads of the coils to include and in the estimating of the moment of inertia of the winding.

The second method of obtaining Poisson's ratio is the 5 mc/s pulse technique, see Smith (1965). The specimen used in this measurement was a cylinder 1" in length and about $\frac{3}{4}$" in diameter (which had been cut from the same block of glass which gave the 5" x $\frac{1}{2}$" cylinder), and was annealed in the same manner as the other rods. This technique gives v_l and v_s, the former being the velocity of longitudinal propagation in an unbounded medium, given by $\left\{(\lambda + 2\mu)/\rho\right\}^{\frac{1}{2}}$, v_s being the shear velocity.

TABLE (4.5)

Data calculated from 5 mc/s pulse technique measurements for glass

(1)	v_l (m/s)	5611.9 ± 0.5
(2)	v_s (m/s)	3332.1 ± 0.5
(3)	density, (gm/cc)	2.568 ± 0.001
(4)	$\mu' \times 10^{11}$ (dyn,/cm^2)	2.852 ± 0.002
(5)	$\lambda' \times 10^{11}$ (dyn./cm^2)	2.385 ± 0.002
(6)	$E' \times 10^{11}$ (dyn./cm^2)	7.003 ± 0.002
(7)	v_E (m/sec.)	5222 ± 2
(8)	σ	0.2277 ± 0.0012

Notes:

(3) average of measurements taken from the three previously described cylinders and the 1" x $\frac{3}{4}$" cylinder

(8) calculated from $\sigma = \frac{E' - 1}{2\mu'}$

TABLE (4.6)

Calculated values of Poisson's ratio for glass

(1)	(2)	(3)	(4)
0.2257	0.2260	0.2310	0.2277
± 0.0005	± 0.0006	± 0.0035	± 0.0012

Notes:

(1) average of first twelve values of data (c) of Figure (4.3)

(2) f_E and $f_s(2)$ for data (c), Table (4.2)

(3) f_E and directly measured value of f_s = 13.14 kc/s

(4) 5 mc/s pulse method, see Table (4.5)

TABLE (4.7)

Calculated values of moduli for glass

	(1)	(2)	(3)	(4)	(5)	
$E' \times 10^{-11}$	7.045 ± 0.003	7.044 ± 0.003	7.039 ± 0.003	7.003 ± 0.002	-	(dyn./cm^2)
$\mu' \times 10^{-11}$	2.870 ± 0.002	2.874 ± 0.002	2.872 ± 0.002	2.852 ± 0.002	2.856 ± 0.009	"
$\lambda' \times 10^{-11}$	2.39 ± 0.02	2.36 ± 0.02	2.36 ± 0.02	2.385 ± 0.002	-	"

Notes:

(1) from (c) of Table (4.4), μ' obtained from $v_s(2)$

(2) from (a) of Table (4.4), μ' obtained from $v_s(2)$

(3) from (b) of Table (4.4), μ' obtained from $v_s(2)$

(4) data from 5 mc/s pulse method

(5) result of direct measurement of f_s = 13.14 kc/s

Table (4.5) gives the data from the 5 mc/s pulse method. Table (4.6) gives values of Poisson's ratio for all three methods, dispersion, shear mode resonance and pulse technique. As can be seen, values (1) and (2) obtained from the dispersion measurements, are somewhat lower than values (3) and (4) which were derived by the two other methods, though the experimental errors nearly cover the range of values. Table (4.7) gives the values of Young's modulus and the Lamé elastic constants obtained from measurements on the various samples of glass used; λ' was calculated from E' and μ' by the relationships shown in Appendix 1. From this table can be seen more clearly the agreement between the values of μ' obtained by the pulse method and the direct measurement of the shear mode frequency, these values being quite distinctly lower than the values of μ' obtained from the value of f_s given by the universal point theory, for all three rods. Although the 5 mc/s pulse method value of E' is lower than those values deduced from the fundamental resonant frequency of a rod, Poisson's ratio is practically unaltered, see Table (4.6).

(iv) Display of data using method of Edmonds and Sittig

Having obtained independent values of the shear

velocity, it is now possible to display the dispersion data in the manner of Edmonds and Sittig, see section (1.i). Figure (4.7) shows the theoretical curve for $\sigma = 0.2252$, and the experimental points A, B, C, which have been derived from data (a) of Figure (4.3). Points A are the values for the resonant frequencies to which have been added the correction of 4.2 c/s; the value of f_s used to obtain $f_n/n.f_s$ $(= v_n/v_s)$ is 13.167 kc/s, see Table (4.2). Points B are the values for the uncorrected resonant frequencies, the first four points only having been given as the others are equal to points A. It is not surprising that points A fit the theoretical curve so well, because f_s was interpolated from these phase velocity measurements. Points C are the experimental points which result from the use of $f_s = 13.14$ kc/s which is the value obtained from the direct measurement of the fundamental shear mode frequency and the uncorrected values of f_n (data (a)). As can be seen, the use of a decreased value of f_s is to displace upwards the values of the ordinates in Figure (4.7). At $d/L = 0$, the value of the ordinate is

$$\left\{2(1 + \sigma)\right\}^{\frac{1}{2}} - \left\{2(1 + 0.2)\right\}^{\frac{1}{2}}$$

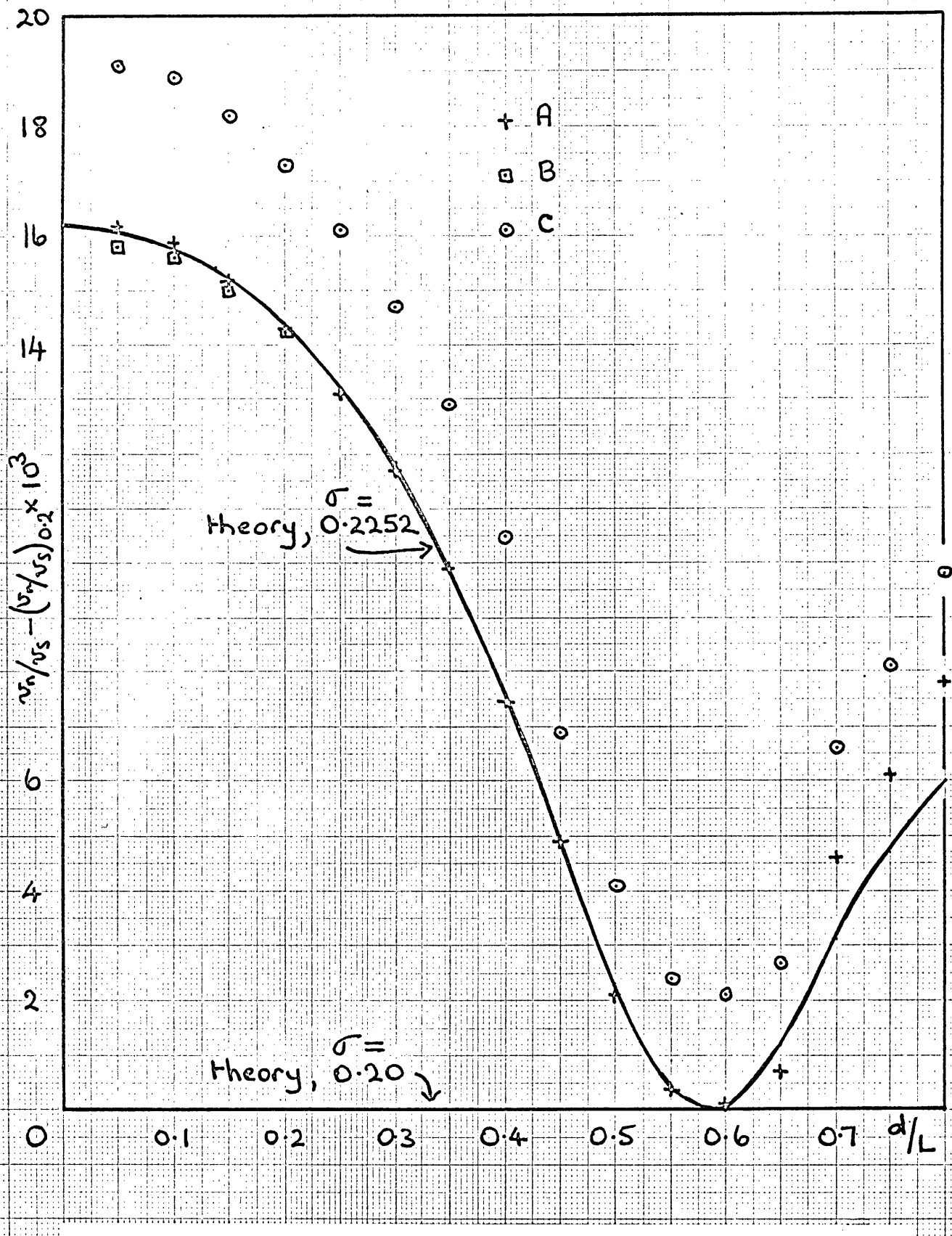

FIG.(4.7) Velocity dispersion in a 5" x ½" glass cylinder presented in the manner of Edmonds and Sittig, (1957).

which results from the definition of Poisson's ratio as

$$\sigma = \tfrac{1}{2}(v_E/v_s)^{\frac{1}{2}} - 1$$

and the knowledge that $v_n = v_E$ at $d/L = 0$. Hence the ordinate for $d/L = 0$ in Figure (4.7) is a measure of the Poisson's ratio of the material of the rod. The extrapolated value of points C at $d/L = 0$ gives a Poisson's ratio of 0.2302 which is the value resulting from $f_s = 13.14$ kc/s and $f_E = 20.610$ kc/s, this latter value being that resulting from the uncorrected value of f_1 for data (a), as indeed it should be.

Care must be taken in comparing the experimental data of Figures (4.4) and (4.7), which are derived from the same values of the resonant frequencies. For $d/L > 0.6$ in Figure (4.7), the experimental points A do not lie between the theoretical curves for 0.2 and 0.2252, whereas these same data points do on Figure (4.4). This apparent contradiction arises from the fact that the data of Figure (4.4) depends upon $n.f_E/f_n$, whereas that of Figure (4.7) is a measure of $f_n/n.f_s$. In Figure (4.4), the value of f_E is derived from f_1 which is too low by an amount equal to the end-effect correction; even on adding this correction to the f_n values above $d/L = 0.6$,

the dispersion is too low to give $\sigma = 0.2252$, and thus it must be explained in terms of the f_n values being too high. Too high a value of f_n will increase the values of $f_n/n.f_s$ as shown in Figure (4.7). The low d/L value deviation from a constant Poisson's ratio shown in both graphs arises from the fact that the f_n values are low due to end-effect, the correction required becoming less and less important as n increases. In this case, the effect will show up as a decrease in the ordinates of both graphs as the reduction in f_1 is greater than the reduction in $f_2/2$ for Figure (4.4).

(d) Summary of findings for the glass specimens

Subject to the conditions concerning end-effect referred to in section (4.c.i), it can be said that the value of Poisson's ratio given by the exact theory for the short cylinders used, in terms of both the velocity dispersion and the universal point, is one that can be obtained by measurements independent of the exact theory. In fact, there is a slight difference in the values, which is not accounted for by experimental error. Nonetheless, the closeness of the values of Poisson's ratio has only been equalled by Zemaneck's work (1962) on a well-annealed aluminium cylinder which had a value of d/21 of 0.0071

compared with the value of 0.05 resulting from the longest cylinder used in the present investigation.

The method of Edmonds and Sittig has been shown to depend critically on the value of v_s used in the calculations. From Figure (1.1), it is possible to calculate the value of f_s (in the manner described above) derived from the universal point; the value obtained is 6.63 kc/s. However, the authors quote a measured value of f_s (derived from the average of the first 17 harmonics) of 6.462 kc/s. The difference in these two values explains the deviation of the experimental curve from the universal point in Figure (1.1). Thus, the adherence of the dispersion data to the theory at the universal point would give a value of σ of 0.324, whereas that obtained from the measured values of f_s and f_E would be 0.393. The authors concluded that the deviation of the experimental data from the universal point was due to anisotropy of the material of the rod. The question of the effect of anisotropy is considered further on in this chapter.

(e) Polystyrene rod measurements and discussion

(i) General observations

In order to minimise the presence of strain anisotropy in the rods, a careful annealing process was followed. The block of material, from which a rod was to be turned was annealed at about 110°C for about one hour, after which it was allowed to cool to room temperature very slowly (over about ten hours). This temperature is above the glass transition temperature, and therefore distortion of the shape of the block sometimes occurred. A rod was then turned slowly from the block, plenty of coolant being used in the process. The rod was then annealed once more, the temperature of the oven being close to but less than the estimated glass transition temperature of 95°C, in order to avoid distortion of the shape of the rod. Measurements were made of the resonant frequencies of the rod, subsequent annealings being sometimes necessary, as determined by a large scatter in the values of the resonant frequencies. The measurements of resonant frequency were made under the same conditions of temperature stability as were applied to those for the glass rods, see section (4.c.i).

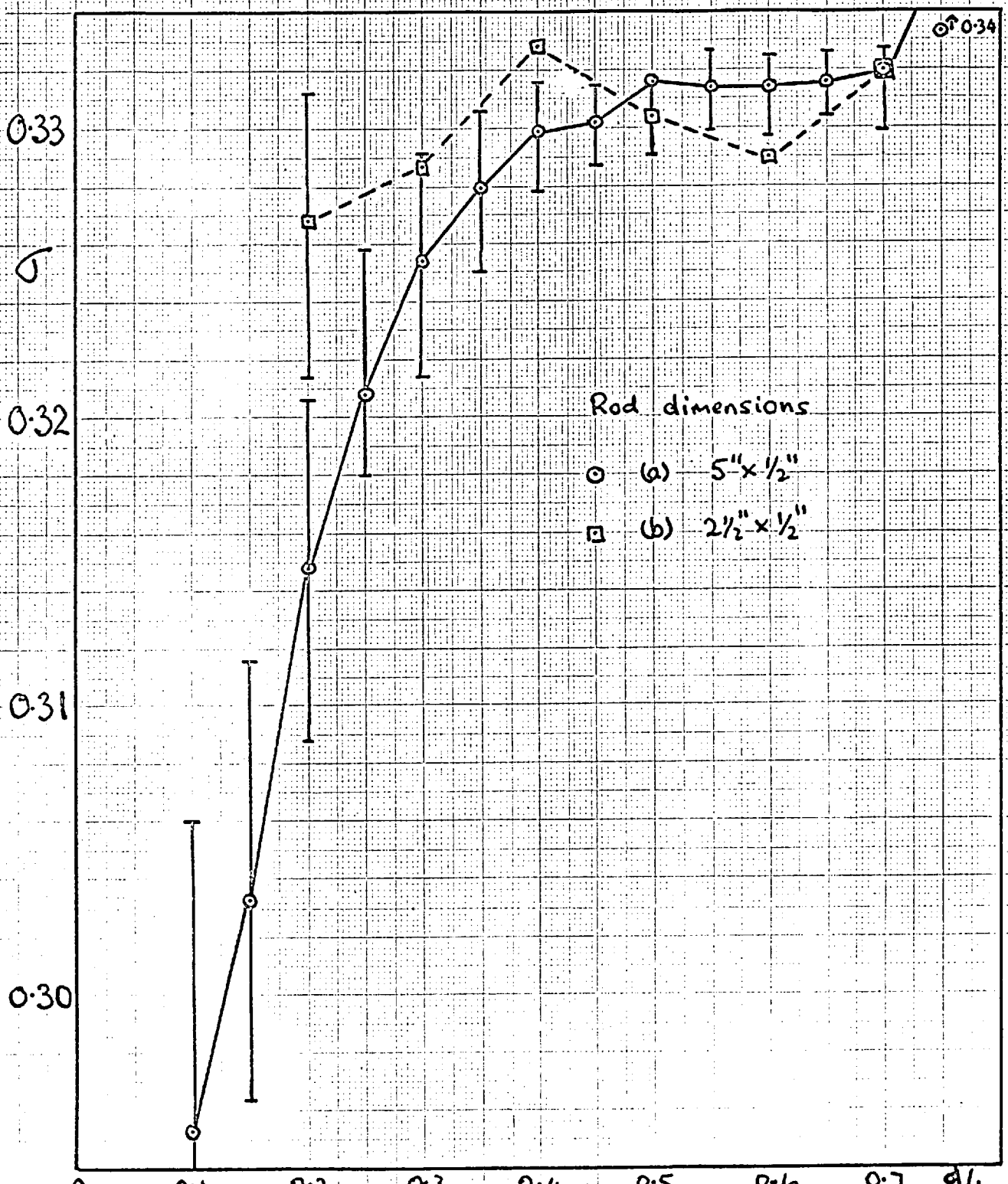

FIG.(4.8) Poisson's ratio calculated from the velocity dispersion in two polystyrene cylinders of different dimensions using the exact theory.

Figure (4.8) shows the values of Poisson's ratio obtained by method 2 for two cylinders of polystyrene, (a) a 5" x $\frac{1}{2}$" rod and (b) the same rod shortened to $2\frac{1}{2}$" x $\frac{1}{2}$", a measure of the spread of values observed for the 5" rod being shown by the appropriate vertical lines. The spread of values of the $2\frac{1}{2}$" rod is such that it is probably not quite correct to say that Poisson's ratio for the two rods is solely a function of d/L, as was the case for the glass rods, see Figure (4.5).

Figure (4.9) incorporates the same data as Figure (4.8) with a correction of 12 c/s added to each of the values of the resonant frequencies of the 5" rod, and a correction of 24 c/s added to each of those of the $2\frac{1}{2}$" rod. These are the averages of Δf obtained from the values shown in Figure (4.9), which were derived from equation (4.1). The horizontal lines of Figure (4.9) are the values of σ resulting from f_E and $f_s(1)$ for the two rods shown in Table (4.8) which shows the values of various constants of polystyrene derived from measurements on both rods. The principal source of error in the values of f_E is the error in the value of Δf. It is likely that the

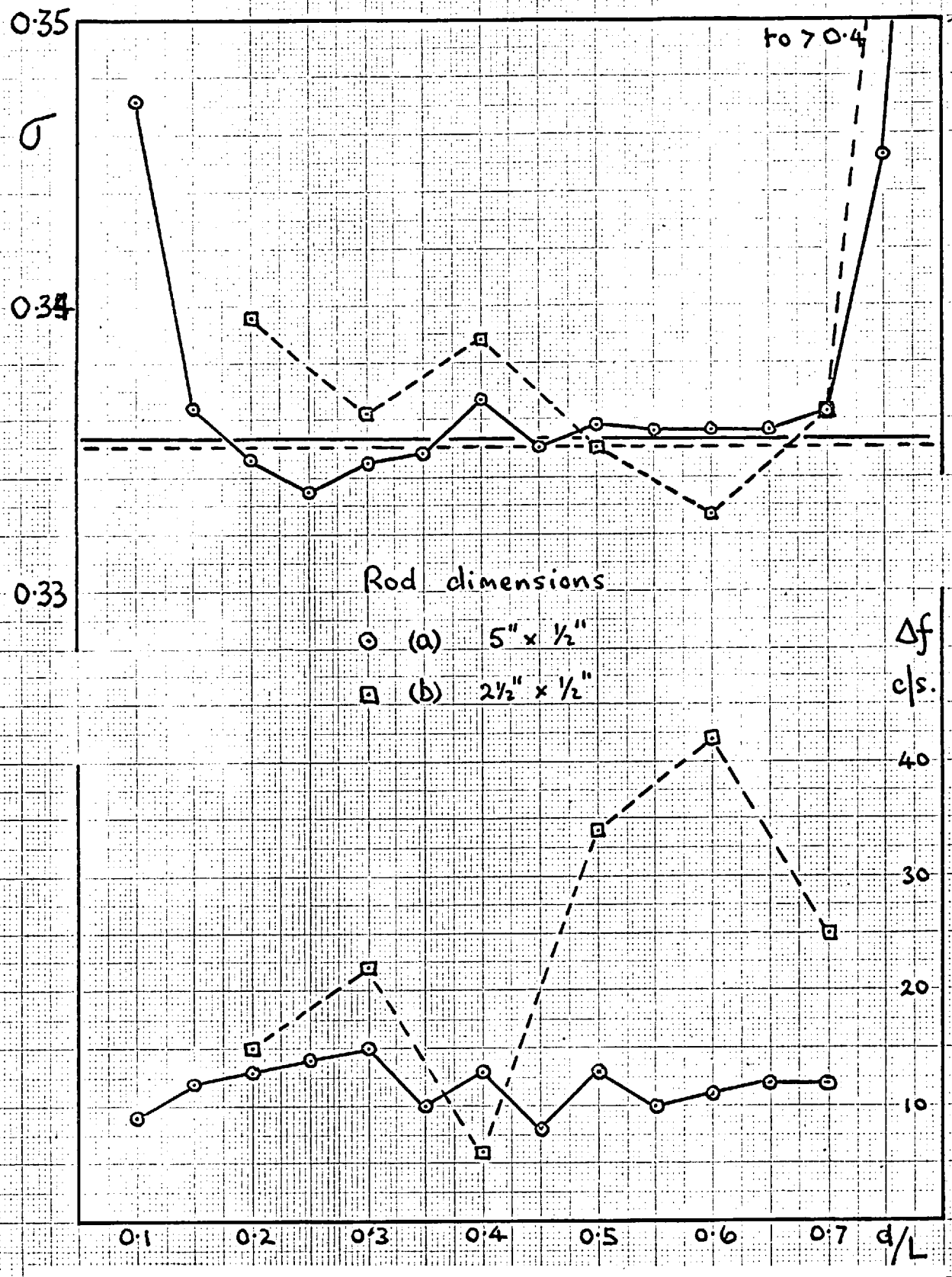

FIG.(4.9) Corrected values of Poisson's ratio and corresponding Δf values for two polystyrene cylinders of different dimensions.

value of Δf for the 5" rod is constant, though no such statement seems valid for the $2\frac{1}{2}$" rod. An attempt was made to measure the fundamental shear mode frequency in the manner described in section (3.d.ii), but the resonance was so broad and shallow, and the loading correction so great, that it is only possible to say that the value obtained was of the same order as that derived from the universal point theory. However, values of Young's modulus and the shear modulus were obtained from static loading measurements, a value of $\sigma = 0.32 \pm 0.02$ resulting. These measurements are not very accurate, depending as they do on the fourth power of the radius of the rod under test.

TABLE (4.8)

Calculated data for polystyrene rods

		$5" \times \frac{1}{2}"$	$2\frac{1}{2}" \times \frac{1}{2}"$
(1)	Δf (c/s)	12 ± 2	24 ± 12
(2)	f_E (kc/s	7.330 ± 0.002	14.669 ± 0.012
(3)	$f_s(1)$ (kc/s)	4.487 ± 0.001	8.987 ± 0.002
(4)	$f_s(2)$ (kc/s)	4.489 ± 0.002	8.977 ± 0.002
(5)	$\sigma(0)$	0.3353 ± 0.0009	0.3365 ± 0.0025.
(6)	$\sigma(1)$	0.3354 ± 0.0011	0.335 ± 0.003
(7)	$\sigma(2)$	0.3342 ± 0.0011	0.338 ± 0.003
(8)	v_E (m/s)	1862 ± 2	1863 ± 2
(9)	$v_s(2)$ (m/s)	1140 ± 1	1140 ± 1
(10)	ρ (gm/cc)	1.050 ± 0.002	
(11)	$E' \times 10^{-10}$ (dyn/cm^2)	3.640 ± 0.005	3.650 ± 0.006
(12)	$\mu' \times 10^{-10}$ (dyn/cm^2)	1.36 ± 0.02	1.36 ± 0.02
(13)	$\lambda' \times 10^{-10}$ (dyn/cm^2)	2.84 ± 0.5	2.94 ± 0.5

Notes:

(3) obtained from linear interpolation between appropriate resonances

(4) computer-interpolated from all resonant frequencies

(5) average of values of σ for $d/L < 0.70$

(6) calculated from f_E and $f_s(1)$

(7) calculated from f_E and $f_s(2)$

(10) average of values obtained from both rods

Whilst it can be said that the overall behaviour of the polystyrene rods is similar to that of the glass rods, certain differences do exist. The constant value of the correction is applicable for a slightly greater range of d/L values for the polystyrene than for the glass rods, i.e. 0.70 as opposed to 0.65. Above these values of d/L, whilst the resonant frequencies of the glass rods seem to be greater than required to give a constant Δf, those of the polystyrene rods are less. Another difference is in the scale of correction required to produce a constant Poisson's ratio at low d/L values; $\Delta f/f_E$ for the glass is about 1/5000, whereas that for the polystyrene is about 9/5000.

Figure (4.10) shows the data of the 5" rod displayed in Edmonds' and Sittig's manner, for values of f_n/n as measured and after the addition of the end-effect correction to f_n. The deviation from the theoretical curve of 0.335 at d/L = 0.6 is due to two effects. Of the 0.0005 deviation, 0.0002 is due to the fact that the correction of 12 c/s had not been added to the resonant frequencies used, and the remainder is accounted for by the fact that the value of Poisson's ratio at this value of d/L is 0.3356, and not 0.335. Displacement upwards of the theoretical plot of

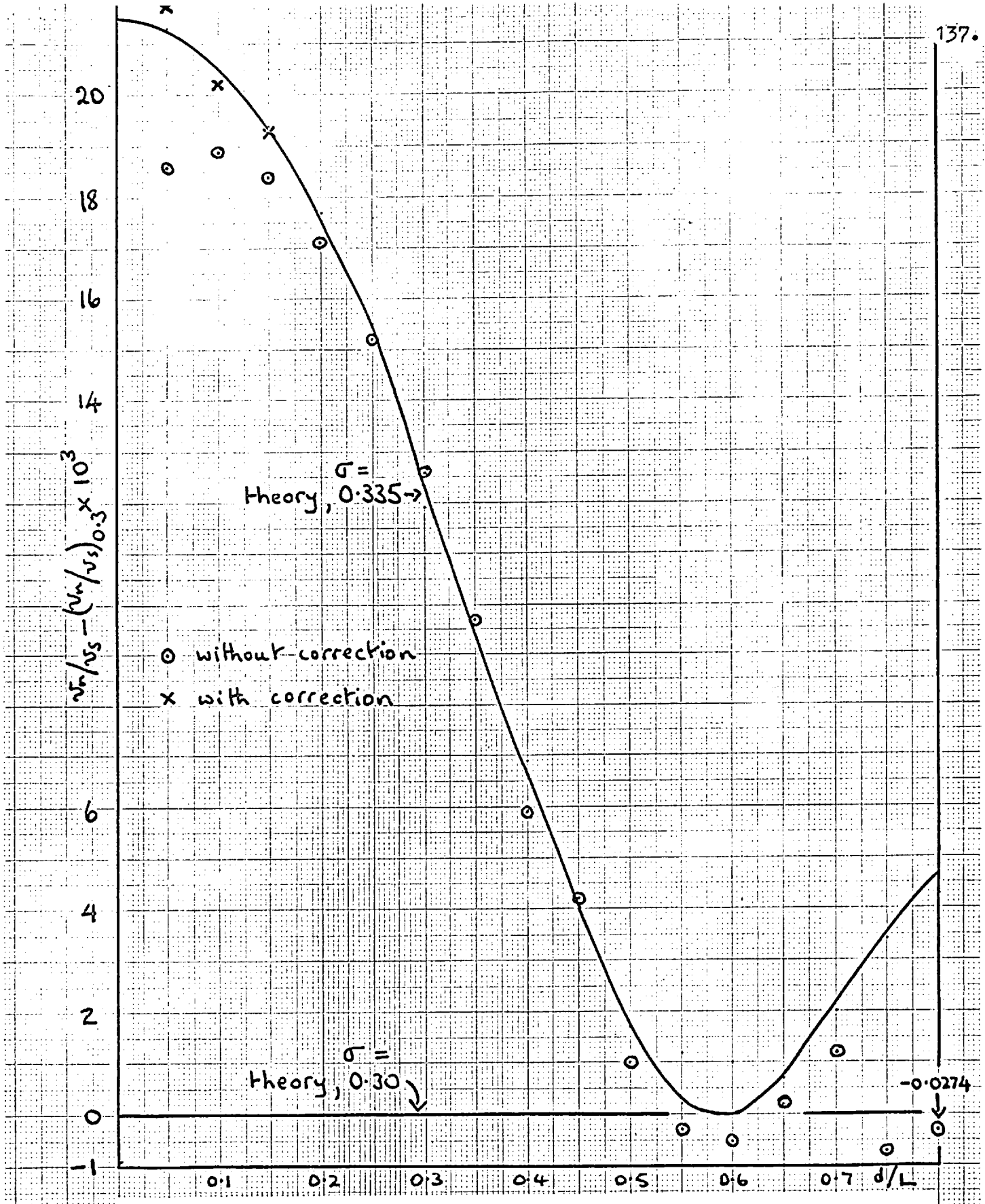

FIG.(4.10) Velocity dispersion in a 5" x ½" polystyrene cylinder presented in the manner of Edmonds and Sittig, (1957).

Figure (4.10) by 0.0003 gives an ordinate value of 0.0218, which is equal to a Poisson's ratio of 0.3354, which agrees with/value expected. The deviation at the low d/L values is due mostly to the lack of the correction, as is shown by the experimental points included in Figure (4.10) which have been calculated from the resonant frequencies to which the correction of 12 c/s had been added.

The table below shows the values obtained by others for some of the constants of polystyrene.

TABLE (4.9)

Constants of polystyrene at room temperature

Observer	$E' \times 10^{-10}$ dyn/cm^2	$\mu' \times 10^{-10}$ dyn/cm^2	σ	Comments
(1) Mason (1958)	5.28	1.2	0.41	-
(2) Wada (1959)	3.7	1.39	0.33	at 33 and 66 kc/s
(3) Wada (1959)	-	-	0.33	at 1 mc/s
(4) Nielsen (1962)	3.4	-	0.33	-

Wada et al. have calculated Poisson's ratio at 33 kc/s from -40°C to 80°C and show that it remains constant at 0.33 for the whole temperature range. As can be seen, Mason's values (quoted from the American Institute of Physics Handbook, McGraw-Hill, 1957) differ from the

others quoted, though no mention is made of the type of material used.* The values obtained from the present investigation of velocity dispersion seem to agree well with the values of Wada et al.

It can be concluded that the velocity dispersion in the polystyrene cylinders used can be expressed in terms of the exact theory for infinite loss-less cylinders subject to the condition that at low d/L values a suitable and more-or-less constant correction is made to the values of the resonant frequencies. The very high value of σ for d/L = 0.1 for the 5" rod is due to the correction there being 9 c/s whereas the average correction (which was used in calculating σ versus d/L) is 12 c/s. This n = 1 and 2 value of Δf was consistently lower than the average value for many sets of readings, and it may be that the use of an average value for Δf is erroneous. The high d/L values of Δf will be referred to in Chapter 5.

---

* The value of the Lame elastic constants quoted by Mason in the A.I.P. Handbook (1957 and 1962) are incompatible with the value of E quoted, and as given in Table (4.9). Thus $\mu = 1.2_{10}$ $\lambda = 3.4 \times 10^{10}$ dyn./cm^2 which give values of E and σ as 3.28×10^{10} dyn./cm^2 and 0.37 respectively. These values are much nearer those of Wada and of Nielsen, and also of the present investigation. It is possible that the error is a typographical one.

(ii) Effect of pin support position on values of resonant frequencies

Figure (4.11) shows the results of an experiment carried out to investigate the effect of the position of pin supports on the resonant frequencies of a 5" x $\frac{1}{2}$" polystyrene rod. The rod was supported at five different places along its length, specified by the letters (a) to (e). The positions were:

(a) one support at $\frac{1}{4}$" from each end

(b) one support placed at $1\frac{1}{4}$" from each end

(c) one support placed at $1\frac{1}{2}$" from each end

(d) one support placed at $1\frac{3}{4}$" from each end

(e) one support only, and that placed at the centre of the rod

Table (4.10) shows the values of f_E and f_n for the first four resonances used in the calculation of Poisson's ratio from the dispersion measurements which are shown in Figure (4.11). Figure (4.12) is a full-size diagram of the positions of the supports. It is suggested that Figure (4.11) shows the increasing of the values of the resonant frequencies due to the pin supports being close to the end of the cylinder. As the supports are moved nearer to the centre of therod, the effect diminishes, disappearing entirely when the support is at the centre. It is to be

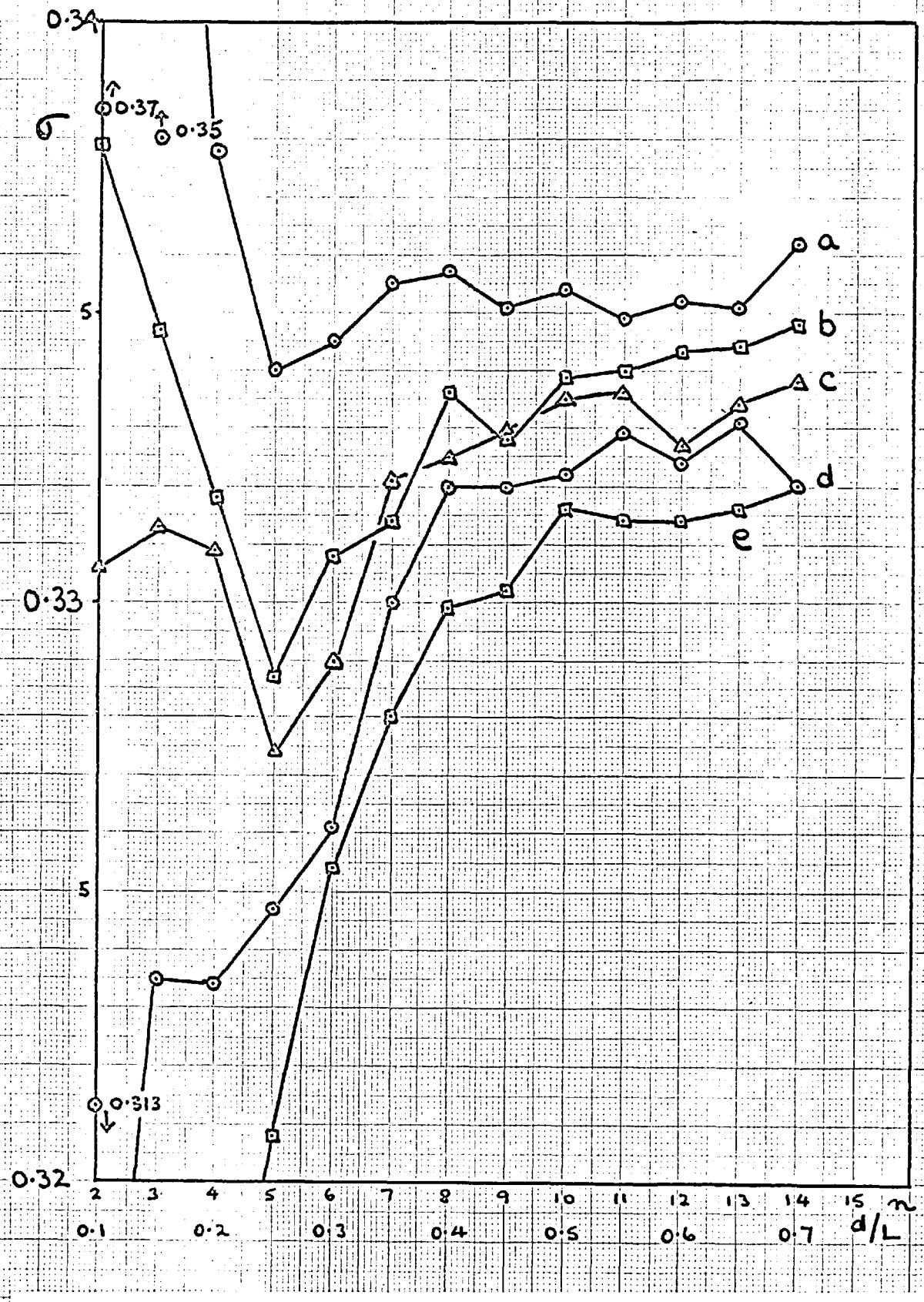

FIG.(4.11) Poisson's ratio calculated from the velocity dispersion of a 5" x $\frac{1}{2}$" polystyrene cylinder for five positions of its pin supports.

TABLE (4.10)

f_n (kc/s) versus support position for polystyrene rod

	1	2	3	4	f_E
a	7.332	14.624	21.859	28.998	7.337
b	7.326	14.620	21.855	28.989	7.331
c	7.325	14.619	21.853	28.989	7.330
d	7.323	14.619	21.853	28.993	7.328
e	7.318	14.614	21.851	28.987	7.323

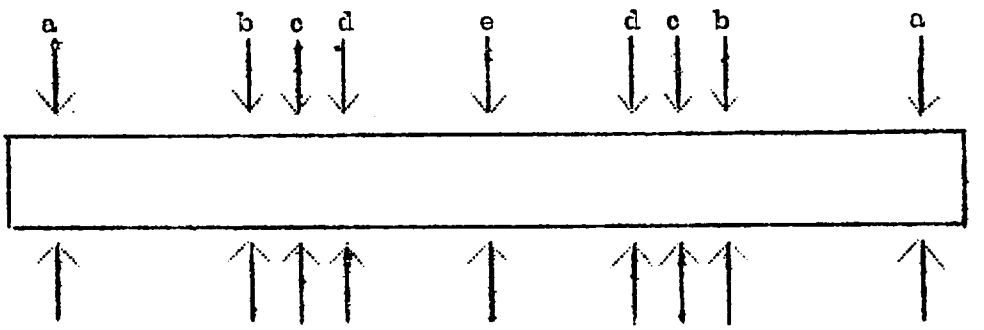

FIGURE (4.12)

Positions of supports on polystyrene rod, full size

noted that the increase in resonant frequency decreases with increasing value of n.

Appendix 6 gives a theory of the effect of a constraint placed on the ends of a rod, excited into E-mode resonance; the derivation follows Parfitt's (1954) for a centrally placed constraint. This latter theory predicts an increase in the values of the frequencies of those resonances of even number; no effect should be observed on the odd number resonances as the supports are then placed at anti-nodes. The effect of an increase in the value of the odd number resonances would be to decrease the value of the Poisson's ratio for these values, as calculated from dispersion, by method 1 or 2, though no such effect is noted for the values (e) of Figure (4.11). The theory given in Appendix 6 predicts that the values of all the resonant frequencies are increased when a constraint is applied at each end, and by an amount which is inversely proportional to n^2, though the effect demonstrated in Figure (4.11) and Table (4.10) is proportional to $1/n$, rather than to $1/n^2$. From the values of f_1 for data (a) and data (e), it is possible to estimate the value of e_o, the stiffness constant of the constraint, for $E = 3.4 \times 10^{10}$ dynes/cm^2 and $n = 1$. The value obtained is 4.8×10^{-8} dynes/cm^3.

Unfortunately, use of the values of the other resonances, (a) and (e), in a similar manner gives a value of e_o which doubles as n increases by unity from n = 1. A more serious fault of the theory however, is that the effect of a support at each end is less than that of one support in the middle (compare equations (A6.6) and (A.6.11)) which seems unlikely, particularly as no effect of a central constraint has been detected. Perspex rod resonances showed some indication of the effect similar to that found in the polystyrene rod, but the Q values of the resonances of perspex rods are so low that accurate measurement of the resonant frequencies was impossible. It is not surprising that a glass rod did not show any support effect because the pins of the support system do not penetrate the surface of the rod, it being hard and brittle. However, an aluminium rod is soft enough for steel pins to penetrate its surface, and yet no increase in the values of the resonant frequencies were observed. Reference to equation (A6.12) offers some explanation. The increase in frequency predicted by this theory is proportional to $(e_o/E)^2$. As the value of E of aluminium is about a factor of 20 greater than that of polystyrene, the constraint on an aluminium rod must be 20 times

greater for a shift in the resonant frequencies equal to that observed in the polystyrene rod. The most important variable determinants of e_o are the length of the pin between cylinder and fastening point and the tension of the spring holding the top pin, neither of which is capable of increasing the value of e_o by the amount required.

(f) Perspex rod measurements and discussion

As for the polystyrene cylinders, care had to be taken with the annealing process for the perspex cylinders. The glass transition temperature of perspex is about 120°C and therefore the block from which the cylinders were to be turned was heated slowly up to a temperature of 135°C and left there for about an hour, after which it was slowly cooled to room temperature. After turning the rods from the block, they were annealed at temperatures close to but below 120°C, e.g. 100°C to 110°C.

Whilst the problem of annealing the specimen rods was great, the main experimental problem was the accurate determination of the values of the resonant frequencies.

The Q values of the glass cylinder resonances were of the order of 5,000 and those of the polystyrene rods 300. However, the Q values of the perspex rods were only of the order of 30, which resulted in an experimental error in values of f_n/n of $\pm$ 5 c/s for the higher n values.

Notes for Table (4.11) (following)

* by definition

(3) calculated from uncorrected resonant frequencies and $\sigma = 0.350$

(4) Δf calculated for $\sigma = 0.35$

(5) Δf calculated for $\sigma = 0.30$

(6) calculated from dispersion data derived from resonant frequencies corrected by $\Delta f = 100$ c/s

TABLE (4.11)

Calculated values of σ and Δf for 5" perspex rod

n	d/L	(1) f_n/n(kc/s)	(2) v_m/v_n	(3) σ(1)	(4) Δf(1)(c/s)	(5) Δf(2) (c/s)	(6) σ(2)
1	0.05	8.560	1.00076*	0.350*	-	-	0.300*
2	0.10	8.590	0.9973	-	100	90	0.35_0
3	0.15	8.595	0.9970	-	130	115	0.28_5
4	0.20	8.555	1.0014	~0.11	130	.95	0.31_0
5	0.25	8.535	1.0040	~0.14_5	180	125	0.27_5
6	0.30	8.440	1.0148	0.23_0	165	100	0.30_5
7	0.35	8.380	1.0222	0.23_5	220	120	0.29_0
8	0.40	8.335	1.0278	0.21_6	320	185	0.26_0
9	0.45	8.115	1.0556	0.26_7	245	95	0.31_1
10	0.50	7.965	1.0759	0.26_6	285	115	0.29_6
11	0.55	7.745	1.1064	0.27_6	270	80	0.31_3
12	0.60	7.535	1.1373	0.27_2	290	115	0.29_3
13	0.65	7.280	1.1765	0.27_5	265	95	0.31_3

Table (4.11) shows the values of f_n/n obtained for a 5" x $\frac{1}{2}$" perspex rod, held centrally by one pin support, and excited by the condenser microphone technique. It is immediately seen that the values of f_n/n for n = 2 and 3 are higher than that for n = 1. The cause of this is the very high value of the end-effect correction which produces a greater effect in the values of the resonant frequencies than does the dispersion. Values of the end-effect correction have been calculated for two values of Poisson's ratio, 0.35, which is the value quoted by the manufacturers (I.C.I. Ltd.), and 0.30 which was found by trial and error to be the value of σ which gave a more or less constant value of Δf, whose average value was 100 $\pm$ 15 c/s. If constancy of Δf is the criterion which determines the value of Poisson's ratio, then Table (4.11) shows that this value is 0.30.

Table (4.12) gives values of the constants of perspex calculated from the measurements taken from the 5" rod and from a rod made from the same block and of dimensions $2\frac{1}{2}$" x $\frac{1}{2}$". It is seen that the values of σ resulting from the

TABLE (4.12)

Calculated data for perspex

Rod length	5"	$2\frac{1}{2}$"
(1) Δf, c/s	100±15	300±50
(2) f_E, kc/s	8.67±0.02	17.47±0.05
(3) $f_s(1)$, kc/s	5.37±0.01	-
(4) $f_s(2)$, Kc/s	5.30±0.06	10.68±0.05
(5) $\sigma(0)$	0.30±0.02	0.31$_5$±0.02
(6) $\sigma(1)$	0.30±0.01	-
(7) $\sigma(2)$	0.34±0.03	0.34±0.03
(8) v_E, m/s	2202±5	2218±5
(9) $v_s(2)$, m/s	1346±4	1356±5
(10) ρ, gm/cc	1.181±0.001	1.178±0.001
(11) $E' \times 10^{-10}$, dyn./cm^2	5.73±0.01	5.80±0.01
(12) $\mu' \times 10^{-10}$, dyn./cm^2	2.13±0.01	2.17±0.01
(13) $\lambda' \times 10^{-10}$, dyn./cm^2	4.7±0.1	4.5±0.1

Notes:

(3) obtained by a linear interpolation

(4) obtained by a computer interpolation

(5) average of values from column (6) of Table (4.11) and equivalent for $2\frac{1}{2}$" rod

(6) calculated from $f_s(1)$ and f_E

(7) calculated from $f_s(2)$ and f_E

dispersion data and from the universal point theory are about the same, within the large experimental errors. Due to the high damping factor of perspex it was quite impossible to measure Poisson's ratio by either of the two other methods available, though static loading experiments gave a value of 0.33 ± 0.03.

The table below shows the values of certain constants of PMMA obtained by other workers. As for the polystyrene, no mention is made of the nature of the material under test, and some of the data is offered with no reference to the method of measurement.

TABLE (4.13)

Constants of PMMA at room temperature

Observer	$E' \times 10^{10}$ dyn./cm^2	$\mu' \times 10^{10}$ dyn./cm^2	Poisson's ratio	Comments
(1) Mason (1958)	4.0	1.4	0.4	-
(2) Wada (1959)	6.3	2.2	0.4	at 33 kc/s
(3) Nederveen (1962)	6.0	2.2	0.28-0.50	at 10 kc/s
(4) Nielsen (1962)	3.7	-	0.33	-
(5) I.C.I.Journal	-	-	0.35	statically measured
(6) Heyde mann (1962)	5.0	-	-	50 c/s - 1000 c/s flexural mode

Koppelmann (1958) has measured E' and μ' through a secondary transition (see section (2.f)) in PMMA at room temperature; the position of the transition is at about 5 c/s. A frequency dependent value of σ was obtained, with a minimum occurring at about 10 c/s. Nederveen (1962) has also investigated the material over the same frequency range, but did not find the minimum observed by Koppelmann. The following table shows the findings of these two workers.

TABLE (4.13a)

Frequency dependence of Poisson's ratio for perspex

Frequency c/s	10^{-3}	10^{-2}	10^{-1}	10^{0}	10^{1}	10^{2}	10^{3}
Koppelmann	0.30	0.32	0.31	0.25	0.12	-	0.32
Nederveen	(0.22 - 0.35)		-	0.29 to 0.39	(.30 - 0.45)		

As can be seen, Nederveen quoted very wide tolerances for the possible values of Poisson's ratio arising from inaccuracies in measuring E' and μ'. He did not find the minimum in Poisson's ratio observed by Koppelmann and found that the range of values quoted in Table (4.13a) for the frequencies 10^{-3} to 10^{-2} remained constant to 10^{-6} c/s. Wada showed that σ remained constant at 0.4 from 20°C to 100°C, but that below this temperature it decreased

to 0.35 at - 40°C. Wada's measurements were made at 33 kc/s. The problem of a frequency dependent value of Poisson's ratio will be considered in Chapter 5.

As can be seen from Table (4.12), the value of Poisson's ratio obtained from f_E and $f_s(2)$ agrees reasonably well with the value quoted by Nielsen and the I.C.I. value. However, it has been shown that only a value of Poisson's ratio of 0.30 will give a constant end-effect correction.

Some comment should be made on the difference between static and dynamic values of Poisson's ratio. Landau and Lifshitz (1959), show that the difference between the adiabatic (dynamic) and isothermal (static) values of Young's modulus, E_a and E_i respectively, is given by

$$\frac{1}{E_i} - \frac{1}{E_a} = \frac{\alpha^2 . T}{9 . C_p . \rho} \qquad (4.2)$$

where T is the absolute temperature

α is the coefficient of linear expansion

C_p is the specific heat, and

ρ is the density of the material.

As $\mu_i = \mu_a$ it can be shown that

$$E_a/E_i = (1 + \sigma_a)/(1 + \sigma_i) \qquad (4.3)$$

where σ_a and σ_i are the dynamic and static values of Poisson's ratio, respectively. On putting the appropriate values of the constants into equation (4.2), equation (4.3) shows that for $\sigma_a = 0.3500$, the value of σ_i would be 0.3502, too small a difference to account for the range of values quoted above in Table (4.13).

The experimental results obtained for the perspex cylinders are unsatisfactory in that the large experimental errors involved in the measurement of the dispersion produced large errors in the values of Poisson's ratio so derived. There appears to be a large variation in the value of Poisson's ratio observed by workers in the field, the most obvious reason for this being the presence of a frequency-dependent molecular process in the range of frequency (or temperature) used. It is possible, nevertheless, to conclude with reasonable confidence that the data of Table (4.11) exhibits the behaviour predicted by the exact theory, if a suitable correction is made to f_n, though whether for a value of σ obtainable by other methods seems open to doubt. The value of the work done on the perspex cylinders is that the end-effect correction on the resonant frequencies is so large that it is easily observed for the 5" x $\frac{1}{2}$" cylinder. Resonances higher than the thirteenth were very difficult to measure with any confidence; it is

probably safe to say that they are lower than would be given by the exact theory after addition of the constant end-effect, being similar to those of the polystyrene cylinders in this respect, and not like those of the glass cylinders.

The values of E' obtained from the 5" and the $2\frac{1}{2}$" cylinders are not the same, even when taking account of the experimental errors. If the end-effect corrections were not added to the values of the fundamental resonant frequency used to obtain f_E and hence E', however, the values of E' obtained from the 5" and the $2\frac{1}{2}$" rod would be 5.60×10^{10} dynes/cm^2 for both. This point will be returned to in Chapter 5.

(g) The effect of material anisotropy on the measurements

Two aluminium alloy cylinders of dimensions $8\frac{1}{3}$" x $\frac{1}{2}$" were cut from different blocks of commercial material which had been annufactured by an extrusion process. Thus the material of the cylinders was anisotropic, and no attempt was made to correct this. The values of the resonant frequencies of the rods were measured, after which they were shortened and the new resonance frequencies determined.

Values of Poisson's ratio calculated by method 2 from the uncorrected values of the resonant frequencies for the

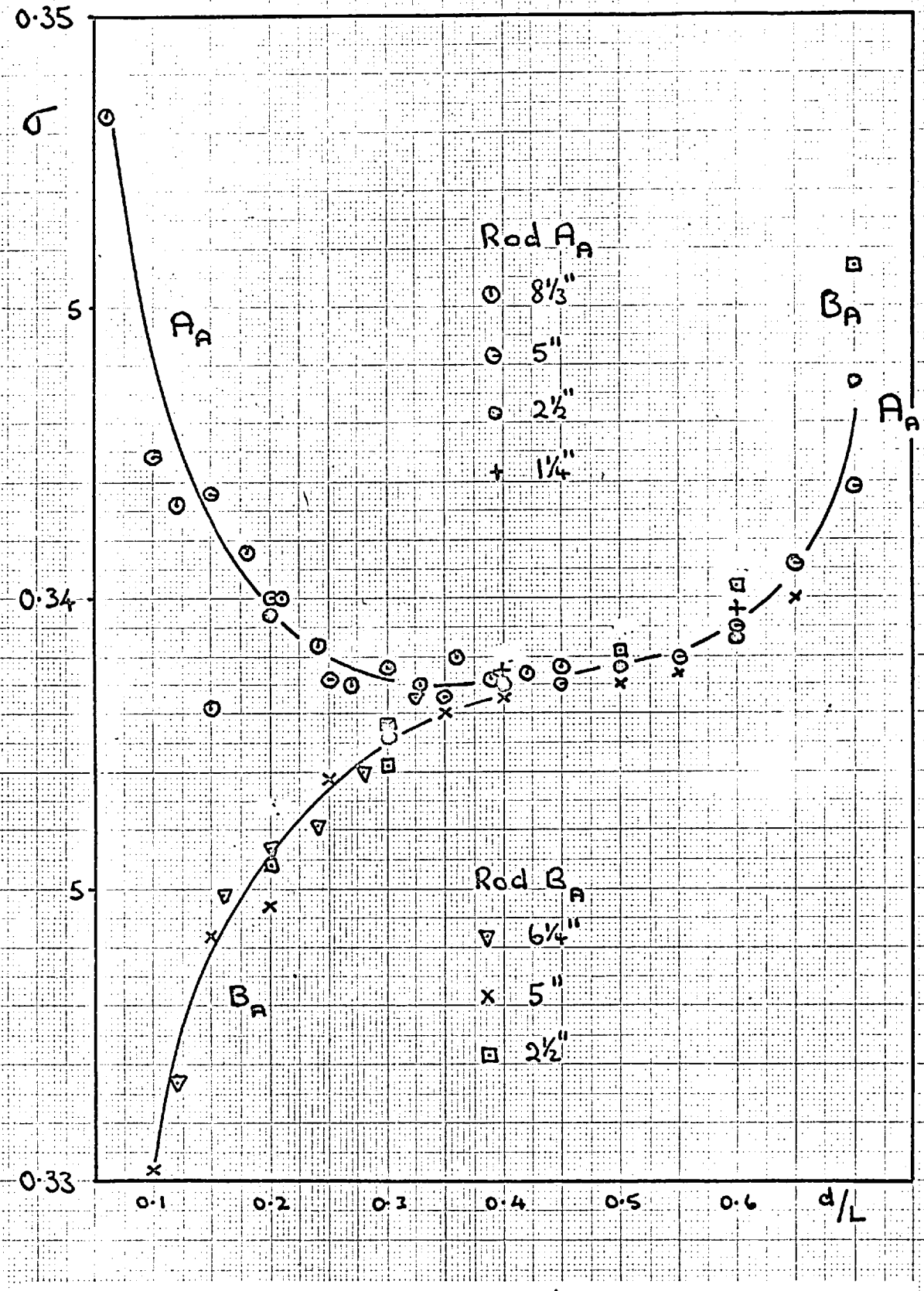

FIG.(4.13) Poisson's ratio, as given by the exact theory, for successively shorter lengths of two anisotropic aluminium alloy cylinders.

rods are shown in Figure (4.13). From Figure (4.13) it is seen that Rod A_A would give a negative value of the end-effect correction, whilst Rod B_A would give a positive value, which is to be expected.

Figure (4.14) shows the data presented in the manner of Edmonds and Sittig, the values of f_s used to obtain the experimental points being directly measured, as described in section (3.d.ii). The values of v_s obtained directly and by interpolation at the universal point are shown in Table (4.14), with v_E obtained from f_1 (with no adjustment for end-effect); the values of Poisson's ratio resulting from these values used in equation (1.22) are also given.

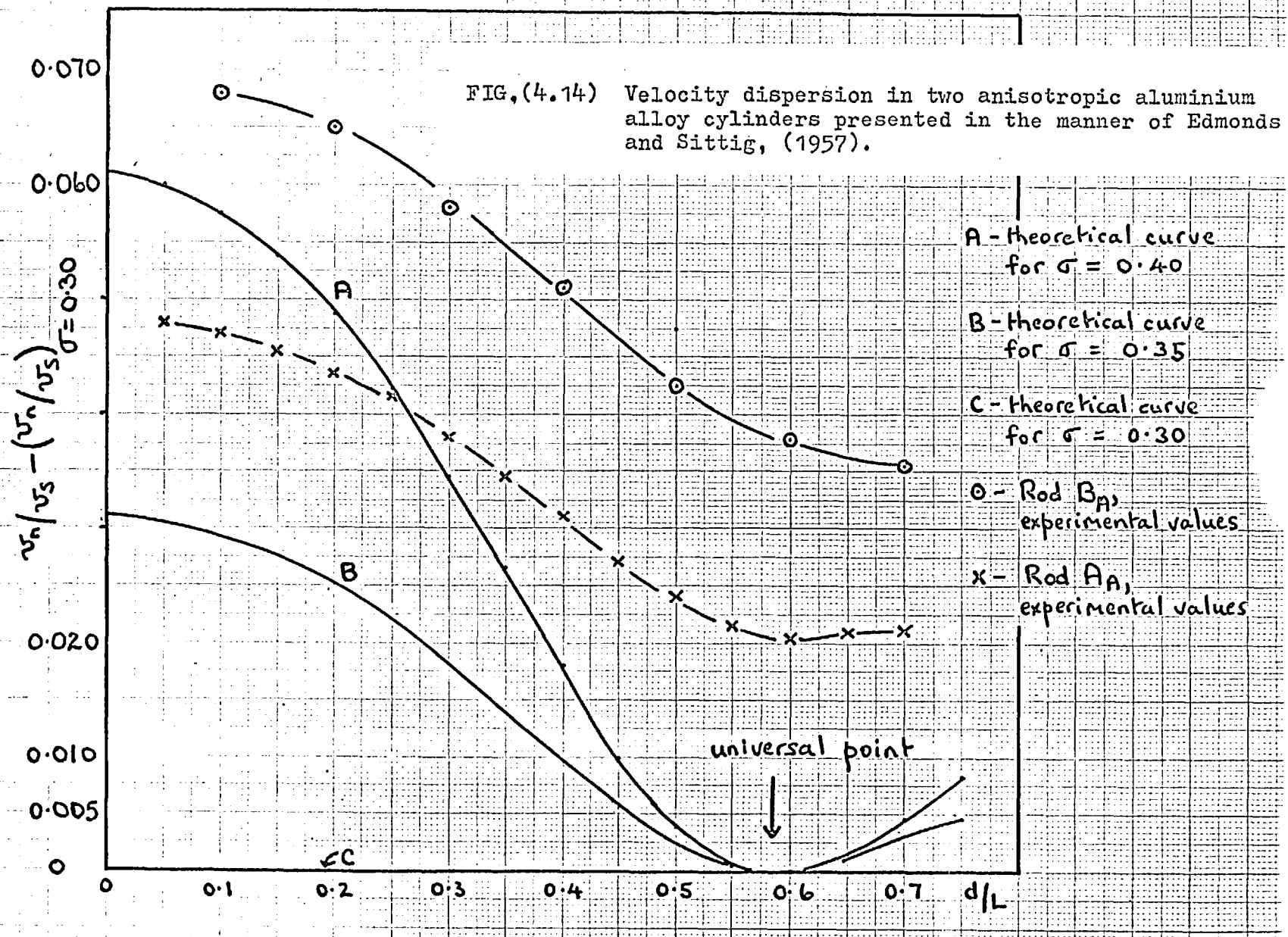

FIG.(4.14) Velocity dispersion in two anisotropic aluminium alloy cylinders presented in the manner of Edmonds and Sittig, (1957).

TABLE (4.14)

Calculated values of v_E, v_s and σ for rods A_A and B_A

	A_A	B_A
(1) v_E, m/s, measured	5164±2	5196±2
(2) v_s, m/s, measured	3116±9	3096±9
(3) σ (m)	0.373±0.009	0.408±0.009
(4) v_s, m/s, interpolated	3157±2	3167±2
(5) σ (i)	0.338±0.002	0.346±0.002

Notes:

(3) calculated from equation (1.22) and values of (1) and (2)

(4) linear interpolation between eleventh and twelfth resonances for 5" x ½" rod

(5) calculated from equation (1.22) and values (1) and (4)

As can be seen, the interpolated and directly measured values of v_s are quite different, and this is assumed to be due to anisotropy of the material of the cylinders, as is the negative end-effect of Rod A_A of Figure (4.13).

In order to investigate the effect of anisotropy on the values of E', μ' and σ, two further cylinders of aluminium alloy were made. The dimensions of these rods were 5" x $\frac{1}{2}$", which were used for measurements of velocity dispersion and 1" x 1" which was used for the 5 mc/s pulse technique measurements. These cylinders, machined from commercial rod, originally of $1\frac{1}{4}$" in diameter, were cut such that their axes were in the same direction as the axis of the original rod.

After measurements had been made on both rods, they were heated to 400°C for two hours and then allowed to cool slowly in the oven over a period of eight hours. Measurements were then made on both cylinders. Following this first heat treatment, the cylinders were once more heated to 400°C and then suddenly quenched in water at room temperature. The measurement of the various constants of the material of the cylinders was again made. Table (4.15) shows the values of these constants before any heat treatment and after each of the heat treatments described

above. The effect of these heat treatments on grain size and direction, as observed on the etched surface of a test cylinder of the same material using a low-powered microscope, was negligible.

TABLE (4.15)

Effect of heat treatment on constants of aluminium alloy

	BEFORE		AFTER 1st		AFTER 2nd	
	rod resonace	5mc/s pulse	rod resonance	5mc/s pulse	rod resonance	5mc/s pulse
(1) E'	7.497	-	7.560	-	7.632	-
(2) $\mu'(2)$	2.797	-	2.813	-	2.835	-
(3) $\mu'(m)$	2.717	2.773	2.775	2.720	2.785	2.740
(4) $\lambda'(2)$	5.95	-	6.20	-	6.37	-
(5) $\lambda'(m)$	8.55	5.914	7.28	6.066	7.94	6.127
(6) σ (2)	0.3400	-	0.3440	-	0.3460	-
(7) σ (m)	0.3795	0.3405	0.3620	0.3450	0.3700	0.3455
(8)	12%	-	5%	-	7%	-

Notes: Units of (1) to (5) are 10^{11} dyn./cm^2. No end-effect corrections have been added.

(2) is the computer interpolated value. (3) is the directly measured value. (4) is calculated from (1) and (2). (5) is calculated from (1) and (3). (6) is calculated from (1) and (2). (7) is calculated from (3) and (5). (8) is

$$[\sigma(m) - \sigma(2)] / \sigma(2)$$

Errors: (1) $\pm$ 0.003, (2) $\pm$ 0.002, (3) Rod, $\pm$ 0.006; 5 mc/s $\pm$ 0.002, (4) $\pm$ 0.02, (5) Rod, $\pm$ 0.06; 5 mc/s $\pm$ 0.002, (6) $\pm$ 0.0015, (7) Rod, $\pm$ 0.0010; 5 mc/s $\pm$ 0.0002.

Figure (4.15) shows the effect of the heat treatment on the dispersion measurements as displayed in the manner of Edmonds and Sittig. Plot A is the theoretical plot for $\sigma = 0.35$, plot B for $\sigma = 0.30$ and plots C, D, E are the experimental plots of the dispersion before heat treatment, after the first and after the second heat treatments respectively. The values of v_s used in these last three plots is the value obtained by a direct measurement of the fundamental shear mode frequency which also gave the values of μ' shown as $\mu'(m)$ of Table (4.15), for the rod resonance column.

The first conclusion to be drawn from Figure (4.15) is that heat treatment results in the ordinate of this graph being either increased or decreased, depending on the effect of the heat treatment on the value of v_s as measured by the fundamental shear mode frequency. The deviation from zero of the ordinate at the universal point is therefore seen as arising from a difference between the values of v_s resulting respectively from an interpolation at the universal point and from this direct measurement of the fundamental shear mode frequency. This difference is observed in the difference between the values of $\mu'(m)$ and $\mu'(2)$, and between $\sigma(m)$ and $\sigma(2)$ of Table (4.15). Row (8) of this table shows the percentage difference between $\sigma(m)$ and $\sigma(2)$, showing that heat treatment

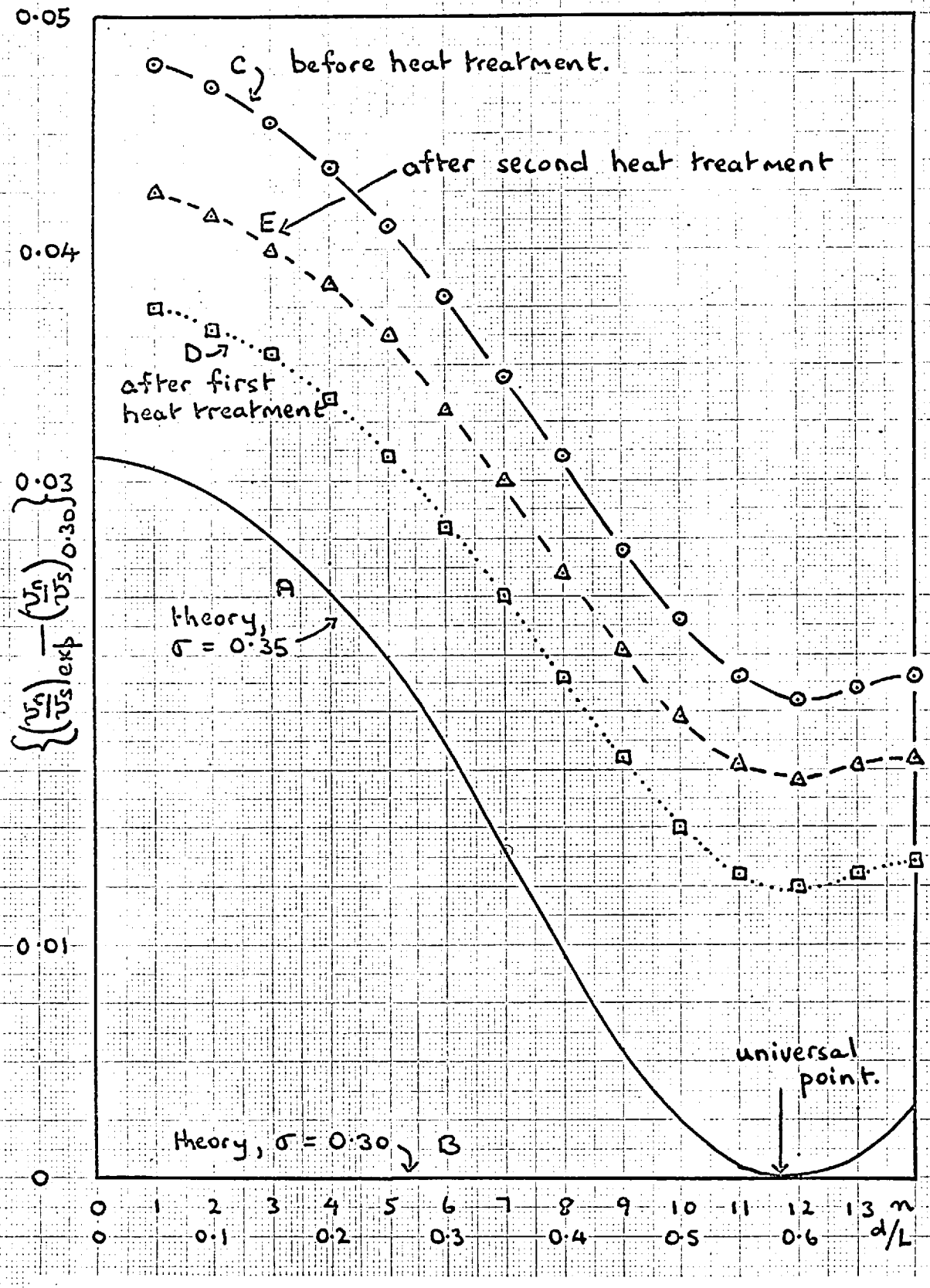

FIG.(4.15) The effect of heat treatment of a 5" x $\frac{1}{2}$" aluminium alloy cylinder on the velocity dispersion, as presented in the manner of Edmonds and Sittig, (1957).

affects the deviation from the universal point. Plots C, D and E can be made to pass through the universal point, for this is what is in effect done on obtaining a value of v_s from the theory of the universal point. It can therefore be concluded that this is the cause of the deviation from the universal point of the experimental plot obtained by Edmonds and Sittig (1957) and reproduced as Figure (1.1). The deviation from the theoretical shape of the plot at high d/L values will be referred to in Chapter 5. It is to be remembered that even if the experimental plots C, D and E were made to go through the universal point, then they would only meet at that point. This is shown by the difference in the values of σ (2) before and after the heat treatment. This value of Poisson's ratio is the one to which the experimental values of dispersion most closely fits when use is made of the exact theory tables of v_E/v_n as a function of d/L and σ , a constant value being obtained as a function of d/L only when an appropriate correction is made to the resonant frequencies.

The values of Δf obtained both before and after heat treatment are negative and exhibit a good deal of scatter. However, it was observed that the range of values did not change much after the heat treatments. The values of Δf obtained for rod B_A of Table (4.14) were positive and showed a

reasonable constancy, having an average value of about 8 c/s for the 5" long cylinder, being therefore about twice as big as that for the glass cylinder of the same dimensions. No firm conclusions on the effect of heat treatment on the values of Δf are possible from the data obtained in these experiments, and further comment is reserved until Chapter 5.

TABLE (4.16)

Comparison of Poisson's ratio for heat-treated rod

	Before	After 1st	After 2nd	Rod B_Δ
(1) σ (2)	0.340	0.344	0.346	0.353
(2) σ (m), 5mc/s	0.3405	0.3450	0.3455	0.346
(3) σ (m), rod	0.3795	0.3620	0.3700	0.408

Notes:

(1) obtained from f_E and the value of f_s resulting from a computer interpolation at the universal ^{s}point

(2) resulting from the 5 mc/s pulse experiments

(3) resulting from f_E and the value of f_s obtained by a direct measurement

Errors: (1) $\pm$ 0.0015 (2) $\pm$ 0.0002 (3) $\pm$ 0.0010

Table (4.16) shows the values of $\sigma(2)$, and of $\sigma(m)$ obtained from the rod in resonance and the 5 mc/s pulse measurements taken from Table (4.15). Values of Poisson's ratio for the rod B_A of Table (4.14) are also given. It is seen that the agreement between $\sigma(2)$ and $\sigma(m)$ for the 5 mc/s pulse experiments is better than the agreement between the two values of $\sigma(m)$. Though no such simple conclusion can be drawn for the values of μ' obtained by the three methods described above, see Table (4.15); the corresponding values of λ' seem to bear the same relationship to each other as do the values of Poisson's ratio, though this follows from the relatively small differences between the values of μ'obtained by the three methods. Without more detailed knowledge of the nature of the anisotropies causing the differences in values of Poisson's ratio, further comment is not possible.

Zemaneck and Rudnick (1961) presented data which showed that for d/L values up to 0.30, Rayleigh's approximate solution of the wave equation gave dispersion values which were closer to those determined experimentally than given by the exact solution, for a value of the Poisson's ratio of the aluminium cylinder obtained from a measurement of the first resonances of the E-mode and of the shear mode.

TABLE (4.17)

Comparison of exact solution and Rayleigh's approximate solution for rod A_A

d/L	(1) v_n/v_E exp.	(2) $(v_n/v_E)_e$ 0.340	(3) $(v_n/v_E)_R$ 0.349	(4) $(v_n/v_E)_e$ 0.379	(5) σ_R	(6) σ_e
0.10	0.9970_5	0.99711	0.99699	0.99642	0.3445	0.3424
0.15	0.9933_0	0.99340	0.99324	0.99186	0.3465	0.3421
0.20	0.9879_5	0.98800	0.98798	0.98529	0.3493	0.3406
0.25	0.9808_0	0.98071	0.98122	0.97654	0.3527	0.3391
0.30	0.9714_0	0.97126	0.97295	0.96541	0.3591	0.3392
0.35	0.9596_0	0.95933	0.96319	0.95167	0.3657	0.3386

Notes:

(1) experimental values, calculated by method 1

(2) theoretical values for $\sigma = 0.340$, from exact solution

(3) theoretical values for $\sigma = 0.349$, from Rayleigh's solution

(4) theoretical values for $\sigma = 0.379$, from exact solution

(5) values of σ calculated from column (1) and Rayleigh's solution

(6) values of σ calculated from column (1) and exact solution, see Figure (4.13).

Table (4.17) shows a comparison of the dispersion, v_n/v_E, obtained experimentally from rod A_A, with that calculated from both the Rayleigh solution and the exact solution for three values of Poisson's ratio. As can be seen, whilst the experimental values of the dispersion (column (1)) give a Poisson's ratio of about 0.34 (column (6)), a value of 0.349 will give values of dispersion from the Rayleigh solution (column (3)) closer to the experimental values than does the value of Poisson's ratio of 0.379 obtained from f_E and f_s both obtained experimentally, and the exact solution. The values of Poisson's ratio resulting from the use of the experimentally-obtained dispersion in Rayleigh's solution are given in column (5) and column (6) gives the values of σ obtained from the same dispersion data used with the exact solution. Whilst Table (4.16) does not reproduce the findings of Zemaneck and Rudnick (in their investigation, the values of σ · · in columns (5) and (6) were the same), it is obvious that there can be a closer fit of the experimentally-determined dispersion values to Rayleigh's approximate solution for some given value of σ than to the exact theory for the value of σ obtained from f_E and f_s for cylinders which are not isotropic.

(h) General discussion of velocity dispersion measurements

It has been shown that the velocity dispersion as measured in short cylinders is as predicted by the exact theory, if the resonant frequencies are suitably corrected. Up to a certain value of d/L (0.60 for glass, 0.70 for polystyrene, and about 0.70 for perspex), this correction is constant, and seems to depend on the nature of the material. Thus, for rods of dimensions 5" x $\frac{1}{2}$", the value of $\Delta f/f_E$ for glass, polystyrene and perspex are 1/5000, 9/5000 and 70/5000. More will be said on this subject in Chapter 5. The value of Poisson s ratio calculated from the value of f_s which is obtained from the theory of the universal point is the same as the average value resulting from the dispersion calculations, subject to the conditions concerning end-effect referred to above.

Within experimental error, it has been shown that values of Poisson's ratio obtained independently of the dispersion calculations are close to those derived from the latter and from the theory of the universal point, for the well-annealed glass cylinder. Due to the high internal losses of the polystyrene and perspex, the alternative methods were insufficiently accurate for measurements to be made.

A considerable variation in the quoted values of Poisson's ratio for polystyrene and perspex seems to exist in the literature, for which no explanation is offered.

The effect of anisotropy of the specimen under test on the values of the Lame elastic constants is considerable, the precise effect produced depending on the nature of the anisotropy. It is concluded that the deviation of experimental plots of dispersion shown by Edmonds and Sittig is due to the anisotropic nature of the cylinder under test, and that the fitting of Rayleigh's approximate solution to the experimental values obtained by Zemaneck and Rudnick, rather than to the exact solution, may well be due to the same effect, as these latter authors pointed out.

Finally, in reference to the three problems posed in section (1.h), it can be said that:

1. Subject to a suitable and small correction, the phase velocity dispersion in short and almost loss-less cylinders does follow the dependence on d/L and Poisson's ratio as given by the theory.

2. Rods made from materials having a finite damping coefficient seem to obey the exact theory, subject to the

application of an appropriate correction, as previously described.

The question of a possible end-effect is raised in Chapter 5.

CHAPTER 5

DISCUSSION OF THE ΔF CORRECTION TERM

(a) Summary of experimental findings and their significance

(i) Dependence of $\Delta f/f_E$ on damping factor

It was shown in section (4.h) that the value of $\Delta f/f_E$ depended on the material of the rod under test. It was decided therefore to investigate the dependence of $\Delta f/f_E$ on damping factor, and Figure (5.1) shows this dependence for ten similar rods of different materials, dimensions 5" x $\frac{1}{2}$". The value of Δf will be shown to depend critically on the correction for dispersion, c_n, occurring in equation (4.1) which itself is determined by Poisson's ratio. The value of Poisson's ratio is known only for glass and polystyrene with any confidence and therefore, the values of Δf for $\sigma = 0.2$, 0.3 and 0.4 were calculated. The damping factor is frequency-dependent and therefore a range of values of δ_E exists. Thus it is seen that the values of $\Delta f/f_E$ can occur at any point within a rectangle whose dimensions are defined by the frequency dependence of δ_E and by the dependence of Δf on σ.

Quoted values of Poisson's ratio are shown in Table (5.1) along with the source and method of calculation. The values of $\Delta f/f_E$ for these values of σ are shown in Figure (5.1) at the mean value of δ_E and the line A has been drawn through the values of $\Delta f/f_E$ obtained for the glass and polystyrene rods, which, it is felt, are known with the most confidence. The range of values quoted for the Mn/Cu alloy are taken from the static loading measurements of E' and μ for a range of alloys which had been differently heat-treated. Figure (5.1) must be interpreted with caution because:-

1. the value of Δf used is derived from the n = 1 and 2 resonances only, for most of the specimens
2. the rods are likely to be anisotropic due to strain (ebonite, tufnol and the metals), and to density variations arising from voids (solder, bismuth, thallium) and arising from the nature of the material (tufnol is a resin-bonded paper product).

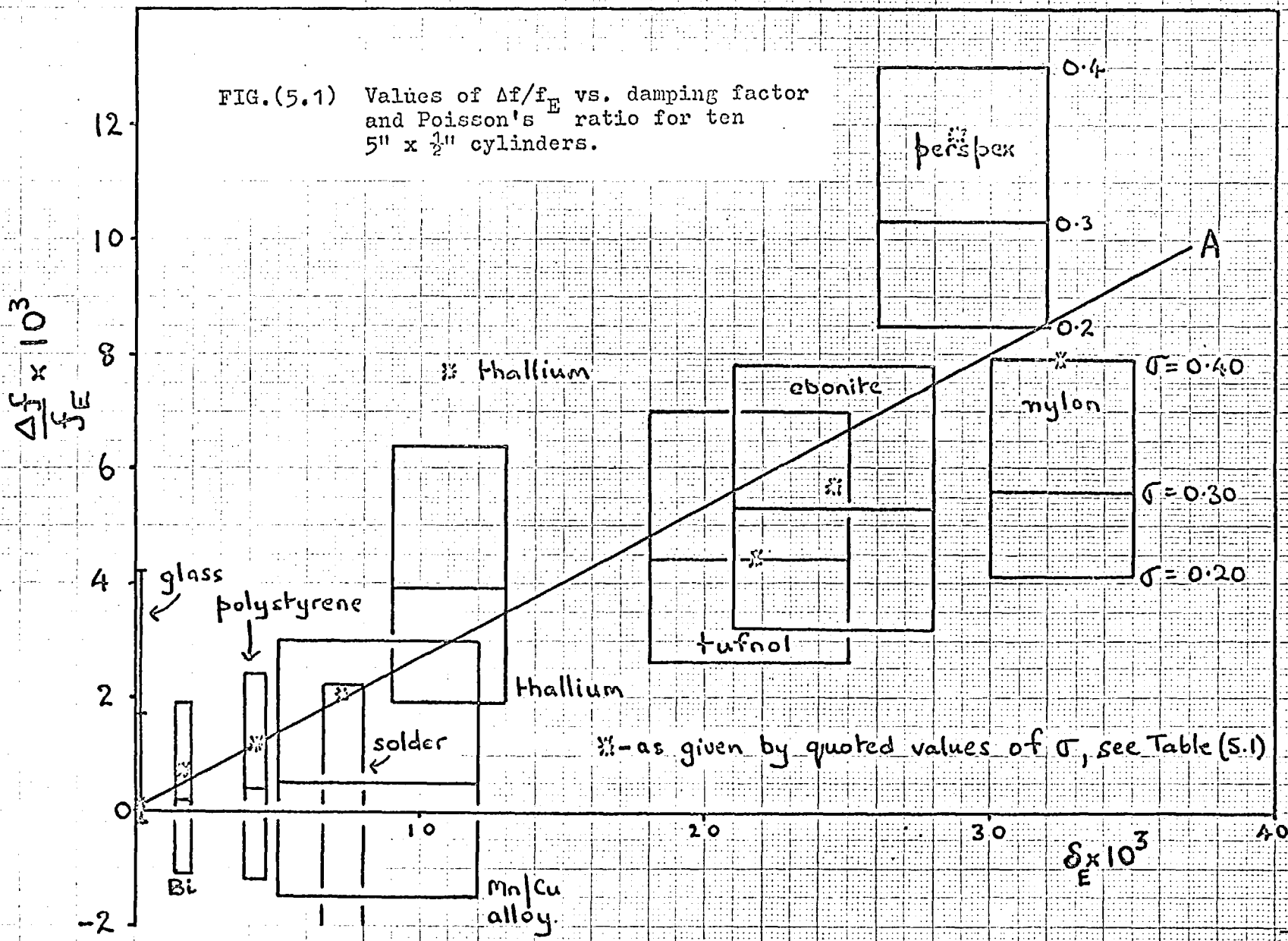
FIG.(5.1) Values of $\Delta f/f_E$ vs. damping factor and Poisson's ratio for ten 5" x ½" cylinders.
$\frac{\Delta f}{f_E} \times 10^3$
$\delta_E \times 10^3$
12
10
8
6
4
2
0
-2
10
20
30
40
A
0·4
0·3
0·2
perspex
thallium
ebonite
nylon
tufnol
σ = 0·40
σ = 0·30
σ = 0·20
glass
polystyrene
thallium
solder
Bi
Mn/Cu alloy
※-as given by quoted values of σ, see Table (5.1)

TABLE (5.1)

Quoted values of Poisson's ratio used in Figure (5.1)

Material	Poisson's ratio	Source	Method
glass	0.225	present investigation	dispersion calculations
bismuth	0.33	Rare Metals Handbook, Chapman & Hall, 1961	-
polystyrene	0.335	present investigation	dispersion calculations
Mn/Cu alloy	0.16 - 0.38	Admiralty Materials Lab. Report A/81(S)	static loading
solder	0.39	present investigation	universal point theory
thallium	0.45	Schramm 1962	pulse method
tufnol	0.30	present investigation	static loading
ebonite	0.32	present investigation	static loading
nylon	0.4	American Institute of Physics Handbook, 1957	-
perspex	0.35	I.C.I. Trade Journal "Mechanical Properties of Perspex"	static loading

Cylinders of teak and of softwood were also investigated and found to have large negative values of Δf for all values of σ. It was shown in section (4.g) that this phenomenon was likely to be symptomatic of anisotropy due in the case of the wooden cylinders to the grain.

(ii) Dependence of Δf on rod dimensions

It was shown experimentally in Chapter 4 that a constant value of Δf was obtained for a wide range of d/L values. However, another finding to be investigated is the seeming independence of the Poisson's ratio of the length of the cylinder. This was observed for the glass cylinders, Figure (4.5), for the aluminium cylinders, Figure (4.13), and to a lesser extent for the polystyrene cylinders, Figure (4.8).

It was decided to investigate the significance of this in terms of the different values of Δf observed experimentally for the rods of different lengths by means of an empirical relationship whose basis would be the observed independence of σ of l.

The value of σ at d/L = 0.20 for the glass cylinders is set at 0.2231, see Figure (4.5), and it is assumed that the ideal value of v_E is 5237.4 m/s, see Table (4.4). The value of the correction due to dispersion at d/L = 0.20

and $\sigma = 0.2231$ is 1.00533, and therefore the following equation can be written:

$$v_E^* = 1.00533 v_n^* \qquad (5.1)$$

where v_E^* and v_n^* are the "Young's modulus" velocity and the phase velocity respectively calculated from the appropriate resonant frequencies uncorrected for end-effect. However, the ideal value of v_E has been defined as 5237.4 m/s and thus

$$(5237.4) = (f_1 + \Delta f) \times 21 \times c_1$$

or

$$f_1 = (5237.4)/21 \times c_1 - \Delta f \qquad (5.2)$$

where c_1 is the dispersion correction for the fundamental resonance, 1 is the length of the cylinder, Δf is the effective end correction, and f_1 is the observed value of the fundamental resonant frequency (uncorrected).

Equations (5.1) and (5.2) give a value of f_n, the uncorrected value of the resonant frequency at $d/L = 0.20$; n is defined therefore by the value of 1 and d from the relation $n.d/21 = 0.20$. Hence f_n is given by

$$f_n = n \times [\, (5237.4)/21 \times c_1 - \Delta f \,] \times c_1/(1.00533) \qquad (5.3)$$

It is now possible to calculate the values of Δf at d/L = 0.20 for a whole range of rods of different dimensions, subject only to the condition that their dimensions are such that n.d/21 = 0.20 gives an integral value of n. Following the method used in Chapter 4, c_1 is given by the appropriate value of d/21 and σ = 0.2250 in order to try to reproduce the behaviour of the glass cylinder.

Four rods of dimensions given below in Table (5.2) are defined such that 21/I. will give an integral value of n.

TABLE (5.2)

Dimensions of four rods

Name	Diameter(in.)	Length (in.)	d/21	n
A	0.5	50	0.005	40
B	0.5	25	0.01	20
C	0.5	12.5	0.02	10
D	0.5	5	0.05	4

Use can now be made of equation (4.1) to calculate the effective end correction for each of the four rods described above, an illustrative calculation for rod D of Table (5.2) being shown below.

Fromequation (5.2):

$$f_1 = (5237.4)/[\ 2 \times (2.54) \times 5 \times (1.00032)\ ] - \Delta f$$

$$f_1 = (20.6131) - \Delta f \qquad \text{(in kc/s)}$$

From equation (5.3):

$$f_4 = 4 \times [\ (20.6131) - \Delta f\ ] \times (1.00032)/(1.00533)$$

Equation (4.1) then becomes:

$$4 \times [\ (20.6131) - \Delta f + \Delta f\ ] \times (1.00032) = \left\{ [\ (20.6131) - \Delta f] \times 4 \times (1.00032)/(1.00533) + \Delta f \right\} \times (1.00533)$$

and therefore:

$$(2.9955) \times \Delta f = 13.9 \text{ c/s} = K$$

$$\Delta f = 4.6 \text{ c/s.}$$

Table (5.3) gives the values of Δf for the four rods, calculated in the manner shown below.

TABLE (5.3)

End-effect correction as a function of dimensions

Name	K(c/s)	Δf(c/s)	$K/\Delta f$	(21/5d - 1)
A	14.0	0.36	38.9991	39
B	13.8	0.73	18.9977	19
C	14.0	1.56	8.9963	9
D	13.9	4.6	2.9955	3

The values of $K/\Delta f$ shown in this table are those resulting from the calculations as shown above. It is obvious from Table (5.3) that an approximate empirical relationship between Δf and the rod's dimensions can thus be written:

$$\Delta f = \frac{K}{(21/5d - 1)} \qquad (5.4)$$

where K is some function of the material of the cylinder. The dependence of K on δ_E can be obtained by noting that Table (5.3) defines K as 3x (the value of Δf for the 5" x $\frac{1}{2}$" rod). Hence Figure (5.2) can be obtained from the same data which produced Figure (5.1). The line is drawn through the two points which are known with reasonable confidence(for glass and for polystyrene) and seems to give a linear dependence of K on δ_E. The equation of this dependence is

$$K = 600.\ \delta_E + 12 \quad \text{(in c/s)} \qquad (5.5)$$

which with equation (5.4) gives the following empirical relationship between Δf, δ_E and the rod dimensions.

$$\Delta f = \frac{600.\ \delta_E + 12}{21/5d - 1} \qquad (5.6)$$

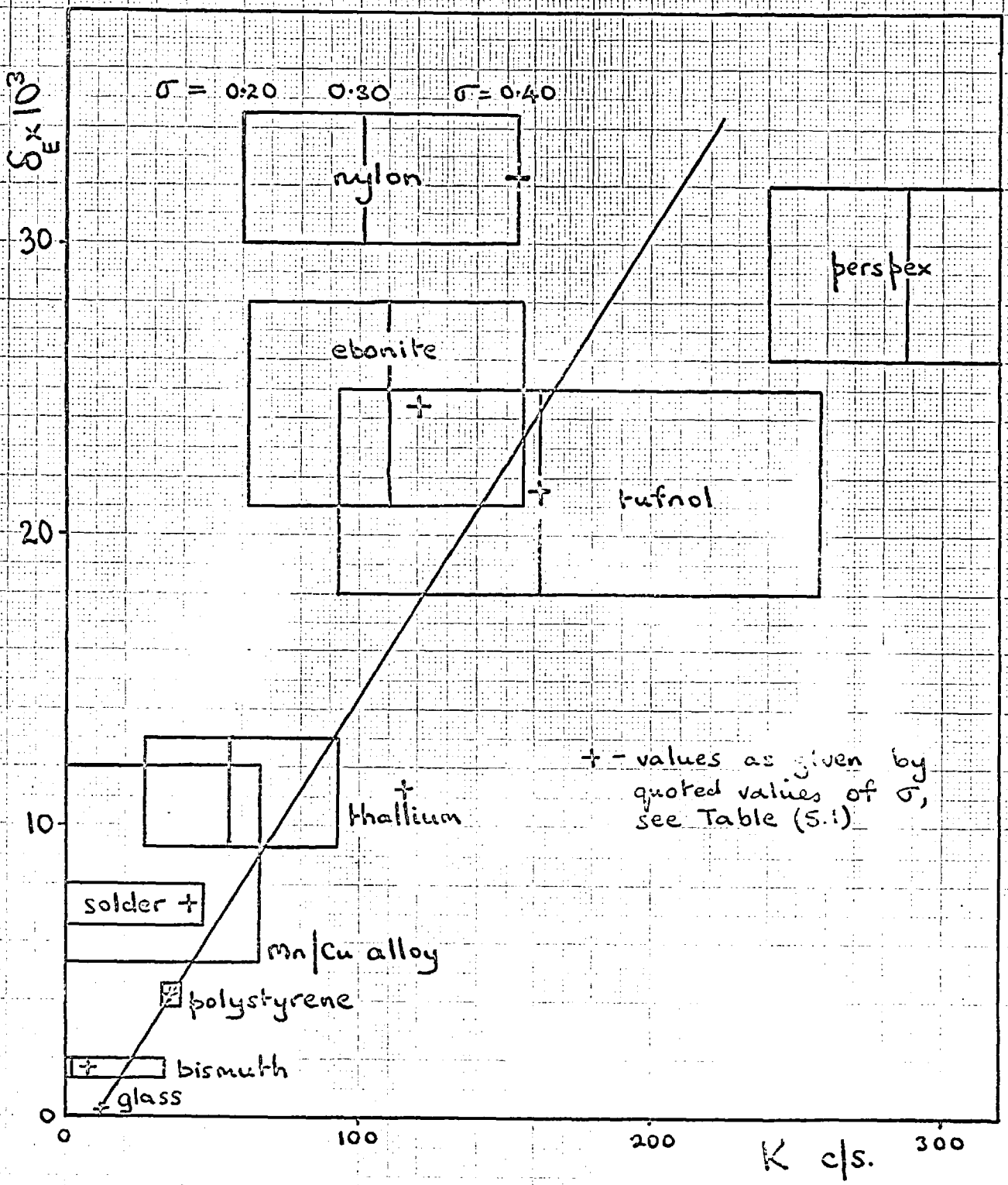

FIG.(5.2) Dependence of K on damping factor for ten materials, as calculated from data derived from 5" x $\frac{1}{2}$" cylinders.

Equation (5.6) is seen to be valid only for rods whose dimensions obey the condition that $21/5d < 1$. This condition is due to the derivation of the theory from the consideration of the dependence of σ on d/L at 0.20.

Table (5.4) shows the experimentally determined values of Δf for perspex, polystyrene and glass rods of different dimensions. It is to be noted that for the perspex rods a value of $\sigma = 0.30$ has been used in deriving the values of Δf.

TABLE (5.4)

Observed values of Δf(c/s) for different rods

Rod length	$8\frac{1}{3}$"x$\frac{1}{2}$"	5"x$\frac{1}{2}$"	$2\frac{1}{2}$"x$\frac{1}{2}$"	$2\frac{1}{2}$"x$\frac{1}{4}$"
Glass	-	4.1 ± 0.7	12.2 ± 1.6	4.3 ± 2.3
Polystyrene	-	12 ± 2	24 ± 12	-
Perspex	95 ± 10	100 ± 15	300 ± 50	-
(21/5d - 1)	5.7	3	1	3

It is seen that, in terms of the value of Δf for the 5" x $\frac{1}{2}$" rod, Δf for the $8\frac{1}{3}$" x $\frac{1}{2}$" rod should be 1/5.7 times as great, that of the $2\frac{1}{2}$" x $\frac{1}{2}$" rod should be three times greater and that of the $2\frac{1}{2}$" x $\frac{1}{4}$" rod should be the same. It is not surprising that the experimentally obtained values for the glass cylinders obey these rules, as the behaviour of the glass cylinders was the basis of the theory. As

can be seen, Δf values for the polystyrene cylinders only just agree with the predictions, as is the case for the shortest perspex cylinder. However, Δf for the longest perspex cylinder is too high, the predicted value (based on the value of the 5" x $\frac{1}{2}$" rod) is 53 c/s.

The data from the other cylinders (see Figure (5.2)) cannot be used to check the validity of equation (5.4) as the relationship between the values of Δf for different rod dimensions will hold only for the exact value of Poisson's ratio of the material, which is unknown. Measurement of Δf values for rods of dimensions $2\frac{1}{2}$" x $\frac{1}{2}$" were made for the range of materials of Figure (5.2), but are not shown due to the large range of values resulting from the use of the range of Poisson's ratio from 0.2 to 0.4. For example, the values of Δf for the glass rod of these dimensions for σ = 0.2, 0.3 and 0.4 are -58.0, 266.0, and 693.9 c/s respectively, compared with -4.3, 34.5 and 87.9 c/s respectively for the 5" x $\frac{1}{2}$" rod.

Measurements were made, however, on relatively long and thin rods of perspex and polystyrene, their dimensions being respectively, 6.629" x 0.192" and 6.416" x 0.236". Defining K as three times the value of Δf for the 5" x $\frac{1}{2}$" rod, the theoretical values of Δf for these rods are 23 and 3.6 c/s respectively. The values obtained experimentally

were 40 ± 20 c/s and 7 ± 3 c/s, agreement between theory and experiment only being attained by using the extreme values of the experimental errors.

Equation (5.5) implies that an end-effect correction exists even for a perfectly loss-less material, which is consistent with the description by Zemaneck (1962) that the end-effect is caused by the boundary conditions being inapplicable for rods of finite dimensions. Figure (5.2) implies that there is also a contribution to end-effect due to the internal friction of the material. The implication of equation (5.6) that an infinitely long and thin, loss-less cylinder would have an end-effect should not be considered too seriously, as this prediction was derived from cylinders whose dimensions were anything but infinite.

Another check on the validity of the empirical theory developed in this section is its prediction of the values of Poisson's ratio as a function of d/L for very long and thin cylinders, an experiment which could not be carried out with the apparatus available. Table (5.5) gives the values of v_E^*/v_n^* for glass and polystyrene cylinders of dimensions 50" x $\frac{1}{2}$"; the results for an equivalent perspex cylinder are not shown as values greater than unity do not occur until d/L = 0.18, i.e. the 36th resonance.

Table (5.5) shows that at low enough values of d/L, values of v_E^*/v_n^* less than unity will occur for any cylinder and not only for those made of high-loss materials.

TABLE (5.5)

Calculated velocity dispersion in cylinders as given by empirical theory

n	GLASS		POLYSTYRENE		d/L
	v_E^*/v_n^*	σ	v_E^*/v_n^*	σ	
2	0.99995	-	0.99913	-	0.01
4	0.99997	-	0.99917	-	0.02
6	1.00002	0.12-0.15	0.99921	-	0.03
8	1.00010	0.16	0.99935	-	0.04
10	1.00021	0.185	0.99958	-	0.05
12	1.00034	0.195	0.99985	-	0.06
14	1.00051	0.204	1.00020	0.13	0.07
16	1.00071	0.21	1.00061	0.195	0.08

Figure (5.3) shows the values of σ of three cylinders, normalised by σ_T, the "true" Poisson's ratio which has been calculated as 0.2257 for the theoretical values and 0.2252 for the experimental values (those of data (a) of Figure (4.2)) for the glass; 0.3352 and 0.3356 for the polystyrene, respectively; and for the perspex cylinder, two theoretical values have been used, 0.30 and 0.31, the

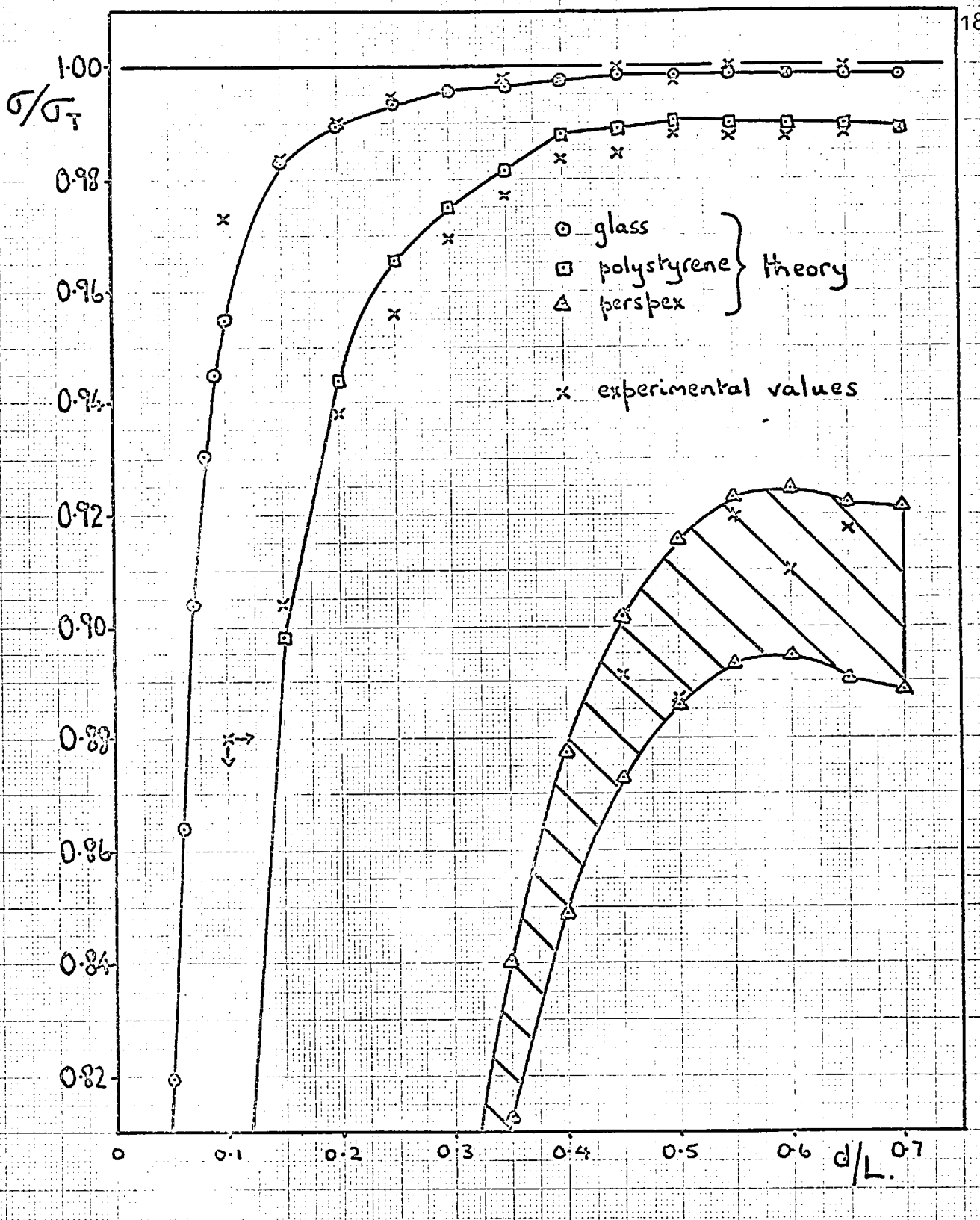

FIG.(5.3) Normalised values of Poisson's ratio as given by the empirical theory for a 50" x $\frac{1}{2}$" cylinder compared with the experimental values obtained from a 5" x $\frac{1}{2}$" cylinder, for three materials.

experimental value employed being 0.30. As can be seen from Figure (5.3), there is a reasonable agreement between the theoretical and experimental values for the 5" x $\frac{1}{2}$" glass and polystyrene cylinders, except for the first experimental points shown which are for the n = 2 resonance. It is to be noted that this lack of agreement for the polystyrene cylinder is shown in Figure (4.12) as the very high value of σ for d/L = 0.10, the cause of this being the difference between the average value of Δf and the value at d/L = 0.10, which are 12 and 9 c/s respectively.

Of course, the theory does not attempt to explain the high d/L value behaviour of the Poisson's ratio and therefore the curves shown in Figure (5.3) should be terminated at 0.65 for the glass and at 0.70 for the perspex and polystyrene cylinders.

To summarise the value of this empirical theory, it has been shown that

1. It is reasonably successful in predicting the values of Δf for the shorter cylinders, the experimental value for the longest perspex cylinder being too high.
2. Use of the theory to predict the behaviour of long, thin rods of perspex, polystyrene and glass produces curves of

σ versus d/L which reflect the behaviour of short cylinders, except at low values of d/L for these latter cylinders.

(b) Comparison with theory

(i) Dependence on damping factor

Edmonds (1961) and Parfitt (1954) have both theoretically considered the dependence of f_n on the value of the damping factor, the former for the exact theory and the latter for the simple (dispersionless) theory. Edmonds corrected the exact equation (equation (1.4)) for first order effects only, and showed that the solution could then be separated into real and imaginary parts, the former giving the frequency equation as before and the latter giving a relationship between Q and δ_E which will be considered in Chapter 6. Thus internal friction has no first order effect on the values of the resonant frequencies.

Parfitt obtained equation (1.20) as the relationship between resonant frequency and δ_E from the simple (dispersionless) theory. As can be seen, this equation supports Edmonds' findings that there are no first order effects. However, Parfitt's correction is insufficient in two respects. First, it is not large enough, for whilst the correction calculated for polystyrene is of the order of

2×10^{-3} for the n = 1 resonance, equation (1.21) predicts a correction of $\delta_E^2/8$ which is of the order of 10^{-6}. Secondly, the correction is proportional to frequency which is not the dependence observed experimentally. (There is a slight dependence on n in equation (1.21) but this is of the magnitude of δ_E^4 and therefore negligible as $\delta_E = 3 \times 10^{-2}$ for perspex).

It is therefore seen that theoretical dependence of f_n on damping factor is insufficient to explain the experimental observations.

(ii) Dependence on rod dimensions

Zemaneck (1962) is the only worker to have theoretically and experimentally investigated the phenomenon of end-effect, and his particular interest was in the prediction of the frequency of end-resonance (see Appendix 2) which he did with great success, see Figure (5.4). His work however, was concerned with the dispersion in a "semi-infinite" cylinder of dimensions 120" x $1\frac{1}{2}$", and he did not investigate the dependence of end-effect on dimensions.

As pointed out in Appendix 2, the end-effect cannot be calculated exactly as it depends upon contributions from an infinite number of modes, and therefore Zemaneck calculated values of the end-resonance frequency and of

end-effect for the first 3, 5, 7 and 9 pairs of modes. The frequency of end-resonance was found to depend only slightly on the number of modes used in the calculation after the first three pairs, and Figure (5.4) shows the experimental verification of the position of the 9 mode end-resonance frequency.

However, the values of the end-effect below end-resonance were found to be very dependent upon the number of modes included in their calculation, but for all numbers of modes investigated, were found to be approximately proportional to the third power of the frequency. This prediction is obviously at variance with the experimental findings reported here of an end-effect which is independent of frequency for a wide range of values.

The relationships between θ , Δf and g, which are all expressions of end-effect (see equations (1.15), (1.17) and (1.18)) are as follows.

$$g = \theta^{o}/180^{o} = \frac{n.\,\Delta f}{(f_n + \Delta f)} \qquad (5.7)$$

Using these to convert the experimentally observed values of Δf into value of θ gives Figure (5.5) as the dependence of θ on d/L for the 5" x $\frac{1}{2}$" rods of glass, polystyrene and perspex. A direct comparison between Figures (5.4) and

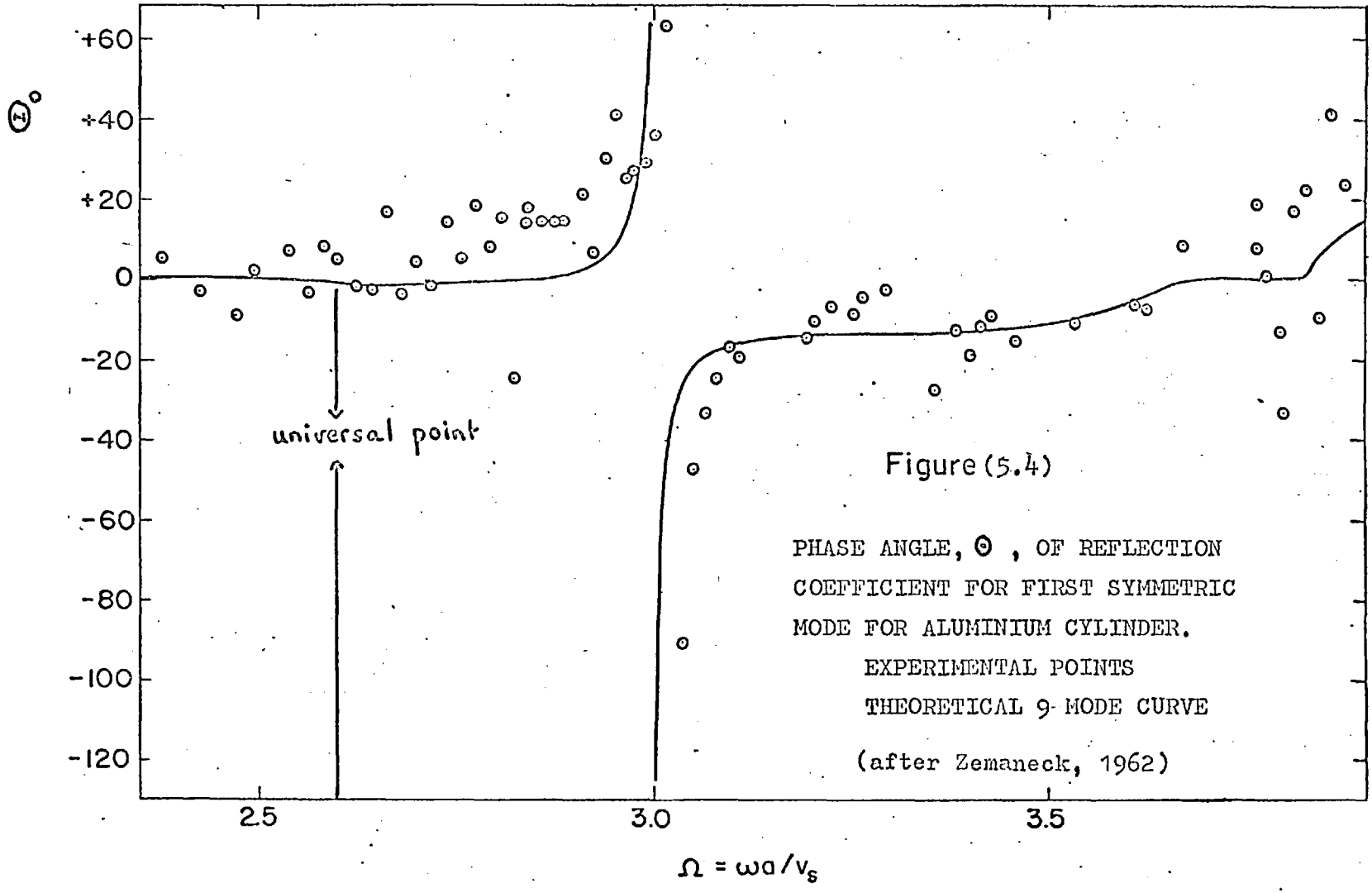

Figure (5.4)

PHASE ANGLE, Θ , OF REFLECTION COEFFICIENT FOR FIRST SYMMETRIC MODE FOR ALUMINIUM CYLINDER.
EXPERIMENTAL POINTS
THEORETICAL 9-MODE CURVE

(after Zemaneck, 1962)

(5.5) is only possible at the universal point due to the different abscissa scales. However, the position of end-resonance shown in Figure (5.4) is seen to be above that of the universal point and occurs at about d/L = 1.0.

As can be seen from Figure (5.4), Zemaneck's experimental values of Θ exhibit considerable scatter, a phenomenon attributed in the present work to anisotropy of the cylinder. It is to be remembered, however, that these values of the end-effect have been obtained experimentally by noting the positions of the nodes along the length of the cylinder at resonance.

The maximum value of Θ obtained theoretically by Zemaneck for a loss-less cylinder was of the order of 0.05° which is the value reached just before the end-effect diminishes to zero at the universal point. Whilst this is of the order of magnitude of the values of Θ obtained experimentally for the glass cylinder, see Figure (5.5), there is no agreement between the experimentally observed frequency dependence reported here and the theoretically predicted dependence of Zemaneck, the latter giving a value of Δf which is almost zero for the fundamental and increasing as the third power of frequency thereafter. In the present investigation, the correction Δf was defined primarily to explain deviations from the exact theory at

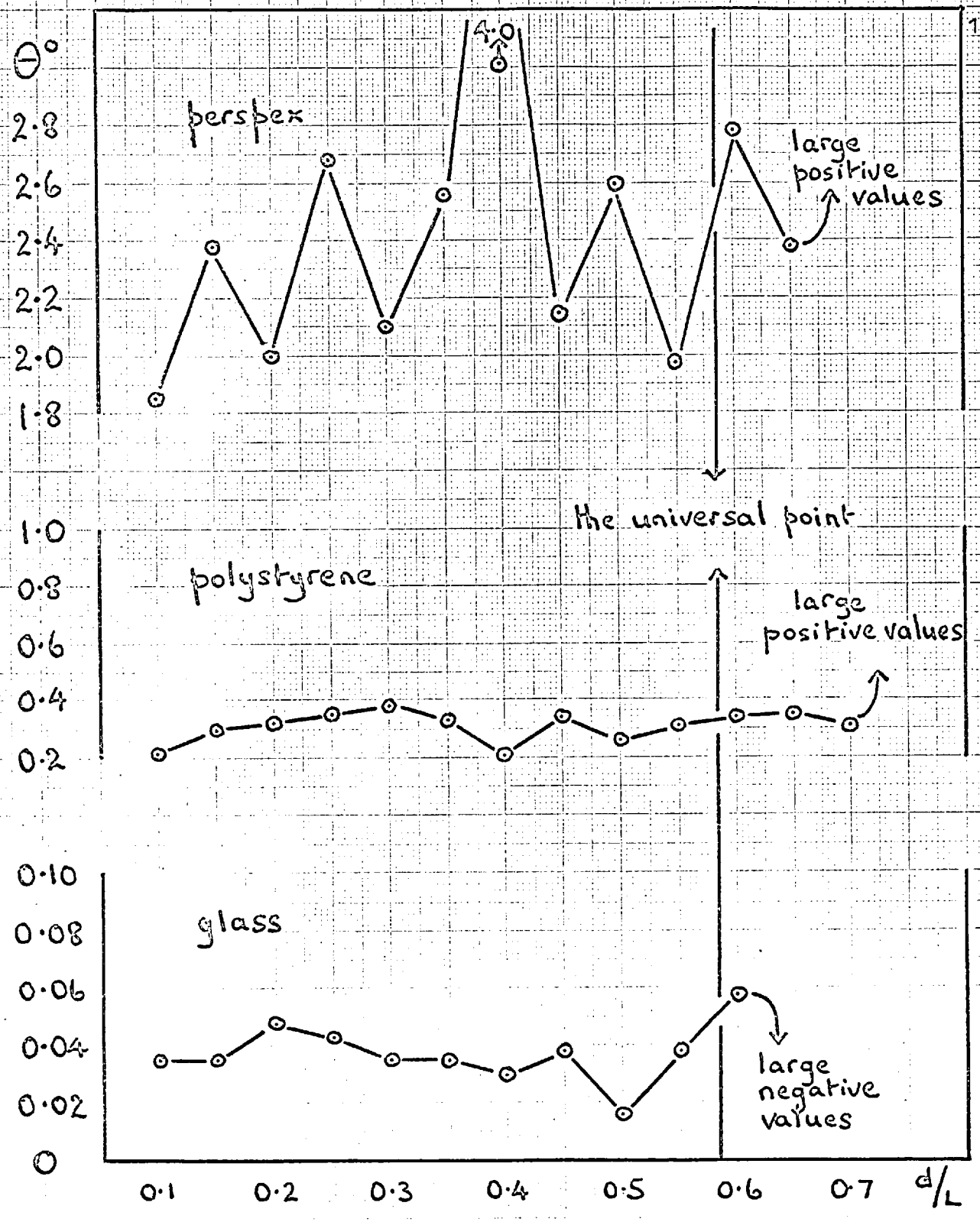

FIG.(5.5) Phase angle of reflection coefficient, θ , vs. d/L obtained from experimental values of f for three 5" x ½" cylinders.

the low frequencies for which Zemaneck found little or no end-effect. Therefore it is necessary to investigate other possible causes of the correction Δf calculated in the present investigation.

(c) Frequency dependence of E', μ' and σ

The derivation of a constant value of Poisson's ratio in the manner of Chapter 4 implies that Poisson's ratio and Young's modulus are independent of frequency. It has been seen, however, that the value of Poisson's ratio of perspex below 10^3 c/s is very dependent upon frequency, though the precise form of this dependence seems to be in doubt, see Table (4.13a). It is obvious, then, that the derivation of a constant value of Poisson's ratio from the dispersion data need not represent its actual dependence in the frequency range considered. A further problem exists in that even if Poisson's ratio is independent of frequency, then Young's modulus need not be. Thus a frequency indpendent Poisson's ratio is the result of the frequency dependence of E^* and μ^* being such that $\sigma^* = E^*/2\mu^* - 1$ is constant.

Confirmation of the existence of an end-effect can only be achieved by comparing the same resonant frequencies of two cylinders of the same material but different lengths

(to eliminate the possible frequency dependence of E'), and with the same value of d/L (to eliminate the effect of a possible frequency-dependent Poisson's ratio). The fundamental frequency of the $2\frac{1}{2}$" x $\frac{1}{2}$" rod and the n = 2 resonance of the 5" x $\frac{1}{2}$" rod are two such frequencies, both having a value of d/L = 0.10. Table (5.6) shows the values of these two resonances for the two rods of glass, perspex and polystyrene respectively.

TABLE (5.6)

Frequencies (c/s) for two rods at contstant d/L (0.10) but different lengths

Dimensions	(1) 5" x $\frac{1}{2}$"	(2) $2\frac{1}{2}$" x $\frac{1}{2}$"	(3) (2) - (1)	(4) c/s	(5) c/s
glass	41,469±8	41,458±17	-11±25	-8	-8
polystyrene	14,623±3	14,627±5	+4±8	-24	-10
perspex	17,200±10	17,170±10	-30±20	-200	-200

Notes:

(1) n = 2 resonance for the 5" x $\frac{1}{2}$" rod

(2) n = 1 resonance for the $2\frac{1}{2}$" x $\frac{1}{2}$" rod

(3) difference between cols. (1) and (2)

(4) difference that should exist between cols. (1) and (2) if the empirical theory of section (5.a.ii) were correct. This is the difference between the values of Δf for the two rods as given by the theory, i.e. 4 - 12 = - 8 c/s

(5) difference between measured values of Δf for these two resonances

If there is no end-effect, then the frequencies shown in cols. (1) and (2) should be equal and col. (3) should be zero. As can be seen, the difference between the two frequencies is zero within experimental error (which arises principally from the impossibility of measuring the lengths of the cylinders better than 1/1000"), except for the perspex cylinder. If there is an end-effect as given by the empirical relationship of section (5.a.ii), then cols. (3) and (4) should be the same. This is true, within experimental error, only for the glass cylinders. Col. (5) of this table is the difference between the measured values of Δf for the resonances in question, and the agreement between these values and those of col. (3) is no better than the agreement between cols. (3) and (4).

It is to be concluded, therefore, that the correction previously termed the "end-effect" is not entirely due to such an effect but must also be due in part to the frequency dependence of Young's modulus and/or Poisson's ratio. Without knowledge of the dependence of either one or the other of these on frequency, it is seen that analysis of Δf is very difficult, though if the frequency dependence of E' of perspex and polystyrene is as shown in Figure (5.6),

then no correction is required to give a constant value of σ. These values have been obtained from the resonant frequencies assuming that σ is constant at 0.35 and 0.335 respectively for perspex and polystyrene. A similar graph can be plotted for the glass cylinder, but the dependence of E' upon frequency is very slight.

(d) Evidence of a frequency-dependent Young's modulus

Reference to Figure (A1.1f) shows that an increase in the elastic moduli of a material is to be expected on increasing the frequency of measurement through a relaxation. Evidence of the existence of such processes in perspex and polystyrene is given in Chapter 2. Marx and Siverten (1953) have shown that relaxation processes occur in inorganic glasses and Mason (1958), in a review, has shown that they are to be expected in metals, though for these last two groups of materials not usually at the frequencies occurring in the present investigation. Since Δf has been shown to be at least in part dependent upon the variation of E' with frequency, the values of Δf must be regarded as some measure of this dependence.

Wegel and Walther (1935) showed that the dependence of the damping factor for a variety of materials could be expressed as a power law in the following manner:

$$\delta \propto f^{q} \qquad (5.8)$$

where q is a constant whose magnitude depends upon the particular material and generally of the order of -0.29 to +0.55. Parfitt (1954) used the same power law to describe the frequency dependence of E', i.e.

$$E' \propto f^{p} \qquad (5.9)$$

Using this form of the frequency dependence of E', it is shown in Appendix 7 that the relationship between p of equation (5.9) and $\Delta f/f_1$ is as follows, assuming that no contribution from end-effect exists in the values of Δf;

$$p = 2. \left\{ 1 - \log [n] / \log [n + (n-1). \Delta f/f_1] \right\} \qquad (5.10)$$

Parfitt (1954) obtained a value of +0.017 for p for perspex for the same frequency range as considered in the present investigation. In obtaining this value, he had to correct the values of f_n for velocity dispersion, using a value of Poisson's ratio of 0.338.

For relatively long and thin rods, the value of Poisson's ratio used is not of great importance as the correction for dispersion is small. However, for the $8\frac{1}{3}$" x $\frac{1}{2}$" perspex cylinder used in the present investigation, the value of p depends on the value of Poisson's ratio used in estimating this correction. Hence p = +0.020 for σ = 0.33, whereas

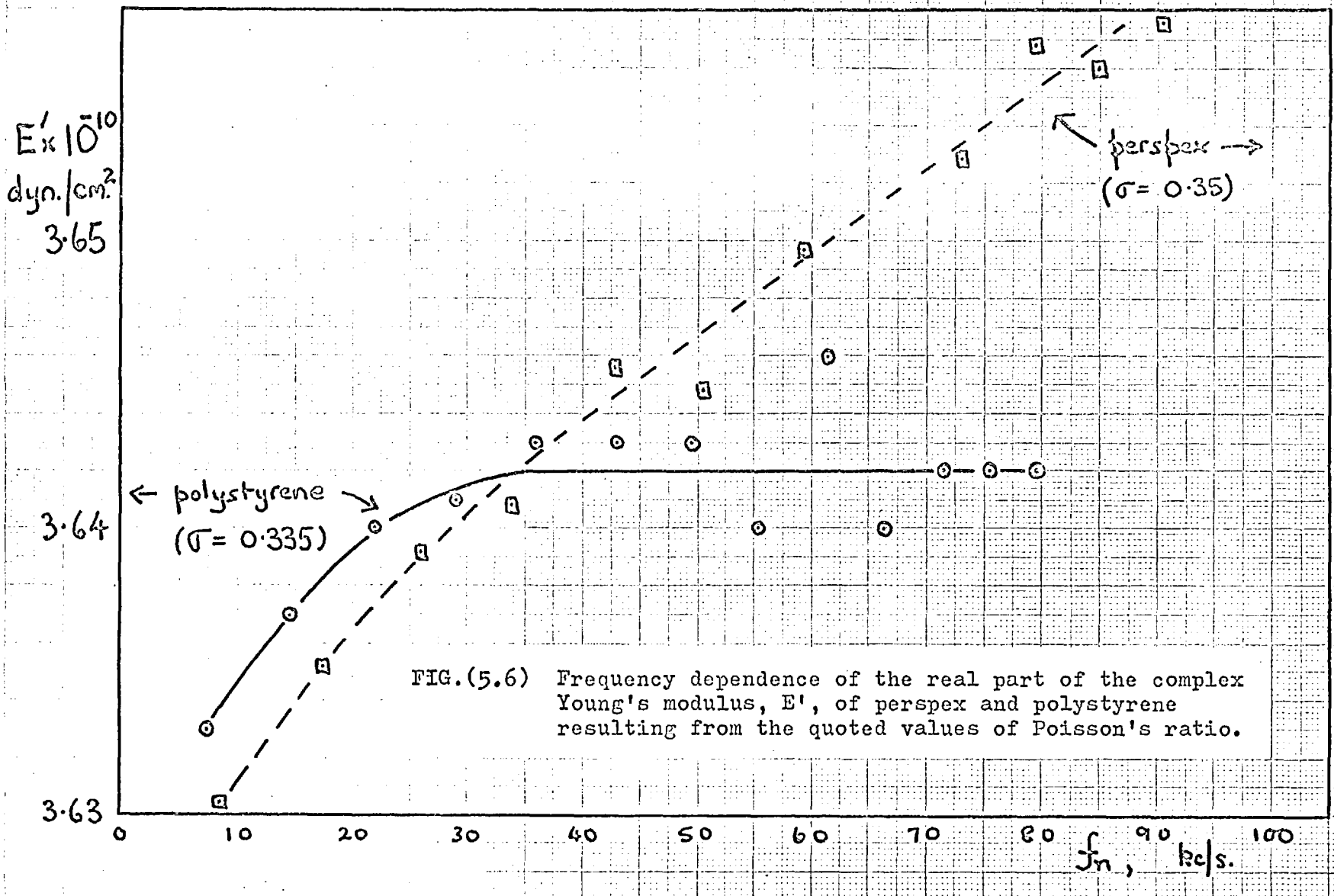

FIG.(5.6) Frequency dependence of the real part of the complex Young's modulus, E', of perspex and polystyrene resulting from the quoted values of Poisson's ratio.

$p = +0.024$ for $\sigma = 0.35$. If Poisson's ratio is also frequency-dependent a more complicated situation exists.

Values of p for polystyrene and glass of the order of 0.003 and 0.0004 respectively, are sufficient to give a constant value of Poisson's ratio for the 5" x ½" cylinders investigated. Negative values of Δf can only be explained in terms of a Young's modulus which decreases with increasing frequency, see Appendix 7 and equation (5.10), a phenomenon not explained by simple relaxation theory. It is considered therefore, that the cause is the anisotropic nature of the materials of the cylinders exhibiting these negative values.

The values of E' for polystyrene in Figure (5.6) agree well with Parfitt's values, not only in magnitude but also in frequency dependence, in that he observed a constant value for E' above 50 kc/s. The density of the sample that he used was the same as that of the samples used in the present investigation - 1.050 gm/cc. In correcting for dispersion, Parfitt used a value of Poisson's ratio of 0.337, which he obtained from the measurement of the fundamental resonances of both the shear and E-modes.

Figure (5.7) shows the frequency dependence of E' for perspex obtained in the present investigation compared with that found by Parfitt (1954). As can be seen, there are two differences, the first one being in the frequency

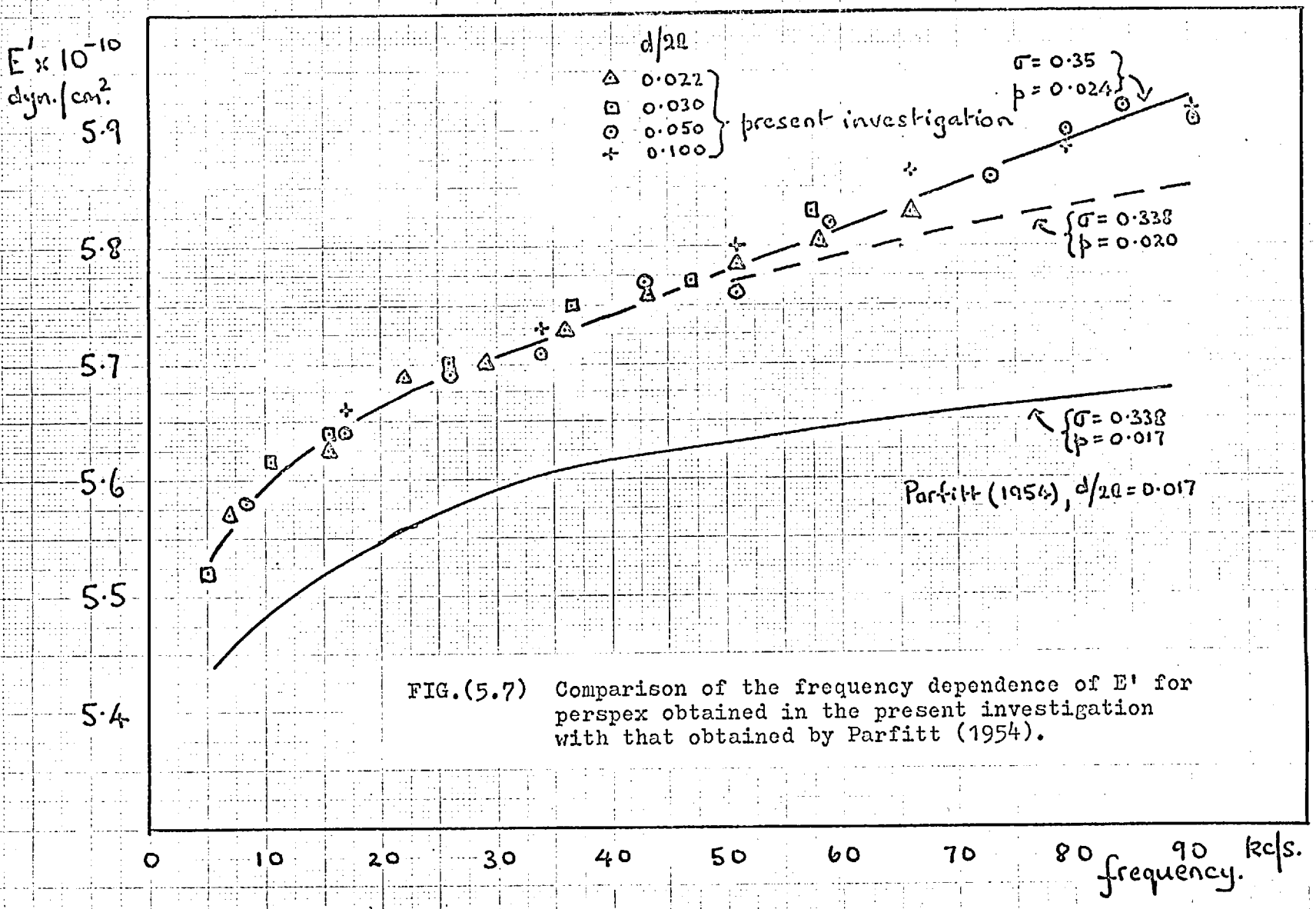

FIG.(5.7) Comparison of the frequency dependence of E' for perspex obtained in the present investigation with that obtained by Parfitt (1954).

dependence, even when using the same value of Poisson's ratio to correct for dispersion that Parfitt used in his calculations. However, the value of Poisson's ratio which gives the same value of p for the present investigation as obtained by Parfitt is 0.315, which falls within the range of possible values of Poisson's ratio quoted, see Table (4.13a). The second difference is in the value of E' at any given frequency, for even if the same frequency dependence is derived for the present investigation as Parfitt's, these values are about 2 per cent higher than his. The density of the perspex investigated by Parfitt was quoted as 1.155 $\pm$ 0.005 gm/cc, whereas that of the present investigation is 1.180 $\pm$ 0.002 gm/cc. Thus the materials are not exactly similar, a point which will be returned to in Chapter 6.

(e) The influence of a frequency-dependent E' upon Δf values

From values of the resonant frequency which obey the relationship $E' \propto f^p$, where p is assumed to have a typical value of 0.02, values of Δf have been calculated for different rod lengths. These are given in Table (5.7) below, for frequencies which have been chosen to produce large values of Δf in order to emphasise the variations calculated. Hence Table (5.7) does not represent the

behaviour of any particular rod used in the present investigation. The frequencies shown are corrected for dispersion and the diameters of the rods are therefore of no significance.

TABLE (5.7)

Effect of $E' \propto f^{0.02}$ on values of Δf for different rod lengths

Rod length	10"		5"		$2\frac{1}{2}$"	
Frequencies c/s	n	Δf (c/s)	n	Δf (c/s)	n	Δf (c/s)
9,930	1	-	-	-	-	-
20,000	2	140	1	-	-	-
40,270	4	180	2	270	1	-
60,640	6	210	3	320	-	-
81,100	8	240	4	370	2	560
101,600	10	260	5	400	-	-
204,620	20	320	10	510	5	820

It is seen that the values of Δf calculated from equation (4.1) for the resonant frequencies of a rod of given length are not constant, but increase with n, the number of the resonance. Further, on halving the rod length, the value of Δf is seen to double approximately, if a mean value for Δf is chosen.

These results do not agree with the experimentally observed constant values of Δf as obtained from equation (4.1) for glass and perspex, and with the prediction derived from the empirical relationship of section (5.a.ii), in which the value of Δf is that given by equation (5.4). This latter equation predicts a value of Δf which also depends on the diameter of the rod, a shortening of the rod from 5" to $2\frac{1}{2}$" resulting in a trebling of the value of Δf, and not a doubling, as given for a frequency-dependent Young's modulus.

Reference to equation (4.1) shows that the values of Δf are very dependent on the value of Poisson's ratio used to calculate the dispersion correction, e_n. Table (5.8) below, shows this dependence calculated for the n = 1 and n = 10 resonances of the 5" x $\frac{1}{2}$" glass rod, which occur at values of d/L of 0.05 and 0.50, respectively.

TABLE (5.8)

Dependence of Δf on value of σ used in equation (4.1)

(1) σ	(2) c_1	(3) c_{10}	(4) $10xf_1xc_1$ c/s	(5) $f_{10}xc_{10}$ c/s	(6) Δf c/s
0.220	1.00030	1.05854	206,150	205,774	-48
0.224	1.00031	1.06003	206,150	206,063	-10
0.225	1.00032	1.06040	206,160	206,135	-3
0.226	1.00032	1.06077	206,160	206,207	+5
0.227	1.00032	1.06114	206,160	206,279	+13
0.230	1.00033	1.06226	206,160	206,497	+38

Notes:

(2) v_E/v_n at d/L = 0.05 and the value of σ as given by exact solution

(3) v_E/v_n at d/L = 0.50 and the value of σ as given by exact solution

(6) values of Δf resulting from use of values (4) and (5) in equation (4.1).

As can be seen, the difference between the values of Δf depends primarily in the change in the value of c_{10} and very little in the change in c_1. Therefore by choosing a value of Poisson's ratio higher than the one used to calculate the constant values of Δf for Figure (4.3), resulting values of Δf will increase with n number as shown below in Table (5.9).

TABLE (5.9)

Dependence of Δf on σ as a function of n for successive resonances of the 5" x ½" cylinder

Resonance	2	4	6	8	10	12	
σ = 0.2258	4	3	4	3	4	3	c/s
σ = 0.2270	5	5	7	10	13	16	c/s

Notes: values of Δf are calculated from the data which gave plot (c) of Figure (4.3).

Hence, there is perhaps some significance in the values of Poisson's ratio obtained by the independent methods for the glass being higher than those values resulting from the dispersion measurements, see Table (4.6). However, if Poisson's ratio is also frequency-dependent, the issue becomes much more complicated.

From Figure (4.9), it can be seen that values of Δf for the 5" x ½" polystyrene rod for the n = 2 to 5 resonances

increase with n, the n = 2 value being consistently lower than the value of Δf averaged over the n values. However, the increase in Δf values of the $2\frac{1}{2}$" x $\frac{1}{2}$" polystyrene rod is not considered to be experimentally significant, as an opposite trend was observed on occasions, the average value of Δf being still about the same as that quoted. This average value is seen to be about twice that of the 5" x $\frac{1}{2}$" rod, as predicted by Table (5.6).

It is of interest to see if a frequency-dependent E' will give values of Poisson's ratio versus d/L which are indepndent of the length of the cylinder, as experimentally observed for the glass and the aluminium cylinders. Choosing the n = 8, 4 and 2 resonances for 10", 5" and $2\frac{1}{2}$" rods respectively, $n.f_1/f_n$ (which is v_E/v_n for the uncorrected resonances) can be calculated at the common value of d/L = 0.20. The values are 0.9795, 0.9864 and 0.9931, and are less than unity because of the largeness of Δf, as explained previously. Nonetheless, it is seen that the value of v_E/v_n for the $2\frac{1}{2}$" rod is greater than that of the other two, which results in the general conclusion that Poisson's ratio at the same value of d/L increases as the length of the rod decreases. Reference to Figure (4.5) shows that, the values of Poisson's ratio for the $2\frac{1}{2}$" x $\frac{1}{2}$" glass rod are, if anything, lower than those of the longer rod,

though within experimental error, they are the same. However, it is seen from Figure (4.8) that the values of Poisson's ratio for the shorter polystyrene rod are greater than those for the longer rod. Thus the experimental evidence concerning the dependence of Poisson's ratio on length of cylinder for the same d/L value is contradictory.

(f) The values of Δf at high frequencies

The sudden increase (for perspex and polystyrene) and decrease (for glass) of Δf for values of d/L in excess of 0.65 is unlikely to be due to changes in the frequency dependence of Young's modulus. An increase in Δf is equivalent to an increase in E' which would be ascribed to a relaxation process, no such processes having been reported at these high frequencies (in the vicinity of 80 kc/s). For the glass cylinders, a negative Δf is equivalent to a decrease in E', which is unaccounted for by simple relaxation theory.

However, there are three possible explanations of this sudden change in the behaviour of the resonances which result from the properties of cylinders in longitudinal resonance, which will now be described.

(i) Mode conversion

It has been seen, Appendix 2, that the boundary conditions at the end faces of a cylinder of finite length are satisfied only by the production of modes different from the propagating mode. At low frequencies these modes do not propagate along the length of the cylinder, as their amplitudes diminish to zero very close to the end-face. However, above a certain frequency the first pair of these modes do begin to propagate. For an aluminium alloy, Zemaneck has shown that the onset of propagation of the first pair of these modes is defined by $\omega a/v_s = 3.68$. Applying this condition to the glass cylinder, the first pair of modes would begin to propagate at a frequency of about 290 kc/s, i.e. the frequency of the 23rd or 24th resonance, and therefore above the limit of detection. In any case, as the distinct change in the values of Δf occurs at about the 14th resonance, it seems that the possibility of these high number resonances being other than those of the L(0,1) mode is a remote one.

(ii) Cut-off frequency

The cut-off frequency is derived from equation (A2.19) by letting (γa) tend to zero, whilst $\omega a/v_s$ remains finite (i.e. the wavelength becomes infinite), and is the frequency

beyond which the mode does not propagate. The exact theory for a loss-less infinite cylinder predicts no cut-off for the L(0,1) mode. However, reference to Table (4.11) shows that there must be a frequency for cylinders of low Q value resonances, beyond which the resonances begin to merge together. For the 5" x ½" perspex cylinder, it is estimated that merging occurs at about the 17th resonance. Biesterfeldt et al. (1960) have reported on this matter, showing that the simple (dispersionless) theory predicts a cut-off due to damping in the material at about the 20th resonance for $\delta_E = 10^{-2}$ (for perspex, $\delta_E = 3 \times 10^{-2}$), but noted that this frequency is considerably higher than that observed experimentally. They also showed that the non-symmetric loading of the cylinder due to the drive and detection system contributes to the lowering of the experimentally-observed cut-off frequency.

(iii) End-resonance effect

From Figure (5.4) it is seen that above the frequency of end-resonance, the value of Θ is negative for a range of values of $\omega a/v_s$. On the assumption that the correction Δf has some relation to end-effect, a constant value of σ of 0.225 can be obtained from the n = 14 and higher resonances of the 5" x ½" glass cylinder by assuming a negative end-effect. The value of Θ obtained from Δf for this cylinder

are of the order of -2.8^{o}, whilst those shown in Figure (5.4) above the frequency of end-resonance are of the order of -10^{o}. However, end-resonance occurs in Zemaneck's aluminium cylinder at frequencies much higher than those given by n = 14 for the glass cylinder, and the behaviour of the polystyrene, perspex and aluminium cylinders is such that a large positive value of θ would be required to give a constant value of Poisson's ratio.

To summarise, the possible explanations are:

1. A combination of a cut-off frequency lower than expected together with the detection of other modes.
2. An end-resonance frequency lower than expected, followed by a large negative value of θ as given by Zemaneck, for the glass, but by a large positive value for the perspex, polystyrene and aluminium cylinders.

Certain similarities of the behaviour of all four cylinders should be pointed out.

1. The deviation at high frequencies from the constant value of σ. The sudden change in the value of Δf is independent of the length of the cylinder.
2. The value of d/L at which this deviation is observed is about the same for all four materials, being of the order of 0.65.

(g) Conclusions from investigation of velocity dispersion in short cylinders

Without a detailed knowledge of the frequency dependence of Young's modulus and Poisson's ratio, it is seen that velocity dispersion measured in short cylinders cannot be compared with that predicted from the exact theory for infinitely long and thin rods, to the accuracy with which the values of the resonant frequencies of the short rods can be measured. Further, no attempts can be made to investigate the possible occurrence of end-effects.

The following conclusions can be drawn from the present investigations:

1. For well-annealed short cylinders, the universal point occurs at the value of d/L as given by the exact theory, and has been shown to be independent of Poisson's ratio, as predicted by the exact theory.
2. Deviations from the exact theory relationship of the behaviour of long cylinders (Zemaneck and Rudnick) and of short cylinders (Edmonds and Sittig) is attributable to anisotropy of the material of the cylinders, due either to strain or preferred orientation of the crystallites.
3. Except for some variation attributable to a frequency-dependent Young's modulus, it is seen that the exact solution applies to the velocity dispersion measurements made on the

short cylinders investigated for values of d/L up to 0.65 - 0.70 depending upon the material of the cylinder. This is true for both high and low-loss materials. Above this value of d/L, a constant Poisson's ratio can only be obtained by increasing the value of the correction found necessary at lower values of d/L for perspex and polystyrene, and by decreasing this value for glass. The cause of this change in the value of the correction is possibly due to the behaviour of resonant cylinders at high d/L values, as discussed in the previous section.

CHAPTER 6

YOUNG'S MODULUS AND DAMPING FACTOR MEASUREMENTS

(a) Preliminary discussion

The exact nature of polymer samples investigated is rarely stated by authors when quoting values of constants of the polymer under test. As a result, it is perhaps not surprising that differences in the quoted values of a given constant exist, an example being shown in Figure (5.7), where the frequency dependence of E' quoted by Parfitt (1954) and that found in the present investigation can only be made to agree by assuming different values of Poisson's ratio. Another example is shown below in Table (6.1), which gives the values of damping factor observed by three different authors for, nominally the same material.

TABLE (6.1)

Damping factor (x 10^2) of polystyrene at three frequencies

Frequency of measurement kc/s	10	20	50	Temperature
Parfitt (1954)	4.1	3.8	3.6	23°C
Biesterfeldt et al. (1960)	5.3	..	-	-
Present investigation	4.7	4.4	4.3	23°C

Biesterfeldt et al. do not quote the temperature at which their measurements were made. However, if their value is to be consistent with the temperature dependence found in the present investigation, their measurements would have had to have been made at about 40°C.

In order to correlate the polymer measurements of different observers, it is essential that the method of measurement and as exact a characterisation of the polymer as possible is stated. This latter requirement is difficult to realise, particularly with large specimens. Depending on the property to be investigated, one specimen can be different from another in the following ways:

1. Sample dimensions
2. Average molecular weight
3. Impurity content due to
   - (i) Polymerising agent
   - (ii) Filler
   - (iii) Plasticiser, including water
4. Annealing history

The consequences of possible variations in the measured properties due to the above items will be considered in following sections.

(b) Nature of the polymers investigated

(i) Perspex, polymethyl methacrylate

Three types of polymethyl methacrylate were available:

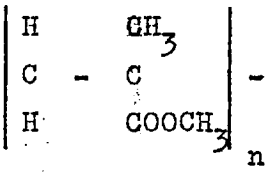

1. I.C.I. Ltd. brand "perspex". The average molecular weight is considered by the manufacturer to be "of a few million", the precise value varying from batch to batch. The molecular weight distribution was described as "wide".

2. A polymethyl methacrylate (considered by the manufacturer, Mill Plastics Ltd., to be of the same molecular weight as perspex) containing 10% dibutyl phthalate, a plasticiser.

3. A molecular weight regulated sample of polymethyl methacrylate (0.05% lauryl mercaptan was added during the polymerisation) of an average molecular weight much lower than that of perspex.

In the present investigation the perspex specimens are type 1.

(ii) Polystyrene

Three types of polystyrene were available:

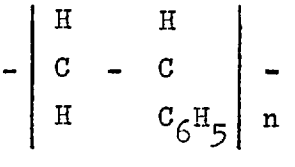

1. Shell Chemical Co. product of average molecular weights

$\bar{M}_n$, number average = 120,000

$\bar{M}_w$, weight average = 266,000

$\bar{M}_v$, viscosity average = 233,000

The distribution was lognormal. Appendix 8 discusses the measurement of average molecular weights and the relationships between them.

2. Monsanto Chemicals product of $\bar{M}_w$ = (50,000 to 60,000)

3. Monsanto Chemicals product of $\bar{M}_w$ = (55,000 to 65,000)

Reference to polystyrene in the present investigation implies type 1.

(c) Dependence of measurements on rod dimensions

(i) Young's modulus

As described in the previous chapter, the problem is one of correction of the resonant frequencies for dispersion, which is dependent upon Poisson's ratio. If the rod is short and stubby, major differences in the possible frequency dependence of E' will result from an inaccurate estimation of Poisson's ratio. For long and thin rods, the dispersion is small and not so dependent on Poisson's ratio. For example, a rod of dimensions 6" x $\frac{1}{4}$" will have its tenth longitudinal resonance at d/L = 0.2. An inaccuracy of 3% in Poisson's ratio produces an error in the correction for dispersion of 0.06% resulting in an error of the order of 0.1% in E'.

(ii) Damping factor

It was felt desirable to determine whether rod dimensions had any measurable influence on the damping factor. Figure (6.1) shows the damping factor of polystyrene at 23°C obtained from the measurement of Q_E of the resonances of two rods, originally of dimensions 7.4" x 0.25" and 5" x ½" but successively shortened to lengths shown in Figure (6.1). As can be seen, there is no observable difference in the values obtained at a given frequency. The range of values of d/21 for the 5 rods are given in Figure (6.1). At a frequency of about 55 kc/s the value of d/L for the series of rods of 0.25" diameter is 0.19, whereas that for the rods of ½" diameter is 0.40. As can be seen even for a doubling in the value of d/L, there is no observable difference in the measured value of damping factor at this frequency.

As described in section (1.g), Edmonds (1961) has theoretically investigated the effect of finite internal losses on the exact solution of the frequency equation. The effect on the resonant frequencies has been discussed in the previous chapter and in Appendix 2, the latter also containing the theoretical relationship between the Lamé elastic constants, Q and the rod dimensions. Edmonds investigates the values of λ" as obtained by L(0,1) mode resonances and by flexural mode resonances(using shear mode

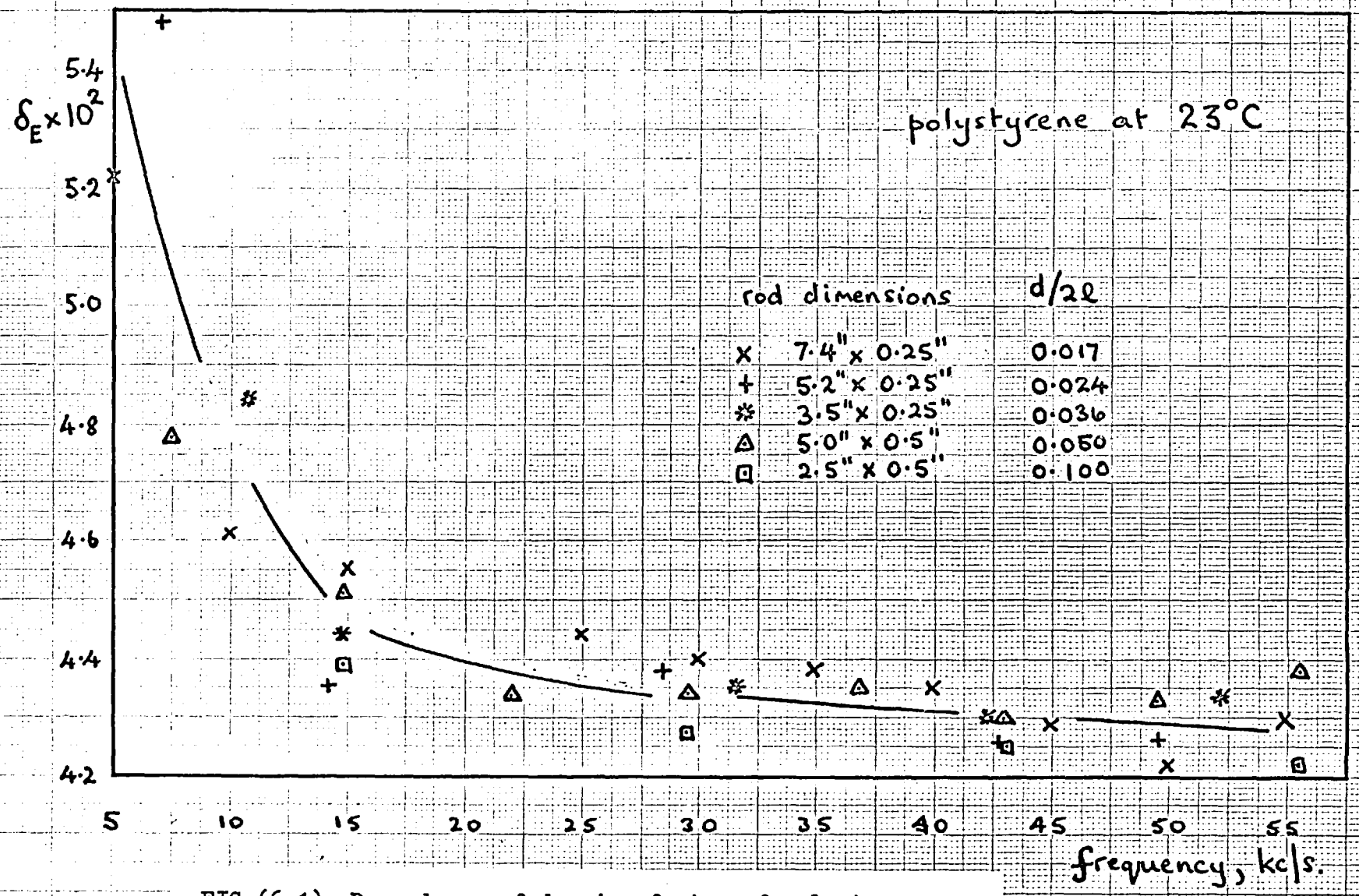

FIG.(6.1) Dependence of damping factor of polystyrene on frequency as given by the Q of resonances of rods of different dimensions.

resonances to give μ^{*}) which he finds to be different when calculated from the experimental data of these two modes of Biesterfeldt et al. (1960), see Figures (6.2a) and (6.2b) which are taken from Edmonds' paper. Figure (6.2c) shows the values of 1/Q for the polystyrene rod when in torsional, bending (flexural) and longitudinal (L(0,1)) mode resonance as a function of frequency, which were obtained by Biesterfeldt et al.

No measurements of the damping factor in shear mode resonance were made in the present investigation. However, Parfitt (1954) did measure both Q_E and Q_μ for a polystyrene rod of square cross-section from 3 - 50 kc/s. From his data it is possible to construct an experimental plot of $Q_E \cdot \mu$ " versus $\omega a/v_n$ and this is shown in Figure (6.3) as plot (b). Plot (a) is the approximate experimental plot transferred from Figure (6.2a). Of course, plot (b) is not entirely valid as the data is taken from a square cross-section rod (the value of one side has been taken as "d") whereas Biesterfeldt et al. worked on a cylindrical rod, for which shape Edmonds established the theoretical predictions. Plot (c) is taken from the experimental data of Figure (6.1) for the 5" x $\frac{1}{2}$" rod with values of μ" calculated from these Q_E values, assuming that the same frequency dependence exists for Q_μ as for Q_E. As the

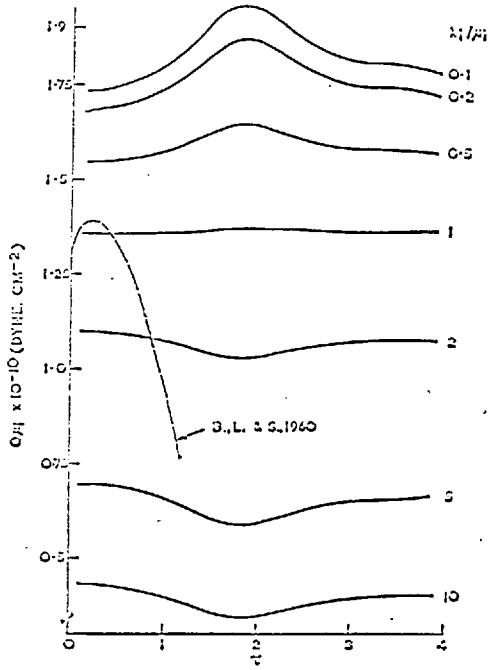

(a)

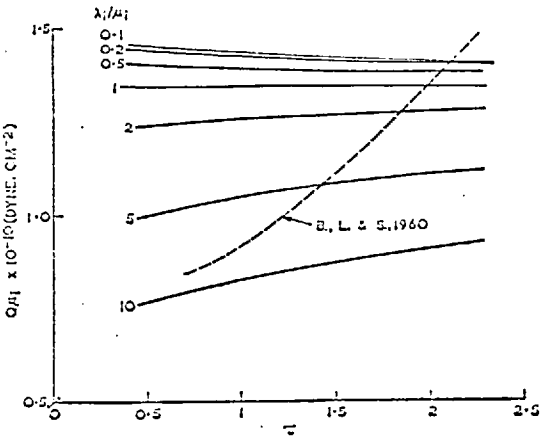

(b)

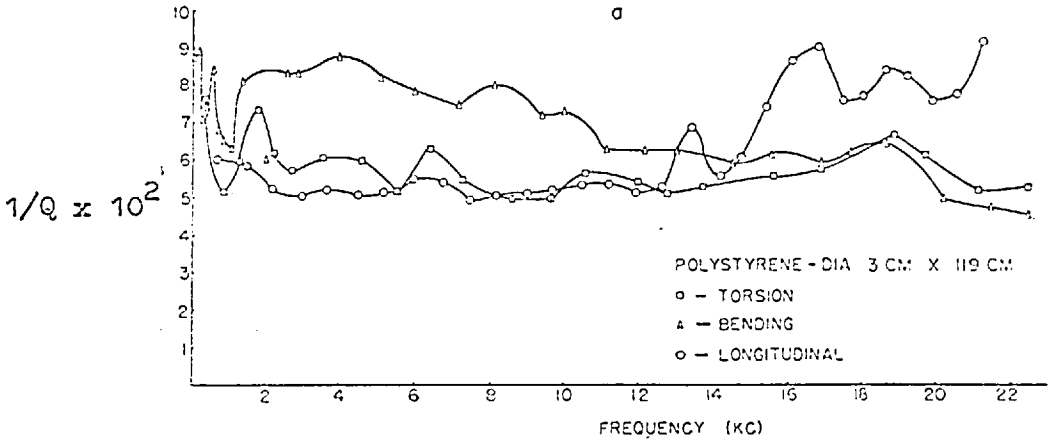

(c)

FIG.(6.2) THEORETICAL AND EXPERIMENTAL VALUES OF Q.μ" FOR POLYSTYRENE
(a) FOR YOUNG'S MODULUS MODE RESONANCES
(b) FOR FLEXURAL MODE RESONANCES (after Edmonds, 1961)

(c) EXPERIMENTAL VALUES OF 1/Q VS. FREQUENCY FOR POLYSTYRENE FOR TORSION, BENDING (FLEXURAL) AND LONGITUDINAL (YOUNG'S MODULUS) MODE RESONANCES. (after Biesterfeldt et al., 1960)

In the present terminology, $\tau = \omega . a/v_n$ and $\mu_i = \mu''$, $\lambda_i = \lambda''$

shear mode resonance frequencies are lower than the E-mode resonance frequencies for the same value of n, the plot of $Q_E \cdot \mu''$ versus $\omega a/v_n$ will not be linear and of zero slope, as would be the case for the same parameter plotted as a function of frequency.

There are two differences between plot (a) and plots (b) and (c), of Figure (6.3). First, the latter two do not show the peak of plot (a). Now although the frequency ranges of plot (a) and plots (b) and (c) are different (300 - 20,000 c/s as opposed to 5 - 55 kc/s), neither are sufficiently low enough to cover the whole range of the secondary transition which could explain the peak, see Figures (6.1) and (6.2c). The only explanation of this peak lies in the peak in the values of δ_μ shown at about 2 kc/s in Figure (6.1c) which is as likely to be due to scatter in the experimental measurements as to a relaxation process, for such a process would then show in the plot of δ_E at about the same frequency, see Ferry (1961), page 310.

The second difference lies in the decrease in ordinate values of plot (a) of Figure (6.3) which is not observed in plot (c). In part, some of the decrease could be accounted for by the frequency dependence of the damping factors, as is shown by the comparison of frequencies on plots (a) and (c) of Figure (6.3), except that Figure (6.2c) shows

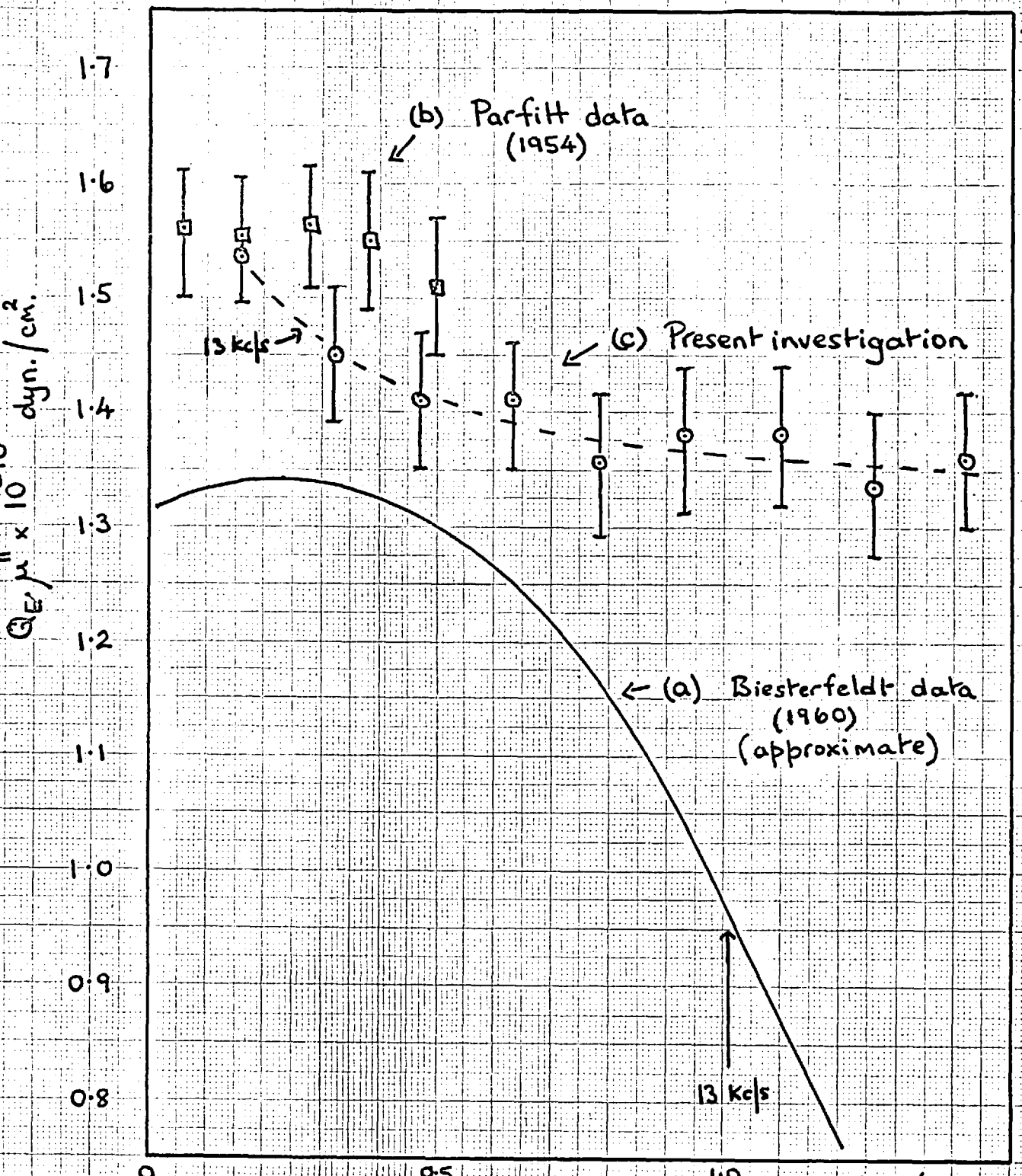

FIG.(6.3) Comparison of the values of $Q_E.\mu''$ derived from data from three different sources.

a damping factor in both the shear and E-modes to be reasonably independent of frequency. Above 13 kc/s on this graph, the value of δ_E does begin to increase, which would account for the decrease in $Q_E \cdot \mu''$ above 13 kc/s in plot (a) of Figure (6.3). However, the increase in δ_E above 13 kc/s (see Figure (6.2c)) is due to the proximity of the cut-off frequency as shown in the Biesterfeldt paper (their Figure 4) at about 22 kc/s when the ratio of the detected signal at resonance to that at the minimum between resonances tends to unity, thus invalidating the use of 1/Q as a measure of damping factor.

For the purposes of the present investigation, it is concluded from Figure (6.1) that the range of dimensions of rods used have no influence on the value of δ_E obtained. A comparison of the values of δ_E as given by Figures (6.1) and (6.2c) at the same frequency for the same material - "polystyrene" - underlines the problem of characterisation of polymers.

(d) Dependence of measurements on the nature of the specimen

(i) The occurrence of "bubbles" in polystyrene

All manufacturers claimed that their products would contain only a small amount of polymerising agent, and were otherwise free of filler or plasticiser. However, the samples of the Shell Chemical polystyrene used, which were cut from a block of the material manufactured by Shell, were found to

contain some absorbed impurity. Figure (6.4) shows a photograph of three samples of polystyrene. Specimen A is a portion of a commercial polystyrene rod, B is a sample of the Shell Chemical polystyrene, and sample C is another sample of the Shell Chemical product, but manufactured in a manner different from sample B. This photograph was taken after the samples had been heated to 200°C for about one hour, no bubbles or impurities being visible in the samples before this heat treatment.

Specimen A, being commercial rod, was probably formed by extrusion of the molten polymer. Specimen B was turned from a block which was either cast from the molten material or formed by the dissolving of the polystyrene pellets (of approximate dimensions 3 - 5 mm) in a suitable solvent (toluene, perhaps) and subsequent evaporation. In the case of specimen B, it was impossible to discover which method of manufacture had been used. Specimen C was made from the same batch of pellets as sample B, except that they were melted under a reduced air pressure of about 2 mm Hg.

The source of the bubbles in A and B is not chemical degradation, otherwise bubbles would be observed in specimen C. In any case, degradation is considered to take place at temperatures above 260°C, which was not

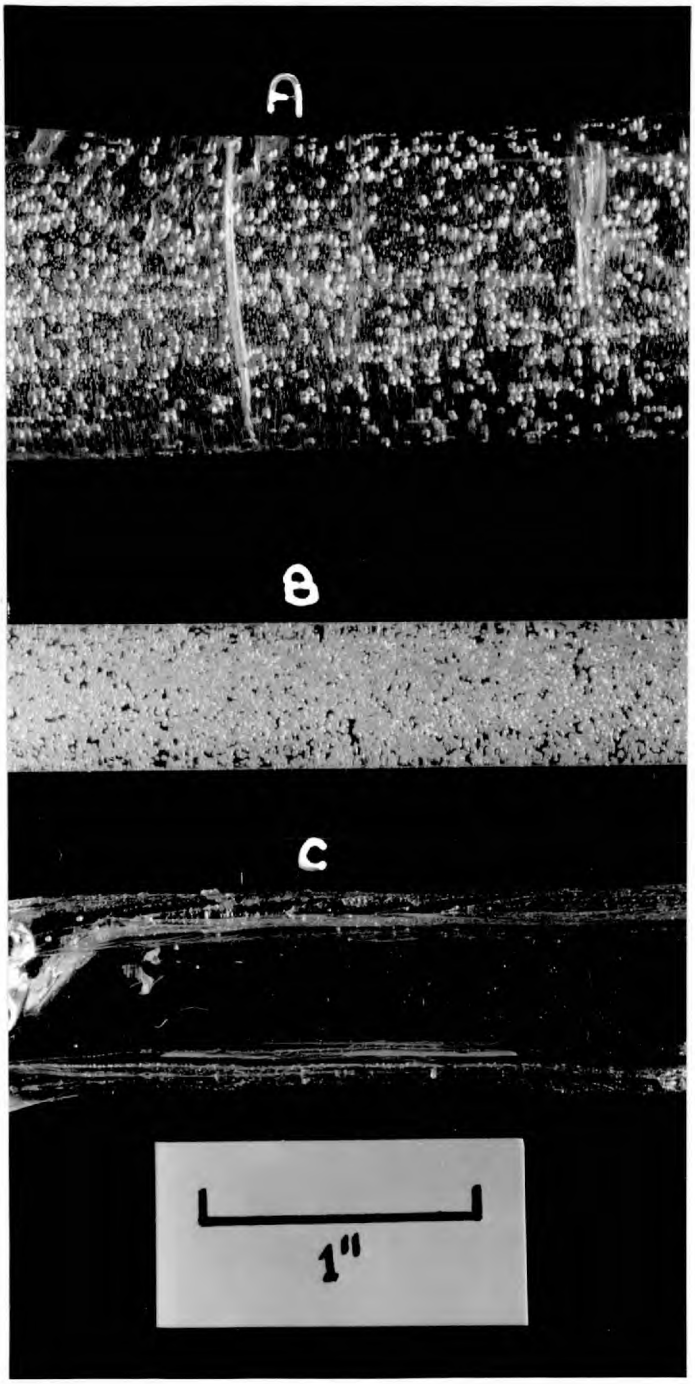

FIG.(6.4) Three polystyrene samples after heat treatment.

reached in the experiments reported here. A further check on this was made in heating samples cut from the same block as specimen B to 120°C for about 15 hours. Towards the end of this period, very small bubbles were seen to have appeared, thus demonstrating that the phenomenon could not be explained by degradation. It is suggested that the critical temperature is the glass-transition temperature, above which the viscosity of the rubber-like material is low enough to allow the absorbed impurity to appear as bubbles.

The bubbles are due to either

1. air trapped between the pellets of the material as they coalesce on melting and subsequently absorbed as the molten polymer is compressed in the extrusion process - specimen A, or
2. air or absorbed solvent - specimen B.

The source of the bubbles is not the pellets themselves, as was established by heating the pellets up to melting temperatures when no bubbles appeared. Bubbles did not appear in any of the polymethyl methacrylate samples up to temperatures at which they began to degrade. The method of manufacture of specimen C suggests that absorbed air can be a source of bubbles, but does not indicate whether the bubbles in specimen B are due to air or to solvent.

(ii) The effect of bubbles on the measured constants of polystyrene

The crude technology available for the manufacture of polystyrene in vacuo produced a specimen rod of distorted shape. Measurement of the damping factor, of E' and of the density of this sample(C) was carried out, however, and the values are shown below in Table (6.2) along with the values obtained for sample B both before and after the heat-treatment which produced the bubbles.

TABLE (6.2)

Calculated constants of three kinds of polystyrene at 15 kc/s

Sample	B before heating	B after heating	C	errors
density, gm/cc	1.050	1.010	1.053	$\pm$0.001
E'x10^{-10}dyn./cm^2	3.64_0	3.35_0	3.45_0	$\pm$0.005
damping factor x 10^2	4.5	4.7	4.4	$\pm$0.2

1. Density

As can be seen, there is little significant difference between the densities of sample B before heating and sample C even though the greater proportion of the source of the bubbles seems to have been eliminated (a few small bubbles, which cannot be seen in Figure (6.4), do exist in sample C

after heating). The density of sample B after heating, containing the bubbles, is of course lower than that of either samples B before heating and C. Some trouble was taken to measure the density of the pellets from which samples B and C were made, the former by the manufacturer and the latter by the author. The pellets are in the form of short cylinders, 0.2 cm in diameter, and 0.4 - 0.8 cm in length, the ends being broken and uneven. The pellets were put in a clean beaker and covered in distilled water. The beaker was then immersed in the tank of an ultrasonic cleaner which not only removed the fine polystyrene dust covering the pellets but "ground" the rough ends of the pellets. The density of the clean pellets was determined, using a specific gravity bottle, a large number of the pellets being tipped into the partially water-filled bottle. This method was found to be most unsatisfactory as air bubbles were also introduced with the pellets, giving values of the density ranging from 1.017 to 1.045 gm/cc, even when some of the air bubbles were removed by immersing the filled s.g. bottle in the ultrasonic cleaner. Finally, it was decided to introduce the pellets one-by-one into the s.g. bottle from a beaker which contained distilled water. On carefully selecting the pellets so that those with major cracks and those few with voids were excluded,

a value of 1.097 ± 0.002 gm/cc was obtained. A second measurement, using different pellets, confirmed this value. As can be seen, this value is 4% - 5% greater than either of the two values of density quoted in Table (6.2) for samples B before heating and C after heating.

It appears that some major impurity is introduced into samples when they are manufactured from pellets. The values of density quoted in Table (6.2) show that a brief vacuum treatment of the molten polymer is not sufficient to increase the density to that of the pellets, though the trend is in the right direction. Without more information on the mode of manufacture of the samples, and also of the pellets, it is not possible to discuss the source of the bubbles further. It is concluded that the quoted constants of commercial samples of polystyrene have to be considered with great care.

2. Young's modulus

There are real differences between the values of E' for the three samples. Without some knowledge of the physical states of sample B before heating and sample C it is not possible to say why E' of the former should be greater than for the latter. McKenzie (1950) has considered the effect of a uniform distribution of voids in a material on the values of the elastic constants. He

has shown that the change in Young's modulus, ΔE, observed in the sample with voids and of measured density, ρ_m, is given by

$$\frac{\Delta E}{E} = -[1 - \rho_m/\rho_i] \cdot 3 \cdot \frac{(9 + 5\sigma)(1 - \sigma)}{2(7 - 5\sigma)} \qquad (6.1)$$

where ρ_i is the density and E is the Young's modulus of the (ideal) material without voids respectively. Putting the following values into equation (6.1)

$$\rho_m = 1.010 \text{ gm/cc}; \quad \rho_i = 1.050 \text{ gm/cc}; \quad \sigma = 0.335$$

gives a value of $\Delta E/E$ of - 0.076. If the value of E of the ideal material is put at the value obtained for sample C, Table (6.2), then $\Delta E/E$ for sample B after heating is - 0.029. However, using the value of E obtained for sample B before heating for this ideal value gives $\Delta E/E$ = - 0.080, which implies that the material surrounding the bubbles in sample B after heating is more akin to that of sample B before heating than to that of sample C.

3. Damping factor

The damping factor values shown in Table (6.2) are seen to be the same within experimental error. Ying and Truell (1956) have calculated the energy scattered from spherical cavities embedded in an isotropic solid medium for longitudinal waves and have found that the losses due to scattering are small when the wavelength is large compared

with the diameter of the cavities, as in Rayleigh scattering. Their formula for scattering cross-section (which is the ratio of the total energy scattered per unit time to the incident energy per unit area per unit time) is

$$\frac{16.\pi^3}{9} \cdot g_c \cdot \frac{1}{L^2} \cdot \left\{\frac{\pi d}{L}\right\}^6$$

where d is the diameter of the cavities and g_c is some function of v_1/v_s and is of the order of 15 for polystyrene; all the other symbols have been used before. For d = 0.02 cm and L = 2 cm (the wavelength of the 10th resonance), the value of the scattering cross-section is 10^{-7} cm^{-2} which is clearly negligible.

The damping in sample C is seen to be no different from that in the other two samples.

(iii) The effect of molecular weight

Perspex The damping factor of the molecular weight regulated sample was found to be the same as that of the ordinary perspex, within experimental error. Young's modulus, E', of the molecular weight regulated sample was found to be about 3% lower at all frequencies than that of the ordinary perspex.

Polystyrene There were no differences between the values of either E' or damping factor for the two low molecular weight samples. The value of E' for the high molecular

weight sample was about 3% higher at all frequencies than that of the low molecular weight samples. The damping factor of the high molecular weight sample was about the same as that of the low molecular weight samples, within experimental error.

As pointed out in section (2.a), the effect of molecular weight on the glass transition temperature is negligible for values of $\bar{M}_n$ above about 20,000. Benbow and Wood (1958) have measured the damping factor of three low molecular weight organic glasses and three polymers (polyethylene, polystyrene and perspex) and have shown that the damping factor of two of the former lies between those of the perspex and the polystyrene. Whilst this evidence is hardly conclusive, it appears that the effect of molecular weight on the properties of polymers, when the molecular weight is in excess of a certain value, is negligible for polymers below their glass transition temperature.

(iv) The effect of plasticiser on the properties of perspex

The sample of PMMA containing 10% dibutyl phthalate had a damping factor which was 34% higher at all frequencies than that of the pure material, as given by the perspex specimens. The value of E' of the plasticised PMMA was about 1% lower than that of perspex.

Parfitt (1954) found that perspex plasticised with 5% dibutyl phthalate had a damping factor of about the same magnitude as the pure material, and E' was about 4% lower than for the unplasticised polymer. Heijboer (1956) has investigated the effect of this same plasticiser on the secondary transition of perspex, see section (2.h) for a description of the effect on the position of the maximum. The height of the maximum was found to increase with increasing amount of plasticiser, 10% of dibutyl phthalate increasing the damping factor by about 16% at all frequencies up to 1 kc/s.

There is little agreement between these three quoted effects of dibutyl phthalate on PMMA, which is perhaps due to differences in the pure material, though Heijboer's measurements were made at a lower frequency than those of Parfitt and of the present investigation.

(v) The effect of absorbed water on the constants of perspex and polystyrene

The resonant frequencies and damping factor of a rod of perspex and of polystyrene were measured and the rods were weighed. After total immersion in water for 10 days, the same constants were once more measured. The percentage increase in weight of the perspex rod was 0.25% and no

increase in weight was noted for the polystyrene rod. No detectable changes in E' or damping factor of the polystyrene or of the perspex were found.

The amount of absorbed water to be expected is very small. I.C.I. Ltd. quote an increase in weight of 2% for a sample of perspex totally immersed for a period of 240 days. Monsanto Ltd. quote an increase in weight of 0.03% for a polystyrene sample similarly treated.

Yamamoto et al. (1957) have investigated the effect of totally immersing a perspex sample for a period of two months. The only differences they reported were in the shifting of the β -transition (see section (2.h)) and the appearance of a new peak in the damping factor versus temperature graph at about 10°C; the frequency of observation was 37 kc/s..

Whilst it appears that the amount of absorbed water likely to be present in the polymer samples used in the present investigation has no effect on the measured constants of the samples, they were stored in an air-tight dessicator containing silica-gel.

(vi) The effect of thermal history

A block of polystyrene was heated slowly to 115°C (i.e. just above T_g) at which temperature it was maintained for about two hours and was then slowly cooled to room

temperature, over a period of eighteen hours. After removal from the oven, it was kept at room temperature for a week, after which a rod of dimensions $7\frac{3}{4}$" x $\frac{1}{4}$" was slowly machined from the block, using plenty of coolant. The specimen rod was then annealed at 85°C (i.e. just below T_g) for three hours after which it was allowed to cool to room temperature in the oven overnight. After a week, the damping factor of the specimen rod was measured as a function of frequency, which will be referred to as measurement A.

The sample was heated in situ to 36°C at which temperature it was maintained for two hours, when it was considered that temperature equilibrium had been established. The vacuum chamber was then removed from the higher-temperature bath and placed in the bath at room temperature, where it was maintained for a week. The damping factor of the polystyrene rod was again measured, which will be referred to as measurement B. This procedure was repeated twice, for temperatures of 60°C and 75°C, after each heating the vacuum chamber was returned to the room temperature bath followed by the measurement of the damping factor after a period of some days. These measurements are referred to as C and D respectively. Finally, the rod was slowly annealed as described above in an attempt to remove the effects of the severe heat treatment to which it had been

subjected, after which the damping factor was once more measured - measurement E.

TABLE (6.3)

Dependence of measured damping factor (1/Q) of polystyrene at 9 kc/s on thermal history

Measurements	A	B	C	D	E	Errors
(1) H eated to (deg.C):	85	36	60	75	85	±1
(2) Cooled to (deg.C):	23	23	23	23	23	±1
(3) Equilibrium time (hours):	10	1	1	1½	10	-
(4) Approximate cooling rate (deg.C/hour):	6	13	37	34	6	-
(5) Time of measurement (hours):	180	48	150	240	80	-
(6) Limiting damping factor: ($x10^{3}$)	4.5	4.7	4.9	5.4	4.6	±0.2

Notes:

(3) Time of attainment of temperature equilibrium.

(4) Cooling rate is not linear, which is assumed in this calculation.

(5) Time after which value of damping had reached values shown in (6) after attainment of 23°C.

(6) Value of damping factor obtained after length of time shown in (5).

Table (6.3) shows the effect of the various heat treatments on the measured damping factor at 9 kc/s. The damping factor as measured at 23°C was to a certain extent dependent upon the time of measurement after thermal equilibrium had been achieved. Thus the value of damping factor measured immediately after the attainment of 23°C following cooling from 60°C was found to relax from 5.2×10^{-2} to 4.9×10^{-2} after 150 hours, see Table (6.3). A similar effect was noted in the measurements that were made after cooling from 75°C, though none was observed for the sample when cooled from 36°C. Measurement of the density of similarly treated samples of polystyrene showed no change in the density, within the experimental error of 1/1000. As can be seen from Table (6.3), the measured damping factors differ for the same material with varying cooling rates and initial elevated temperature, though it is to be noted that a final slow annealing of the specimen removes the effects of the previous quenching.

The amount of the relaxation noted in the damping factor for measurement C, 0.3×10^{-2}, is of the order of magnitude of the experimental error, though the trend to lower values is a consistent one. Such an effect was noted by Parfitt (1954), though on a larger scale, for specimens which had been cooled from above the glass transition temperature, though

he also detected a related decrease in the density of the specimen. It is seen from the present investigation, therefore, that the attainment of temperature equilibrium need not be proof of the completion of the annealing process even when cooling the specimen from temperatures below T_g.

In performing his experiments, Parfitt was careful to avoid the possibility of strain occurring in his samples. Investigation of samples heat-treated in a manner similar to those referred to in Table (6.3) by means of polarised light, showed that substantial strain existed in them. It is therefore concluded, that the different values of damping factor shown in Table (6.3) are due to different amounts of strain existing in the specimens. The fact that a slight relaxation was noted in the values of damping factor of samples cooled from below the glass transition temperature implies that free volume might be changed by such a process, but by an amount that is very small.

(vii) Conclusions

It is seen that the most likely cause of differences in the quoted values of the damping factor of nominally the same polymer is the thermal history of the specimen under test. Whilst plasticiser content has some effect on the values of damping and of E', and whilst molecular weight

differences seem to influence the value of E', it is considered that thermal history of the sample is the one quality of the polymer which should be referred to in characterising the specimen. As a result of this conclusion, all specimens used in the present investigation were annealed following the procedure described at the beginning of section (6.d.vi).

(e) Temperature and frequency dependence of the components of the complex Young's modulus

(i) Frequency dependence

Figure (6.5) shows the frequency dependence of the real and imaginary components of Young's modulus for perspex and polystyrene. The comparison of the values of E' of the present investigation with those obtained by Parfitt (1954) has been carried out in section (5.d). The values of E" obtained by Parfitt for perspex are shown in Figure (6.5), and do not compare well with those of the present investigation, even for the lower temperature at which Parfitt's measurements were made (19.5°C), see Figure (6.7) As described in section (6.a), the damping factor of polystyrene obtained in the present investigation is slightly higher than that obtained by Parfitt.

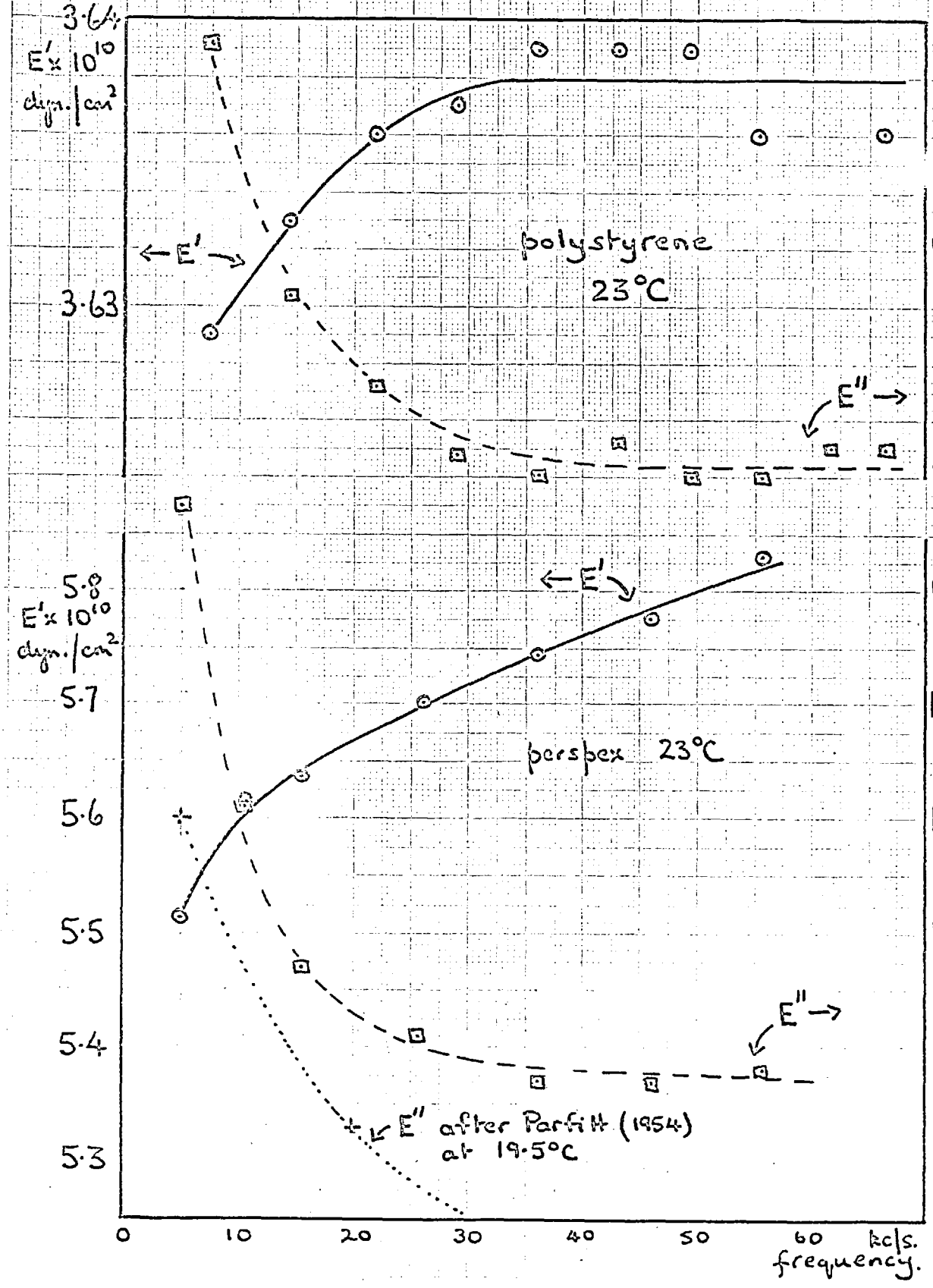

FIG.(6.5) The frequency dependence of the complex Young's modulus of polystyrene and perspex.

(ii) Temperature dependence

Figure (6.6) shows the dependence of E" and E' on temperature for perspex. The measurements were taken for an increasing and a decreasing temperature (shown by arrows ⟶ increasing, ⟵ decreasing), to investigate possible hysteresis effects referred to in section (6.c.viii). As can be seen, no such effect was detected. The temperature dependence observed by Parfitt for Young's modulus is also shown in Figure (6.6). Whilst the dependence of E' seems to be about the same (except for a magnitude difference), his values of E" are possibly approaching the maximum of the glass transition more rapidly than those observed in the present investigation.

Figure (6.7) shows the temperature dependence of Young's modulus for polystyrene. Compared with Parfitt's results, it seems that the value of E" is approaching the maximum of the glass transition more rapidly, implying either a lower glass transition temperature or a broader maximum for the polystyrene used in the present investigation compared with that for the polystyrene used by Parfitt. No hysteresis effects are noted in the temperature dependence of either E' or E" for the present investigation.

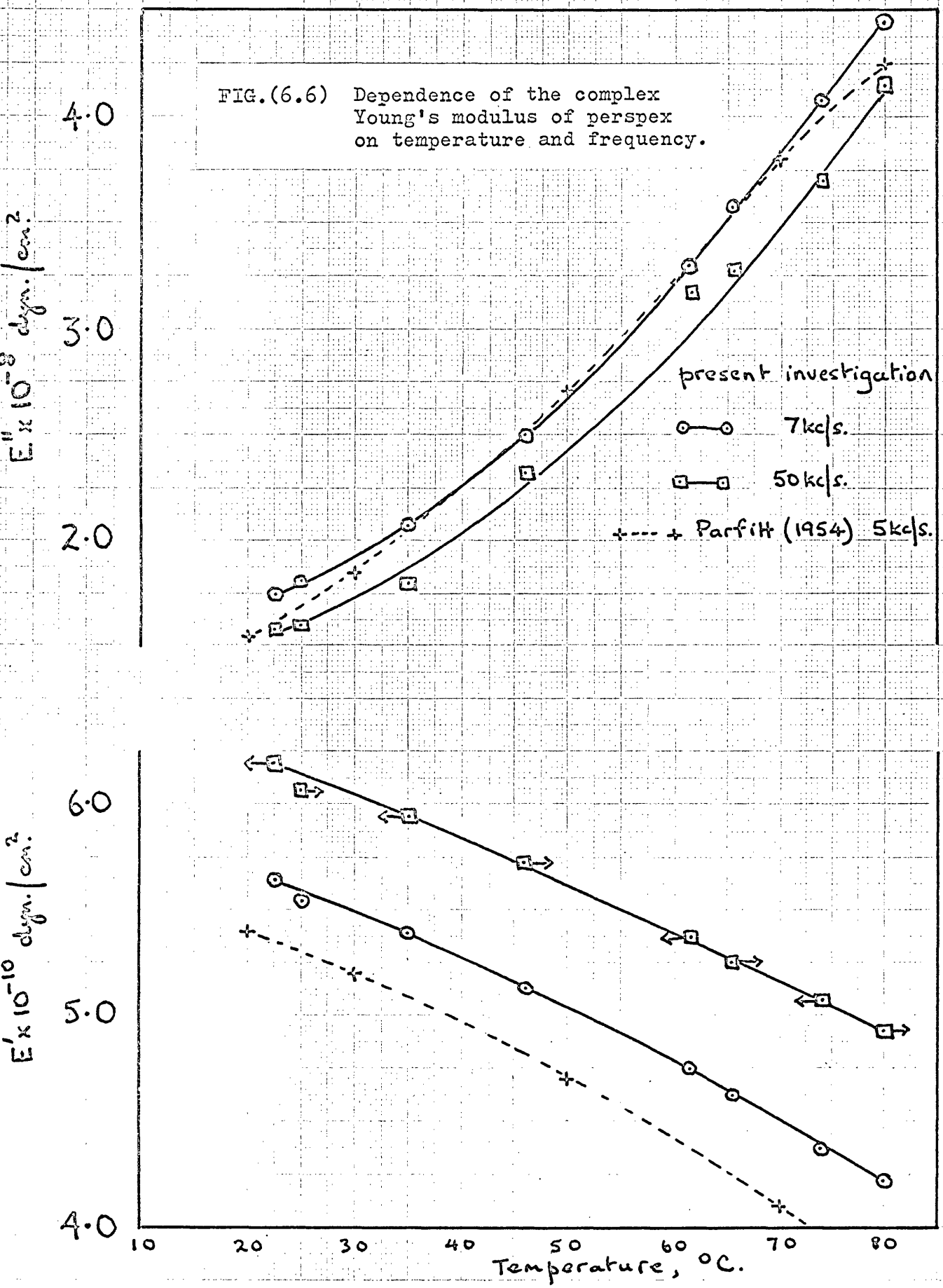

FIG.(6.6) Dependence of the complex Young's modulus of perspex on temperature and frequency.

FIG.(6.7) Dependence of the complex Young's modulus of polystyrene on temperature and frequency.

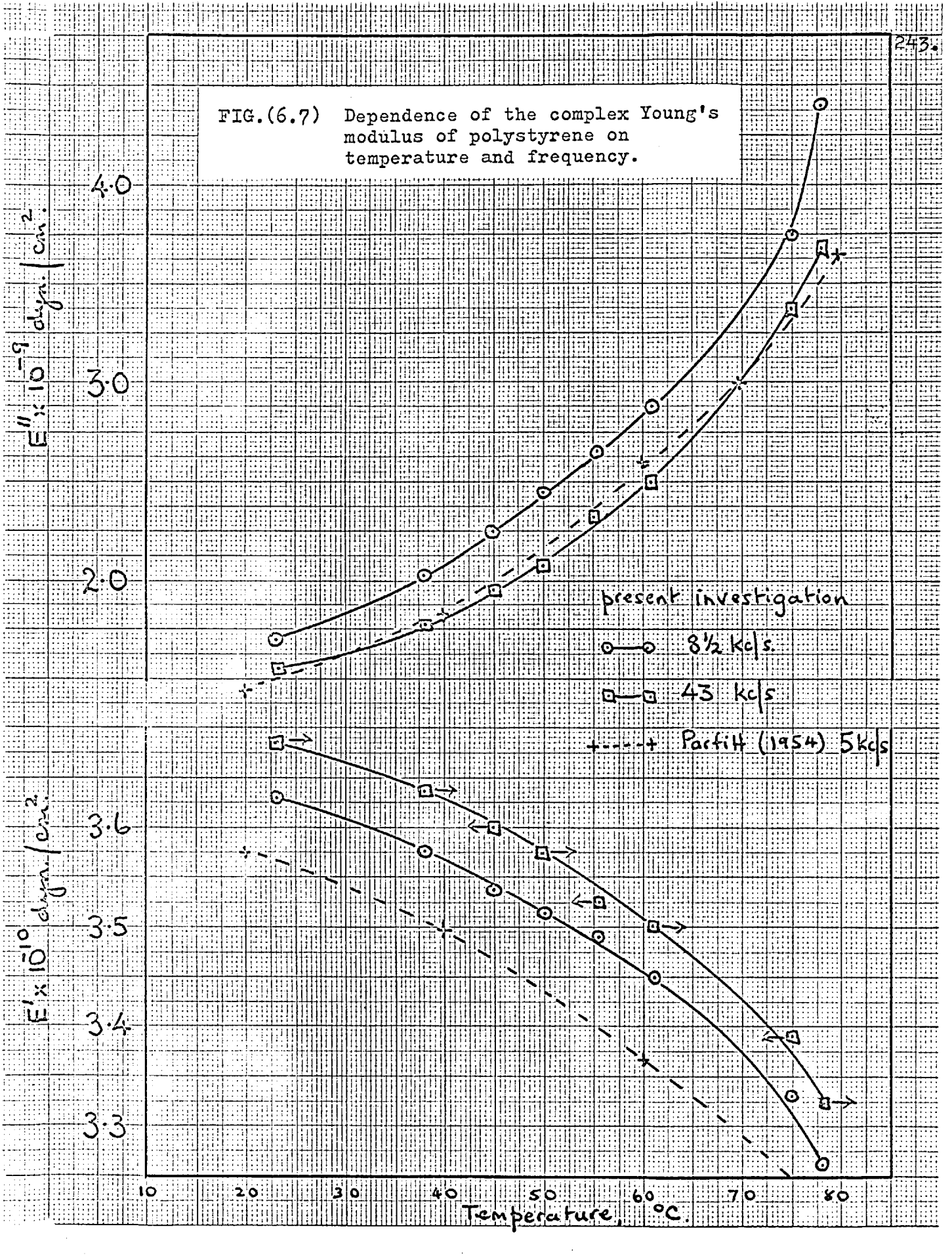

(f) The effect of subjecting the specimens to pressure

(i) General comments

The effect of increasing the temperature of a polymer is to increase the kinetic energy of the molecules which makes for a decreased packing of the molecules and therefore a lower density. At the glass transition temperature, the motion of the molecules is so large that segments of the backbone chain are in motion and the properties of the material are rubber-like. At the melting point, the individual molecules, which were pinned together along their lengths in the rubber state, break free one from another and begin to flow if subjected to a suitable pressure gradient.

An increasing pressure has an opposite effect, in that the molecules are forced closer and closer together such that a polymer which was previously rubber-like will become glass-like at a certain pressure, depending on the temperature of the polymer. Thus, the higher the temperature, the greater the pressure required to bring about the glass transition from the rubber-like state. Matsuoka and Maxwell (1958) have shown that once polystyrene, polyethylene and polypropylene are in the molten (as distinct from the rubber-like) state however, a pressure of 30,000 p.s.i. (2,000 atm.) is insufficient to

bring about the glass transition.

Because of the molecular structure of amorphous polymers, the attainment of the glass-like state by the application of pressure, is also dependent upon the rate of pressure increase. Thus, the above authors have shown that the glass transition of a high molecular weight polystyrene at 120°C occurs at about 10,000 p.s.i. but increases to 15,000 p.s.i. when the rate of pressure increase is reduced to about 1/300 of the former rate. Hence, for a slower application of pressure, more time is available for the polymer molecules to adjust to this inhibition of their motion. Also the final volume change is greater and the less is the free volume. Further, as Matsuoka and Maxwell point out, "in packing the mold for injection molding, if .... the time of pressure application is shortened, less material will enter the mold per cycle since the melt is less compressible at a rapid rate of compression". Thus, the ultimate properties of a particular specimen will depend on the method of its manufacture.

These conclusions on the behaviour of polymer samples subjected to an increase in temperature and pressure are relevant to the present investigation, which is concerned with the possible changes in the density and the damping factor of perspex and polystyrene samples after the application of

pressure at given temperatures. Thus, that no changes in these constants were noted for the application of pressures up to 7,000 p.s.i. followed by a heating of the samples to 80°C, is not surprising, as the confining pressure would have been sufficient to stop any changes in the packing of the molecules resulting from the increased temperature.

Even so, increasing the pressure slowly after the temperature had been increased to values less than 80°C did not produce changes in the density and damping factor of the samples, as measured after the temperature and pressure had been decreased (the former slowly, the latter rapidly) to normal laboratory values. It is concluded that the critical temperature for such experiments is the glass transition temperature, which is (90 - 95)°C for polystyrene and about 120°C for perspex.

As the method of heating the pressure apparatus was the pumping of hot water through a jacket, experimental results above T_g for perspex were therefore unobtainable, and the following section describes experiments carried out on polystyrene samples.

(ii) Measurements on polystyrene

Two polystyrene rods were annealed at the same time in the manner described at the beginning of section (6.d.vi) and then placed in the dessicator for a week. They were then considered to have reached volume equilibrium and their densities were measured using a specific gravity bottle. The damping factor of the material of each rod was then measured as a function of frequency. Within experimental error, the densities and damping factors of the two rods were found to be identical.

Both rods were placed in the brass cylinder of the pressure vessel and covered with mercury, see section (3.j), which was then placed in the pressure vessel with the bleed valve open. The temperature of the pressure vessel was then raised slowly to 98 $\pm$ 2^{o}C and maintained there for two hours after which the bleed valve was closed and the pressure raised slowly to 6,000 p.s.i. These temperature and pressure conditions were maintained for three hours after which the temperature was slowly reduced (over about two hours) to room temperature (23^{o}C) and maintained there overnight (about 12 hours). The pressure which had been maintained at 6,000 p.s.i. throughout these temperature changes, was then suddenly

released. The densities of the rods were then measured, after which one of them was placed in the resonance-measuring apparatus for damping factor measurements to be made over a period of time. The density of the other sample was periodically measured using a specific gravity bottle.

Figure (6.8) shows the dependence of volume of one rod and the damping factor of the other as a function of time after the release of pressure in the pressure vessel.

(iii) Discussion of results and comparison with the findings of other workers

As can be seen from Figure (6.8), the density and the damping factor have both been increased by applying pressure when the specimens were above the glass transition temperature. That the damping factor should increase with an increased density is contrary to the assumption that internal friction decreases with decreasing free volume. Section (6.d.vi) considered the effect of thermal history on the damping of the polymer specimen, where it was concluded that internal strains brought about by the heat treatment produced the changes in damping factor noted. It is concluded therefore, that the increased damping factor noted

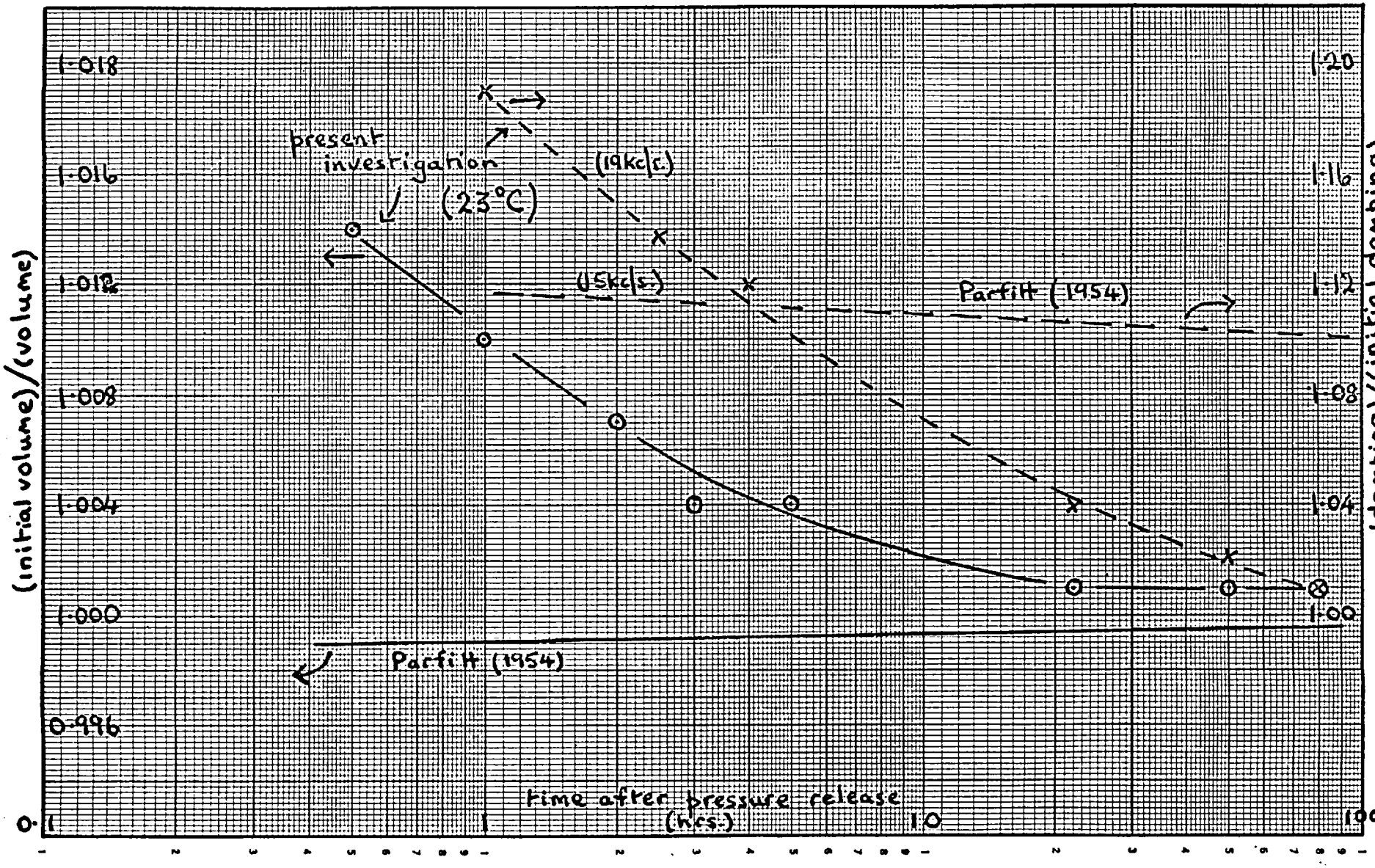

FIG.(6.8) Variation of volume and damping factor of a polystyrene specimen with time after release of pressure.

after the release of pressure is due to strains in the sample produced by the temperature/pressure treatment.

This explanation is consistent with the observed relaxation of the values of both damping factor and density to the values measured before the treatment. Thus the stressed, high density state of the polymer molecules relax to a more typical value (as determined by the temperature of the specimen, i.e. 23°C) on release of the pressure, even though the specimen is then below its glass transition temperature, below which only minor changes in the motion of the molecules are considered possible.

In terms of the free volume, the effect of the heat/pressure treatment of the polystyrene specimens as described above is as follows. As the temperature of the specimens rises, their free volume slowly increases, showing a sudden jump in value to 2.5% of the volume above T_g (see Kovacs, 1964). The increasing pressure then produces a response which may be regarded primarily as the collapse of free volume (Ferry, 1961, page 409). If pressure were to be released whilst at a temperature above T_g, the free volume would quickly assume its former

proportions, whereas maintaining the pressure whilst decreasing the temperature of the specimen below its glass transition temperature should result in a "freezing-in" of the new molecular configuration of higher density. Figure (6.8) shows that this new (denser) configuration is not fixed, but relaxes back to the state expected of a polystyrene sample which had been cooled through the glass transition without any confining pressure acting. Any possible decrease in the damping factor of the specimen is, by this explanation, hidden in the increase in damping factor due to the strains set up by the pressurising of the specimen.

Delaying the final release of pressure in the pressure vessel for one week after the attainment of room temperature by a polystyrene sample similarly treated, produced a slightly less rapid decrease in density than that shown in Figure (6.8) and to a value which was marginally higher than that shown for 50 hours, implying that some small relaxation in volume had taken place within the glass-like state, whilst under pressure.

Figure (6.8) also shows the change in damping factor

with time that Parfitt (1954) produced in a polystyrene sample by heat-treatment. He cooled a specimen from 97°C to 60°C in three minutes and then more slowly cooled the specimen down to room temperature in order to avoid the setting up of strains within the specimen. The volume change that he produced by this process was 0.15%, which is seen to be about an order of magnitude less than by the present method. He found that the volume and damping factor decreased logarithmically with time, whereas the increase in volume and decrease in damping factor found in the present investigation is seen to be faster than this, the relation between the initial volume v_i (before temperature/pressure process), the instantaneous volume, v, and time being expressed by the relation:-

$$(v_i - v) \propto t^s \qquad (6.2)$$

where s is of the order of -0.71, for the time period up to 22 hours after the release of pressure, no detectable changes either in volume or damping factor being observed after this period.

Due to the possibility of the polystyrene sample containing some impurity, as discussed earlier in this

chapter, the high rate of volume relaxation may not be significant, for if the impurity acts as a plasticiser, the friction between molecules will be substantially reduced. However, plasticiser in the form of dibutyl phthalate has been shown to increase the damping factor of perspex by a large amount, as was noted in section (6.d.iv), though no effect on the damping factor of a polystyrene specimen from which the prime source of the "bubble" impurity had been removed was noted, Table (6.2). Further investigation of this volume relaxation effect on pure samples of polystyrene is obviously desirable.

Matsuoka and Maxwell (1958) have obtained a value of 2.4% for the change in volume produced in a polystyrene sample by 6,000 p.s.i. at a temperature of 99°C, which is seen to be of the order of magnitude to be expected of the volume change produced by the present experiment. However, their value of ~~compressibility~~ bulk modulus of polystyrene below the glass transition (at 37°C) is of the order of (15×10^{10}) dyn./cm^2, whereas that derived from the values of E' and μ' obtained in the present investigation (see Table (4.8)) and the Lamé elastic constant relationships (Appendix 1) is (3.74×10^{10}) dyn./cm^2. This latter value is of the

order of magnitude that Wada's data (1959) would give for K from these relationships, see Table (4.9). Using the Lamé elastic constants λ and μ quoted by Mason (1958) gives a value of K of (4.2×10^{10}) dyn./cm^2. There appears, therefore, to be some doubt about the use of the Lamé elastic modulus relationships for estimation of the compressibility.

(g) Conclusions from Young's modulus and damping factor measurements

The experiments on polystyrene reported here have been carried out on samples which have been shown to contain an impurity which produces bubbles in the specimen at temperatures above T_g. Below this temperature, bubbles were not observed. Hence some doubt must be associated with the values of constants quoted here, though experiments on a crude sample of polystyrene made in vacuo (which process seemed to remove most of the "bubble" impurity) suggested that the density and the damping factor are little affected by the impurity, though the value of E' decreased, see Table (6.2). It has been shown that the density of pellets of polystyrene (which can be looked upon as the raw material for specimen

manufacture) is about 4% higher than specimens formed into blocks.

The dimensions of rods whose resonances give values of δ_E have been shown to have no effect on the magnitude of the damping factor for values of d/L from 0.017 to 0.100, when compared at a constant frequency. The most likely cause of differences in the quoted values of constants for, nominally, the same polymer is considered to be due to the different thermal histories of the specimens investigated.

The effect of 7,000 p.s.i. on the volumes of perspex and polystyrene specimens below their glass transitions has been shown to be negligible. However, when a polystyrene specimen is compressed whilst above its glass transition temperature, followed by a cooling to room temperature, the resulting change in volume is not a permanent one, for the volume of the specimen soon relaxes to the value noted before the compression took place. Hence, whilst a pressure of 7,000 p.s.i. was insufficient to materially affect the volume of the glass-like polystyrene, the internal pressure produced in the specimen by the compression above T_g was sufficiently high at room temperature to change the volume of the

specimen by about 2%, and over the relatively short length of time of about 20 hours. The magnitude of the volume change is to be expected from the work of Matsuoka and Maxwell (1958) but the rate of the relaxation is high compared with those produced by quenching. The extent to which the rate of volume relaxation is dependent on the purity of the specimen is unknown.

SUGGESTIONS FOR FURTHER WORK

Velocity dispersion in finite cylinders

Further experimental work on short cylinders needs undertaking to establish the magnitude of the end-effects. Before this can be done, however, the frequency dependence of Young's modulus and Poisson's ratio must be unambiguously determined, preferably by a method other than the resonances of cylinders, e.g. a pulse technique. One possible method of determining the order of magnitude of the end-effect is by means of a cylinder of such dimensions that one of its resonances occurs at a value of d/L of 0.58606, i.e. the universal point. Comparison of the frequency of this resonance, which is not influenced by end-effect, with the other resonances may offer some estimate of the magnitude of the end-effect. Such an experiment will require very small tolerances on the dimensions of the cylinder and on the temperature stability of the apparatus, even assuming that the density of the material is uniform throughout the cylinder. For this latter cordition to hold, it is felt that the use of either fused quartz or optical quality glass is essential.

The behaviour of the resonances of short cylinders at high d/L values (i.e.> 0.65) is still unexplained, particularly the difference between that of the glass cylinders and of the cylinders made of aluminium and the

polymers. Apparatus which will detect the nodal distributions along the length of the cylinder and across an end-face, in order to determine their mode(s), is required as the starting point of any further investigation of this region.

Polymer studies

The exact nature of the "bubble" impurity in polystyrene, and its effect on the measured constants of this polymer, need determining before any further work on polystyrene can be undertaken, particularly at temperatures above the glass transition. Other polymers should perhaps be carefully investigated in order to determine if any similar impurities occur.

The limited pressure experiments on polystyrene have indicated the existence of relatively fast relaxations of molecules nominally "fixed" in the glass-like state. It is suggested that further work on such pressure effects would be more conveniently carried out on polyvinyl acetate, an amorphous polymer whose glass transition temperature is about 30°C. Thus the required temperature range of the pressure experiments will be much more easily obtained. The dependence of the rate and magnitude of volume relaxation on pressure and on the temperature at which the pressure is applied is considered worthy of investigation.

APPENDIX 1

Brief review of viscoelastic behaviour

As Ferry (1961) expresses it, the "classical theory of elasticity deals with mechanical properties of perfectly elastic solids, for which, in accordance with Hooke's law, stress is always directly proportional to strain but independent of the rate of strain. The theory of hydrodynamics deals with properties of perfectly viscous liquids for which, following Newton's law, the stress is always directly proportional to the rate of strain but independent of the strain itself."

However, these categories are idealised and any real solid shows deviations from Hooke's law under suitably chosen conditions and "it is probably safe to say that any real liquid would show deviations from Newtonian flow if subjected to sufficiently precise measurement..." (Ferry, 1961, page 1).

A viscoelastic solid is one for which a time dependency of the reaction of the solid to some constraint is apparent, and therefore its behaviour has to be expressed in terms of both elastic and viscous effects. It is assumed that the behaviour of the materials considered are linearly dependent on the stress amplitude.

The simplest way of showing the behaviour of a viscoelastic material is in terms of the Burgers spring and dashpot elements.

A Hookean solid is a perfectly elastic spring and a Newtonian liquid is a perfectly viscous dashpot. A spring and a dashpot together in parallel is known as a Voigt solid following this author's work (1892) on the behaviour of such a system to an externally applied stress. A spring and dashpot in series ia a Maxwell (1867) liquid. Figure (A1.1) shows these models and the appropriate differential equations relating stress, S, to strain, ε, through the elastic constant of the spring, c, and the viscosity constant, η, for these models, are given below.

(a) $S = c.\varepsilon$

(b) $S = \eta . \frac{d\varepsilon}{dt}$

(c) $S = c.\varepsilon + \eta . \frac{d\varepsilon}{dt}$

(d) $S + \frac{\eta}{c} . \frac{dS}{dt} + \eta . \frac{d\varepsilon}{dt}$

(e) $(1 + \frac{c_2}{c_1}) S + \frac{\eta}{c_1} . \frac{dS}{dt} = c_2 . S + \eta . \frac{d\varepsilon}{dt}$

It should be pointed out that the constants c and η do not necessarily represent the behaviour of any identifiable molecule or part thereof comprising the material; they serve to express mechanical effects observed in materials in bulk.

Equations similar to those above can be written for any kind of stress/strain behaviour, be it mechanical or otherwise, e.g. section

(a) Hookean solid

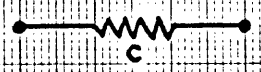

(b) Newtonian liquid

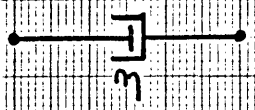

(c) Voigt solid

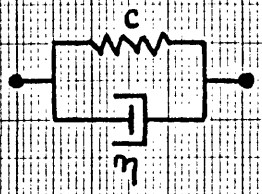

(d) Maxwell liquid

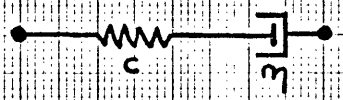

(e) Simple relaxing medium

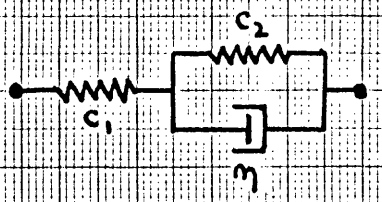

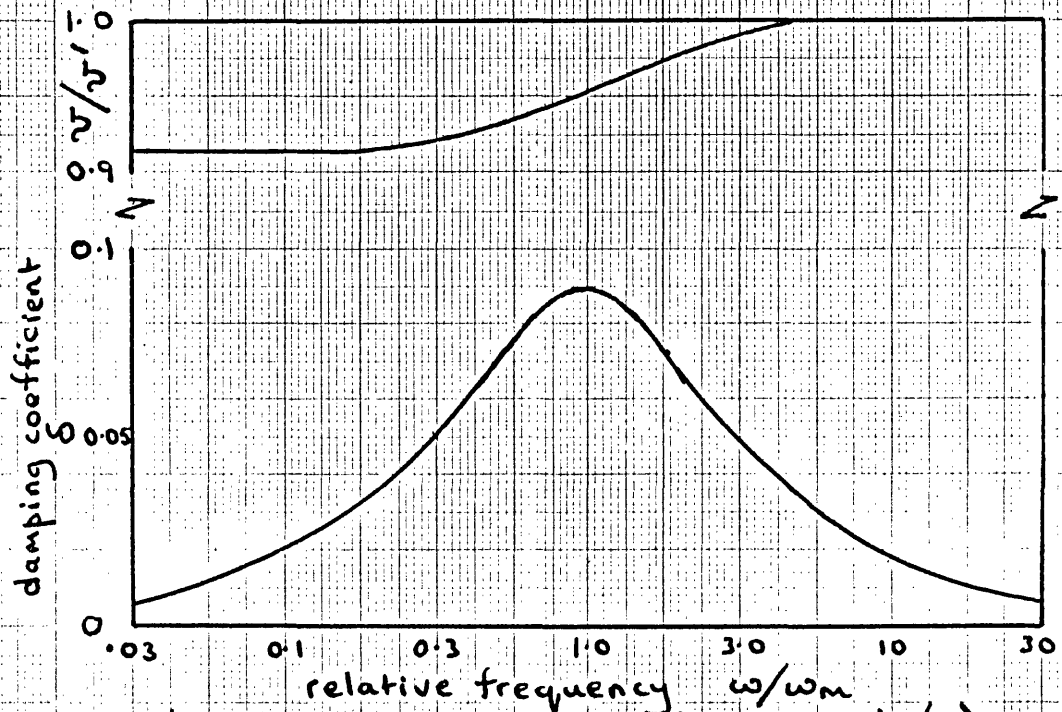

(f) Velocity and damping for Model (e)

FIG.(A1.1) VISCOELASTIC MODELS.

(2.2e) deals with the temperature dependence of volume of a viscoelastic material starting from a Voigt type equation. Nor is one limited to the use of the Voigt or the Maxwell models; systems of numbers of each type or both types together, either in parallel or series, can be put together, though the complexity of the analysis of such systems grows with each addition.

One much used model (Zener, 1948; Mason, 1958; Kovacs, 1961) shown in Figure (A1.1e), is called the simple relaxing solid model. Zener has shown that such a model subjected to a sinusoidally varying strain demonstrates several mechanical phenomena which are observed in solids. On applying a tension to its terminals, it will immediately extend by stretching the spring c_1 which will be followed by a further slow or "retarded" extension as the piston moves through the dashpot, allowing spring c_2 to extend. The model thus demonstrates creep. Solution of the differential equation for equation (e) above by setting $\frac{dS}{dt} = 0$ shows the creep to be exponential with a time constant η / c_2, which is usually called the retardation time. If the terminals are suddenly pulled apart, by a distance ε, at first c_1 only is extended, but over a period c_2 will yield and the tension in the model will decrease, or relax, from the value $c_1 . \varepsilon$ to $\varepsilon . c_1 . c_2/(c_1 + c_2)$, the time constant in this case being $\eta/(c_1 + c_2) = \tau$. The model thus demonstrates stress relaxation and τ is called the relaxation time.

At frequencies low with respect to $1/\tau$, the elastic behaviour of the model is that of the two springs c_1 and c_2 together in series, thus having an elastic constant of $c_1c_2/(c_1 + c_2)$, and at high frequencies, the elastic constant will be c_1. At frequencies inbetween, the elastic constant undergoes a transition from one value to the other, which would be observed experimentally as a transition of the phase velocity as shown in Figure (A1.1f), where v is the velocity at frequency ω and $v' = (c_1/\rho)^{\frac{1}{2}}$, ρ being the density of an equivalent material; ω_m is given by $\frac{1}{\tau} \cdot [c_2/(c_1 + c_2)]^{\frac{1}{2}}$

When the simple relaxing model (and indeed any material showing internal energy losses) is subjected to a sinusoidally varying stress, the strain is neither perfectly in phase with the stress, as for a perfectly elastic solid, nor exactly 90^o out of phase, as for a perfectly viscous liquid, but somewhere inbetween, dependent upon the values of c_1, c_2, η and the value of $1/\tau$ compared with the frequency with which the stress is applied.

The strain can be resolved into an in-phase and a quadrature component, the former being a measure of the stored (recoverable) energy, whilst the latter is associated with the irreversible energy loss in the material. Hence both strain and stress can be looked upon as complex, which results in Young's modulus, for example, being complex, as is shown as follows:-

$$S^*/\varepsilon^* = E^* = E' + jE'' = E'(1 + j\delta_E)$$

where $\delta_E = E''/E'$ is the damping coefficient or damping factor. Similar equations can, of course, be written for the other forms of deformation such as bulk and shear. The damping coefficient is therefore the irrecoverable part of the energy associated with the excitation of the model, and is linked in a real material to molecular processes.

Evaluating δ for the simple relaxing model shows that it has a maximum value at $\omega = \omega_m$ and falls off very rapidly at both high and low frequencies, as shown in Figure (A1.1f). Few processes of a viscoelastic nature can be expressed in terms of a single value of τ resulting from the setting up of a simple Burgers type model, and even relaxation peaks similar in shape to those of the simple relaxing model cannot be explained in this manner. Most experimentally observed relaxation processes can only be expressed in terms of a distribution of relaxation times, which is equivalent to the setting up of models comprising large numbers of elements, as described earlier in this section.

The value of δ can be determined from the 3 db Q factor of the resonance of an isotropic rod, see Mason (1958, page 190) for example. For the rod excited into Young's modulus mode resonances, the following relationship holds:-

$$1/Q_E = (\omega_1 - \omega_2)/\omega_o = \quad \delta_E \qquad \text{(A1.2)}$$

where ω_1 and ω_2 are the frequencies at which the amplitude of the resonance has fallen by 3 db on each side of the maximum. Similar relationships can be written for rods excited into other mode resonances. Parfitt (1954) has reviewed the different theoretical forms taken by the damping factor and shows some of the relations that exist between them.

Gross (1953) and Ferry (1961) have reviewed the theory of viscoelasticity and the latter also quotes experimental evidence.

The Lamé elastic constants

The Lamé elastic constants, λ and μ (sometimes called the Lamé elastic moduli), referred to in the present work, are derived from the following stress/strain relationships for a perfectly isotropic medium. T_n and S_n are respectively the stress and strain in the n-direction.

$$T_1 = (\lambda + 2\mu).S_1 + \lambda(S_2 + S_3) \quad ; \quad T_4 = \mu.S_4$$

$$T_2 = (\lambda + 2\mu).S_2 + \lambda(S_1 + S_3) \quad ; \quad T_5 = \mu.S_5$$

$$T_3 = (\lambda + 2\mu).S_3 + \lambda(S_1 + S_2) \quad ; \quad T_6 = \mu.S_6$$

It can be shown (Mason, 1958) that

(1) shear modulus = μ

(2) Young's modulus, $E = \mu.(3\lambda + 2\mu)/(\lambda + \mu)$

(3) Poisson's ratio, $= \lambda/(2\lambda + 2\mu) = E/2\mu - 1$

(4) bulk modulus, $K = \lambda + \frac{2}{3}\mu$

and hence a knowledge of two of the above constants will allow calculation of all of them.

In accounting for internal losses in a material, the complex notation described earlier is used, when Poisson's ratio is shown to be given by

$$\sigma^* = \sigma' + j\,\sigma'' = E^*/2\,\mu^* - 1$$

$$= \frac{\mu'(E' - 2\mu') + \mu''(E'' - 2\mu'')}{2(\mu'^2 + \mu''^2)}$$

$$+ j.\left\{\frac{\mu'(E'' - 2\mu'') - \mu''(E' - 2\mu')}{2(\mu'^2 + \mu''^2)}\right\}$$

Writing $\delta_E = E''/E'$ and $\delta_\mu = \mu''/\mu'$, it can be shown that

$$\sigma' = \frac{(E'/2\mu' - 1) + \delta_\mu[(E'/2\mu').\delta_E - \delta_\mu]}{1 + \delta_\mu^2}$$

Following Edmonds' finding that first order effects of the damping factor on the resonant frequencies of a cylinder are negligible, and that the value of Young's modulus resulting

from the resonant frequencies is the real part of the complex modulus, equation (1.22) can be written:

$$\sigma'_o = E'/2\mu' - 1$$

Substituting this value of Poisson's ratio into the equation above, it is seen that

$$\sigma' = \sigma'_o \frac{(1 + \delta_\mu \cdot \delta_E)}{1 + \delta_\mu^2} + \frac{\delta_\mu \cdot (\delta_E - \delta_\mu)}{1 + \delta_\mu^2}$$

As $\delta_\mu \sim \delta_E$ for polymers, then $\sigma'_o = \sigma'$ to a first approximation

For polystyrene: $\delta_E = 4.0 \times 10^{-3}$, and $\delta_\mu = 4.5 \times 10^{-3}$ (Parfitt, 1954) and therefore $\sigma' = \sigma'_o - 2 \times 10^{-6}$

For perspex: $\delta_E = 3.0 \times 10^{-2}$ and assuming $\delta_\mu = 3.5 \times 10^{-2}$ and therefore $\sigma' = \sigma'_o - 1.5 \times 10^{-4}$.

It is therefore seen that the use of equation (1.22) to give the real part of Poisson's ratio is justified in terms of the accuracy with which values have been quoted.

APPENDIX 2

Theory of velocity dispersion in cylinders

The equation of motion for an isotropic elastic solid is

$$(\lambda + 2\mu)\nabla(\nabla.\bar{u}) - \mu\nabla x\nabla x\bar{u} = \rho\frac{\partial^2\bar{u}}{\partial t^2} \qquad (A2.1)$$

where λ and μ are the two Lame constants (μ being the shear modulus), $\bar{u}$ is the displacement vector, t is the time and ρ the density of the medium. In applying this equation to a cylinder, cylindrical coordinates are chosen with the z-direction along the axis of the cylinder, which is the propagation direction. Scalar and vector potentials are defined such that

$$\varphi = \nabla.\bar{u} \qquad (A2.2)$$

$$\bar{\Psi} = \nabla x\,\bar{u} \qquad (A2.3)$$

and from (A2.3) it follows that

$$\nabla.\bar{\Psi} = 0 \qquad (A2.4)$$

Substituting (A2.2) and (A2.3) into (A2.1) gives

$$(\lambda + 2\mu)\nabla\varphi - \mu\nabla x\bar{\Psi} = \rho\frac{\partial^2\bar{u}}{\partial t^2} \qquad (A2.5)$$

and taking the gradient of (A2.5) gives

$$\nabla^2 \varphi = \frac{1}{v_1^2} \cdot \frac{\partial^2 \varphi}{\partial t^2} \tag{A2.6}$$

where v_1 is the velocity of longitudinal (compressional) waves in infinite media. Taking the curl of (A2.5) gives

$$\nabla^2 \underline{\Psi} = \frac{1}{v_s^2} \cdot \frac{\partial^2 \underline{\Psi}}{\partial t^2} \tag{A2.7}$$

where v_s is the velocity of shear waves in infinite media. Equation (A2.7) separates into three components, which are

$$\nabla^2 \psi_r - \frac{\psi_r}{r^2} - \frac{2}{r^2} \cdot \frac{\partial \psi_\theta}{\partial \theta} - \frac{1}{v_s^2} \frac{\partial^2 \psi_r}{\partial t^2} = 0 \tag{A2.8}$$

$$\nabla^2 \psi_\theta - \frac{\psi_\theta}{r} + \frac{2}{r^2} \cdot \frac{\partial \psi_r}{\partial \theta} - \frac{1}{v_s^2} \frac{\partial^2 \psi_\theta}{\partial t^2} = 0 \tag{A2.9}$$

$$\nabla^2 \psi_z - \frac{1}{v_s^2} \cdot \frac{\partial^2 \psi_z}{\partial t^2} = 0 \tag{A2.10}$$

and combining (A2.8) and (A2.4) yields

$$\frac{\partial^2 \psi_r}{\partial r^2} + \frac{3}{r} \frac{\partial \psi_r}{\partial r} + \frac{1}{r^2} \psi_r + \frac{1}{r^2} \frac{\partial^2 \psi_r}{\partial \theta^2} + \frac{\partial^2 \psi_r}{\partial z^2} - \frac{1}{v_s^2} \frac{\partial^2 \psi_r}{\partial t^2} = \frac{2}{r} \cdot \frac{\partial \psi_z}{\partial z} \tag{A2.11}$$

Equations (A2.6), (A2.10) and (A2.11) can be solved by the separation

of variables, and give

$$\varphi = A J_n(hr) \exp\left[j(\omega t - \gamma z + n\Theta)\right]$$

$$\Psi_z = C J_n(kr) \exp\left[j(\omega t - \gamma z + n\Theta)\right]$$

$$\Psi_r = \frac{B}{r} J_n(kr) - j \frac{\gamma}{k^2} \frac{\partial}{\partial r}\left[J_n(kr)\right] \cdot \exp\left[j(\omega t - \gamma z + n\Theta)\right] \qquad \text{(A2.12a)}$$

where $\omega = 2\pi$ times the frequency, f.

γ is the propagation constant which equals $2\pi/L$, L being the wavelength.

n is an integer starting at zero.

$$h^2 = (\omega/v_l)^2 - \gamma^2$$

$$k^2 = (\omega/v_s)^2 - \gamma^2 \qquad \text{(A2.12b)}$$

$J_n(x)$ is the Bessel function of the first kind of order n.

Only that portion of the solution to the differential equation which remains finite at $r = 0$ has been retained.

From equation (A2.3) the three components of $\overline{\Psi}$ are

$$\Psi_r = \frac{1}{r}\frac{\partial u_z}{\partial \theta} - \frac{\partial u_\theta}{\partial z}$$

$$\Psi_\theta = \frac{\partial u_r}{\partial z} - \frac{\partial u_z}{\partial r}$$

$$\Psi_z = \frac{\partial u_\theta}{\partial r} + \frac{u_\theta}{r} - \frac{\partial u_r}{\partial \theta} \qquad \text{(A2.13)}$$

Plane wave type solutions are assumed for the three components of displacement of the form

$$u_r = U(r).\cos(n\theta).\exp[j(\gamma z - \omega t)]$$

$$u_\theta = V(r).\sin(n\theta).\exp[j(\gamma z - \omega t)]$$

$$u_z = W(r).\cos(n\theta).\exp[j(\gamma z - \omega t)] \qquad \text{(A2.14)}$$

Substituting (A2.14) and (A2.12) into (A2.13) gives U(r), V(r) and W(r), which are unknown, in terms of three constants A, B, C which are also unknown.

$$U(r) = \frac{A}{(\omega^2/v_l^2)} \cdot \frac{d}{dr}[J_n(hr)] + \frac{B}{(\omega^2/v_s^2)} \cdot \frac{d}{dr}[J_n(kr)] + \frac{C}{k^2} \cdot n \cdot \frac{J_n(kr)}{r}$$

$$V(r) = \frac{A}{(\omega^2/v_l^2)} n \cdot J_n(hr) - \frac{B}{(\omega^2/v_s^2)} \cdot n \cdot \frac{J_n(kr)}{r} - \frac{C}{k^2} \cdot \frac{d}{dr}[J_n(kr)]$$

$$W(r) = j\frac{A\gamma}{(\omega^2/v_R^2)} \cdot J_n(hr) + j\frac{B}{(\omega^2/v_s^2)} J_n(kr) \cdot \frac{K^2}{\gamma} \qquad \text{(A2.15)}$$

The constants A, B, C are found by applying the boundary conditions that the cylindrical surface is traction-free.

$$T_{rr}\Big|_{r=a} = 0 = \lambda\left[\frac{u_r}{r} + \frac{\partial u_r}{\partial r} + \frac{1}{r}\frac{\partial u_\theta}{\partial \theta} + \frac{\partial u_z}{\partial z}\right] + 2\mu\frac{\partial u_r}{\partial r}$$

$$T_{r\theta}\Big|_{r=a} = 0 = \mu\left[\frac{1}{r}\frac{\partial u_r}{\partial \theta} + r\frac{\partial}{\partial r}\left(\frac{u_\theta}{r}\right)\right]$$

$$T_{rz}\Big|_{r=a} = 0 = \mu\left[\frac{\partial u_r}{\partial z} + \frac{\partial u_z}{\partial r}\right]$$

(A.216)

where T_{rr}, $T_{r\theta}$, T_{rz} are the stress components in the directions given and a is the radius of the cross-section of the cylinder.

Substituting (A2.15) into (A2.14) and these in turn into (A2.16) leads to three homogeneous equations in terms of A, B, C. The only non-trivial solutions for these constants are those for which the determinant of the coefficients of A, B, C is equal to zero. This determinant is

$$\begin{matrix} A_{11} & A_{12} & A_{13} \\ A_{21} & A_{22} & A_{23} \\ A_{31} & A_{32} & A_{33} \end{matrix} \qquad \text{(A2.17)}$$

where

$$A_{11} = \left[n^2 - 1 - \frac{\Omega^2}{2} + (\gamma a)^2\right] J_n(ha)$$

$$A_{12} = \left[n^2 - 1 - (ka)^2\right] J_n(ka)$$

$$A_{13} = 2(n^2 - 1)\left[ka\, J_{n-1}(ka) - n\, J_n(ka) - (ka)^2 J_n(ka)\right]$$

$$A_{21} = ha\, J_{n-1}(ka) - (n+1)\, J_n(ka)$$

$$A_{22} = ka\, J_{n-1}(ka) - (n+1)\, J_n(ka)$$

$$A_{23} = \left[\, 2n^2 + 2n - (ka)^2 \,\right] J_n(ka) - 2ka\, J_{n-1}(ka)$$

$$A_{31} = ha\, J_{n-1}(ha) - n\, J_n(ha)$$

$$A_{32} = \left\{ \frac{\Omega^2}{2(\gamma a)^2} - 1 \right\} \cdot \left[\, ka\, J_{n-1}(ka) - n\, J_n(ka) \,\right]$$

$$A_{33} = n^2\, J_n(ka)$$

$$\Omega = \frac{\omega a}{v_s}$$

The equation formed by expanding (A2.17) is the so-called frequency equation which for a given value of n relates the phase velocity to the wavelength. Thus if Ω and γa are chosen as dimensionless variables, (A2.17) is seen to relate these two as a function of Poisson's ratio. In terms of these variables, (ha) and (ka) can be written as

$$(ha)^2 = \alpha^2 \cdot \Omega^2 - (\gamma a)^2$$

$$(ka)^2 = \Omega^2 - (\gamma a)^2$$

where $\alpha^2 = v_s^2/v_l^2 = \frac{1 - 2\sigma}{2(1 - \sigma)}$

where σ is Poisson's ratio.

Equation (A2.17) has two sets of solutions represented by L(n,m) and F(n,m), n and m being integers. L(n,m) represent the symmetric modes of propagation and F(n,m) the anti-symmetric ones, or in more common parlance, the longitudinal and flexural modes. Thus there is a family of longitudinal modes of propagation specified by $n = 0,1,2,3,4,5 \ldots \infty$. For each one of these modes there is an infinite number of dispersion curves specified by $m = 1,2,3,4,5 \ldots \infty$, and these are called branches. To find the solution for the L(0,1) mode, the first symmetric mode, n is set to zero and m is set to 1, in equation (A2.17) when the determinant becomes simpler, factoring into two equations

$$ka\, J_0(ka) - 2J_1(ka) = 0 \qquad \text{(A2.18)}$$

$$[\Omega^2 - 2(\gamma a)^2]^2 J_0(ha) J_1(ka) + 4(\gamma a)^2 ha\, ka \cdot J_0(ka) J_1(ha) - 2\Omega^2 ha\, J_1(ha) J_1(ka) = 0 \qquad \text{(A2.19)}$$

Equation (A2.18) is the frequency equation for torsional waves. This equation determines an infinite set of roots, given by $ka = (ka)_q$, q being an integer which specifies the modes, see Mason (1964, page 134); ka = 0 is the simplest solution and represents the lowest order torsional mode, in which the phase velocity is v_s. This phase velocity is independent of frequency and hence is non-dispersive, and

$$v_s = (\mu/\rho)^{\frac{1}{2}} \qquad \text{(A2.18a)}$$

Equation (A2.19) is the frequency equation for the longitudinal modes of propagation, and its solution is not easy for rods of finite length due to the difficulty of applying the boundary conditions for the ends of the rod. These boundary conditions are that the normal and shear stresses T_{zz} and T_{rz} vanish at the ends given by $z = 0$ and $z = l$, l being the length of the rod.

To find T_{zz} and T_{rz}, the axial and radial displacements must first be obtained. Let them be, respectively,

$$u_r = U(r) \exp[\, j\,(\gamma z - \omega t)\,] \tag{A2.20}$$

$$u_z = W(r) \exp[\, j\,(\gamma z - \omega t)\,] \tag{A2.21}$$

Note that these are the same as (A2.14) with $n = 0$. Combining (A2.20) and (A2.21) with (A2.12) and (A2.13), the solutions for $U(r)$ and $W(r)$ are given as

$$U(r) = -Ah\, J_1(hr) + C\gamma\, J_1(kr) \tag{A2.22}$$

$$W(r) = j\, A\gamma\, J_0(hr) + j\, C\, kJ_0(kr) \tag{A2.23}$$

One of the boundary conditions for the traction-free surface is

$$T_{rz}\Big|_{r=a} = \mu\left[\frac{\partial u_r}{\partial z} + \frac{\partial u_z}{\partial r}\right] = 0 \tag{A2.24}$$

and from this boundary condition, equations (A2.20, 21, 22, 23) give

$$A[\, -2\gamma\, hJ_1(ha)] + C\,[\,(\gamma^2 - k^2)\, J_1(ka)] = 0 \tag{A2.25}$$

The ratio A/C depends on the relationship between Ω and γa given in equation (A2.19). Because there is an infinity of values of γa for any Ω, γa will be assigned a subscript to identify it with a particular root of

(A2.19). Thus we write $\gamma a = (\gamma a)_{n)}$ and the ratio A/C is given as

$$\left(\frac{A}{C}\right)_n = \frac{J_1(k_n a)\,[2(\gamma a)^2 - \Omega^2]}{2(\gamma a)_n\, h_n a\, J_1(h_n a)} \qquad (A2.26)$$

Equation (A2.23) can be written as

$$W_n(r) = W_{n,1}(r) + W_{n,2}(r) = j\, A_n\, \gamma_n\, J_o(h_n r) + j\, C_n\, k_n\, J_o(k_n r) \qquad (A2.27)$$

and therefore

$$\frac{W_{n1}(r)}{W_{n2}(r)} = \frac{A_n \cdot \gamma_n \cdot J_o(h_n r)}{C_n \cdot k_n \cdot J_1(k_n r)} \qquad (A2.28)$$

Substituting for A/C from (A2.26) gives

$$\frac{W_{n1}(r)}{W_{n2}(r)} = \frac{J_o(h_n r)[\,2(\gamma a)_n^2 - \Omega^2\,]J_1(k_n a)}{k_n a J_o(k_n r)\; 2h_n a J_1(h_n a)} \qquad (A2.29)$$

and comparing (A2.29) with (A2.27), it is seen that the following equations hold

$$j\, A_n\, \gamma_n = [2(\gamma a)_n^2 - \Omega^2\,]J_1(k_n a) \cdot K_o \qquad (A2.30)$$

$$j\, C_n\, k_n = 2k_n \cdot a \cdot h_n \cdot a \cdot J_1(h_n a) \cdot K_o \qquad (A2.31)$$

where K_o is a constant.

Substituting (A2.30) and (A2.31) into (A2.27) gives the axial displacement

$$U_{zn} = Z_n(r)\, \exp[\, j(\gamma_n z - \omega t)\,]\; K_o \qquad (A2.32)$$

$$Z_n(r) = \left[\, 2(\gamma a)_n^2 - \Omega^2 \,\right] J_1(k_n a)\, J_o(h_n a \tfrac{r}{a}) + 2k_n\, a h_n a\, J_1(h_n a)\, J_o(k_n a\, \tfrac{r}{a}) \tag{A2.33}$$

and the radial displacements

$$U_{rn} = j\, R_n(r) \exp\left[\, j(\gamma_n z - \omega t)\,\right] K_o \tag{A2.34}$$

$$R_n(r) = \frac{h_n a}{(\gamma a)_n} \Big\{ \left[2(\gamma a)_n^2 - \Omega^2 \right]\left[J_1(k_n a)\, J_1(h_n a \tfrac{r}{a}) \right] - 2(\gamma a)_n^2\, J_1(h_n a)\, J_1(k_n a\, \tfrac{r}{a}) \tag{A2.35}$$

Equations (A2.32) and (A2.34) are therefore the axial and radial displacements as a function of the radius for the first branch of the first symmetric mode. Using (A2.16), (A2.32) and (A2.34), the normal and shear stresses are obtained; the normal stress is

$$T_{zzn} = \frac{j\mu}{a} H_n \cdot ZZ_n(r) \cdot \exp\left[\, j(\gamma_n z - \omega t)\,\right] K_o \tag{A2.36}$$

$$H_n^{-1} = (\gamma a)_n \tag{A2.37}$$

$$ZZ_n(r) = \left[2(\gamma a)_n^2 - \Omega^2 \right]\left[2(\gamma a)_n^2 - \Omega^2(1 - \alpha^2) \right] J_1(k_n a)\, J_o(h_n a\, \tfrac{r}{a}) + 4(\gamma a)_n^2\, h_n a \cdot k_n a\, J_1(h_n a)\, J_o(k_n a\, \tfrac{r}{a}) \tag{A2.38}$$

and the shear stress is

$$T_{rzn} = -\frac{2\mu}{a} \cdot RZ_n(r) \exp\left[\, j(\gamma_n z - \omega t)\,\right] K_o \tag{A2.39}$$

$$RZ_n(r) = h_n a \left[2(\gamma a)_n^2 - \Omega^2 \right]\left[J_1(k_n a)\, J_1(h_n a\, \tfrac{r}{a}) - J_1(h_n a)\, J_1(k_n a\, \tfrac{r}{a}) \right] \tag{A2.40}$$

If $\gamma_2 = -|\gamma_2| = -\gamma_1$, then it can be shown that

$$H_2 = H_1,\quad ZZ_2(r) = ZZ_1(r),\quad RZ_2(r) = RZ_1(r)$$

$$T_{zz2} = - T_{zz1}, \quad T_{rz2} = T_{rz1} \qquad (A2.41)$$

i.e. the sign of the shear stress T_{rz} is independent of the sign of γ or the direction of propagation, but that the normal stress T_{zz} is dependent upon the sign of γ. This dependence is introduced by the function H.

Zemaneck (1962) has calculated relative values of T_{rz} and T_{zz} for Poisson's ratio of 0.3317. T_{rz} is zero at the centre and at the edges, and for $\Omega < 2.6$ T_{rz} is 2 orders of magnitude less than the normal stress, T_{zz}. From equation (A2.41), T_{zz} can be made to vanish, as it is an odd function, if the incident wave is reflected with no phase shift. The resultant normal stress then assumes the form

$$T_{zz} = A.\sin(\gamma z)$$

and this assumption is the low frequency approximation and results in the familiar equation relating wavelength to length of the cylinder

$$L = 2l/n \qquad (A2.42)$$

The derivation of the frequency equation then continues as from section (1.c).

At high frequencies (see section (1.e)), T_{rz} is far from zero and both this component and T_{zz} can only be made to vanish if it is assumed that higher branches of the L(0,m) mode, which are non-propagating below frequencies given by $\omega a/v_s = 3.68$, are generated at the end face so as to cancel out the excess strain which results from assuming that only the

m = 1 branch of this first symmetric mode is reflected. Zemaneck has shown that the frequency defined above is that at which the m = 2 and m = 3 branches begin to propagate. At higher frequencies, more and more pairs of branches begin to propagate, and "it is apparent that the calculation of the resonant frequencies of a finite bar would be extremely difficult if not impossible" (Zemaneck). Zemaneck's chief use of these newly-propagating modes is to calculate the frequency of "end resonance" and he shows that using an increasing number of pairs of such modes results in a more accurate value of this frequency, as given by experiment.

The "end-resonance" effect

The amplitude of these newly-propagating modes dies away rapidly with increasing distance from the end-face of the cylinder, such that far from the end face only the reflected L(0,1) mode would ordinarily be observed. However, this "energy storage" phenomenon would be observed in changes of the phase and amplitude of the reflection coefficient of the mode concerned. (Mason, 1964, page 146). At certain frequencies, this stored energy at the end-face of the rod causes large amplitude displacements near the end face, and this is the cause of the phenomenon of "end-resonance", when the phase angle of the reflection coefficient undergoes a sudden change of 360°, and which has been observed by Zemaneck (1962) at the value of $\omega a/v_s$ as given by the theory; Oliver (1957 first observed the end resonance effect.

If the reflection coefficient for the incident mode or the amplitude coefficient for the n^{th} branch which is generated at the end face is

$$A_n = |A_n| \cdot \exp(j\,\Theta_n) \qquad (A2.43)$$

then the normal and shear stresses can be expressed in terms of the propagating mode and its higher branches, and at the end-face they become

$$T_{zz}(r) = \sum_{n=0}^{\infty} A_n . T_{zzn}(r) = 0 \qquad (A2.44)$$

$$T_{rz}(r) = \sum_{n=0}^{\infty} A_n . T_{rzn}(r) = 0 \qquad (A2.45)$$

Zemaneck uses the following convention for n; the incident mode is denoted by n = 0 and its reflection by n = 1. For frequencies less than $\Omega = 3.68$, branches whose propagation constants are imaginary are referred to by n values greater than 1. The first pair of these are denoted by n = 2 and 3, the second pair by n = 4 and 5, and so on. In any pair, one branch is the complex conjugate of the other, and this description is based on the concept that a source located at infinity is assumed to excite the L(0,1) mode. This motion is reflected with a reflection coefficient A_1 on reaching the traction-free interface at z = 0. Higher branches are generated in sufficient amplitude to cancel the residual stress. In trying to satisfy the boundary conditions shown as equations (A2.44) and (A2.45) above, it is obviously not practical to include an infinite number of A_n values, though Zemaneck has calculated the reflection coefficients and phase shifts for the first 9 values in these equations. At the

universal point, he has been able to show that the phase shift is zero, and that close to $\Omega = 3.0$, it undergoes a jump of 360^{o} in value, which effect is known as "end-resonance".

Finite internal losses in the rod

Section (1.g) refers to the work of Edmonds in accounting for first order effects due to finite internal losses in the rod. He shows that $Q_E \cdot \mu''$ is dependent only upon $\omega a/v_E$ and upon λ''/μ'', assuming that these parameters are independent of frequency.

In making the Lame constants, angular frequency and phase velocities complex, the propagation constant, γ , must remain real so that the wavelength is real. This condition dictates that $\omega'/\omega'' = v_1'/v_1''$. Putting these complex terms into equation (1.12) gives

$$(x^{*} - 1)^2 \Phi (P^{*}a) - (2\varepsilon x^{*2} - 1)[x^{*} - \Phi(Q^{*}a)] = 0 \qquad (A2.48)$$

where $2\varepsilon^{*2} = \beta_o$ of equation (1.12).

Edmonds expands this equation by Taylor's theorem and on keeping only the first order imaginary terms shows that the real part of the resulting equation is equal to equation (1.12a).

By further manipulation it is possible to arrive at the following equation

$$A_o \frac{\lambda'' + 2\mu''}{\lambda' + 2\mu'} + B_o \mu''/\mu' - C_o \cdot \omega''/\omega' = 0 \qquad (A2.49)$$

where A_o, B_o and C_o are functions which contain only the real parts of the parameters used, one of which is $\omega a/v_E$, ignoring any end-effect corrections.

Writing $1/Q_E = \omega''/\omega'$, equation (A2.49) can be written as

$$Q_E \cdot \mu'' \cdot \left[B_o / \mu' + A_o \frac{(\lambda''/\mu'' + 2)}{\lambda' + 2\mu'} \right] = C_o \qquad \text{(A2.50)}$$

and hence $Q_E \cdot \mu''$ is a function of λ''/μ'' and of the three functions A_o, B_o and C_o, which contain the parameter $\omega a/v_n$

APPENDIX 3

Theoretical values of dispersion in an infinite cylinder

These values have been interpolated from Bancroft's original table (1941). Other tables given by Bradfield (1964) give the values of v_n/v_E for d/L values less than 0.45.

The values of v_E/v_n given here are considered to be accurate to within $\pm$ 0.00001; this is the worst deviation that the curve fitting computer programme gives for the values of dispersion as shown in Bancroft's table.

The table presents values of d/L from 0.45 to 1.00, and values of Poisson's ratio from 0.15 to 0.40.

d/L_σ	0.45	0.50	0.55	0.60	0.65	0.70
0.15	1.02181	1.03337	1.05222	1.08183	1.12251	1.16999
0.16	1.02435	1.03682	1.05655	1.08649	1.12667	1.17329
0.17	1.02698	1.04034	1.06089	1.09113	1.13088	1.17672
0.18	1.02968	1.04390	1.06523	1.09575	1.13513	1.18027
0.19	1.03245	1.04751	1.06956	1.10036	1.13942	1.18391
0.20	1.03528	1.05116	1.07389	1.10495	1.14374	1.18763
0.21	1.03817	1.05484	1.07822	1.10952	1.14807	1.19143
0.22	1.04111	1.05854	1.08254	1.11408	1.15242	1.19528
0.23	1.04410	1.06226	1.08685	1.11861	1.15678	1.19919
0.24	1.04713	1.06600	1.09115	1.12313	1.16115	1.20315
0.25	1.05020	1.06976	1.09544	1.12764	1.16551	1.20714
0.26	1.05330	1.07353	1.09971	1.13212	1.16988	1.21116
0.27	1.05643	1.07731	1.10398	1.13659	1.17425	1.21521
0.28	1.05959	1.08109	1.10823	1.14104	1.17861	1.21929
0.29	1.06278	1.08488	1.11248	1.14548	1.18297	1.22339
0.30	1.06599	1.08868	1.11671	1.14990	1.18733	1.22750
0.31	1.06921	1.09248	1.12092	1.15431	1.19168	1.23163
0.32	1.07246	1.09629	1.12513	1.15870	1.19604	1.23578
0.33	1.07572	1.10009	1.12932	1.16307	1.20038	1.23994
0.34	1.07900	1.10390	1.13350	1.16743	1.20473	1.24411
0.35	1.08229	1.10770	1.13767	1.17177	1.20906	1.24829
0.36	1.08559	1.11151	1.14183	1.17610	1.21339	1.25247
0.37	1.08890	1.11531	1.14597	1.18041	1.21771	1.25665
0.38	1.09222	1.11910	1.15010	1.18470	1.22201	1.26083
0.39	1.09555	1.12289	1.15421	1.18898	1.22629	1.26501
0.40	1.09889	1.12666	1.15831	1.19323	1.23054	1.26916

d/L	0.75	0.80	0.85	0.90	0.95	1.00
σ						
0.15	1.21939	1.26754	1.31290	1.35479	1.39293	1.42739
0.16	1.22189	1.26946	1.31441	1.35602	1.39398	1.42833
0.17	1.22457	1.27156	1.31608	1.35739	1.39516	1.42940
0.18	1.22740	1.27381	1.31790	1.35891	1.39648	1.43059
0.19	1.23036	1.27620	1.31988	1.36057	1.39793	1.43190
0.20	1.23344	1.27874	1.32199	1.36236	1.39950	1.43333
0.21	1.23663	1.28140	1.32423	1.36428	1.40120	1.43487
0.22	1.23992	1.28418	1.32659	1.36633	1.40301	1.43651
0.23	1.24330	1.28706	1.32907	1.36849	1.40494	1.43827
0.24	1.24675	1.29005	1.33165	1.37076	1.40697	1.44012
0.25	1.25028	1.29313	1.33434	1.37313	1.40910	1.44208
0.26	1.25387	1.29629	1.33713	1.37561	1.41134	1.44413
0.27	1.25752	1.29953	1.34000	1.37818	1.41367	1.44627
0.28	1.26122	1.30283	1.34295	1.38083	1.41608	1.44850
0.29	1.26496	1.30621	1.34598	1.38357	1.41858	1.45081
0.30	1.26875	1.30964	1.34905	1.38639	1.42116	1.45320
0.31	1.27257	1.31312	1.35224	1.38927	1.42382	1.45566
0.32	1.27642	1.31665	1.35546	1.39223	1.42654	1.45820
0.33	1.28030	1.32023	1.35874	1.39524	1.42933	1.46081
0.34	1.28420	1.32384	1.36207	1.39832	1.43218	1.46348
0.35	1.28813	1.32749	1.36545	1.40144	1.43509	1.46621
0.36	1.29208	1.33118	1.36887	1.40462	1.43806	1.46900
0.37	1.29604	1.33489	1.37233	1.40785	1.44107	1.47184
0.38	1.30002	1.33863	1.37583	1.41113	1.44414	1.47474
0.39	1.30401	1.34240	1.37936	1.41444	1.44725	1.47768
0.40	1.30801	1.34618	1.38293	1.41780	1.45041	1.48067

APPENDIX 4

Definitions of spin-lattice relaxation time and second moment

The resonance observed in nuclear magnetic resonance experiments results from the excitation by R.F. photons of nuclei from one magnetic spin quantum state to another. The spin-lattice relaxation time, T_1, is the time constant which controls the return of these excited nuclei to their original quantum state, a process which is brought about by a coupling between these nuclei and the thermal photons of the lattice. The spin-spin relaxation time, T_2, is the relaxation time which controls the return of the excited nuclei to their initial states by coupling with the other nuclei.

The shape of the resonance envelope which can be expressed as the function $g(H)$, can be expressed numerically by calculating the m^{th} moment of the resonance curve defined by

$$\Delta H_M^m = \frac{\int_{line} g(H).(H - H_o)^m. \, d(H - H_o)}{\int_{line} g(H). \, d(H - H_o)}$$

The second moment is given by putting $m = 2$. These moments are a measure of the width of the resonance curve which for dipolar broadening decreases as motion of the molecular environment of the nuclei increases. The broadening of the envelope results from the fact that

the nuclei see not only the applied magnetic field, but also that resulting from the magnetic moments of the nuclei comprising their environment. As motion of these nuclei increases, these deviations from the applied magnetic field are averaged out and the resonance envelope width decreases.

As the motion of the lattice increases, more thermal phonons will become available to bring about the de-excitation process described above, which will result in the process occurring more quickly. Hence, T_1 will decrease with increasing molecular motion. It is therefore obvious that the measurement of these two parameters during the progress of a transition like those occurring in the glass-like state will be a means of observing these transitions.

Abragam (1961) and Slichter (Frechette, 1958) give more detailed definitions of these parameters and their dependence upon molecular motion.

APPENDIX 5

Details of electronic circuits

The oscillator

Figures (A5.1a) and (A5.1b) show the circuit of this oscillator. One of the fractional detuners provides a change in frequency of ± 4%, and the other ± 0.4%, the former being adequate to cover Q measurements at room temperature in perspex and the latter in polystyrene. The H.T. supplies of 270 and 350 volts, both stabilised, are provided by commercial apparatus. The range of the oscillator is from 50 c/s to 350 kc/s.

The drive amplifier

Figure (A5.2) shows the circuit. This device also provides the 200 volts D.C. potential between the end of the rod and the earthed plate which together form the condenser microphone which drives the rod. The peak-to-peak voltage of the oscillatory potential must not exceed one quarter of the D.C. potential, i.e. no more than 50 volts, for Parfitt (1954) has shown that above this fraction second harmonic distortion can occur.

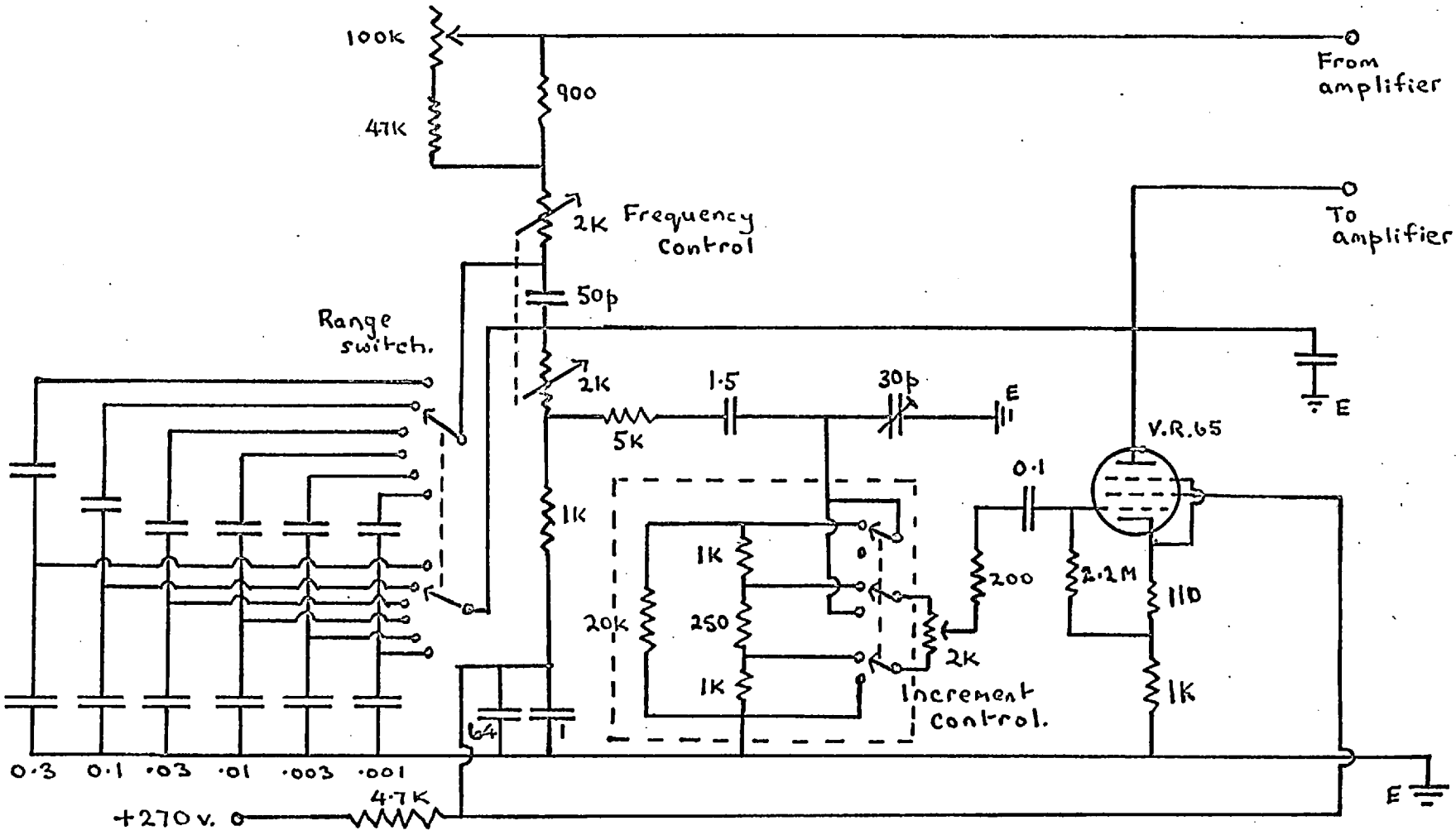

FIG.(A5.1a) Oscillator tuning and increment circuit.

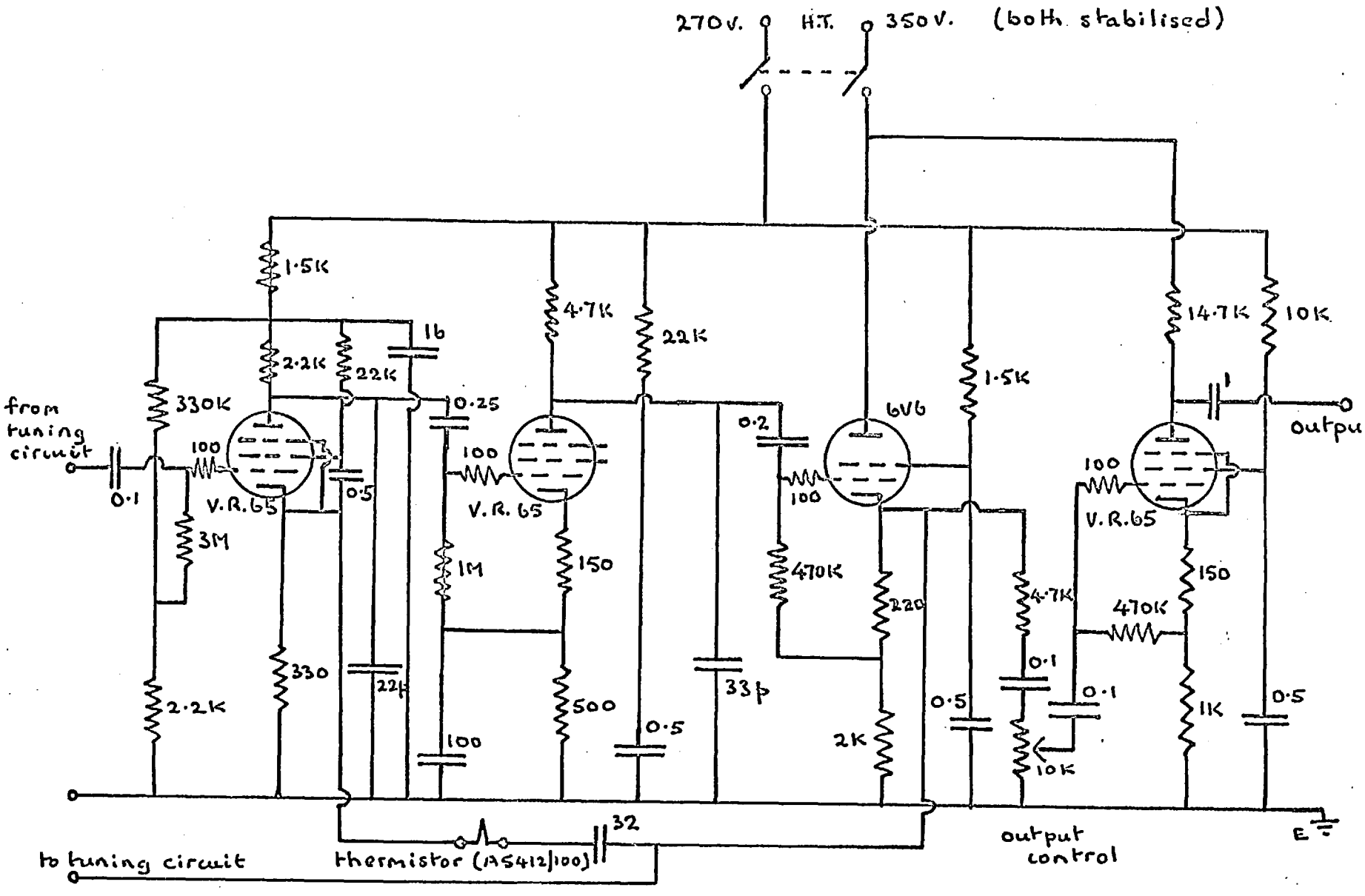

FIG.(A5.1b) Maintaining amplifier for oscillator.

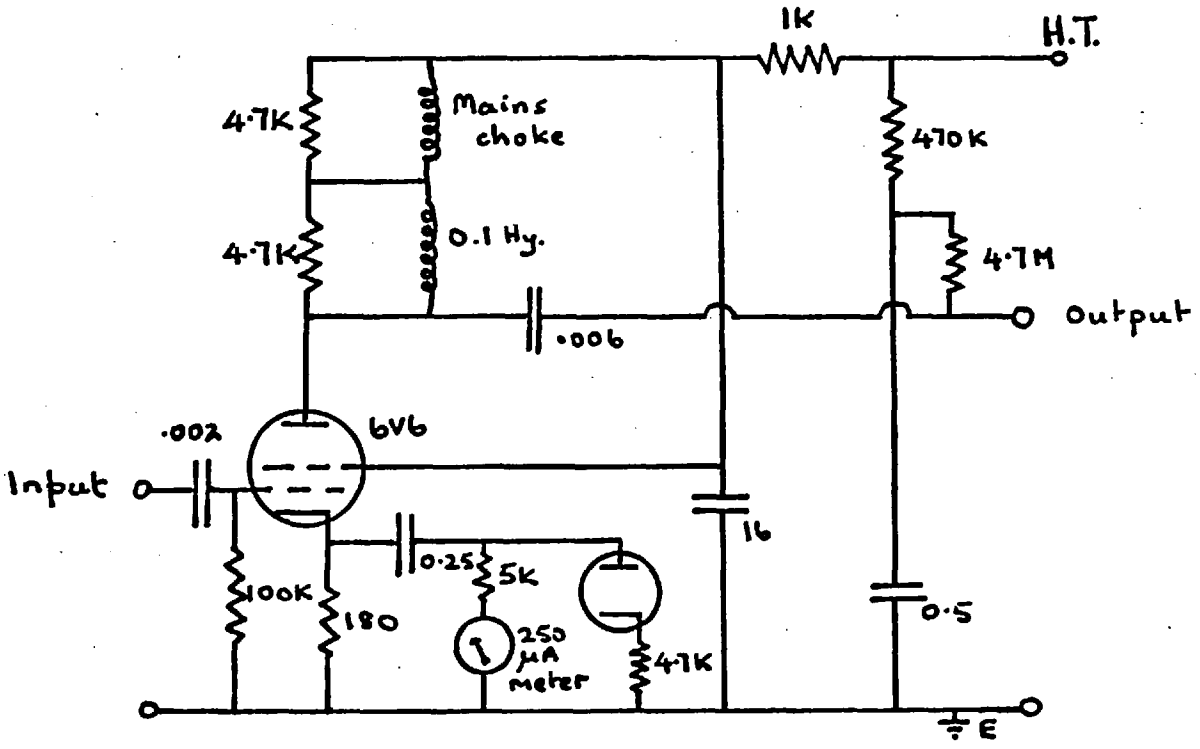

FIGURE (A5.2) THE DRIVE AMPLIFIER

The detection amplifier

The circuit of this apparatus is shown in Figure (A5.3). The D.C. polarising potential applied to the detector condenser microphone is also supplied by this circuit, which is essentially a resistance coupled amplifier, employing negative feedback to minimise the effects of variations of valve properties and to improve the linearity of the frequency characteristics. In the untuned range, the amplifier has a frequency response which is flat from 2 kc/s to 140 kc/s; its gain is such that a full scale deflection of the meter is obtained for a signal of 75 microvolts at the input. The first stage of the circuit, the pre-amp. stage, is built into a small box (shown by the broken lines in Figure (A5.3)) which is connected to the amplifier proper by leads. This arrangement allows the pre-amp. to be as close as possible to the detecting condenser microphone, thus minimising lead capacitance which reduces the sensitivity of the detector.

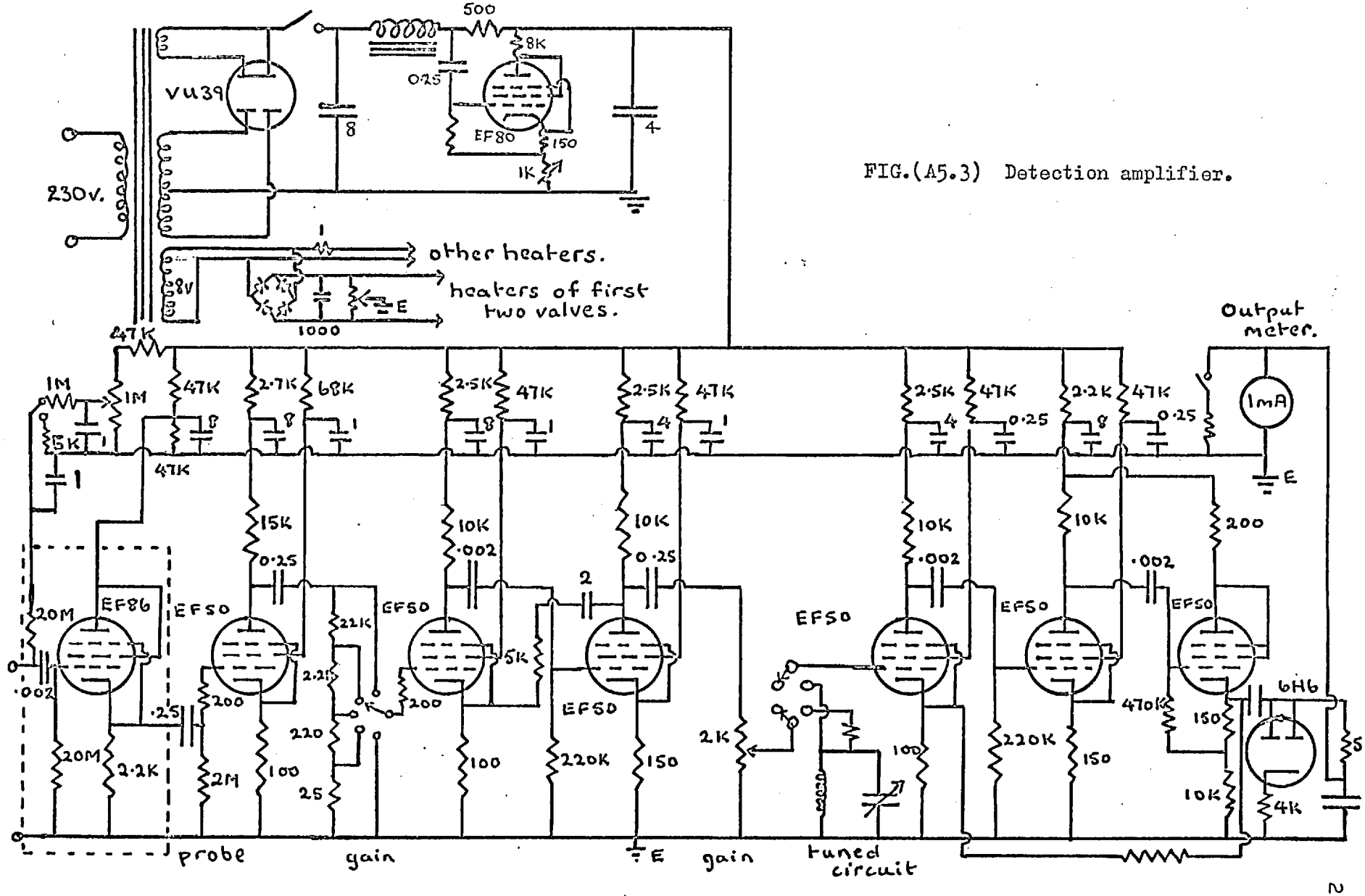

FIG.(A5.3) Detection amplifier.

Appendix 6

Effect of a constraint on each end of the rod

Let us consider shear mode propagation; it can be shown (Kolsky, 1950) that the wave equation can be written as

$$G^{*} \cdot \frac{\partial^2 u}{\partial x^2} = \rho \cdot \frac{\partial^2 u}{\partial t^2} \qquad \text{(A6.1)}$$

where G^{*} is the complex shear modulus and ρ is the density and u is the angular rotation through which diametrical planes rotate, and which has a solution

$$u(x,t) = U(x) \cdot \exp(j\omega t)$$

where ω is the angular frequency. Equation (A6.1) can therefore be written as

$$G(1 + j\delta) \frac{\partial^2 U}{\partial x^2} + \rho \cdot \omega^2 U = 0 \qquad \text{(A6.2)}$$

which has a solution

$$U(x) = P.\exp(-\gamma x) + Q.\exp(+\gamma x) \qquad \text{(A6.3)}$$

where $\gamma = \alpha + j\beta$

$$\alpha = \omega.\delta/2.(\rho/G)^{\frac{1}{2}}$$

$$\beta = \omega . (\rho / G)^{\frac{1}{2}} \qquad (A6.4)$$

P and Q are determined from the boundary conditions on the rod, that at the driven end, the couple in the cylinder which is given by

$$C = G^{*}\Gamma . \frac{\partial^2 U}{\partial x^2} \qquad (A6.5)$$

must be equal to the driving couple $C_o . \exp(j\omega t)$, and at the free end must be zero. Γ is the second moment of ~~inertia of a~~ area cross section ~~about the axis~~ of the rod.

If δ tends to zero, then the solution of this equation is the familiar one which relates the wavelength of propagation at resonance to the length of the rod, as shown in equation (1.7) and where the frequency of excitation is given by

$$\omega_n = n . \omega_o$$

If δ is kept in the solution, then the relationship

$$\omega_n = n . \omega_o . (1 + (\delta^2/8)(1 + 2p + (1/8)(3 + 2p)\ b\ \delta^2))^{-1}$$

where $b = \pi^2 n^2/6$ and p is given by putting δ proportional to ω^{-p}, is derived, see section (1.i).

Parfitt (1954) has considered the effect of a central constraint on a cylinder excited into shear mode resonance,

and finds that the frequencies of the odd harmonics (n = 1 is the fundamental) are unaffected (the constraint is always at a node for these resonances) whereas for the even number harmonics, the frequency is shifted upwards by an amount given by

$$\omega_n = 2n\,\omega_o + 2S_o\,\omega_o^2/\pi^2\omega \qquad (A6.6)$$

where $S_o = g_o 1/2G\Gamma$, g_o being the stiffness of the constraint. Using Parfitt's method, let us now consider such a constraint at each end of the rod.

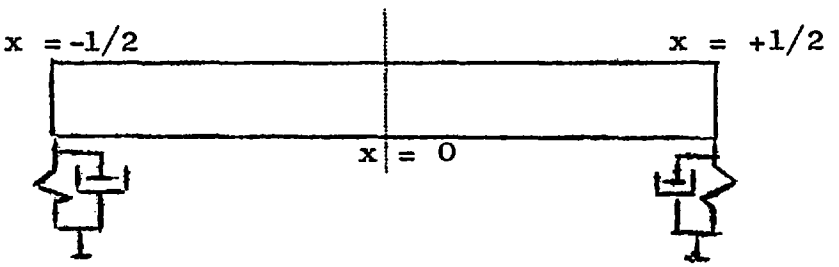

The stiffness and the damping of the constraint are g_o and Δ . Therefore the couple per unit angle of twist is $g_o(1 + j\Delta)$ The boundary conditions are:-

1. at $x = -\frac{1}{2}$

$$g_o(1 + j\Delta).U(-1/2) + G(1 + j\delta)\Gamma\frac{\partial U}{\partial x} = 0$$

2. at $x = \frac{1}{2}$

$$g_o(1 + j\Delta).U(1/2) + G(1 + j\delta)\Gamma\frac{\partial U}{\partial x} = C_o$$

These two conditions are sufficient to determine P and Q of equation (A6.3) and it can be shown that the ratio of U_o (defined by $C_o 1/G\Gamma$) to U_1, the complex amplitude of oscillation at the free end is given by

$$U_o/U_1 = 1g_o/G\Gamma .(1 + j\,\Delta).\ \sinh(\gamma\, 1).(Z^2 - 1)/Z \qquad (A6.7)$$

where $Z = G\Gamma\,\gamma\ (1 + j\,\delta)/g_o(1 + j\,\Delta)$

By putting δ^2 and Δ^2 equal to zero, it can further be shown that the square of the modulus of this ratio is given by:-

$$1^2.(1 - g_o^2/G^2\,\Gamma^2\,\beta^2)^2.\ \Big\{\ (\sinh\alpha 1).\ \cos(\beta\,1).(\alpha - \beta\,\varepsilon_o + \Delta\beta\ ) + \cosh(\alpha 1).\sin(\beta\ 1).(\beta\ + \alpha.\varepsilon_o - \Delta.\alpha\ ))^2 + (\sinh(\alpha\ 1).\ \cos(\beta 1).\ (\ \beta\ + \alpha.\varepsilon_o - \Delta\alpha\ ) - \cosh(\alpha 1).\ \sin(\beta 1).\ (\ \alpha\ - \beta.\varepsilon + \Delta\beta\ ))^2\ \Big\} \qquad (A6.8)$$

where $\varepsilon_o = \delta\ - \Delta$

Let us now assume that δ and Δ are equal to zero, when the above relationship becomes

$$\Big\{\ U_o/U_1\ \Big\}\ = \beta 1.(1 - g_o^2/G^2\,\Gamma^2\,\beta^2).\sin(\beta\,1) \qquad (A6.9)$$

Resonance condition is given by differentiating with respect to $\beta 1$ and setting to zero the above expression, when

$$\sin(\beta 1).(1 + g_o^2/G^2\,\Gamma^2\,\beta^2) + \beta 1.\cos(\beta 1).(1 - g_o^2/G^2\,\Gamma^2\,\beta^2) = 0$$

or when

$$\tan(\beta 1) = (M - 1)/(M + 1).\,\beta 1 \qquad \text{(A6.10)}$$

where $M = g_o^2/G^2\Gamma^2\beta^2$

Writing $\tan(X) = \tan(X - 2n\pi) - X - 2n\pi$ we have,

$$(\beta 1 - 2n\pi) = \beta 1.(M - 1)/(M + 1)$$

But $\beta 1 = \omega\pi/\omega_o$, by the simple theory, and so

$$(\omega/\omega_o - 2n).(1 + N\omega_o^2/\omega^2) = \omega/\omega_o.(N\,\omega_o^2/\omega^2 - 1)$$

where $N = g_o^2 1^2/G^2\Gamma^2\pi^2$

which gives $\omega = n\omega_o.(1 + N\omega_o^2/\omega^2)$ (A6.11)

This equation is valid for Young's modulus mode of excitation when g_o is replaced by e_o, the form of N then becoming

$$N = e_o^2/E^2.\pi^2$$

Thus equation (A6.11) can be written

$$\omega = n.\omega_o(1 + e_o^2/E^2.\pi^2.n^2) \qquad \text{(A6.12)}$$

This solution suggests that the resonant frequencies of a rod so constrained will be increased by an amount which is proportional to the square of the ratio of the stiffness of the constraint to the Young's modulus of

the material of the rod, and inversely proportional to the square of the number of the resonance. Although equation (A6.11) agrees with (A6.6) in the direction of the frequency shift, the amount of the shift given by the latter is more than that given by the former, as g_o/G will always be less than one. This prediction is contradicted by experimental evidence.

Appendix 7

The relationship between p and Δf, the two expressions of a frequency dependence of E'

Ideally, the resonant frequencies f_1 and f_n of a rod, after suitable correction for velocity dispersion, are given by

$$n.f_1/f_n = 1 \qquad (A7.1)$$

In fact, only by the use of the correction Δf can such an equation be written, i.e.

$$\frac{n.(f_1 + \Delta f)}{(f_n + \Delta f)} = 1 \qquad (A7.2)$$

Assuming that $E' \propto f^p$ is the frequency dependence of the real part of Young's modulus, it is seen that

$$n.f_1/f_n = (E'_1/E'_n)^{\frac{1}{2}} = (f_1/f_n)^{p/2} \qquad (A7.3)$$

From (A7.2), $f_1/f_n = [\, n + (n - 1).\, \Delta f/f_1 \,]^{-1}$

and $n.f_1/f_n = n/[\, n + (n - 1).\, \Delta f/f_1 \,]$

Substituting these into equation (A7.3) gives

$$p = 2.\left\{ 1 - \log [n] / \log[\, n + (n - 1).\, \Delta f/f_1] \right\} \qquad (A7.4)$$

as the relationship between p and Δf.

If Δf is negative, then $\log [n] / \log[\, n + (n - 1)\, \Delta f/f_1]$ is greater than unity, and p becomes negative.

Appendix 8

Characterisation of polymers

Linear polymers consist of a distribution of molecular weights. Both the shape of this distribution envelope and the magnitude of any particular component depend upon the particular process which produced the polymer.

A lognormal distribution is one which is described by the following equation, see Kendall and Stuart (1958).

$$dF(z) = \frac{A}{(2.\pi.z)^{\frac{1}{2}}} . \exp\left[-\tfrac{1}{2}(B + A\log z)^2\right] . dz$$

where $z = (x - C).D$

and A, B, C and D are constants.

For comparison, the Gaussian or normal distribution is

$$dF(x) = \frac{1}{(2.\pi)^{\frac{1}{2}}} . \exp\left(-\tfrac{1}{2}x^2\right). dx$$

where $dF(x)$ is the frequency of occurrence of the variable x between x and $(x + dx)$.

Whereas a Gaussian distribution is symmetrical in shape about some mean value, the lognormal distribution envelope is assymetric having a brief tail on the low "x" side of the maximum and a sharp cut-off on the high "x" side, the magnitude of the tail and the sharpness of the cut-off depending on the constants A, B, C and D.

Because of this distribution of molecular weights of linear polymers, two average molecular weights have been defined.

1. The number-average molecular weight, $\bar{M}_n$

$$\bar{M}_n = \sum_i X_i M_i = \frac{\sum_i N_i M_i}{\sum_i N_i}$$

where X_i = the mole fraction of species i

M_i = molecular weight of species i

N_i = number of molecules of species i

It follows that the definition of the number-average molecular weight is

$$\frac{\text{total weight of polymer}}{\text{total number of moles of polymer molecule}}$$

2. The weight-average molecular weight, $\bar{M}_w$

$$\bar{M}_w = \sum_i W_i M_i = \frac{\sum_i N_i M_i^2}{\sum_i N_i M_i}$$

In determining the average molecular weight from some property of the polymer in solution and its dependence on molecular weight, the particular average that is obtained

will depend upon this dependence. Hence, let it be assumed that a constant of the polymer in solution, P, is such that

$$P_i = K.M_i^a.c_i$$

where K is a constant and c_i is the weight concentration of the species i of molecular weight M_i. Hence $c_i = N_iM_i$. It follows that

$$P = \sum_i P_i = \sum_i K.M_i^a.c_i$$

and therefore $\bar{M}_p$, the particular average molecular weight given by the measurement of constant P, is given by

$$\bar{M}_p = \left[\frac{P}{K \sum_i c_i}\right]^{1/a} = \left[\frac{\sum_i c_i M_i^a}{\sum_i c_i}\right]^{1/a}$$

Substituting $c_i = N_iM_i$ into this relationship gives

$$\bar{M}_p = \left[\frac{\sum_i N_i M_i^{a+1}}{\sum_i N_i M_i}\right]^{1/a}$$

For light scattering experiments,

<u>a = 1</u> $\bar{M}_p$ is tho <u>weight-average</u> molecular weight.

For osmotic pressure and freezing point depression experiments,

<u>a = - 1</u> $\bar{M}_p$ is the <u>number-average</u> molecular weight.

For viscosity experiments, the situation is less well-defined. If the Staudinger equation holds, then a = 1 and the molecular weight obtained is the weight-average molecular weight, sometimes referred to as the "Staudinger molecular weight". The Staudinger equation does not apply over a wide range of concentrations however, and a has a value which generally lies between 0.5 and 1.0. Therefore, the molecular weight resulting from viscosity experiments, and referred to as the viscosity-average molecular weight, $\bar{M}_v$, lies somewhere between the number-average and the weight-average molecular weights.

The above analysis of the various average molecular weights is taken from "Physical Chemistry of High Polymeric Systems" by H. Mark and A.V. Tobolsky, which is Part II of the series "High Polymers" by Interscience Publ. Inc., New York.

REFERENCES

Abragam, A. (1961) "The Principles of Nuclear Magnetism", Clarendon Press, Oxford

Abramson, H.N. (1957) J.A.S.A. 29, 42

Adem, J. (1954) Quart. Appl. Math. 12, 261

Alfrey, T. (1948) "Mechanical Behaviour of High Polymers" Interscience Publ. Inc., N.Y.

Allen, G. et al. (1961) Polymer 2, 375

Araki, Y. (1965) J. App. Pol. Sci. 9, 421

Bancroft, D. (1941) Phys. Rev. 59, 588

Bekkedahl, N. (1949) J. Res. N.B.S. 43, 145

Benbow, J.J. and D.J.C. Wood (1958) Trans. Farad. Soc. 54, 1581

Bergmann, L. (1949) Zeits. f. Phys. 125, 405

Biesterfeldt, H.J. et al. (1960) J.A.S.A. 32, 749

Boyer, R.F. and R.S. Spencer (1946) "Adv. in Colloid Sci." Vol. II Interscience Publ. Inc., N.Y.

Bradfield, G. (1964) Notes on Applied Science, No. 30 (N.P.L./D.S.I.R.) H.M.S.O.

Charlesby, A. and N.H. Hancock (1953) Proc. Roy. Soc. A218, 245

Chree, C. (1889) Trans. Camb. Phil. Soc. 14, 250

Condon, E.U. (1954) Glass Industry 33, 307 and 322

Crissman, J.M. et al. (1965) J. Pol. Sci. 3A, 2693

Daane, J.H. and R.E. Barker (1964) J. Pol. Sci. 2B, 343

Davies, R.O. and G.O. Jones (1953) Proc. Roy. Soc. 217A, 26

Doolittle, A.K. (1951) J. App. Phys. 22, 1471

Dudek, T.J. and J.J. Lohr (1965) J. Appl. Pol. Sci. 9, 3795

Edmonds, P.D. (1961) J.A.S.A. 33, 615

Edmonds, P.D. and E. Sittig (1957) Acustica 7, 299

Ellerstein, S.M. (1963) J. Pol. Sci. 8B, 443

Ellerstein, S.M. (1964) J. Pol. Sci. 4B, 379

Ferry, J.D. (1961) "Viscoelastic Properties of Polymers" Wiley

Flory, P.J. (1955) Int. Symp. on Macromol. Chem. Supplement to "La Ricerca Scientifica"

Frechette, V.D. (1960) Ed. of "Non-Crystalline Solids", Wiley

Gross, B. (1953) "Mathematical Structure of the Theories of Viscoelasticity", Hermann et Cie., Paris

Haward, R.N. et al. (1966) J. Pol. Sci. 4B, 375

Heijboer, J. (1956) Kolloid-Z. 148, 36

Holden, A.N. (1951) Bell System Tech. J. 30, 956

Hudson, G.E. (1943) Phys. Rev. 63, 46

Hughes, D.S. et al. (1949) Phys. Rev. 75, 1552

Illers, K.H. and E. Jenckel (1958) Rheol. Acta 1, 322

Jenckel, E. and R. Heusch (1953) Kolloid-Z. 130, 89

Kauzmann, W. (1948) Chem. Rev. 43, 219

Kendall, M.G. and A. Stuart (1958) "Advanced Theory of Statistics", Vol. I, Griffin and Co., London

Kolsky, H. (1953) "Stress Waves in Solids", O.U.P.

Kovacs, A.J. (1961) Trans. Soc. Rheol. 5, 285

Kovacs, A.J. et al. (1963) J. Phys. Chem. 67, 152

Kovacs, A.J. (1964) Adv. Pol. Sci. 3, 394

Krause, S. et al. (1965a) J. Pol. Sci. 3A, 3573

Krause, S. et al. (1965b) J. Pol. Sci. 3A, 1631

Krim, S. and A.V. Tobolsky (1951) Textile Res. J. 21, 805

Kynch, G.J. and W.A. Green (1957) Quart. J. Mech. and Appl. Math. 10, 61

Koppelmann, J. (1958) Rheol. Acta 1, 20

Landau, L.D. and E.M. Lifshitz (1959) "Theory of Elasticity" Dover Publ., N.Y.

Lewis, A.F. (1963) J. Pol. Sci. 1B, 649

Love, A.E.H. (1944) "Treatise on the Mathematical Theory of Elasticity", Dover Publ., N.Y.

Marx, J.W. and J.M. Sivertsen (1953) J. App. Phys. 24, 81

Mason, W.P. (1958) "Physical Acoustics and the Properties of Solids", Van No strand Co., Inc.

Mason, W.P. (1964) Ed. of "Physical Acoustics" 1A, Academic Press

Matsuoka, S. and B. Maxwell (1958) J. Pol. Sci. 32, 131

McKenzie, J.K. (1950) Proc. Phys. Soc. 63B, 2

McKinney, J.E. et al. (1960) Trans. Soc. Rheol. 4, 347

McLoughlin, J.R. and A.V. Tobolsky (1951) J. Pol. Sci. 7, 658

McPherson, A.T. and D.A. Cummings (1935) J. Res. N.B.S. 14, 553

Melchore, J.A. and H.F. Mark (1953) Modern Plastics 31, 141

Miklowitz, J. (1960) App. Mech. Rev. 13, 865

Monaglio, G. and F. Danusso (1963) Polymer 4, 445

Morse, P.M. and H. Feshbach (1963) "Methods of Theoretical Physics" McGraw-Hill, N.Y.

Nederveen, Ir. C.J. (1962) 4th Int. Cong. on Acoustics, Copenhagen P16

Nielsen, L.E. (1962) "Mechanical Properties of Polymers" Reinhold Publ. Corp., N.Y.

O'Reilly, J.M. (1962) J. Pol. Sci. 57, 429

Parfitt, G.G. (1954) Ph.D. Thesis, London University

Parfitt, G.G. (1956) Proc. 9th Int. Cong. on Appl. Mech., Brussels, p.360

Pasquine, A. and M.N. Pilsworth (1964) J. Pol. Sci. 2B, 253

Paterson, M.S. (1964) J. App. Phys. 35, 176

Pochhammer, L. (1876) J. Reine Angew. Math. 81, 324

Powles, J.G. (1956) J. Pol. Sci. 22, 79

Powles, J.G. and P. Mansfield (1962) Polymer 3, 336

Powles, J.G. and J.H. Strange (1963) Polymer 4, 401

Powles, J.G. et al. (1964) Polymer 5, 523

Prins, J.A. (1965) Ed. of "Non-Crystalline Solids", North Holland Publ. Co., Amsterdam

Rady, A.A.G. (1957) Ph.D. Thesis, London University

Rayleigh, Lord (1887) "Theory of Sound" Vol. I, Dover Publ., N.Y.

Read, B.E. and G. Williams (1961) Polymer 2, 239

Richards, W.T. (1936) J. Chem. Phys. 4, 449

Saito, N. (1963) "Solid State Physics" 14 Academic Press, N.Y.

Schramm, K.H. (1962) Z.Metallkunde 53, 729

Shear, S.K. and A.F. Focke (1940) Phys. Rev. 57, 552

Singh, H. and A.W. Nolle (1959) J. App. Phys. 30, 337

Sittig, E. (1957) Acustica 7, 157

Smith, R.T. (1965) Ph.D. Thesis, London University

Smothers, W.J. and Y. Chiang (1958) "D.T.A., Theory and Practice" Chem. Publ. Co., N.Y.

Snowdon, J.C. (1964) J.A.S.A. 36, 502

Spinner, S. et al. (1960) J. Res. N.B.S. 64A, 147

Spinner, S. and W.E. Tefft (1962) J. Res. N.B.S. 66A, 193

Tool, A.Q. and C.G. Eichlin (1931) J. Am. Ceram. Soc. 14, 276

Treloar, L.R.G. (1958) "The Physics of Rubber Elasticity", O.U.P.

Turnbull, D. and M.H. Cohen (1961) J. Chem. Phys. 34, 120

Wada, Y. et al. (1959) J. Phys. Soc. Japan 14, 104

Wegel, R.L. and H. Walther (1935) J. App. Phys. 6, 141

Wunderlich, B. and D.M. Bodily (1964) J. App. Phys. 35, 103

Wunderlich, B. (1964) J. App. Phys. 35, 95

Yamamoto, K. and Y. Wada (1957) J. Phys. Soc. Japan 12, 374

Ying, C.F. and R. Truell (1956) J. App. Phys. 27, 1086

Zemaneck, J. (1962) Ph.D. Thesis U.C.L.A.

Zemaneck, J. and I. Rudnick (1961) J.A.S.A. 33, 1283

Zemansky, M.W. (1957) "Heat and Thermodynamics", McGraw-Hill, N.Y.

Zener, C.M. (1948) "Elasticity and Anelasticity in Metals", Univ. of Chicago Press